CIVIL ENGINEERING STUDIES
STRUCTURAL RESEARCH SERIES NO. 344

INVESTIGATION OF PRESTRESSED REINFORCED CONCRETE FOR HIGHWAY BRIDGES
PART VI:
BOND CHARACTERISTICS OF PRESTRESSING STRAND

by
M. F. STOCKER
M. A. SOZEN

Issued as a Part of Progress Report No. 18 of
The Investigation of Prestressed Reinforced
Concrete for Highway Bridges
Project IHR-10
Illinois Cooperative Highway Research Program

Conducted by
THE STRUCTURAL RESEARCH LABORATORY
DEPARTMENT OF CIVIL ENGINEERING
ENGINEERING EXPERIMENT STATION
UNIVERSITY OF ILLINOIS
in cooperation with

THE STATE OF ILLINOIS
DIVISION OF HIGHWAYS

and

THE U.S. DEPARTMENT OF COMMERCE
BUREAU OF PUBLIC ROADS

UNIVERSITY OF ILLINOIS
URBANA, ILLINOIS
JUNE 1969

PRIVATE COMMUNICATION
NOT FOR PUBLICATION

INVESTIGATION OF PRESTRESSED REINFORCED CONCRETE FOR HIGHWAY BRIDGES

PART VI: BOND CHARACTERISTICS OF PRESTRESSING STRAND

By

M. F. Stocker
M. A. Sozen

Issued as a Part of Progress Report No. 18 of
The Investigation of Prestressed Reinforced
Concrete for Highway Bridges
Project IHR-10
Illinois Cooperative Highway Research Program

Conducted by

THE STRUCTURAL RESEARCH LABORATORY
DEPARTMENT OF CIVIL ENGINEERING
ENGINEERING EXPERIMENT STATION
UNIVERSITY OF ILLINOIS

in cooperation with

THE STATE OF ILLINOIS
DIVISION OF HIGHWAYS

and

U. S. DEPARTMENT OF TRANSPORTATION
FEDERAL HIGHWAY ADMINISTRATION
BUREAU OF PUBLIC ROADS

UNIVERSITY OF ILLINOIS
URBANA, ILLINOIS

June, 1969

ACKNOWLEDGMENTS

This study was carried out as a part of the research under the Illinois Cooperative Highway Research Program Project IHR-10, "Investigation of Prestressed Reinforced Concrete for Highway Bridges." The work on the project was conducted by the Department of Civil Engineering of the University of Illinois in cooperation with the Division of Highways, State of Illinois, and the U. S. Department of Transportation, Bureau of Public Roads.

At the University, the work covered by this report was carried out under the general administrative supervision of D. C. Drucker, Dean of the College of Engineering, Ross J. Martin, Director of the Engineering Experiment Station, N. M. Newmark, Head of the Department of Civil Engineering, and Ellis Danner, Director of the Illinois Cooperative Highway Research Program and Professor of Highway Engineering.

At the Division of Highways of the State of Illinois, the work was under the administrative direction of Virden E. Staff, Chief Highway Engineer, and J. E. Burke, Engineer of Research and Development.

The program of investigation has been guided by a Project Advisory Committee consisting of the following:

Representing the Illinois Division of Highways:

J. E. Burke, Engineer of Research and Development,
Illinois Division of Highways

Floyd K. Jacobsen, Bureau of Design,
Illinois Division of Highways

C. E. Thunman, Jr., Engineer of Bridge and Traffic Structures, Bureau of Design, Illinois Division of Highways

Representing the Bureau of Public Roads:

W. J. Wilkes, Chief, Bridge Division, Bureau of Public Roads

Representing the University of Illinois:

C. E. Kesler, Professor of Theoretical and Applied Mechanics

Narbey Khachaturian, Professor of Civil Engineering

R. E. Lloyd, C. Galambos, E. G. Paulet, and W. N. Richardson, U. S. Bureau of Public Roads, and W. J. Mackay, Illinois Division of Highways, also participated in the meetings of the Advisory Committee and contributed materially to the guidance of the program.

The investigation was directed by Dr. C. P. Siess, Professor of Civil Engineering, as Project Supervisor and as ex-officio chairman of the Project Advisory Committee. Immediate supervision of the investigation was provided by Dr. M. A. Sozen, Professor of Civil Engineering, as Project Investigator.

Acknowledgment is due to J. B. Reber and J. Kontoudakis, former Research Assistants in Civil Engineering, for their invaluable help.

This report was written as a thesis under the direction of Professor M. A. Sozen

TABLE OF CONTENTS

TABLE OF CONTENTS (continued)

TABLE OF CONTENTS (continued)

TABLE OF CONTENTS (continued)

LIST OF TABLES

LIST OF FIGURES

LIST OF FIGURES (continued)

LIST OF FIGURES (continued)

LIST OF FIGURES (continued)

LIST OF FIGURES (continued)

LIST OF FIGURES (continued)

LIST OF FIGURES (continued)

LIST OF FIGURES (continued)

LIST OF FIGURES (continued)

LIST OF FIGURES (continued)

LIST OF FIGURES (continued)

LIST OF FIGURES (continued)

LIST OF FIGURES (continued)

LIST OF FIGURES (continued)

1. INTRODUCTION

1.1 Object and Scope

The main objective of the investigation described in this report was to provide a fundamental understanding of the bond characteristics of prestressing strand as affected by various critical variables.

The scope of the investigation may be divided into four parts:

(1) The experimental study included 486 tests of simple pull-out specimens with short embedment lengths. The tests provided the necessary information on the relationship between bond force and slip. The major variables investigated were: size of strand, strength, consistency, curing conditions, age, and settlement conditions of concrete, lateral confining pressure, and time effects.

Some tests with plain wire and twisted square bars were made to study the influence of steel surface and torsional stiffness on bond of strand.

(2) The object of the theoretical investigation was to develop a hypothesis on the nature of bond for plain wire and strand. A simple conceptual model was designed to explain the fundamental bond characteristics of strand.

(3) An important object of the investigation was to study the question of the direct applicability of results from pull-out tests to the design of prestressed members. A simple analytical procedure is discussed to project the results of the short-length pull-out tests to practical problems such as calculating, for instance, the anchorage length of strand in a prestressed beam for a given prestress.

The results from the analytical method are compared with data from tests on five pretensioned prestressed beams and several pull-out tests with large embedment lengths.

(4) Practical recommendations related to the bond strength of prestressing strand are given for design purposes.

1.2 Strand as Prestressing Reinforcement

Seven-wire strand is manufactured by "stranding" hard-drawn or non-stress-relieved wire. The head of the stranding machine preforms the six exterior wires permanently and lays them around a straight center wire. This preforming process makes it possible to unravel strand and put it back together without difficulty.

After stranding, the strand is stress-relieved in a carefully controlled time-temperature operation. This is mostly achieved by an electrical induction process at temperatures on the order of 650°F.

Prestressing strand differs from ordinary seven-wire strand in that the center wire has a slightly larger diameter than the exterior wires. This is to ensure that the straight center wire does not slip, when under stress, with respect to the exterior wires. The center wire is held in place only by friction with the exterior wires which tend to straighten themselves when stretched and thus subject the center wire to lateral forces. It was found by the manufacturers that an increase of the diameter of the center wire by four percent with respect to that of the exterior wires is enough to prevent slipping. The larger size of the center wire leads to spaces between the exterior wires and enables concrete matrix to fill the spaces between the individual wires (Fig. 1.1).

The pitch of seven-wire strand is usually between 12 to 16 times the nominal diameter. The modulus of elasticity is approximately 28×10^6 psi.

Seven-wire strand is available in two grades: (a) ASTM Grade (A416) with a minimum tensile strength of 250 ksi and (b) Grade 270 K with a minimum tensile strength of 270 ksi.

At the beginning of the development of prestressing strand, use was limited to strands of small diameters (1/4 in., 3/8 in.). Following the trend to transfer more prestressing force to the concrete by means of less tendons for practical reasons, larger strand sizes have been developed (7/16, 1/2, 6/10 in.).

Recently, some exploratory tests with deformed (dimpled) seven-wire strand were reported (Hanson, N. W., 1969)*. The test results indicated improved bond properties compared with those of conventional seven-wire strand.

1.3 Previous Investigations of Bond Characteristics of Prestressing Strand

The following section presents a brief description of investigations related to bond of strand which were conducted at various laboratories. Most of the studies were performed by measuring, in one way or another, the anchorage length or the flexural bond strength in prestressed beams.

---

*References are arranged in alphabetical order in the List of References. The numbers in parentheses refer to the year of publication.

(1) Debly (1956) conducted a series of four prestressed-beam tests reinforced with two 7/16-in. strands to provide information on the bond characteristics of prestressing strand. For an effective prestress after release ranging from 148 to 167 ksi, the anchorage length was found to vary from 24 to 32 in. The higher values were obtained for a larger concrete cover under the strand. The anchorage length was determined by measuring the concrete strain at the level of the reinforcement.

(2) Base (1958) reported an extensive investigation of the variation of the anchorage lengths developed by various prestressing steels in practice. The anchorage length was determined by measuring the concrete strain along the reinforcement. Measurements were taken on beams produced in prestressing plants throughout England. The investigation included plain wire, indented wire, crimped wire, and 5/16-in. strand. The anchorage length of 5/16-in. strand was found to vary from 9 to 19 in. The prestressing force was not reported.

The effect of time on the anchorage length of 0.2-in. wire was studied in laboratory tests.

(3) Ratz, Holmjanski, and Kolner (1958) conducted tests on approximately 200 concentrically prestressed concrete prisms to study the effect of the concrete strength on the anchorage length of various deformed wires and 7x1.6-mm strand (0.19-in. strand). Bond was found to be a direct function of the concrete strength for any type of wire and strand. On the basis of a direct relation between tension in the

steel and displacement within the anchorage zone, a formula was developed to compute the slip of the steel at any point within the anchorage zone.

In most of the tests, only the end slip of the wire or strand was measured. The anchorage length was determined analytically on the basis of the end slip. The results indicated that the anchorage length of the strand prestressed to approximately 170 ksi varied from 5 to 19 in. with the concrete strength varying from 6000 to 2400 psi.

(4) Dinsmore, Deutsch, and Montemayor (1958) performed 42 prestressed pull-out tests and four prestressed-beam tests to study the anchorage lengths required to transfer the prestressing force and to develop the strength of clean 7/16-in. strand. The test results were found to vary over a wide range. The anchorage length necessary to transfer the prestress (effective prestress after release = 138-166 ksi) ranged from 9 to 36 in. The variation of the results was attributed partly to the degree of vibration of the concrete.

An anchorage length of four ft (110 diameters) was found sufficient to develop the strength of the strand.

(5) Rüsch and Rehm (1963) carried out an extensive investigation on concentrically prestressed concrete beams to determine the anchorage length of 16 different types of prestressing steel. Three beams were reinforced with 7x3-mm strand (0.35-in. strand). The anchorage length was based on strain measurements on the concrete along the reinforcement.

It was found that, in general, an increase of the concrete strength led to a decrease of the anchorage length. The anchorage length of the strand for a prestress of 128 ksi after transfer of the prestressing force varied from 26 in. to 34 in., depending on the concrete strength and the type of stress release.

The type of release of the prestressing force was found to cause a significant difference in the anchorage length. The effect of time on the anchorage length was studied over a period of six months.

(6) Kaar, LaFraugh, and Mass (1963) investigated the influence of the concrete strength on the anchorage length of seven-wire strand by testing 36 rectangular concrete prisms. The tests included 1/4, 3/8, 1/2, and 6/10-in. strand. The anchorage length was determined from concrete strain measurements.

The test results indicated that the concrete strength, varying from 1660 to 5500 psi, had only little influence on the anchorage length of strands up to 1/2-in. diameter.

The increase of the anchorage length with time observed for a period of one year was found to be, in general, less than 10 percent.

(7) Preston (1963) reported a comparative investigation of the anchorage length of clean 1/2-in. strand with tensile strengths of 250 and 270 ksi. In addition, 1/2-in. strand with a rusted surface was included in the investigation.

The results indicated that the bond characteristics were approximately identical for the two types of strand. The corrosion of

the steel surface was found to lead to a 25-percent reduction in the anchorage length.

(8) Hanson and Hulsbos (1965) studied the load capacity of pretensioned prestressed concrete I-beams with web reinforcement. In the course of this investigation, including 18 beams, the anchorage length of 7/16-in. strand prestressed to approximately 155 ksi, was found to be approximately 18 in.

(9) Over and Au (1965) investigated the influence of the strand size on the anchorage length with the aid of six square concrete prisms prestressed concentrically with 1/4, 3/8, and 1/2-in. strand. It was observed that the anchorage length increased with the strand diameter.

(10) Hanson (1969) studied the influence of surface roughness on anchorage bond and flexural bond strength in 12 prestressed beams using 7/16-in. and 1/2-in. strand. The surface conditions tested were: clean "as received", partially rusty, and rusty. Specially deformed (dimpled) strand was included in the investigation.

Hanson found that a 30-percent improvement in the anchorage length can be obtained with rusted strand. The deformed strand showed a similar improvement over the clean "as received" strand. Similarly, the flexural bond strength of the beams containing rusted or deformed strand was higher than that for clean strand.

Test data and numerical results from the above investigations concerning the anchorage length of clean seven-wire strand are summarized in Table F.4.

2. OUTLINE OF EXPERIMENTAL INVESTIGATION

The experimental program included 486 simple pull-out tests and five prestressed-beam tests. The specimens were reinforced with seven-wire, round-wire strand (nominal diameter: 1/4, 3/8, 7/16, and 1/2 in.), plain wire (diameter: 0.084, 0.130, 0.147, and 0.171 in.), and twisted square bars (width: 5/16 in.).

The pull-out specimens consisted of 4 by 4 by 9-in. concrete prisms with the steel embedded in the center of the specimen parallel to the longer side. In 433 specimens, the bonded length was only one in. In the remaining specimens, the bonded length was varied from 0.5 to 20 in. During the test, the bond force and the slip were measured until, at a slip of 0.15 in., the test was discontinued. The pull-out tests were performed in series containing 4 to 17 specimens cast from the same batch of concrete. The properties of each test series are listed in Table B.1 through B.4. The range of the variables investigated is given below:

Seven-wire strand:

Effect of bonded length:

Variation: 0.5 to 2.0 in.	
1/4-in. strand	12 tests
3/8-in. strand	12 tests
7/16-in. strand	12 tests
1/2-in. strand	12 tests
Variation: 1.0 to 20.0 in.	
7/16-in. strand	22 tests

Effect of test setup:

Variation: rotational restraint of strand vs. concrete

7/16-in. strand 9 tests

Effect of strand diameter and concrete strength:

Variation: strand diameter: 1/4 to 1/2 in.

concrete strength: 2300 to 7600 psi

1/4-in. strand 36 tests

3/8-in. strand 36 tests

7/16-in. strand 36 tests

1/2-in. strand 36 tests

Effect of curing conditions:

Variation: moist to dry, two concrete strengths

7/16-in. strand 18 tests

Effect of concrete consistency:

Variation: 0.2 to 7.5-in. slump

7/16-in. strand 25 tests

Effect of depth of concrete below strand:

Variation: 2 to 30 in.

7/16-in. strand 30 tests

Effect of lateral pressure:

Variation: 0 to 2500 psi, two concrete strengths

7/16-in. strand 35 tests

Effect of time:

Variation: age of concrete at test: 1 to 64 weeks

7/16-in. strand 17 tests

Variation: duration of sustained load: 1 to 64 weeks

7/16-in. strand 20 tests

Plain wire:

Effect of wire diameter and concrete strength:

Variation: diameter: 0.084 to 0.171 in.

concrete strength: 2200 to 8300 psi

d = 0.084 in. 9 tests

d = 0.130 in. 9 tests

d = 0.147 in. 9 tests

d = 0.171 in. 9 tests

Effect of curing conditions:

Variation: moist to dry

d = 0.147 in. 6 tests

Effect of lateral pressure:

Variation: 0 to 2000 psi, two concrete strengths

d = 0.147 in. 26 tests

Square Bars:

Effect of twist angle:

Variation: 0 to 46 degrees, two test setups

d = 5/16 in. 17 tests

The five pretensioned prestressed beams were 9 ft long and had a cross section of 6 by 12 in. They were reinforced with two 7/16-in. strands. The concrete strength was approximately 5600 psi. The prestress immediately before release was on the average 167 ksi.

The only variable included was the depth of the concrete below the strand. In three beams, the strand was placed two in. from the bottom of the beam with respect to the direction of casting. In two beams, the strand was placed two in. from the top.

The anchorage length of the strand, which was determined by measuring the concrete strain distribution along the beam, was measured immediately after release of the prestress and after periods of 1, 6, 15 and 35 days.

3. DETERMINATION OF BONDED LENGTH AND SUPPORT CONDITIONS FOR THE TEST SPECIMEN

3.1 General Remarks

With respect to bond, it is virtually impossible to devise a single type of test specimen and test it under such conditions that the results would be applicable to the whole domain of bond conditions in practice. In general, bond exists under a wide variety of stress combinations with the concrete and the steel stressed differently in different directions.

In prestressed reinforced concrete, the needs are more specific. Of interest is primarily the anchorage bond with the concrete in compression in a direction parallel to the steel which is in tension. Flexural bond becomes critical as the ultimate load is approached in flexural members. In that case, both the concrete and the steel are in a state of tension. In addition to stresses parallel to the reinforcement, the concrete may be subjected to both tensile and compressive stresses which are caused by loads, reaction forces, or transverse prestressing.

Since the objective of this investigation was not to provide data applicable to specific bond conditions but to develop an understanding of the nature of bond and to study the effect of many variables, the test specimen had to be simple both for manufacture and for analysis. Pull-out tests provide a more satisfactory solution to these requirements than beam tests. With a short bonded length, the maximum forces in the specimen could be kept low. Thus, the overall stresses in the concrete

and the lateral elastic deformations of the steel due to axial stresses were kept to a minimum. In order to eliminate the confining forces, induced by friction between the concrete specimen and the supporting element, the steel at the loaded end was left unbonded within the concrete specimen over a length of four in.

Even with the stress conditions for the test specimen defined satisfactorily, the direct applicability of the results is not assured. Extraneous restraints in the test setup may have measurable effects. The following is a discussion of two test conditions which may influence the results of the pull-out tests.

3.2 Effect of Bonded Length

Bond is generally described by the relationship between slip and bond force. This relationship, however, may be regarded as a unique bond property only if the measurements are obtained under very special conditions. In general, the bond stress (i.e. force per bonded unit area) or the unit bond force (i.e. force per bonded unit length) is a nonlinear function of the slip. Since the slip varies along the bonded length because of a nonuniform elastic deformation of the steel, caused by a change in steel stress, the bond stress distribution is nonlinear. The same is true for the distribution of steel stress and slip.

The only quantities that are usually obtained from measurements in pull-out tests are the magnitudes of the slip and the steel stress at the ends of the bonded length. In order to determine a direct relationship between slip and bond force, the distribution of both

quantities along the bonded length would have to be known. Approximations can be made by taking average values assuming, for example, a constant bond stress distribution. The bond-slip relationship, obtained in this manner, would not represent a generally valid bond property but it would pertain to a certain bonded length only. This explains in part why test results of various investigations compare so unfavorably, and why attempts to project from one test condition to another have often failed.

There are three possible approaches to obtaining a direct bond-slip relationship:

(a) The steel stress and the slip along the bonded length are measured. In the realm of current technology, this method has the disadvantages of demanding precision difficult to achieve and instrumentation likely to cause disturbance of bond.

(b) Series of pull-out tests with different bonded lengths could be conducted, and a relationship between the average bond values and the bonded length could be established. Extrapolations would make it possible to determine the average bond force-slip relationship for any desired bonded length. This method, however, would lead to a very extensive test program, since the bonded-length effect would have to be tested for all variables investigated.

(c) The third method appears to be the least expensive and most successful one. It was used by Rehm (1961) in an investigation of bond characteristics of plain and deformed bars. The ideal would have been to test reinforcement with an infinitesimally small bonded

length thus assuring a practically uniform slip, and consequently a uniform bond stress distribution. A direct bond force-slip relationship would be obtained in that case. In practice, of course, a bonded length of finite value had to be chosen. The limits of the length to be chosen depend on many factors such as uniformity of steel surface, aggregate size, relative effect of boundary conditions on total length, maximum pull-out force to be obtained, and the shape of the bond force-slip relationship.

In the investigation described in this paper, the third method was chosen. Before one bonded length for all pull-out tests was decided upon, four test series (SA09-1, SA09-2, SA08-3, SA09-4) were carried out with different bonded lengths. Each series involved a single strand size and consisted of 12 specimens. Three specimens were tested at each of the following bonded lengths: 0.5, 1.0, 1.5, and 2.0 in. The average results, plotted in terms of unit bond force, are shown in Fig. 3.1 and 3.2.

Within each test series and at slips of less than 0.01 in., the differences in the unit bond force-slip relationships were not significantly greater than the differences which would have been obtained if the average results from four groups of three tests with the same bonded length had been compared. This observation is supported by the distribution of a population of 35 tests with a bonded length of one in. (see Fig. 5.3).

At large slips, the unit bond force of the specimens with a bonded length of 0.5 in. increased less than that of specimens with

larger bonded lengths. This fact may be attributed to an imperfection of the test specimens used. As described in section A.4, wax was used at the ends of the bonded length to stop the fresh concrete from running inside the steel pipes that prevented bond between the strand and the concrete outside the desired length. During the pull-out test, the strand was pulled out at least 0.15 in. This meant, that at the trail end of the bonded length, a piece of strand was pulled into the concrete that was unbonded and coated with wax. Thus, the average bond strength over the total length decayed with increasing slip. The amount of loss in bond quality, caused by the imperfection of the test specimens, was constant for every bonded length, the effect on the unit bond force, however, increased the shorter the bonded length became.

Test results obtained with very short embedment lengths are very sensitive towards any imperfections. Therefore, the theoretical advantage of making the bonded length as short as possible is offset by practical considerations. This fact was indicated by the relatively large scatter of the individual tests with bonded lengths of 0.5 in. As a result of these tests, a bonded length of one in. was chosen as the standard bonded length for all pull-out tests since it was the shortest length giving reliable and consistent test results.

An estimate of the differential slip between trail end and attack end of the bonded length may be obtained with the following assumptions: (a) The steel stress decreases linearly from the attack end to the trail end, where it has to be zero. (b) The concrete

deformations are negligible. Thus, the differential slip, ds, will be approximately

$$ds = \frac{P\,L}{2\,A\,E} \tag{3.1}$$

where P = pull-out force, L = bonded length, A = steel area, and E = modulus of elasticity of the strand. For a 7/16-in. strand and a bonded length of one in., the differential slip at a pull-out force of 700 lb is found to be 0.00011 in.

Since the differential slip was of an order that barely could be measured with 0.0001-in. dial indicators, it was not necessary to measure the attack-end slip. For large bonded lengths, however, the measurement of the attack-end slip was a necessity. In those cases, the differential slip became an influential magnitude, and the error in assuming a constant bond stress distribution along the bonded length was significant. Two test series (SA09-18, SA10-19), carried out with specimens of different bonded lengths, confirmed that fact.

Test series SA09-18 included 14 specimens with 7/16-in. strand. Three specimens were tested with each of the following bonded lengths: 1, 3, 8, 15 in., and two specimens with a bonded length of 20 in. Test series SA10-19 included 9 specimens; the bonded lengths were 1, 3, and 8 in. The attack-end slip was measured in both test series in addition to the trail-end slip for bonded lengths greater than one in. Figure 3.3 and 3.4 show the measured force-slip relationships. At an attack-end slip of 0.0001 in., the total load developed was approximately 200 to 300 lb regardless of the bonded

length. The attack-end slip increased proportionally with the load until the trail end started to slip. The relationship between the attack-end slip and the load was virtually independent of the bonded length which indicates the progressive character of the bond mechanism.

After a measurable trail-end slip had developed, the rate of slippage increased suddenly. This break is understandable if the bond force-slip relationship of the one-in. specimen is observed. The bond force increases initially with practically no trail-end slip. After reaching a certain load, the slip increases suddenly while the load stays almost constant. The bond-slip curve may be compared to an elasto-plastic stress-strain curve. The bonded piece of strand is pulled out at approximately constant force after the slip had extended over the total length. The attack-end and trail-end slips progress at the same rate, with the attack-end slip exceeding the trail-end slip by the amount of the differential slip. For bonded lengths less than 8 in., the differential slip was too small to be shown graphically in Fig. 3.3 and 3.4.

The relationship of the unit bond force versus the trail-end slip was plotted in Fig. 3.5 and 3.6. The shape of the unit bond force-slip relationship of the one-in. specimens should be compared with the shape of the curves in Fig. 3.2. The difference was caused by the fact that a new coil of 7/16-in. strand was used in test series SA09-18 and SA10-19.

The shape of the unit bond force-slip relationship of the one-in. specimen affects the magnitude of the average bond force

calculated for tests with larger bonded lengths. If the unit bond force of the one-in. specimen is constant throughout the whole range of slip, the unit bond force-slip relationship would be identical for every bonded length. In the case of a negative slope for the unit bond force-slip relationship, the unit bond force will decrease with increasing bonded length. In the case of a positive slope, it will increase with increasing bonded length. These trends are indicated by the curves in Fig. 3.5 and 3.6. At small slips, the unit bond forces decreased with increasing bonded lengths as expected. The trend of the decrease was in the right order for both test series although the relative magnitudes were not as consistent. The typical scatter of bond tests, especially with short bonded lengths, is such that three ostensibly identical tests are not sufficient to produce completely reliable average values. The reduction in unit bond for the one-in. specimen at a slip of approximately 0.01 in. became less pronounced for larger bonded lengths since, for the longer specimens, the unit bond force was averaged over larger slip ranges.

The results shown in Fig. 3.5 and 3.6 are analysed in detail in Chapter 13.

3.3 Effect of Support Conditions

Strand belongs neither to the category of deformed bars nor to that of plain bars. Provided the concrete specimen does not split, deformed bars fail in bond by shearing off the concrete keys between

their deformations. Plain bars are pulled out of the concrete suddenly after the initial bond force at a slip of approximately 0.0001 in. has been exceeded. Strand, with its long-pitched, helical arrangement of the exterior wires, untwists itself when forced to slip through the rigid concrete embedment.

Two test setups may be used with respect to the untwisting of the strand: (a) the concrete specimen may be restrained completely from rotating, and (b) the concrete specimen may be permitted to rotate freely. In the first case, the strand is forced to untwist itself with respect to the rigid concrete specimen. In the second case, the strand retains its original geometric shape while the concrete specimen rotates.

Untwisting of the strand tends to increase the contact pressure between the strand and the concrete because the strand possesses some torsional stiffness. The higher contact pressures should cause the bond strength to increase. If the concrete specimen is allowed to rotate, the torsional restraint vanishes. No increase of contact pressure occurs.

In order to investigate the effect of the rotational restraint on bond, a series of tests (SA08-5) was carried out using strand with a diameter of 7/16 in. The series included nine specimens: Five specimens were free to rotate during the test, four specimens were completely restrained. The average bond-slip relations are plotted in Fig. 3.7. The difference in bond force was very small. In fact, the bond force at small slips was even lower for the restrained specimens. However, the rate at which the bond force increased with increasing slip was greater for the specimens restrained from rotation than for those free to rotate.

In addition to the bond force, the relative rotation of the strand versus the concrete prism was measured for both types of test setups. As expected, the measured rotation of the unrestrained concrete specimen around the strand was exactly equal to the amount the strand untwisted with respect to the fixed concrete specimen.

Summarizing the test results, it may be concluded that the torsional restraint of the test setup, and consequently the torsional stiffness of strand, had very little influence on bond as measured in the pull-out tests.

Since in practice the concrete is usually restrained from rotation, all further pull-out tests with strand were performed on torsionally restrained specimens.

4. TESTS WITH PLAIN WIRE

Seven-wire strand is manufactured by twisting six plain wires helically around a straight center wire. Although strand consists only of plain wires, the arrangement of the exterior wires results in an overall surface geometry which increases bond beyond the value depending on the surface characteristics of the individual wires. To develop a basic understanding of the bond characteristics of strand, it was necessary to study bond related to the surface characteristics of the plain wires separately. This could be achieved by conducting pull-out tests with plain wire having the same surface characteristics as the exterior wires of the strand. Because the exterior wires of the strand could not be straightened without modifying their surface, the straight center wires of the strand were used for this purpose. The surface characteristics of the center wire might differ a little from that of the exterior wires because of the manufacturing process of the strand and the protected position of the center wire against physical and chemical wear. However, the effect of this difference on bond was assumed to be small.

Three pull-out test series (WA08-1, WB08-1, WC08-1) were conducted using the center wires of 1/4-in., 3/8-in., 7/16-in., and 1/2-in. strand. For each series of twelve specimens, a different concrete mix was used. The compressive strength of the concrete at the time of testing was approximately 2200, 5000, and 8300 psi.

The bond stress-slip relationships (Fig. 4.1) were typical for plain wire, although plotting the slip to a logarithmic scale may

obscure this fact. An example of a bond stress-slip curve, with the slip plotted to a linear scale, is shown in Fig. B.1. Initially, the bond stress increased at a slip too small to be measurable. At a slip of approximately 0.0001 in., the maximum bond stress was reached. This point in the bond stress-slip curve was clearly marked by a sudden drop of the load with an attendant increase of slip. The bond stress kept decreasing until it approached a nearly constant value at a slip of approximately 0.1 in.

The average bond-slip curves, shown in Fig. 4.1, indicate that at higher concrete strengths the bond stress increased with the wire size. This trend was very pronounced in test series WB08-1 with a concrete strength of 8300 psi. Considering the relatively great scatter that is typical for bond tests, especially with short embedment lengths, and the fact that the individual results of tests with different wire sizes overlapped one another by a large margin, it is not expedient to draw definite conclusions. There was neither a statistical nor a theoretical basis to confirm the above observation.

The maximum bond stress for the individual tests (Fig. B.46, B.47, and B.48) ranged from 235 to 425 psi. The lower values were obtained with low-strength concrete, the higher values with high-strength concrete. In order to determine the influence of the concrete strength on bond, the bond stresses of all four wire sizes were averaged. In this manner, one bond stress-slip relationship was obtained for each test series (Fig. 4.2). The results demonstrate that the concrete strength had an increasing effect on the bond stress throughout the

entire range of slip. The influence, however, was very small. Although the concrete strength varied from 2000 to 8000 psi, the bond stress increased by only 10 percent at a slip of 0.0001 in. and by approximately 50 percent at a slip of 0.15 in.

In contrast to the foregoing observations, Rehm (1961) found that the bond stress of plain round bars varied approximately proportionally with the concrete strength, at least within the range of 1000 psi to 5200 psi. Rehm tested plain round steel bars with diameters of 16 mm (5/8 in.) using pull-out tests with a bonded length equal to the diameter of the bar. It should be mentioned, however, that the bars, tested by Rehm, had a rougher surface than the center wires of strand. The surface was classified as "partly scarred mill scale."

Another three test series with plain wire (WAP15-1, WAP17-2, WBP66-1) were performed in connection with the phase of the test program to investigate the influence of lateral pressure on bond. Specimens with center wires of 7/16-in. strand and concrete strengths of approximately 6000 psi and 8200 psi were tested. The relationships found for these tests were very similar to those in the tests described above (Fig. 4.3).

Test series WBP66-1 produced extremely high bond stresses compared with the results of series WB08-1 (Fig. 4.1). The difference may be attributed to shrinkage. Although the concrete mix and the concrete strength were practically identical in both series, the age of the concrete at which the tests were carried out differed by almost two months. The shrinkage deformations of the concrete, developed during this period of

time, induced additional lateral stresses acting normal to the surface of the wire. As a consequence of the higher normal stresses, the bond stresses of test series WBP66-1 exceeded those of series WB08-1.

Summarizing the test results obtained with the center wires of strand, it may be concluded that the concrete strength had a well defined but small effect on the bond strength of plain wire. The bond strength increased with the age of the concrete, which is mainly attributable to shrinkage. The maximum bond stress was developed at a slip of approximately 0.0001 in. For an 8- to 17-day old concrete, the average maximum bond stresses varied from 300 to 330 psi depending on the concrete strength. At a slip of 0.1 in., the range of the average bond stresses was as low as 80 to 160 psi.

The above bond values compare very well to results obtained by Keuning (1962) who used pull-out tests to study the bond characteristics of 0.192-in. round prestressing wire. In Keuning's tests, the bonded length was three in. The age of the concrete was nine days, the concrete strength was approximately 4700 psi, and the maximum bond stress was 330 psi. At a slip of 0.1 in., Keuning's tests indicated an average bond stress of 110 psi.

5. EFFECT OF STRAND SIZE

The most commonly used type of strand in prestressed concrete is seven-wire (round-wire) strand. With the exception of extremely small diameters which are used in model structures, the diameter of seven-wire strand ranges from approximately 0.25 in. to 0.6 in. In order to limit the number of tests, it was necessary to study the effect of different variables on bond experimentally with only one strand size. To project those results to other sizes required an investigation of the influence of the strand size on bond.

The investigation described in this report included four different strand sizes with nominal diameters of 1/4, 3/8, 7/16, and 1/2 in. Three different concrete strengths were used ranging from 2300 psi to 7600 psi. A total of 33 tests was performed with 1/4-in., 3/8 in., and 1/2-in. strand, and 54 tests were carried out with 7/16-in. strand (see Table B.1 and B.2) to investigate the effect of the strand size on bond.

Average unit bond force-slip relationships for different strand sizes, as obtained with a concrete strength of approximately 5400 psi, are plotted in Fig. 5.1. With exception of the 3/8-in. strand, the relationships show a similar trend for the various strand sizes. The bond force increased initially without measurable slip. After having reached a certain value (initial bond force), the strand started slipping. The bond strength beyond the initial bond force continued to increase at a small but steady rate.

The 3/8-in. strand displayed a different bond-slip characteristic. The steady increase of the bond strength was interrupted by a sudden decrease of the bond force at a slip of roughly 0.001 in. The rate at which the bond force increased at slips larger than approximately 0.01 in. exceeded that of the other strand sizes.

The unit bond force of the strand increased with the diameter. To determine how much the bond strength was affected by the strand size, the nominal bond stress (i.e. the pull-out force divided by the theoretical surface area) was plotted for each strand size and for each concrete strength in Fig. 5.2. To express bond in terms of bond stress was justified by the facts that the twist angles of the different strands (i.e. the angle formed by the axes of the exterior wires with the longitudinal axis of the strand) were approximately identical and that the torsional stiffness of strand had little influence on the bond strength (see Section 3.3). The latter fact was confirmed indirectly in Fig. 5.2. Although 1/2-in. strand is stiffer with respect to torsion than 1/4-in. strand, the bond stress of both strands increased with slip at approximately the same rate.

The relationships in Fig. 5.2 suggest a slight trend of the nominal bond stress to decrease with increasing strand diameter. A study of all the test data, however, indicated that this trend was statistically not significant. In Fig. 5.3 through 5.5 the mean, the confidence intervals of the mean, and the mean including two standard deviations were plotted versus the strand size for concrete mixes A, B, and C. The confidence intervals indicate the range within which

the average bond stress lies with a probability of 95 percent. The limits determined by two standard deviations enclose ostensibly 95 percent of all test data.

The bands representing the scatter of individual test results for each strand size in Fig. 5.3 through 5.5 overlap one another by such a margin, both for a slip of 0.0001 in. and 0.1 in., that the trend indicated in Fig. 5.2 appears doubtful, or at least not significant. It should be noticed that the confidence interval was relatively small for 7/16-in. strand in Fig. 5.3 because 35 test results were available for this strand size. Only 12 test results could be used for the other strand sizes.

The variation of the nominal bond stress with the strand diameter for each of the three concrete strengths of mix A, B, and C is presented in Fig. 5.6. The variation is shown in terms of confidence intervals of the mean (probability = 95 percent) and in terms of the mean plus two standard deviations. Figure 5.6 illustrates the variation of the nominal bond stress with the concrete strength.

In Fig. 5.7 the average bond forces at different slips (0.0001 in., 0.01 in., 0.1 in.) are plotted versus the strand diameter. Provided that the same bond characteristics pertain to all strand sizes, straight line relationships, starting at the origin of the graph, should be obtained. For practical purposes and within the range of strand sizes tested, the bond force of strand may be assumed to vary approximately linearly with the strand diameter.

6. EFFECT OF CONCRETE PROPERTIES ON BOND OF PLAIN WIRE AND STRAND

6.1 Introductory Remarks

To compare the influence of different concrete properties on bond is extremely difficult, because varying one property of the concrete inevitably results in the change of other properties. By changing, for example, the strength of the concrete, which may be achieved by varying either the mix proportions or the age of the concrete, the characteristics of settlement of the fresh concrete may be altered in one case, the conditions of shrinkage in the other. It is therefore not possible to separate the influence of individual properties to such a degree as to render absolutely reliable relationships between bond strength and individual concrete properties. It is possible, however, by careful selection and control of the concrete mixes, to determine the trend and the significance of the effects different concrete properties exert on bond.

In the following, effects of concrete properties, such as strength, consistency, curing conditions and age on bond of plain wire and strand are described.

6.2 Effect of Concrete Strength on Bond of Plain Wire and Strand

Three different mix proportions for the concrete were used (Section A.2.3) to study the influence of concrete strength on bond. The mix proportions were chosen so that the ratio of the volume of cement plus sand to the volume of gravel, and the consistency of the fresh concrete, as measured by the slump, remained constant for all

three mixes. Necessarily, the amount of cement and the water/cement ratio were different. The properties of the mixes (A, B, C) and the resulting strength characteristics of the concrete are listed in Table A.1. The age of the concrete at the time the tests were performed was eight or nine days. The average compressive strength was approximately 5400 psi, 7500 psi, and 2400 psi. The relation between the compressive strength and the splitting strength of the concrete is shown in Fig. A.2.

Three series of tests with center wires of four different strand sizes (1/4, 3/8, 7/16, and 1/2 in.) were performed to investigate the variation of the bond strength of plain wire with the concrete strength. The average bond-slip relations of these tests are presented in Fig. 4.1. Each curve represents the average of three tests. Since no significant influence of the wire diameter on the bond strength could be found, the bond stresses of all four wire sizes were averaged and plotted in Fig. 4.2. The concrete strength appeared to have a small but definite effect on the bond strength throughout the whole range of slip.

In Fig. 6.1, the bond strength, obtained with different concrete strengths, was expressed in percent of the bond stress developed at a concrete strength of approximately 5000 psi. Each symbol in this graph represents an average of three test results. Taking the mean value of those results, regardless of the wire diameter and the slip at which the results were obtained, it appears that the bond strength increased by roughly four percent for every 1000-psi

increase of concrete strength. Taking into consideration the introductory remarks of this chapter, and the fact that the above result was derived from only twelve tests per concrete strength, the quantitative conclusion is debatable. It shows clearly, however, that the concrete strength has but little influence on the bond strength of plain wire.

A larger number of tests was performed with strand to study the influence of concrete strength on bond. Including all four strand sizes, 36 tests were carried out with a concrete strength of roughly 2400 psi, 71 tests with a concrete strength of 5500 psi, and 47 tests with a concrete strength of 7500 psi. The data from the following series were used to evaluate the effect of concrete strength: series SA09-1 through SA08-14, with the exception of series SA23-8 and SA08-13 (Table B.1), series SB09-1 through SB08-3, and series SC09-1 through SC08-4 (Table B.2).

Figures 6.2 through 6.5 present the average bond-slip relationships of the four strand sizes at various concrete strengths. The trend of the bond strength to increase significantly with the concrete strength was common to all four strand sizes. In order to compare the relative increase of the bond strength of all four strand sizes, the bond strength measured at various concrete strengths was expressed in percent of that bond strength that was found at a concrete strength of approximately 5500 psi (Fig. 6.6). Despite the differences in strand size and slip, the results compare surprisingly well. According to this figure, the unit bond force increased, on the average, at a rate of eight percent per 1000 psi of concrete strength for a slip of

0.0001 in., and at a rate of eleven percent per 1000 psi of concrete strength for a slip of 0.1 in. These numbers are higher than that observed for plain wire. It should be noted, however, that the larger number of tests with strand (154) compared with that for plain wire (36) resulted in more reliable mean values.

Another illustration of the apparent effect of the concrete strength on bond of strand, showing the variation of individual test results, is presented in Fig. 5.6.

6.3 Effect of Concrete Consistency on Bond of Strand

The consistency of the concrete may be measured by the slump the fresh concrete exhibits in a specified test (ASTM C143-66). In order to find the effect of the consistency of concrete on bond, various concrete mixes were designed such that both the strength characteristics and the water/cement ratio remained constant while the consistency was varied. This was achieved by varying the ratio of fine aggregates (cement plus sand) to coarse aggregates (gravel). Two comparable sets of test series were conducted, each set containing three series (SA09-6, SD09-1, SE09-1, and SA09-7, SD09-2, SE09-2). The properties of the concrete mixes used (A, D, E) are listed in Table A.1. The slump values developed by the three concrete mixes were approximately 0.4, 1.5, and 7.0 in. The average strengths of the concrete at the age of nine days were within a range of 800 psi. Since the concrete properties and the curing conditions were comparable the results of both sets of test series were averaged.

Each bond-slip relationship in Fig. 6.7 represents an average of eight or ten identical tests. A comparison of the three bond-slip curves indicates that the bond strength of strand is affected by the consistency of the concrete. Despite the comparatively low strength of the concrete mix yielding the largest slump, specimens with this concrete developed the highest bond strength. This result confirms that the strength of concrete by itself is neither sufficient nor reliable as a sole basis for the prediction of bond strength with respect to concrete properties.

The favorable bond characteristics developed by the high-slump concrete may be attributed to shrinkage. Although the water/cement ratio was identical for all three concrete mixes, the high-slump concrete required more water and cement to reach a comparable strength at a low consistency. Consequently, this mix was bound to develop more shrinkage than the other two mixes. The resulting difference in contact pressures between the concrete and the strand, caused by shrinkage deformations, led to an increase in bond strength.

6.4 Effect of Curing Conditions on Bond of Plain Wire and Strand

The basic method of curing the pull-out specimens that was used throughout the whole test program is described in Section A.4. The specimens were kept moist in their forms for two days. Then, the forms were struck, and the specimens were moved to the fog room with a relative humidity of 100 percent. After being in the fog room for four days, the specimens were stored in a climate-controlled room with a temperature of approximately 73°F and a relative humidity of 50

percent. In order to probe how sensitive bond strength was to different curing conditions, a pilot series of tests was conducted early in the test program, using, compared with the basic method, two extreme curing conditions.

Series SA08-13, including six specimens, was cast with concrete of the proportions of mix A. During the first two days, all six specimens were kept moist within their forms. After removing the forms, three specimens were stored in the fog room with a relative humidity of 100 percent, and three specimens were stored in the climate-controlled room at a relative humidity of 50 percent.

In addition to this series, another series of six specimens (SA08-12) was cast with the same concrete proportions as series SA08-13. However, the specimens were cured in the usual manner described above. At an age of eight days, the specimens of both series were tested.

The results are plotted in the form of bond-slip relationships in Fig. 6.8. The normally cured specimens and those stored in the fog room (moist cured) yielded similar results. However, the specimens stored at a relative humidity of 50 percent (dry cured) developed a significantly higher bond strength although the strength of the dry cured concrete was only insignificantly larger than that of the normal and moist cured specimens.

In order to confirm this variation of bond strength with curing conditions, two other series of tests were carried out: one with 7/16-in. strand (SB18-4) and one with the center wire of this strand (WB18-2). Both series were cast from the same batch of concrete,

which was proportioned according to mix B. Each series included six specimens. Three specimens were dry cured, and three specimens were moist cured. The curing conditions were identical to those of series SA08-13. However, instead of testing the specimens at an age of eight days, the tests were performed after 18 days in order to extend the influence of the two different methods of curing.

The deformations of the concrete caused by shrinkage and swelling were measured from the time the forms were removed until the day of testing. The deformation was measured with an 8-in. Berry gage along four lines located on two opposite faces of the concrete prism (Fig. 6.9). The average results, obtained from six specimens for each type of curing, indicate that the moist cured specimens developed a swelling strain of approximately 5×10^{-5} (of the same magnitude as the reliability of the measurements), and the dry cured specimens a shrinkage strain of roughly 26×10^{-5}. Both changes in strain relate to the state of the concrete two days after casting.

The bond-slip relationships of series WB18-2 and SB18-4 (Fig. 6.10) demonstrate that dry curing of the concrete resulted in significantly higher bond strengths than moist curing, especially at small slips. With increasing slip, the difference between the bond forces developed by dry cured and moist cured specimens decreased. At a slip of 0.15 in., the influence of the different curing conditions on the bond strength of both plain wire and strand was too small to be measurable.

Since the compressive strength of the concrete, determined with cylinders subjected to the same curing conditions as the test

specimens, was identical for both types of curing, the consistent difference in bond strength may only be explained by shrinkage. It should be noted that the swelling measured in the moist cured specimens does not indicate absence of stresses due to early shrinkage in the first two days.

6.5 Effect of Age of Concrete on Bond of Plain Wire and Strand

It was not intended to investigate in this program the influence of the concrete age on bond on a broad scale. In order to perform such an investigation properly, a large number of specimens, cast preferably from one batch of concrete, would be necessary. Sets of tests would have to be conducted in certain intervals of weeks, months and years. Taking into account different storage conditions, this investigation would be a program in itself. Nevertheless, the tests carried out in the executed program at different ages of the concrete provided some valuable data concerning the effect of age on bond.

The age of the concrete at which tests were usually performed was eight or nine days. The preparation and test procedure for specimens being subjected to lateral pressure required a longer period of time to conduct one test series. Therefore, the age at which those specimens were tested varied from 15 to 24 days. One series was tested at an age of 66 days.

Bond-slip relationships of specimens with plain center wire of 7/16-in. strand tested at different ages are compared in Fig. 6.11. The curing conditions and the mix proportions of the specimens compared with one another were identical. The initial bond stress of specimens

4. TESTS WITH PLAIN WIRE

Seven-wire strand is manufactured by twisting six plain wires helically around a straight center wire. Although strand consists only of plain wires, the arrangement of the exterior wires results in an overall surface geometry which increases bond beyond the value depending on the surface characteristics of the individual wires. To develop a basic understanding of the bond characteristics of strand, it was necessary to study bond related to the surface characteristics of the plain wires separately. This could be achieved by conducting pull-out tests with plain wire having the same surface characteristics as the exterior wires of the strand. Because the exterior wires of the strand could not be straightened without modifying their surface, the straight center wires of the strand were used for this purpose. The surface characteristics of the center wire might differ a little from that of the exterior wires because of the manufacturing process of the strand and the protected position of the center wire against physical and chemical wear. However, the effect of this difference on bond was assumed to be small.

Three pull-out test series (WA08-1, WB08-1, WC08-1) were conducted using the center wires of 1/4-in., 3/8-in., 7/16-in., and 1/2-in. strand. For each series of twelve specimens, a different concrete mix was used. The compressive strength of the concrete at the time of testing was approximately 2200, 5000, and 8300 psi.

The bond stress-slip relationships (Fig. 4.1) were typical for plain wire, although plotting the slip to a logarithmic scale may

obscure this fact. An example of a bond stress-slip curve, with the slip plotted to a linear scale, is shown in Fig. B.1. Initially, the bond stress increased at a slip too small to be measurable. At a slip of approximately 0.0001 in., the maximum bond stress was reached. This point in the bond stress-slip curve was clearly marked by a sudden drop of the load with an attendant increase of slip. The bond stress kept decreasing until it approached a nearly constant value at a slip of approximately 0.1 in.

The average bond-slip curves, shown in Fig. 4.1, indicate that at higher concrete strengths the bond stress increased with the wire size. This trend was very pronounced in test series WB08-1 with a concrete strength of 8300 psi. Considering the relatively great scatter that is typical for bond tests, especially with short embedment lengths, and the fact that the individual results of tests with different wire sizes overlapped one another by a large margin, it is not expedient to draw definite conclusions. There was neither a statistical nor a theoretical basis to confirm the above observation.

The maximum bond stress for the individual tests (Fig. B.46, B.47, and B.48) ranged from 235 to 425 psi. The lower values were obtained with low-strength concrete, the higher values with high-strength concrete. In order to determine the influence of the concrete strength on bond, the bond stresses of all four wire sizes were averaged. In this manner, one bond stress-slip relationship was obtained for each test series (Fig. 4.2). The results demonstrate that the concrete strength had an increasing effect on the bond stress throughout the

entire range of slip. The influence, however, was very small. Although the concrete strength varied from 2000 to 8000 psi, the bond stress increased by only 10 percent at a slip of 0.0001 in. and by approximately 50 percent at a slip of 0.15 in.

In contrast to the foregoing observations, Rehm (1961) found that the bond stress of plain round bars varied approximately proportionally with the concrete strength, at least within the range of 1000 psi to 5200 psi. Rehm tested plain round steel bars with diameters of 16 mm (5/8 in.) using pull-out tests with a bonded length equal to the diameter of the bar. It should be mentioned, however, that the bars, tested by Rehm, had a rougher surface than the center wires of strand. The surface was classified as "partly scarred mill scale."

Another three test series with plain wire (WAP15-1, WAP17-2, WBP66-1) were performed in connection with the phase of the test program to investigate the influence of lateral pressure on bond. Specimens with center wires of 7/16-in. strand and concrete strengths of approximately 6000 psi and 8200 psi were tested. The relationships found for these tests were very similar to those in the tests described above (Fig. 4.3).

Test series WBP66-1 produced extremely high bond stresses compared with the results of series WB08-1 (Fig. 4.1). The difference may be attributed to shrinkage. Although the concrete mix and the concrete strength were practically identical in both series, the age of the concrete at which the tests were carried out differed by almost two months. The shrinkage deformations of the concrete, developed during this period of

time, induced additional lateral stresses acting normal to the surface of the wire. As a consequence of the higher normal stresses, the bond stresses of test series WBP66-1 exceeded those of series WB08-1.

Summarizing the test results obtained with the center wires of strand, it may be concluded that the concrete strength had a well defined but small effect on the bond strength of plain wire. The bond strength increased with the age of the concrete, which is mainly attributable to shrinkage. The maximum bond stress was developed at a slip of approximately 0.0001 in. For an 8- to 17-day old concrete, the average maximum bond stresses varied from 300 to 330 psi depending on the concrete strength. At a slip of 0.1 in., the range of the average bond stresses was as low as 80 to 160 psi.

The above bond values compare very well to results obtained by Keuning (1962) who used pull-out tests to study the bond characteristics of 0.192-in. round prestressing wire. In Keuning's tests, the bonded length was three in. The age of the concrete was nine days, the concrete strength was approximately 4700 psi, and the maximum bond stress was 330 psi. At a slip of 0.1 in., Keuning's tests indicated an average bond stress of 110 psi.

5. EFFECT OF STRAND SIZE

The most commonly used type of strand in prestressed concrete is seven-wire (round-wire) strand. With the exception of extremely small diameters which are used in model structures, the diameter of seven-wire strand ranges from approximately 0.25 in. to 0.6 in. In order to limit the number of tests, it was necessary to study the effect of different variables on bond experimentally with only one strand size. To project those results to other sizes required an investigation of the influence of the strand size on bond.

The investigation described in this report included four different strand sizes with nominal diameters of 1/4, 3/8, 7/16, and 1/2 in. Three different concrete strengths were used ranging from 2300 psi to 7600 psi. A total of 33 tests was performed with 1/4-in., 3/8 in., and 1/2-in. strand, and 54 tests were carried out with 7/16-in. strand (see Table B.1 and B.2) to investigate the effect of the strand size on bond.

Average unit bond force-slip relationships for different strand sizes, as obtained with a concrete strength of approximately 5400 psi, are plotted in Fig. 5.1. With exception of the 3/8-in. strand, the relationships show a similar trend for the various strand sizes. The bond force increased initially without measurable slip. After having reached a certain value (initial bond force), the strand started slipping. The bond strength beyond the initial bond force continued to increase at a small but steady rate.

The 3/8-in. strand displayed a different bond-slip characteristic. The steady increase of the bond strength was interrupted by a sudden decrease of the bond force at a slip of roughly 0.001 in. The rate at which the bond force increased at slips larger than approximately 0.01 in. exceeded that of the other strand sizes.

The unit bond force of the strand increased with the diameter. To determine how much the bond strength was affected by the strand size, the nominal bond stress (i.e. the pull-out force divided by the theoretical surface area) was plotted for each strand size and for each concrete strength in Fig. 5.2. To express bond in terms of bond stress was justified by the facts that the twist angles of the different strands (i.e. the angle formed by the axes of the exterior wires with the longitudinal axis of the strand) were approximately identical and that the torsional stiffness of strand had little influence on the bond strength (see Section 3.3). The latter fact was confirmed indirectly in Fig. 5.2. Although 1/2-in. strand is stiffer with respect to torsion than 1/4-in. strand, the bond stress of both strands increased with slip at approximately the same rate.

The relationships in Fig. 5.2 suggest a slight trend of the nominal bond stress to decrease with increasing strand diameter. A study of all the test data, however, indicated that this trend was statistically not significant. In Fig. 5.3 through 5.5 the mean, the confidence intervals of the mean, and the mean including two standard deviations were plotted versus the strand size for concrete mixes A, B, and C. The confidence intervals indicate the range within which

the average bond stress lies with a probability of 95 percent. The limits determined by two standard deviations enclose ostensibly 95 percent of all test data.

The bands representing the scatter of individual test results for each strand size in Fig. 5.3 through 5.5 overlap one another by such a margin, both for a slip of 0.0001 in. and 0.1 in., that the trend indicated in Fig. 5.2 appears doubtful, or at least not significant. It should be noticed that the confidence interval was relatively small for 7/16-in. strand in Fig. 5.3 because 35 test results were available for this strand size. Only 12 test results could be used for the other strand sizes.

The variation of the nominal bond stress with the strand diameter for each of the three concrete strengths of mix A, B, and C is presented in Fig. 5.6. The variation is shown in terms of confidence intervals of the mean (probability = 95 percent) and in terms of the mean plus two standard deviations. Figure 5.6 illustrates the variation of the nominal bond stress with the concrete strength.

In Fig. 5.7 the average bond forces at different slips (0.0001 in., 0.01 in., 0.1 in.) are plotted versus the strand diameter. Provided that the same bond characteristics pertain to all strand sizes, straight line relationships, starting at the origin of the graph, should be obtained. For practical purposes and within the range of strand sizes tested, the bond force of strand may be assumed to vary approximately linearly with the strand diameter.

6. EFFECT OF CONCRETE PROPERTIES ON BOND OF PLAIN WIRE AND STRAND

6.1 Introductory Remarks

To compare the influence of different concrete properties on bond is extremely difficult, because varying one property of the concrete inevitably results in the change of other properties. By changing, for example, the strength of the concrete, which may be achieved by varying either the mix proportions or the age of the concrete, the characteristics of settlement of the fresh concrete may be altered in one case, the conditions of shrinkage in the other. It is therefore not possible to separate the influence of individual properties to such a degree as to render absolutely reliable relationships between bond strength and individual concrete properties. It is possible, however, by careful selection and control of the concrete mixes, to determine the trend and the significance of the effects different concrete properties exert on bond.

In the following, effects of concrete properties, such as strength, consistency, curing conditions and age on bond of plain wire and strand are described.

6.2 Effect of Concrete Strength on Bond of Plain Wire and Strand

Three different mix proportions for the concrete were used (Section A.2.3) to study the influence of concrete strength on bond. The mix proportions were chosen so that the ratio of the volume of cement plus sand to the volume of gravel, and the consistency of the fresh concrete, as measured by the slump, remained constant for all

three mixes. Necessarily, the amount of cement and the water/cement ratio were different. The properties of the mixes (A, B, C) and the resulting strength characteristics of the concrete are listed in Table A.1. The age of the concrete at the time the tests were performed was eight or nine days. The average compressive strength was approximately 5400 psi, 7500 psi, and 2400 psi. The relation between the compressive strength and the splitting strength of the concrete is shown in Fig. A.2.

Three series of tests with center wires of four different strand sizes (1/4, 3/8, 7/16, and 1/2 in.) were performed to investigate the variation of the bond strength of plain wire with the concrete strength. The average bond-slip relations of these tests are presented in Fig. 4.1. Each curve represents the average of three tests. Since no significant influence of the wire diameter on the bond strength could be found, the bond stresses of all four wire sizes were averaged and plotted in Fig. 4.2. The concrete strength appeared to have a small but definite effect on the bond strength throughout the whole range of slip.

In Fig. 6.1, the bond strength, obtained with different concrete strengths, was expressed in percent of the bond stress developed at a concrete strength of approximately 5000 psi. Each symbol in this graph represents an average of three test results. Taking the mean value of those results, regardless of the wire diameter and the slip at which the results were obtained, it appears that the bond strength increased by roughly four percent for every 1000-psi

increase of concrete strength. Taking into consideration the introductory remarks of this chapter, and the fact that the above result was derived from only twelve tests per concrete strength, the quantitative conclusion is debatable. It shows clearly, however, that the concrete strength has but little influence on the bond strength of plain wire.

A larger number of tests was performed with strand to study the influence of concrete strength on bond. Including all four strand sizes, 36 tests were carried out with a concrete strength of roughly 2400 psi, 71 tests with a concrete strength of 5500 psi, and 47 tests with a concrete strength of 7500 psi. The data from the following series were used to evaluate the effect of concrete strength: series SA09-1 through SA08-14, with the exception of series SA23-8 and SA08-13 (Table B.1), series SB09-1 through SB08-3, and series SC09-1 through SC08-4 (Table B.2).

Figures 6.2 through 6.5 present the average bond-slip relationships of the four strand sizes at various concrete strengths. The trend of the bond strength to increase significantly with the concrete strength was common to all four strand sizes. In order to compare the relative increase of the bond strength of all four strand sizes, the bond strength measured at various concrete strengths was expressed in percent of that bond strength that was found at a concrete strength of approximately 5500 psi (Fig. 6.6). Despite the differences in strand size and slip, the results compare surprisingly well. According to this figure, the unit bond force increased, on the average, at a rate of eight percent per 1000 psi of concrete strength for a slip of

0.0001 in., and at a rate of eleven percent per 1000 psi of concrete strength for a slip of 0.1 in. These numbers are higher than that observed for plain wire. It should be noted, however, that the larger number of tests with strand (154) compared with that for plain wire (36) resulted in more reliable mean values.

Another illustration of the apparent effect of the concrete strength on bond of strand, showing the variation of individual test results, is presented in Fig. 5.6.

6.3 Effect of Concrete Consistency on Bond of Strand

The consistency of the concrete may be measured by the slump the fresh concrete exhibits in a specified test (ASTM C143-66). In order to find the effect of the consistency of concrete on bond, various concrete mixes were designed such that both the strength characteristics and the water/cement ratio remained constant while the consistency was varied. This was achieved by varying the ratio of fine aggregates (cement plus sand) to coarse aggregates (gravel). Two comparable sets of test series were conducted, each set containing three series (SA09-6, SD09-1, SE09-1, and SA09-7, SD09-2, SE09-2). The properties of the concrete mixes used (A, D, E) are listed in Table A.1. The slump values developed by the three concrete mixes were approximately 0.4, 1.5, and 7.0 in. The average strengths of the concrete at the age of nine days were within a range of 800 psi. Since the concrete properties and the curing conditions were comparable the results of both sets of test series were averaged.

Each bond-slip relationship in Fig. 6.7 represents an average of eight or ten identical tests. A comparison of the three bond-slip curves indicates that the bond strength of strand is affected by the consistency of the concrete. Despite the comparatively low strength of the concrete mix yielding the largest slump, specimens with this concrete developed the highest bond strength. This result confirms that the strength of concrete by itself is neither sufficient nor reliable as a sole basis for the prediction of bond strength with respect to concrete properties.

The favorable bond characteristics developed by the high-slump concrete may be attributed to shrinkage. Although the water/cement ratio was identical for all three concrete mixes, the high-slump concrete required more water and cement to reach a comparable strength at a low consistency. Consequently, this mix was bound to develop more shrinkage than the other two mixes. The resulting difference in contact pressures between the concrete and the strand, caused by shrinkage deformations, led to an increase in bond strength.

6.4 Effect of Curing Conditions on Bond of Plain Wire and Strand

The basic method of curing the pull-out specimens that was used throughout the whole test program is described in Section A.4. The specimens were kept moist in their forms for two days. Then, the forms were struck, and the specimens were moved to the fog room with a relative humidity of 100 percent. After being in the fog room for four days, the specimens were stored in a climate-controlled room with a temperature of approximately 73°F and a relative humidity of 50

percent. In order to probe how sensitive bond strength was to different curing conditions, a pilot series of tests was conducted early in the test program, using, compared with the basic method, two extreme curing conditions.

Series SA08-13, including six specimens, was cast with concrete of the proportions of mix A. During the first two days, all six specimens were kept moist within their forms. After removing the forms, three specimens were stored in the fog room with a relative humidity of 100 percent, and three specimens were stored in the climate-controlled room at a relative humidity of 50 percent.

In addition to this series, another series of six specimens (SA08-12) was cast with the same concrete proportions as series SA08-13. However, the specimens were cured in the usual manner described above. At an age of eight days, the specimens of both series were tested.

The results are plotted in the form of bond-slip relationships in Fig. 6.8. The normally cured specimens and those stored in the fog room (moist cured) yielded similar results. However, the specimens stored at a relative humidity of 50 percent (dry cured) developed a significantly higher bond strength although the strength of the dry cured concrete was only insignificantly larger than that of the normal and moist cured specimens.

In order to confirm this variation of bond strength with curing conditions, two other series of tests were carried out: one with 7/16-in. strand (SB18-4) and one with the center wire of this strand (WB18-2). Both series were cast from the same batch of concrete,

which was proportioned according to mix B. Each series included six specimens. Three specimens were dry cured, and three specimens were moist cured. The curing conditions were identical to those of series SA08-13. However, instead of testing the specimens at an age of eight days, the tests were performed after 18 days in order to extend the influence of the two different methods of curing.

The deformations of the concrete caused by shrinkage and swelling were measured from the time the forms were removed until the day of testing. The deformation was measured with an 8-in. Berry gage along four lines located on two opposite faces of the concrete prism (Fig. 6.9). The average results, obtained from six specimens for each type of curing, indicate that the moist cured specimens developed a swelling strain of approximately 5×10^{-5} (of the same magnitude as the reliability of the measurements); and the dry cured specimens a shrinkage strain of roughly 26×10^{-5}. Both changes in strain relate to the state of the concrete two days after casting.

The bond-slip relationships of series WB18-2 and SB18-4 (Fig. 6.10) demonstrate that dry curing of the concrete resulted in significantly higher bond strengths than moist curing, especially at small slips. With increasing slip, the difference between the bond forces developed by dry cured and moist cured specimens decreased. At a slip of 0.15 in., the influence of the different curing conditions on the bond strength of both plain wire and strand was too small to be measurable.

Since the compressive strength of the concrete, determined with cylinders subjected to the same curing conditions as the test

specimens, was identical for both types of curing, the consistent difference in bond strength may only be explained by shrinkage. It should be noted that the swelling measured in the moist cured specimens does not indicate absence of stresses due to early shrinkage in the first two days.

6.5 Effect of Age of Concrete on Bond of Plain Wire and Strand

It was not intended to investigate in this program the influence of the concrete age on bond on a broad scale. In order to perform such an investigation properly, a large number of specimens, cast preferably from one batch of concrete, would be necessary. Sets of tests would have to be conducted in certain intervals of weeks, months and years. Taking into account different storage conditions, this investigation would be a program in itself. Nevertheless, the tests carried out in the executed program at different ages of the concrete provided some valuable data concerning the effect of age on bond.

The age of the concrete at which tests were usually performed was eight or nine days. The preparation and test procedure for specimens being subjected to lateral pressure required a longer period of time to conduct one test series. Therefore, the age at which those specimens were tested varied from 15 to 24 days. One series was tested at an age of 66 days.

Bond-slip relationships of specimens with plain center wire of 7/16-in. strand tested at different ages are compared in Fig. 6.11. The curing conditions and the mix proportions of the specimens compared with one another were identical. The initial bond stress of specimens

cast with mix A and tested at ages of 8 and 16 days were almost identical. With increasing slip the 8-day old concrete, although having a lower compressive strength, provided better bond resistance. The 66-day old specimens cast with concrete of mix B developed initial bond stresses almost 30 percent higher than comparable 8-day old specimens. It should be pointed out, however, that the average results were based on only three individual tests.

More test results were available for 7/16-in. strand. Average bond-slip relationships obtained at an age of 8-9, 15, and 22-23 days are shown in Fig. 6.12. The averages were formed from the tests of series SA09-1 through SA08-14, listed in Table B.1 (with the exception of SA08-13), and the series SAP15-1, SAP22-2, SAP23-3 (Table B.3). Although the statistical weight of the test groups varied significantly because of the different number of tests available, a consistent influence of the concrete age on the bond strength may be observed from those results.

The tendency of the bond strength to increase with the age of the concrete was confirmed by the test results of series SAL12-1 which was conducted to study the influence of sustained loading on bond (Fig. 6.13). As part of this investigation, three specimens were tested at an age of 12 days, and three specimens, cast with the same batch of concrete, at an age of 129 days. The concrete strength increased during this time period by approximately 1100 psi. According to the results, described in Section 6.2 this would call for an approximately eight-percent increase of the initial bond strength.

The initial bond strength of the 129-day old specimens increased however by as much as 55 percent. At a slip of 0.01 in., this difference was reduced to 12 percent, and at a slip of 0.1 in. to approximately 3 percent.

Similar test data were obtained from series SAL11-2 and SBL12-1. Three specimens of each series were tested at ages of 11 (SAL11-2) and 12 (SBL12-1) days. Three specimens, cast from the original batch, were tested at ages of 451 (SAL11-2) and 446 (SBL12-1) days. The average bond-slip relationships are shown in Fig. 6.14.

In contrast to the results of series SAL12-1, the initial bond strength of the specimens of series SAL11-2 and SBL12-1 did not increase after the period of approximately 15 months. The average bond strength at large slips, however, was found to have increased by approximately 65 and 30 percent. The increase of the concrete strength during that period was practically negligible.

The test results represented in Fig. 6.12 through 6.14 summarized in Fig. 6.15 seem to indicate different trends for the bond strength versus the age of the concrete at different slips. The initial bond strength appeared to reach a peak value at a concrete age of approximately 20 to 50 days. Beyond this peak, the initial bond strength seemed to decrease gradually with increasing age of the concrete.

The bond strength at large slips appeared to increase steadily with the age of the concrete.

Because of the few test data available and the inconsistent results at large slips (Fig. 6.15), the above trends are not confirmed

reliably enough to draw definite conclusions. It appears that the variation of the bond strength with the age of the concrete is attributable primarily to a variation of contact stresses between the strand and the concrete due to lateral shrinkage of the concrete prism (see Chapters 9 and 14). The increase of the concrete strength during the time periods investigated contributed only a negligibly small amount to the increase in bond strength.

Peattie and Pope (1956), who studied the effect of the age of concrete on the bond resistance of plain bars within the first 28 days of age, came to the conclusion that shrinkage of the concrete closely adjacent to the steel was the primary reason for bond. It was found in their torque - and pull-out tests that the maximum bond capacity was reached within a period of 3 to 14 days. The fact that the maximum bond strength was developed in such a short time while shrinkage continued appreciably up to ages of one to two months, was explained by the exothermic process of hardening of the concrete. The higher temperatures developed in the interior of the specimen, immediately around the steel, accelerated the contraction of the concrete. From the tests described in this investigation, it may be concluded that a longer period of time is needed to develop the maximum bond capacity.

6.6 Concluding Remarks

On the basis of a relatively large number of tests, it has been shown that the concrete strength had relatively little influence on bond of plain wire and strand. Although the ideal condition of separating the effect of the concrete strength on bond could not be

fully achieved, test results indicated that, on the average, the bond strength of plain wire increased by approximately four percent for every 1000 psi of additional concrete strength. For strand, the increase was approximately ten percent.

The primary source of bond was found to be shrinkage. This has been confirmed by tests in which the consistency and the curing conditions of the concrete were varied, while the strength of the concrete was being kept constant. Tests used to study the effect of the age of the concrete indicated the same results. Therefore, bond strength is sensitive primarily to all variables that affect shrinkage, and only secondarily to the strength of the concrete.

7. EFFECT OF SETTLEMENT

Settlement of fresh concrete is caused mainly by a segregation of aggregates and water due to differences in their specific gravities. The solid parts of the mix tend to sink to the bottom while the water tends to rise to the top surface of the concrete. The latter process is referred to as "bleeding." An additional volume change, which is caused by hydration of the cement and which may be described as "chemical shrinkage", adds to the amount of settlement during the very early stages of hardening of the concrete.

If reinforcing bars are held rigidly by the formwork while the settlement of concrete takes place, the steel and the concrete may lose contact on that side of the reinforcement where the settlement is directed away from the steel. Furthermore, the concrete in the immediate vicinity of the steel may be of porous quality because of water and air bubbles which rise during vibration and may get trapped under the reinforcement. The reduced area and quality of contact between steel and concrete must result in a reduction in bond strength.

The amount of settlement depends on many variables, such as the cement and water content of the concrete mix, the surface characteristics of cement and aggregates, the kind and energy of vibration, the type and surface of the formwork, the width of the specimen, and, of course, on the thickness of the concrete layer that settles. It was beyond the scope of this investigation to study the

effect of all those variables with respect to bond of strand. However, two series of tests were carried out to demonstrate the magnitude of the effect of settlement on bond strength.

Series SA09-15 and SA09-16, with a total of 30 individual tests, were conducted to study the influence of the concrete depth on bond of strand. The concrete strength was 5370 psi for SA09-15 and 5150 psi for SA09-16. The slump was 1.5 in. in both series. In the form, the strand was supported in a horizontal position. The cross section vertical to the direction of pouring was constant for all specimens: 4 by 9 in. The depth of the concrete below the center of the strand was varied (2, 6, 10, 15, and 30 in.). The thickness of the concrete above the center of the strand remained two in. for all specimens. The forms were made of oil-treated plywood.

The compaction of the concrete was accomplished with an internal vibrator. For two types of specimens of series SA09-15 (with depths of 15 and 30 in. below the strand), the concrete was vibrated in two stages: the form was filled halfway, vibrated, filled to the top, and vibrated again. One type of specimen in series SA09-15 (with a depth of 10 in. below the strand) was not vibrated. All others were vibrated in one stage.

The average bond-slip relationships of both test series (Fig. 7.1) demonstrated the sensitivity of bond to the depth of concrete under the strand. Specimens with concrete depths of two in. below the strand developed the highest bond force throughout

the entire range of slip. With increasing depth, the bond strength decreased rapidly. However, for depths greater than ten in., the bond force appeared to approach a constant value.

The minimum concrete cover for strand in prestressed concrete ranges from 0.75 to 2 in., depending on the type of structure and the conditions of the environment. Therefore, a concrete depth of two in. under the strand may be considered as the optimum bond condition for horizontal strand. In Fig. 7.2, the average bond forces, developed with specimens of different depths at a certain slip, were expressed as percentages of the average bond force that was obtained with a depth of two in. The results are indicated separately for series SA09-15 and SA09-16. In addition, average values were plotted using the results of both test series, since the concrete properties and the test conditions were nearly identical.

With concrete depths equal to or larger than ten in., the bond strength dropped to values of 60 percent of the maximum bond strength, depending on the slip. Even at the relatively shallow depth of six in., the measured bond strength in series SA09-16 was as low as 65 percent of the bond force for a depth of two in. below the strand. The bond strength may drop even further, if the vibration of the concrete is executed carelessly or omitted completely. This is indicated by the results of series SA09-15. The bond strength developed by the specimens that were not vibrated at all was approximately 30 percent lower than if the specimens had been vibrated.

pressures are listed for each test series in Table B.3. It should be mentioned here that several specimens, which are not included in Table B.3, had to be discarded because there was either too much leakage before the desired lateral pressure could be reached, or the concrete specimen broke when a pressure exceeding 2500 psi had been applied.

8.2 Influence of Test Procedure on Results

The procedure of building the test specimens into the pressure apparatus by pounding in lead seals, as described in Section A.7, was suspected to have some influence on bond of strand or wire. Therefore, two specimens with 7/16-in. strand were built into the pressure apparatus and tested without lateral pressure. The results were compared with test data of two specimens of the same series (SA08-14) which were tested without the pressure apparatus. The bond-slip relationships of the four tests (Fig. 8.1) indicated that the lead-packing procedure had no apparent influence on bond.

8.3 Limits to the Application of Lateral Pressure

The maximum pressure applied in the tests was 2500 psi. This limit was set by the fact that the concrete prisms, which had cylinder strengths ranging from 5300 psi to 8700 psi broke at lateral pressures exceeding 2500. It was possible to apply a lateral pressure of 3000 psi in several tests and to keep this pressure constant, however, the concrete prism broke each time shortly after a small pull-out force had been applied to the strand or wire. The failure was caused by cracking of the concrete near the middle of the specimen in a plane

perpendicular to the direction of the pull-out force. Because of the high lateral pressure, the seal (shim steel) covering the concrete specimen was punched through along the crack permitting oil to leak through the concrete and wedge the prism apart. In several tests, which had been performed under a constant pressure of 1000 or 2000 psi, the pressure was increased after a slip of 0.15 in. had developed. The failure occurred in the same manner as described above at pressures ranging from 3000 to 4200 psi, unless excessive leakage ended the test.

Transverse cracking at approximately one third to nearly one half of the uniaxial compressive strength of the concrete was consistent with major longitudinal cracking observed in uniaxially loaded cylinders at roughly 70 percent of the ultimate load. Presumably, the transverse strain in the biaxially stressed prisms was twice as large as the strain developed by uniaxially loaded specimens.

The above results were confirmed by an investigation of the multiaxial strength of concrete conducted by Fumagalli (1965). It was reported that concrete prisms subjected directly to hydraulic pressure without having a seal between the concrete and the pressure fluid developed an average biaxial compressive strength of 0.36 times the uniaxial strength of concrete. The failure loads found above were a little higher than those reported by Fumagalli. Reasons for this discrepancy were the shim steel seal used in the described investigation, and possibly a small longitudinal restraint caused by the end seals between the pressure chamber and the concrete prism.

The lack of reaching pressures exceeding 2500 psi did not pose a serious impediment to the investigation. The trend of the effect of lateral pressures was indicated well enough by tests obtained with lateral pressures up to 2500 psi.

8.4 Effect of Lateral Pressure on Bond of Plain Wire

Three series of tests were conducted to investigate the influence of lateral pressure on bond of plain wire: series WAP15-1 and WAP17-2 with concrete strengths of approximately 6100 psi, and series WBP66-1 with a concrete strength of 8200 psi. The individual bond-slip relationships are shown in Fig. B.43 through B.45. Since the concrete properties and the age of the concrete of series WAP15-1 and WAP17-2 were comparable, the results of both series were averaged for demonstrating the trends observed.

The average bond stress-slip relationships, as shown in Fig. 8.2 and 8.3, indicate that the shape of the bond-slip curves for plain bars was not altered by varying the lateral pressure. The lateral pressure, however, had a significant influence on the magnitude of the bond strength. Any increase of lateral pressure raised the bond stress by an amount approximately proportional to the lateral pressure.

Figure 8.4 shows the initial bond stresses found in individual tests as functions of the applied lateral pressure. The initial bond stress corresponds to the maximum bond force measured at a slip of approximately 0.0001 in. For specimens with plain wire, this was identical to the maximum bond stress obtained in the test. The following may be gleaned from Fig. 8.4:

(a) The initial bond stress increased in direct proportion to the applied lateral pressure for both concrete strengths.

(b) The results are clearly separated for the two concrete strengths at lateral pressures of zero and 1000 psi. At a lateral pressure of 2000 psi, this separation is not as distinct because two results obtained with the lower-strength concrete turned out to be as high as the results of the higher-strength concrete. Despite those two results it appeared that the concrete properties had a measurable effect on the bond strength of plain wire. It should be noted however, that the difference was presumably not caused so much by the strength, but rather by the age of the concrete, or more precisely by the different amount of shrinkage, as pointed out in Chapter 4 and 6.

8.5 Effect of Lateral Pressure on Bond of Strand

Two preliminary test series (SAP15-1 and SAP22-2) with one or two pressure tests only, and two main series (SAP23-3 and SBP24-1) with eight pressure tests each, were carried out using 7/16-in. strand to study the influence of lateral pressure on bond. The results, plotted in the form of unit bond force-slip relationships, are shown in Fig. 8.5 through 8.7.

Common to all four test series was the significant increase of the maximum bond force with increasing lateral pressure. The maximum bond strength for externally applied lateral pressures equal to or exceeding 1000 psi seemed to be reached at slip values ranging from 0.0003 to 0.0007 in. In contrast to the bond strength developed by

tests without lateral pressure, which tended to increase with increasing slip, the bond strength of specimens subjected to lateral pressures dropped immediately after reaching the maximum bond force. The drop became larger the higher the applied lateral pressure was.

In Fig. 8.8, the maximum bond force of every individual test was plotted versus the lateral pressure. It appears from the plotted data that:

(a) the maximum bond strength of strand was linearly proportional to the externally applied lateral pressure, and

(b) the concrete strength appeared to have no significant influence on the maximum bond strength of strand within the test range of roughly 5000 to 9000 psi. The conditions of shrinkage were approximately the same for all test specimens.

8.6 Effect of Increasing Lateral Pressure on Bond of Plain Wire and Strand at Slips Larger than 0.15 in.

The pull-out tests reported so far were performed under a constant lateral pressure and were usually discontinued when the strand or wire had slipped by an amount of 0.15 in. A variation of the test procedure was used in some of the tests. At a slip of 0.15 in., the test was continued by raising the lateral pressure, which had been constant until then, by 500 psi. After keeping the pressure constant at the new level for approximately 30 seconds, the pressure was raised by another 500 psi. This step-by-step increase of lateral pressure was continued until either the concrete prism broke or the leakage of oil became excessive.

To illustrate the test procedure, two typical force-time relationships, as recorded by the plotter of the testing machine, are shown in Fig. 8.9 for plain center wire and for strand. Neither of the two relations are plotted to scale. The testing machine was operated in such a manner that the moving head of the machine travelled at a constant speed of 0.05 in./min. throughout the whole test.

Initially, the load increased without measurable slip until reaching point A. This point represents the initial bond force. The rate at which the pull-out force increased was relatively low at the beginning of the test. This indicated the tightening of the end anchorage and the joints of the test setup. At point A, the load dropped suddenly to a value far below the initial bond force. From this point on, the force decreased gradually for plain wire until it reached point B. In tests with strand, the force increased steadily after the abrupt drop at A. In the range between points A and B, the force and the slip ceased being smooth functions of the time. The slip of the strand or wire in this region may be described most fittingly as stick-slip motion, a term which is understood without further explanation by looking at the alternating build-up and drop of the bond force indicated in Fig. 8.9.

At point B, a slip of 0.15 in. was developed. Instead of ending the test at B, the lateral pressure was raised by 500 psi (e.g. from 1000 psi to 1500 psi in Fig. 8.9). The bond force responded immediately to the applied pressure and increased to P_2. After reaching the new maximum, P_2, the bond force dropped a little, and a stick-slip

type of motion started again. Another increase of the lateral pressure by 500 psi raised the bond force to P_3 and so forth, until at point C the test was terminated by leakage, or failure of the concrete prism. It was a characteristic feature of the tests that, for plain wire, the bond force in the stick-slip region tended to decrease at all levels of lateral pressure, while it tended to increase for strand.

Untrauer and Henry (1965) investigated the influence of normal pressure (ranging from 0 to 2370 psi) on bond of deformed bars. The bond strength was found to increase in proportion to the square root of the normal pressure in contrast to the linear relationship indicated by the tests reported here. However, the stress conditions in the tests and the steel specimens were not directly comparable. The test specimens used by Untrauer and Henry consisted of 6-in. concrete cubes with the deformed bar (#6 or #9) embedded in the center over the whole length of the specimen. The lateral pressure was applied to two parallel faces of the bond specimen using spherically seated bearing plates. It should be noted that this loading system was basically uniaxial as compared to the biaxial system described in this report. However, because of the frictional restraint between the concrete specimen and the loading plates, the state of normal pressure was probably not uniaxial.

9. EFFECT OF TIME

9.1 Introductory Remarks

The standard pull-out tests were performed within a short period of time (approximately 5 to 10 minutes) while the concrete was still relatively young (8 to 24 days). In order to study the influence of time, three series of tests were made to investigate two effects:

(1) the age of the concrete at the time of the test

(2) sustained loading

Both effects were studied using 7/16-in. strand. The effect of the age of the concrete was discussed in Section 6.5. The effect of sustained loading will be discussed in the following section.

9.2 Effect of Sustained Load on Bond

The basic pull-out specimen described in Section A.3 was used to investigate the bond properties of strand under sustained load. The test setup developed for sustained loading is shown in Fig. A.7. The pull-out specimen with a bonded length of one in. was loaded using a cantilever system. The trail-end slip of the strand versus the concrete was measured with a 0.0001-in. dial indicator. The applied load which could be varied either by changing the weight or the length of the lever arm could be determined with an accuracy of plus or minus 20 lb.

The test procedure was as follows: Three short-time pull-out tests were conducted on identical specimens. The average initial bond force (at a slip of 0.0001 in.) was determined from the data obtained. The long-time test specimens, cast from the same batch, were then loaded

to different percentages of the initial bond force determined from the first three specimens. This load was kept constant throughout the duration of the test. The slip was measured continually.

The first of the three test series, SAL12-1, was a pilot series. The tests were discontinued after a period of four months. The specimens of series SAL11-2 and SBL12-1 were observed over a period of 15 months.

Figure 6.13 shows the average unit bond force-slip relationship for the three specimens of series SAL12-1 tested at an age of 12 days to determine the "short-time" bond characteristics. The concrete cylinder strength was 6000 psi. Based on the initial bond strength of these specimens, loads ranging from 60 to 115 percent of the initial short-time load were applied to ten long-time specimens.

The slip-time relationships are plotted for all ten specimens of series SAL12-1 in Fig. 9.1. Some of the relationships indicate a "negative" slip. This was caused by the method of evaluating the slip measurements. In the pilot series SAL12-1, the slip was measured with a dial indicator mounted on top of the concrete prism, as shown in Fig. A.8. Since the dial readings included the shrinkage deformation of the upper half of the concrete specimen, the shrinkage deformation had to be subtracted from the "slip measurements." Shrinkage deformations were measured on three specimens of series SAL12-1 as indicated in Fig. 9.2. Since the order of magnitude of the time-dependent slip was comparable with the scatter of the shrinkage deformations, this procedure led to "negative slips" in some cases.

For the two test series, SAL11-2 and SBL12-1, another test setup was used to eliminate the effect of shrinkage deformations

on slip measurements. The dial indicator was clamped with a frame to the concrete in the middle of the specimen (Fig. A.7). Thus, the dial recorded the slip of the strand, bonded only in the center of the specimen, versus the concrete at the same level.

The data in Fig. 9.1 indicate that specimens loaded to approximately 100 percent of their initial bond strength did not slip significantly within the time period of observation. The two specimens loaded to 110 and 115 percent of the initial bond strength developed a significant slip with time. The specimen loaded to 110 percent developed a slip of 0.0008 in. after three days, 0.0015 in. after three weeks, 0.0052 in. after eight weeks, and failed completely immediately thereafter. The specimen loaded to 115 percent developed a slip of 0.003 in. after three days, 0.015 in. after three weeks, and 0.21 in. after eight weeks.

Test series SAL11-2 and SBL12-1 consisted of five specimens each. At the time the specimens were loaded, at ages of 11 and 12 days, the concrete strength was 6500 and 8700 psi, respectively. Average bond force-slip relationships obtained from three short-time tests of each series are shown in Fig. 6.14.

The slip-time relationships developed by the specimens of series SAL11-2 and SBL12-1 are presented in Fig. 9.3 and 9.4. The slip was plotted to a logarithmic scale in order to be able to show the total slip of all specimens. One test of series SBL12-1 with a load of 105 percent of the initial bond strength was discontinued after a period of ten weeks when the test setup was disturbed.

The logarithmic plots may give a false impression of the actual slip-time relations, especially in series SBL12-1. To get a better perspective, the slip of the three specimens of series SAL11-2 and SBL12-1 that did not slip immediately after the application of the load by a large amount is plotted to a linear scale in Fig. 9.5 and 9.6.

The two figures (9.5 and 9.6) indicate that up to one half year no significant slip (less than 0.001 in.) developed. This "slip" most likely reflected inelastic deformations due to creep and shrinkage of the annular console of concrete which embraces the bonded length of the strand (Fig. A.8).

The following observations may be made concerning the three series of sustained load tests:

(1) The initial bond strength is sensitive to time (Fig. 9.6).

(2) The initial bond strength may reduce with time to 80 or 70 percent of its initial value. In view of the fact that three specimens of series SAL11-2 did not slip over the whole period of observation lasting 15 months although they were loaded from 80 to 90 percent of the initial bond strength, the assumed reduction may be considered as conservative. It should be noted, however, that the sensitivity of the initial bond strength to time depends on the type of concrete.

(3) The reduction of the initial bond strength may occur a considerable time after the application of the sustained load. In case of series SBL12-1, the reduction took place after a period of approximately one half year.

(4) The concrete immediately surrounding the bonded length of strand in the specimens of series SBL12-1 was cracked to a larger extent than the concrete in the specimens of series SAL11-2. This is shown with two typical photographs in Fig. 9.7 and 9.8. The cracks were made visible by treating the concrete surface with a fluid containing luminescent particles and illuminating it with ultraviolet light.

(5) Specimens which slipped immediately after the application of the load seemed to reach a state of equilibrium at a slip of approximately 0.1 in.

The phenomena observed above may be understood by considering the stress conditions existing in a cross section through the pull-out specimen. The concrete of the specimen will shrink with time. As a result, radial compressive stresses will develop at the contact between the concrete and the comparatively rigid strand. At the same time, circumferential tensile stresses will develop in the concrete. A theoretical distribution of such circumferential stresses based on an elastic solution (see Appendix C.3) is shown in Fig. 9.9.

It was shown in Chapter 8 that the initial bond strength depends on the contact pressure between the strand and the concrete. Consequently, it must be assumed that the initial bond strength will increase as shrinkage progresses with time unless the circumferential stresses in the concrete in the immediate vicinity of the strand exceed the tensile strength of the concrete. In that case, radial cracks will develop and cause the normal contact stress between strand and concrete to decrease. The resulting bond strength will be less than during the uncracked stage.

The above considerations lead to the conclusion that shrinkage has a beneficial influence on the initial bond strength as long as it does not exceed the tensile strength of the concrete. If cracks develop, the majority of the favorable influence of shrinkage on bond will be lost.

In the light of the foregoing explanation, the difference in the test results of series SAL11-2 and SBL12-1 may be understood. The tensile strength of the concrete was almost identical for both series (Table B.2), however the shrinkage strains differed by 20 to 25 percent (Fig. 9.10 and 9.11). It is therefore plausible that shrinkage stresses exceeded the tensile strength in series SBL12-1 (after a period of one halfyear) and led to severe cracking but did not exceed the tensile strength in series SAL11-2.

Theoretically, it is very difficult to predict the time at which severe radial cracking will take place. Even if the shrinkage-time relation is known for the concrete near the surface of the specimen (Fig. 9.10 and 9.11), the rate and amount of shrinkage near the center of the specimen will be uncertain. Furthermore, the prediction of the stress build-up at the contact between strand and concrete due to shrinkage is complicated by the fact that the stresses are continually reduced by creep.

Observation (5) above seems to indicate that the bond strength is less sensitive to time at large slips (approximately 0.1 in.). Apparently, the rate at which the bond-slip relationship increases at large slips (Fig. 5.1) will suffice to prevent further movement.

10. EFFECT OF SHAPE OF STRAND

10.1 Introductory Remarks

As strand moves axially with respect to the concrete in which it is embedded, it rotates about its own axis. If the concrete specimen and the point where the strand is gripped are restrained from rotation, a torque is generated in the strand as it slips. The relation between the rotation of the strand in the concrete and the axial slip can be determined theoretically if the concrete is assumed to provide a completely rigid channel. The angle θ through which the strand rotates may be expressed as

$$\theta = \frac{360\ s}{p} \quad \text{(degrees)} \qquad (10.1)$$

where s = axial slip and p = pitch of the strand in in. The amount of rotation is a typical property of the size, or more accurately, the pitch of the strand.

The rotation-slip relationships of four different strand sizes were measured in over 200 tests as described in Section A.6. The average rotation for each strand size was plotted versus the axial slip in Fig. 10.1. The measured data agree with the theoretical values.

The magnitude of the torsional moment that is generated in strand under the conditions mentioned above depends on the stiffness of the cross section and the pitch of the strand. The results of test series SA08-5 (described in Section 3.3) indicated that this torsional

moment has very little influence on the bond strength of strand as measured in the pull-out tests. Despite the apparent insensitivity of bond to the torsional stiffness of strand, it was desirable for a better understanding of bond to study the effect of the torsional stiffness and the shape of the strand in more detail. For this purpose, tests with twisted square steel bars and straight (nontwisted) strand were performed.

10.2 Tests With Twisted Square Steel Bars

Seven-wire strand is usually manufactured with a standard pitch for each strand size. Because it was desired to vary the pitch, strand was not suitable for this investigation. Instead, cold rolled solid square steel bars were chosen which were twisted on a lathe by different amounts as described in Section A.2.4. The bar cross section was 5/16 in. square. The amount of twist was expressed in terms of the angle α which was formed by the helical edges of the twisted bar and its axis. Pull-out tests were conducted in the same manner as with strand. The bonded length was one in.

Series QB09-1 consisted of 17 pull-out tests: three concrete specimens contained untwisted bars, three contained bars with twist angles of 8 to 14 degrees, three specimens contained bars with twist angles of 27 to 29 degrees, and the rest contained bars with angles of 36 to 46 degrees. The twist angles differed within each group because it was not possible to control the amount of twist on the lathe exactly. Furthermore, the angle of twist varied slightly along the length of a given bar for reasons stated in Section A.2.4. Although the bars were

bonded over a length of one in. only, this nonuniformity was reflected in the scatter of the individual test results (Fig. B.50 through B.51).

The average bond-slip relationships of series QB09-1 are plotted in Fig. 10.2 and 10.3. It was necessary to show the results in two graphs, with the slip plotted both to a linear and a logarithmic scale, in order to emphasize the differences at very small slips as well as at large slips. The graphs contain two major groups of tests:

(a) The concrete specimens were allowed to rotate during the test ($\alpha = 0^{o}$, 11^{o}, 28^{o}, 38^{o}, 44^{o}). The average results are represented by solid lines.

(b) The concrete specimens were restrained from rotating ($\alpha = 37^{o}$, 46^{o}). The results are shown with broken lines.

Within group (a), the initial bond force increased only slightly with the twist angle. The maximum bond force, however, was influenced significantly by the twist angle. After the peak force was reached at slips smaller than 0.007 in., the load dropped suddenly and approached a nearly constant bond force which was 30 to 70 percent lower than the maximum bond force.

Group (b) consisted of only three specimens ($\alpha = 37^{o}$, 37.5^{o}, 46^{o}) which displayed completely different bond-slip characteristics (Fig. 10.3). The initial bond forces at a slip of 0.0001 in. were still of nearly the same magnitude as that of the test specimens with comparable twist angles of the first group. However, while the bond forces of the freely rotating specimens dropped off at slips smaller than 0.007 in., the bond force of the rigidly held specimens kept rising with increasing

slip. The maximum bond force developed by the restrained specimens was several times greater than the bond force of identical but freely rotating specimens. This demonstrates effectively the influence of the torsional stiffness on bond. Twisting of the bars, in the torsionally restrained case, led to increased contact pressures between the steel and the concrete which, in turn, improved the bond strength. In the unrestrained case, any build-up of horizontal restraints was prevented by the freely rotating concrete specimen. Therefore, the torsional stiffness of the bars did not affect the bond strength.

The maximum bond force of the torsionally restrained specimens was approximately 3500 lb. Immediately after reaching the peak force, the load dropped. The bars stopped twisting and were ripped out of the concrete like deformed bars. This is demonstrated by the twist-slip relationships plotted in Fig. 10.4. Exactly at the slip values at which the load started to drop, the twist-slip relations of the restrained specimens turned into horizontal lines. This indicated that the concrete embedment was not rigid enough any more to enforce a further twisting of the steel. The crushing of the concrete keys between two neighboring generators of the twisted bar resulted in a friction surface that was rough enough to cause the bond force to decrease at a relatively slow rate. The high amount of friction kept the twisted bar from instantly rotating back to its original position. A slight rotation with reversed trend is indicated however by the twist-slip relations in Fig. 10.4.

Summarizing the results of the foregoing investigation, it may be concluded that the torsional stiffness and the pitch are important

factors for the bond strength of those bars that tend to rotate when being subjected to bond forces. The pitch of the bar determines the relationship between the axial slip and the amount of rotation (Eq. 10.1). Furthermore, for a given torsional stiffness of the bar, the pitch determines the magnitude of the contact pressure, and consequently the increase in bond strength. Vice versa, the bond strength that can be developed for a constant pitch is proportional to the stiffness of the bar until either the cross section yields or the concrete is crushed under the high contact pressures.

10.3 Tests with Straight (Nontwisted) Strand

The nature of the bond-slip relation of strand differed significantly from that found for plain wire (Fig. B.1). Since the torsional stiffness of strand seemed to be too small as to affect the bond strength of strand to a greater extent (Section 3.3), the bond-slip characteristics of strand must be influenced by the cross sectional shape, or the group arrangement of the wires. In order to investigate this effect, pull-out tests with straight, nontwisted strand were performed.

The straight strand was fabricated in the laboratory by assembling several straight wires to a parallel bundle. Grouping of three or seven wires resulted in straight three- or seven-wire strand. The individual wires were cut from the untwisted center wire of twisted 7/16-in. strand. In order to keep the group of wires in touch during casting, and to assure a uniform slip of all individual wires during the test, the wire bundle was tack-welded approximately two in. below

and above the bonded length. The dimensions of the pull-out specimens were identical to the standard specimens.

Series UA09-1 consisted of three specimens with straight seven-wire strand and two specimens with straight three-wire strand. The average bond stresses of the straight three- and seven-wire strand are plotted in Fig. 10.5. The results are compared with the average bond-slip relationship found for single center wires of strand in series WA08-1. The wires tested in a group developed a higher initial bond stress than a single wire. Grouping of the wires apparently affected also the nature of the whole bond-slip relation. While the bond strength of the single wire decayed rapidly after the initial bond was exceeded, the bond stress of the straight strand decreased only slightly. Beyond a slip of approximately 0.01 to 0.03 in., the bond stress increased again.

In Fig. 10.6, the unit bond force-slip relations of the straight strands are compared with the average unit bond force-slip relation of regular 7/16-in. strand. The initial bond forces of the seven-wire strands were almost identical. The shape of the bond-slip relations was comparable throughout the whole range of slip. The unit bond force of the straight three-wire strand, of course, was less than that of the seven-wire strand because of the difference in the bonded area.

A comparison of the characteristic shapes of unit bond force-slip relationships for regular strand, straight strand, and plain wire is presented in Fig. 10.7.

11. ON THE NATURE OF BOND BETWEEN STEEL AND CONCRETE

11.1 General Concept of Bond

Bond between steel and concrete has been investigated for almost a century, yet the understanding of its nature is still incomplete. The difficulty in developing a clear concept of bond derives from the fact that the sources of bond are of a microscopic nature. Although, as practice shows, it is not absolutely necessary to understand the nature of bond in order to arrive at a satisfactory design with the aid of relevant bond tests, a thorough knowledge of the sources of bond would help reduce the amount of required testing and make it possible to predict and understand the influence of variables to which bond is most sensitive.

The following hypothesis for the nature of bond was arrived at mainly on the basis of experiments and theories which were reported, especially in the past few years, in the literature about friction (Bowden, 1964; Kraghelskii, 1965; Rabinowicz, 1965). In order to explain the mechanism of bond, two basic types of contact between two solid materials shall be discussed:

(a) When two solid materials are placed in contact, they will touch each other only at certain points, no matter how smooth the surfaces of contact may appear (Fig. 11.1a). The individual area at which actual material-to-material contact exists is commonly called the junction. The summed area of the junctions is generally very small compared with the apparent area of contact. If a force perpendicular to the plane of contact exists, and one body is moved with respect to

the other one, parallel to the plane of contact, a force is required to overcome a certain resistance to motion. This resistance is known as friction. It is determined by the shear strength in the junctions, i.e. the real areas of contact. If the friction force is exceeded, shearing may take place either through the junctions, or if one material has less shear strength than the junction itself, the material may shear close to the junction. The friction force remains approximately constant as sliding progresses because a new set of junctions is formed immediately after the destruction of an existing set.

A finite area of contact in the junctions is formed only if a lateral force presses the two materials together. Because of the small area of contact, it may be assumed that the stresses in the junctions are so high, even at extremely small lateral forces, that the material near the junctions yields. Assuming furthermore that the yield stress of the material remains approximately constant, it may be derived that the real area of contact increases in direct proportion to the lateral force. Consequently, the friction force, which depends on the actual shear area, is a linear function of the lateral force. This approach assumes that the unit shear strength of the junctions is not enhanced by the confining effect of the normal force.

(b) When a solid material, like steel, is cast into a viscous material that hardens after some time, like concrete, the contact between the two materials is, in contrast to the above condition, continuous (Fig. 11.1b). The two materials are solidly interlocked with one another. If in this case a force parallel to the plane of contact

is applied to one of the bodies while the other one is fixed, the material with the smaller shear strength shears off through a plane determined approximately by the peaks of the surface of the stronger material. Because the area of contact between the two materials is independent of the lateral force, no contact pressure is required to provide an initial resistance to sliding.

Since the conditions of contact differ from those described in case (a), the phenomenon of the initial shear failure of the interlocks should be distinguished from the phenomenon of friction. The two cases described differ basically only in the initial stage of sliding, because after the shear keys have failed in case (b), a system of two solid bodies sliding on one another is generated. The contact is established by junctions formed by the rough edges of the failure surfaces. This means that a true case of friction is obtained.

The mechanism of bond between steel and concrete may be said to consist of two principal phases: an initial interlocking phase, as described in case (b), and a frictional sliding phase, as described in case (a). The initial shear failure will take place in a plane through the tips of the steel keys because the shear strength of concrete, or rather cement paste, is lower than that of steel. Since it may be assumed that after the failure the indentations in the surface of the steel are still filled with concrete, or cement paste, the new system of contact consists mainly of concrete sliding on concrete (Fig. 11.1c) which becomes a problem of friction.

After the initial shear failure of the interlocking concrete keys, the contact surface is relatively rough. Further sliding leads

to a process of abrasion of the concrete surfaces by which loose wear particles are formed between the two solid concrete layers. The amount of abrasion increases with the distance of sliding. It may be assumed, therefore, that after some slip a thin layer of loose wear particles has formed between the sliding surfaces (Fig. 11.1d)

In the following sections the above concept will be investigated in detail and each phase of bond will be studied in relation to the results of the bond tests.

11.2 Surface Roughness of Steel

The surface of an apparently "plain" bar, produced either by rolling, drawing, or even machining, is marred by a complex of microscopic deformations. Rehm (1961) measured the indentations on the surface of various reinforcing steels with a profile meter, an apparatus that records the vertical movements of a fine needle while it is transversing the surface. The radius of the tip of the needle used was 0.001 in. Therefore, only indentations with openings larger than 0.002 in. could be recorded.

The measured surface profile of cold drawn wire showed indentations with a maximum depth of approximately 0.0008 in. (Fig. D.1). Rehm reported that numerous surface measurements indicated that the depth-to-width ratio of the indentations remained roughly constant. This ratio measured for cold drawn wire was, according to the profiles reported by Rehm, approximately 1:10 to 1:15.

11.3 Interlocking Between Steel and Concrete

After showing that the steel surface of prestressing wire is relatively rough despite its smooth appearance, it is not difficult to imagine that a firm physical interlocking takes place between the steel and the initially semiliquid, later hardening concrete.

An investigation by Martin (1967) indicated that the interlocking is of a much more complex nature than that produced merely by the physical roughness of the steel surface. Martin presented a theory, based mainly on pictures taken with an electron microscope of the contact surface between steel and cement mortar, which assumes that water together with dissolved calcium-hydroxide and other dissolved substances of the fresh cement paste penetrate the complete oxide layer of the steel. The oxide layer, which covers every steel surface after being exposed to air for a short time, is so porous and coarse in its structure that penetration is very easy. The penetration is most probably a simple diffusion. Silicon and calcium do not only move through the oxide layer but are built into the surface of the metallic iron. The movement of the dissolved components of the cement through the oxide layers leads to various types of reactions. Adsorptions along boundary surfaces, recrystallizations in intermediate layers, and epitaxies* at the pure metal result in an extremely interlocked structure between steel and cement.

---

*Epitaxy: oriented growth of one crystalline substance on a substrate of a different crystalline substance.

According to Martin, the interlocking of steel and concrete is not only of a physical but also of a strong chemical nature. Because of this intense interlocking it should be expected that a certain bond force can be applied to a plain wire embedded in concrete before measuring any slip. The typical characteristic of the measured bond-slip relationships of plain center wires of 7/16-in. strand was indeed such that the bond force increased initially without measurable slip (Fig. 11.2). After developing a bond stress in the order of 300 to 400 psi (applied lateral pressure = 0), the bond force dropped suddenly. At the same time, a large slip took place. This abrupt change in bond force suggests that the interlocking structure failed at that point and that the bond force developed from then on was a matter of sliding friction.

For the following discussion of the initial shear failure, the simple conceptual model of a physical interlocking between steel and concrete will suffice. The test results of Fig. 8.2 and 8.3 indicate that the initial bond strength (i.e., the bond strength at which shearing of the interlocking structure takes place) increases with the magnitude of the lateral confining pressure. The relationship appears to be linear (Fig. 8.4). It follows that the shear strength of the concrete keys interlocked with the indentations of the steel surface is affected by the lateral pressure.

A simple calculation will confirm the trend observed in the tests. A simplified cross section through a concrete-steel interlocking at the microscopic level is shown in Fig. 11.3a. It may be assumed that the concrete shears through a plane as indicated in the figure.

An element in the region of the shear failure is subjected to a known normal stress σ_y, an unknown normal stress σ_x, and an unknown shear stress τ_{xy} (Fig. 11.3b). Since the magnitude of both σ_x and τ_{xy} is unknown, let σ_x be a certain portion of τ_{xy}, i.e. $\sigma_x = c\tau_{xy}$. Also assume that the shear failure occurs when the principal tension in the element exceeds the tensile strength of the concrete. Thus,

$$\sigma_I = f_t = \frac{c\tau_{xy} + \sigma_y}{2} + \sqrt{\left(\frac{c\tau_{xy} - \sigma_y}{2}\right)^2 + \tau_{xy}^2} \qquad (11.1)$$

where σ_I = principal tensile stress and f_t = tensile strength of concrete. For the shear stress τ_{xy}, the following expression is obtained

$$\tau_{xy} = \frac{c(\sigma_y - f_t) - \sqrt{c^2(\sigma_y - f_t)^2 - 4 f_t(\sigma_y - f_t)}}{2} \qquad (11.2)$$

By assuming a value for the tensile strength of the concrete, the shear stress may now be plotted as a function of the lateral stress σ_y for various ratios of c. Figure 11.4 shows that the shear stress increases with the lateral pressure. The relationship becomes more and more linear as the value of c increases.

An analysis based on a finite-element method was used to determine the stress distribution in a concrete key of an assumed rectangular shape (see Appendix D). The results indicated that the ratio c was approximately 0.5 (Fig. D.5 through D.7). For a ratio of c = 0.5 the relationship between shear stress and lateral pressure

(Fig. 11.4) was found to be approximately linear. Thus, the trend indicated by the simplified calculation agrees fairly well with the trend observed in the tests.

The magnitude of the shear stresses found by calculation cannot be compared with the measured bond stresses. It was pointed out in Section 11.2 that the indentations on the surface of the steel may have a width-to-depth ratio of approximately 10:1 to 15:1. According to the results of the analysis, the stress transfer from the steel to the concrete is confined approximately to the upper third or upper fifth of the concrete key (Fig. D.5 through D.7). The failure condition assumed in the calculation will be reached in that portion therefore before the rest of the shear key has been stressed to a large extent. The total shearing of the interlocks may be assumed to be a progressive type of failure. Since the measured bond stresses thus represent only average values, the stresses for the conditions of failure are expected to be much higher.

The calculation was not intended to match the test data because of the simplified assumptions made with respect to the mode of failure, the magnitude of the limiting concrete strength, and the distribution of the stresses. However it demonstrates that the approximately linear relationship between the initial bond stress and the lateral pressure, as observed in the pull-out tests, is explainable by means of the hypothesis which assumes that the initial bond failure is a shear failure of the concrete keys.

The analysis of the stress condition within the concrete key of the microscopic interlock is of interest also in relation to the bond

mechanism for deformed bars. In the case of deformed bars, the concrete key in Fig. 11.3a represents ideally the concrete between two lugs. Figure D.8 shows the directions of the principal tensile stresses within the concrete key. If tensile stress is the primary criterion for cracking, the initial cracks should be approximately perpendicular to the direction of the principal tensile stresses. Therefore, cracks should extend from near the bearing face of the key making an acute angle with the longitudinal axis of the reinforcing bar. Viewed in two dimensions, this phenomenon would transform the concrete into a series of discrete columns supporting the bar at one end and bearing on the mass of concrete at the other end (Fig. 11.5). Reactions from these inclined columns would create the excessive hoop stresses around the bar which lead to splitting of the concrete. Depending on the relative size of the shear key and the surrounding mass of concrete, it is, of course, possible that the "columns" fail in shear before splitting of the concrete takes place.

11.4 Frictional Bond

According to the basic quantitative law of friction, the friction force F is determined by

$$F = \mu N \tag{11.3}$$

where μ = coefficient of friction, and N = lateral force acting normal to the direction of sliding.

In Eq. 11.3, the friction force is stated to be independent of the apparent area of contact. This is explained by the fact that the

frictional mechanism is determined by the real area of contact (Fig. 11.1a). The real area, however, is independent of the apparent area and depends only on the magnitude of the lateral force and the yield stress of the material.

On the basis of results from friction tests performed with various materials, the coefficient of friction appears to be a function of the sliding velocity (Bowden, 1964; Rabinowicz, 1965). However, within a wide range of velocities, the friction coefficient remains nearly constant. The small influence of the sliding velocity on the friction coefficient may be explained by the insensitivity of the shear strength of most materials to the rate of loading at moderate to slow loading speeds.

In general, the friction coefficient is also found to be less dependent on the roughness of the sliding surfaces than is commonly assumed. This phenomenon is understandable if it is realized that friction is determined mainly by the shear strength at the junctions. However, the friction coefficient is affected by extremely smooth and extremely rough surfaces. In the first case, the real area of contact is larger than that determined by the yield stress of the material and the lateral force. Therefore, the friction coefficient increases. In the case of very rough contact surfaces, one surface has to be lifted over the other one, or a kind of interlocking may take place that necessitates shear failures through interlocking keys the area of which may exceed that determined by the junctions. Consequently, the friction coefficient increases in that case, too.

The bond-slip relationships for prestressing wire appear to fit into the framework provided by the current concepts of friction.

Two sets of measured bond-slip curves are shown in Fig. 11.2. The curves refer to two different concrete strengths and three levels of confining pressure.

With respect to different bond mechanisms, each bond-slip curve may be idealized by two straight lines as shown in Fig. 11.2: (a) a vertical line which represents the interlocking mechanism between steel and concrete, and (b) a horizontal line which represents the mechanism of sliding friction.

The vertical line is terminated by the bond stress that is developed when the interlocking concrete keys shear off. The ordinate of the horizontal line is determined by the bond stress caused by sliding friction. A third line connecting the end of the vertical line with the beginning of the horizontal line represents a transition from one bond mechanism to the other. Theoretically, the transition may be expected to follow a vertical line, in practice however, the transition occurs gradually along a curve that approaches the horizontal friction line asymptotically.

Both bond mechanisms are related to the shear strength of concrete. However, the areas to be sheared off are different for both cases. During the interlocking phase, the area is determined approximately by the roughness of the steel surface, assuming that the cement matrix of the fresh concrete penetrates into all indentations of the steel. The area is independent of the lateral stress. During the frictional phase,

the area of shear is determined by the lateral force. The initial interlocking mechanism leading to the maximum bond stress cannot be mobilized again after the concrete keys have failed. The mechanism characterizing sliding friction repeats itself endlessly because simultaneously with the destruction of an existing set of junctions a new set is formed.

When the interlocking structure fails, two phenomena occur at the same time: (a) the bond force drops to the friction force because the area of shear is smaller for the sliding system than for the interlocking structure. (b) A further reduction of the bond force takes place because of a loss of contact stress.

The second phenomenon is due to a partial reduction of the intensity of the contact. Concrete is a porous material with voids that range from micro to macro size. It is assumed that shearing of the interlocking keys results in the formation of loose wear particles. Through displacements of the contact surfaces, the wear particles are transported and deposited in pores opened by the shear failure. This is identical to a volume shrinkage of the concrete near the sliding surfaces. The phenomenon may be compared to the behavior of loosely packed sand subjected to shear deformations. Caused by the lateral displacements, the sand grains in the shearing zone rearrange themselves in a more compact manner which results in a reduction of volume.

The apparent shrinkage of the solid volume near the sliding surfaces leads to a decrease in contact pressure because it is extremely sensitive to the quality of contact. A relative separation of the steel

and the concrete in the order of 10^{-5} to 10^{-4} in. would suffice to reduce the contact stress due to external pressures of the magnitudes applied in the tests to zero. (A discussion of this problem is presented in Appendix C).

According to Eq. 11.3, the friction force is determined by the product of the lateral force and the friction coefficient. Since the lateral force acting on the surface of the steel due to shrinkage or externally applied pressure is unknown because of the drop in contact stress following the initial shear failure, it is not possible to determine the coefficient of friction reliably from the data shown in Fig. 11.2.

Before continuing the discussion about the bond mechanisms, attention should be called to the fact that the increase of the bond strength with the lateral pressure was explained by different means for the interlocking mechanism and the frictional mechanism. In the interlocking mechanism, the shear area is assumed to be constant. The shear strength of the material is assumed to increase because of the confining pressure. In the current friction theories, it is assumed that the friction force increases because the shear area of the junctions increases. The shear strength is assumed to remain constant.

Considering the different states of normal stresses that exist in the shear regions of the two bond mechanisms, the different explanations are not unreasonable. In the interlocking phase, complete contact is assumed between the concrete and the steel. Under the lateral pressures applied in the tests, the stresses normal to the shear plane of the

interlocking structure are well below the strength of the material, especially because the material was confined in the directions parallel to the shear plane. Therefore, each increase of the lateral pressure results in an increase of the normal stress in the shear region. Because of the increasing normal stresses, higher shear stresses can be developed.

In the frictional phase, the contact between the steel and the concrete is limited to the junctions. Therefore, the unconfined material at the junctions "yields" at low pressures. Since the normal stress in the junctions cannot increase anymore, the shear strength per unit area remains constant. The increase of the total shear force is possible by expanding the area of the junctions.

11.5 Stick-Slip Motion

In many pull-out tests with plain wire and strand, it was observed that the steel slipped in a regular intermittent motion which is usually described as "stick-slip" motion (Fig. 8.9). This indicated that the friction force did not remain constant as a function of time. According to Rabinowicz (1965), stick-slip motion, which is typical for friction tests, may arise whenever the static coefficient of friction is markedly higher than the kinetic coefficient. Sampson et al (1943) found that for very short periods of stationary contact the kinetic and the static coefficients of friction are identical. However, while the kinetic coefficient may be assumed to remain constant within a wide range of sliding velocity, the static coefficient varies as a

function of the time of contact according to Ishlinski and Kraghelskii (1944). Experiments by Dȍkos (1946) indicate that the static coefficient of friction varies significantly for short times of contact (less than one second) and relatively little for longer periods. The time of contact refers to the period from the beginning of the application of the tangential force to the time the body slides.

In relation to the above, the bond-slip relations observed in the pull-out tests may be interpreted as follows. After the initial shear failure between steel and concrete, the bond force drops to the level of the friction force. Because of the sudden slip, the force comes to an equilibrium at a level below the value of sliding friction. Until the bond force is raised to the level of the friction force, no slip takes place. This short time of contact is enough to initiate a higher static friction coefficient. Therefore, the bond force increases beyond the sliding friction force. After exceeding the static friction force, a sudden slip takes place with an attendant drop in the bond force. Since the bond force drops again below the level of the sliding friction capacity, the following increase of the bond force takes place without slip. Consequently, static friction can develop again. These steps repeat themselves regularly. It may be assumed that the mean value of the friction force between peak and valley of the stick-slip amplitude is the average kinetic friction during the slip.

The amplitude of the stick-slip motion observed in the tests increased with the lateral force because the difference between the static and the kinetic friction force is proportional to the lateral pressure.

11.6 Determination of Friction Coefficient

Several tests in which a constant lateral pressure was applied to the pull-out specimens were continued after a slip of 0.15 in. had developed by increasing the lateral pressure in steps of 500 psi. During that phase of the test, no slip measurements were taken. Typical force-time relationships as recorded by the plotter of the testing machine are shown in Fig. 8.9. The plots indicate that the bond force responded immediately to each increase of the lateral pressure.

The frictional character of the bond mechanism at that stage of the test is demonstrated by the fact that the average bond force remained approximately constant after each increase of the lateral pressure. The slight decrease of the bond force noticed for each period during which the pressure was held constant had approximately the same trend as the bond slip curve at a slip of 0.15 in. (Point B for plain wire in Fig. 8.9). This can be attributed to either a small decline of the contact stress or to the reduction in the friction coefficient resulting from the increasing amount of loose wear particles. The latter cause appears more plausible.

The maximum bond force reached immediately after each pressure increase in tests with plain wire (Fig. 8.9) was slightly larger than the peaks of the following stick-slip motion, because the static friction coefficient developed for that case was higher due to the longer period of contact. Since, according to the previous section, the actual friction coefficient oscillates around the true coefficient of sliding friction as the slip increases, the average friction force determined by the stick-slip motions will be used to calculate the coefficient of sliding friction.

It was assumed in Section 11.4 that at a slip of 0.15 in. the contact pressure was smaller than the externally applied pressure. However, it may be concluded that an increase of the external lateral pressure at that point of the test will result in an equivalent increase of the contact stress because further slip is not likely to lead to a significant compaction of the material near the sliding surfaces as it was the case immediately after the interlocking structure failed. (A detailed discussion of the relationship between the externally applied lateral pressure and the contact stress is given in Appendix C).

Knowing the increase of the contact stress as well as the response of the friction force, it is possible to calculate the friction coefficient μ for each individual increase of lateral stress by the expression

$$\mu = \frac{P_{i+1} - P'_i}{U d\sigma_2} \qquad (11.4)$$

where P_i, P'_i = bond forces according to Fig. 8.9, U = bonded area (= 0.461 in^2 for plain center wire of 7/16-in. strand) and $d\sigma_2$ = increase of the lateral pressure (= 500 psi).

The individual friction coefficients obtained in this manner are plotted in Fig. 11.6 versus the laterally applied pressure. Although the scatter was relatively large, it appeared that the friction coefficient was independent of the lateral pressure within the range from 1000 to 4000 psi. The average coefficient of friction found was $\mu = 0.29$ for concrete mix A (f'_c = 6100 psi) and $\mu = 0.32$ for concrete mix B (f'_c = 8200 psi).

Figure 11.6 does not contain the friction coefficients calculated for the first increase of the lateral pressure because it was found that the coefficient determined from the first increase was significantly lower than the values for the following pressure enhancements (Fig. 11.7). This result agrees fully with the explanation given for the bond mechanism in Section 11.4. The first increase of lateral pressure had to close a "gap" between the two sliding surfaces which was created through the compaction of material between the contact surfaces. Consequently, the contact stress increased by less than 500 psi. For any further increase of the lateral pressure, a fully compacted material at the contact existed which resulted in stress increases comparable to those applied externally.

The friction coefficients mentioned above were only slightly lower than the fictitious coefficients of friction that are obtained for the initial bond if the shear failure of the interlocking structure is explained in terms of friction. The fictitious values which may be determined from the slope of the average bond stress-lateral stress relationships of Fig. 8.4 are found to be 0.33 for concrete mix A and 0.38 for concrete mix B. The small difference between the initial "friction coefficient" and the coefficient of sliding friction indicates that the area of contact through which shearing takes place differs little for both cases.

11.7 Concluding Remarks

The results of pull-out tests with plain prestressing wire agree with the hypothesis that bond of plain bars is caused basically

by two different mechanisms: an initial interlocking mechanism between the steeland the concrete followed by one of sliding friction.

The bond stress developed both during the interlocking and the frictional phase appears to be extremely sensitive to the normal stresses existing at the contact surface between steel and concrete. The initial slip of the steel following the shear failure of the interlocking structure results in a drop of contact stress, and therefore in a relatively large reduction of bond stress.

The coefficient of sliding friction between concrete and plain prestressing wire was found to be approximately 0.30. This value was obtained under the assumption that the contact stress in the tests was equal to the externally applied pressure. It is very unlikely that the contact stress was lower than the external pressure. However, it is conceivable that the contact stress exceeded the external pressure by as much as 20 percent. This would reduce the coefficient of friction to 0.25.

Under conditions where no external pressure is applied, the contact stress necessary to initiate friction after the initial shear failure of the interlocking structure has taken place is supplied primarily by shrinkage.

12. A CONCEPTUAL MODEL FOR BOND OF STRAND

12.1 Introductory Remarks

The basic bond mechanisms governing the bond characteristics of plain wire also determine the bond strength of strand. However, the actual stress distribution existing at the contact surface between the strand and the concrete due to a pull-out force is rather complicated compared with that for plain wire because of the geometry of strand. Provided the concrete specimen and the strand grip are fixed with respect to rotation around the axis of the strand, any slip causes the strand to untwist itself. This property distinguishes strand, with regard to bond, both from plain bars and from deformed bars.

In order to study the principal features determining the bond capacity of strand, it was desirable to design a simple conceptual model which would make it possible to link the bond properties of strand with those of plain wire.

In the following sections, such a model will be developed both for the initial phase of bond which is determined by interlocking between steel and concrete and for the sliding phase which is determined by friction.

12.2 Initial Bond

The initial bond refers to that phase of the bond-slip relation during which no slip between the strand and the concrete has yet developed. The initial bond force, used frequently in the following discussion, refers to the initial bond strength.

To simplify discussion, strand may be thought of as a round bar with several lugs protruding from its surface. These lugs, representing the exterior wires of the strand, run helically around the bar forming an angle α with the axis of the bar (Fig. 12.1a). If only a very small element of the bar is considered, as shown, a two-dimensional model is obtained. Consider this element being pulled down vertically through a mass of concrete. It is assumed that only the lug is bonded to the concrete.

The following forces indicated in Fig. 12.1b act on the lug in the model:

(1) A pull-out force P/n, where n represents the number of lugs, or in the case of strand, the number of exterior wires.

(2) A normal force N/n due to P, acting on the inclined plane of the lug.

(3) A shear force qN/n, where q reflects the increase in the shear strength of the interlocking concrete keys with the normal pressure. The factor q is comparable to the slope of Coulomb's failure envelope. It may be determined from the initial bond stresses obtained for plain wires under various lateral pressures (Fig. 8.4). It was found to be approximately 0.33 for a concrete strength of 6100 psi, and 0.38 for a concrete strength of 8200 psi.

(4) A shear force V/n which represents the interlocking strength between concrete and steel. Qualitatively, the shear force V is determined from the pull-out tests on plain wire. It includes the effect of shrinkage.

(5) A horizontal force F/n which is due to the externally applied lateral pressure.

(6) A shear force $qF\cos\alpha/n$ which is comparable to the shear force qN/n but is caused by external lateral forces not including shrinkage. This force is modified by the angle α because it is assumed that stresses parallel to the shear plane do not have a confining effect on the concrete.

A similar element to that shown in Fig. 12.1a may be considered at the opposite face of the bar. With respect to the axis of the bar, this element presents a mirror image to that in Fig. 12.1b. Consequently, the horizontal components of the forces will create an internal torsional moment. In the case of a freely rotating strand or concrete specimen, however, no external torsional moment can be generated by the strand while untwisting itself in the free length between the strand grip and the bonded length. Therefore, the initial moment must be equal to zero, and the forces of each element must be in equilibrium.

Summing the forces in the x- and y-direction yields:

$$\frac{P}{n}\cos\alpha - \frac{qN}{n} - \frac{V}{n} - \frac{qF\cos\alpha}{n} = 0 \qquad (12.1)$$

$$\frac{P}{n}\sin\alpha - \frac{N}{n} = 0 \qquad (12.2)$$

By eliminating the normal force N, the pull-out force P may be expressed in terms of the shear force V, the lateral confining force F, the factor

q relating the shear strength to the normal stress, and the twist angle α:

$$P = \frac{V + qF\cos\alpha}{\cos\alpha - q\sin\alpha} \qquad (12.3)$$

The shear force V, which represents the bond resistance provided by the interlocking concrete keys, may be determined readily because for plain wire the initial bond force developed is equal to the shear force V ($\alpha = 0$, $F = 0$). Assuming that V is linearly proportional to the bonded area, the initial bond force of plain wire has to be multiplied by the ratio of the actual surface of the strand to that of the plain wire in order to obtain the shear force V for strand. The twist angle α for the various strand sizes is listed in Table A.2.

With Eq. 12.3, it is possible to calculate the initial bond force of strand using data from plain wire tests. In Fig. 12.2, the calculated initial bond force for strand is plotted versus test results obtained with various strand diameters. All the experimental data were derived from specimens cast with concrete mix A and tested at an age of eight or nine days. No lateral pressure had been applied to the specimens ($F = 0$).

The calculated value of the initial bond force compares fairly well with the average value of the test results for 7/16-in. strand and 1/2-in. strand. For 1/4-in. and 3/8-in. strand, the calculated initial bond force lies at the lower boundary of the test results. It should be noted, that the factor q used in the calculation ($q = 0.33$) was derived from tests with center wire from 7/16-in. strand. It is conceivable, that the exterior wires of some strands had different surface characteristics than the center wire of 7/16-in. strand and therefore developed

different initial bond properties. It was pointed out already in Chapter 5 that 3/8-in. strand developed bond-slip characteristics that differed slightly from those of other strand sizes.

For practical purposes, it may be concluded that the initial bond force of strand increases approximately linearly with the strand diameter. The slight deviation of the calculated values from a straight line (Fig. 12.2) derives from small differences between the measured and the nominal geometric properties of strand.

Using Eq. 12.3, it is also possible to calculate the initial bond force developed by strand under laterally applied pressures. In that case, the lateral force F is determined by multiplying the actual bonded area of strand with the lateral stress applied.

Test results obtained with 7/16-in. strand are presented in Fig. 12.3. Compared with the test results of Fig. 12.2, the initial bond forces in the case with no lateral pressure applied are significantly higher. This fact is due to the higher age of the concrete specimens at the time of testing. The trend of the bond strength to increase with the age of the concrete was confirmed for strand in Section 6.5 (Fig. 6.12).

Lacking tests with plain wire comparable in age to tests with strand shown in Fig. 12.3, the initial bond force of strand at zero lateral pressure could not be reproduced theoretically on the basis of wire tests. The increase of the initial bond strength with lateral pressure, however, could be calculated using the second term of Eq. 12.3. The calculated relationship (Fig. 12.3) was obtained using a value of $q = 0.33$ which was derived from wire tests conducted at an age of 15 and 17 days. The theoretical relationship compares fairly well with the test results.

It was mentioned above that for a freely rotating strand or concrete specimen no torsional moment develops. If the concrete specimen and the strand are fixed against rotation, the free length of the strand between the strand grip and the bonded part unwinds while being stretched under the load. As a result, a small torsional moment is applied at the attack end of the bonded length causing an increase of contact pressure between the strand and the concrete. It may be shown, however, that this moment is too small to create a significant increase in bond strength. Tests conducted with both test setups demonstrated that the influence of the torsional moment on the initial bond strength is negligible (Fig. 3.7). For this reason, use may be made of Eq. 12.3 regardless of the test setup.

The model shown in Fig. 12.1 and Eq. 12.3 may also be used for calculating the initial bond force of twisted square bars. Since both the square bars and the strand are manufactured by cold drawing, the same shear force per unit area, representing the interlocking mechanism, may be assumed for both steels. The shear force V is determined by the initial bond force that was developed in one-in. pull-out tests with untwisted square bars. The average value found was 170 lb (Fig. 10.2).

Using the above value in Eq. 12.3, the initial bond force of square bars at an applied lateral pressure of zero psi may be obtained as a function of the twist angle α. In Fig. 12.4, this relationship is compared with various test values of series QB09-1.

The scatter of the test results, especially at large twist angles, is large. This may be deduced from the high degree of nonuniformity in the geometry of the square bars at large twist angles. Nevertheless, the trend of the calculated relationship agrees with the test data.

12.3 Sliding Bond

Sliding bond refers to the phase of bond following the shear failure of the interlocking structure. It is characterized by sliding of the steel with respect to the concrete. The mechanism of sliding depends on the friction properties of the two materials in contact. It may be assumed that the coefficient of sliding friction remains constant within the range of sliding velocities observed in the pull-out tests. Any change in the friction force is therefore assumed to be caused by a change in contact stress between the steel and the concrete.

When strand slips through the concrete it may either wind itself through the concrete like a screw, or it may untwist itself, depending on the test setup. Since strand has some torsional stiffness, the manner in which strand slides through the concrete affects the magnitude of the contact stress between steel and concrete. Consequently, two different cases of sliding have to be investigated: (a) the concrete specimen of the strand is permitted to rotate freely around its axis while the strand is pulled out, (b) the concrete specimen and the strand are held fixed with respect to rotation during the test.

Since the strand in case (a) is not restrained from rotating, no torsional moment will be induced into the concrete prism. In case

(b), the strand is forced to untwist itself through the rigid concrete embedment. Therefore, a torsional moment is generated within the concrete prism due to the rotational stiffness of strand.

In order to study the sliding mechanism of strand, a model very similar to that used for the initial bond may serve as an aid. A smooth prism with a protruding lug slanted at an angle α represents one exterior wire of the strand (Fig. 12.5). Consider only the lug of the prism bonded to concrete. When the prism is pulled down through a mass of concrete, the prism will slide along a plane indicated by the lug.

The following forces indicated in Fig. 12.5b act on the lug of the model:

(1) A vertical pull-out force P/n, where n is the number of lugs or, in the case of strand, the number of exterior wires.

(2) A normal force N/n due to P, acting on the inclined plane of the lug.

(3) A friction force $N\mu/n$, where μ is the coefficient of sliding friction between steel and concrete

(4) A lateral force F/n where F is due either to shrinkage of the concrete or to an externally applied pressure

(5) A friction force $F\mu \cos\alpha/n$

(6) A spring force ks/n which represents a concrete reaction that is equal in magnitude to the force necessary to untwist the strand. The constant k is a spring factor that corresponds to the torsional stiffness of the strand, s is the vertical slip of the strand. The

spring force ks is initiated only in case (b) described above, where the strand is forced to untwist itself.

(7) A friction force $ks\mu \cos\alpha/n$

Summing the forces in the x- and y-direction, the following two equilibrium equations are obtained.

$$\frac{P}{n}\cos\alpha - \frac{N}{n}\mu - \frac{F}{n}\mu\cos\alpha - \frac{ks}{n}\mu\cos\alpha - \frac{ks}{n}\sin\alpha = 0 \qquad (12.4)$$

$$\frac{P}{n}\sin\alpha - \frac{N}{n} + \frac{ks}{n}\cos\alpha = 0 \qquad (12.5)$$

These two equations lead to the following expression for P

$$P = \frac{F\mu + ks\,(2\mu + \tan\alpha)}{1 - \mu\tan\alpha} \qquad (12.6)$$

According to Section 11.6, the friction coefficient μ between prestressing wire and concrete which may be used in the above equation for strand was found to be approximately 0.30. It is not possible, however, to give the magnitude of the lateral force F because both the lateral force due to shrinkage and the contact force between steel and concrete due to the externally applied pressure are unknown (see Section 11.4 and Appendix C). The whole friction force $F\mu$ may be determined approximately, however, by using the friction force developed by plain wires and multiplying it with the ratio of the bonded areas of strand and wire.

In order to determine that part of the pull-out force that is related to the increased contact pressure due to the torsional stiffness

of strand, the spring constant k has to be determined. Because of the composite cross section of strand, it is very difficult to find k for strand theoretically. In view of a better understanding of the effect of the torsional stiffness on bond, it appears therefore expedient to study the influence of the torsional stiffness on the bond force with the aid of twisted square bars.

The torsional moment of a square bar is, according to Timoshenko (1955):

$$T = \frac{0.1406\ G\theta\ a^4}{L} \tag{12.7}$$

where G = shear modulus, θ = torsion angle, a = width of the square bar, and L = length over which the torsion is applied.

The torsional moment may also be expressed in terms of two force couples, Qt, where Q is the resultant force due to the contact pressure caused by the torsional moment, and t is the moment arm as shown in Fig. 12.6. Thus the torsional moment becomes:

$$T = 2Qt \tag{12.8}$$

Combining Eq. 12.7 and 12.8, the force Q is obtained to

$$Q = \frac{0.1406\ G\theta\ a^4}{2Lt} \tag{12.9}$$

This force, however, is identical to the spring force acting in the model of Fig. 12.5. Therefore

$$Q = \frac{ks}{n} \tag{12.10}$$

The torsion angle is related to the slip s by the expression

$$\theta = \frac{2\pi s}{p} \tag{12.11}$$

where p is the pitch of the bar. The pitch, in turn may be expressed in terms of the twist angle α and the width of the bar by the relationship

$$p = a\sqrt{2}\pi\cot\alpha \tag{12.12}$$

Combining Eq. 12.9 through 12.12, the spring constant k can be calculated by the expression:

$$k = \frac{0.1406\ n\ Ga^3\ \tan\alpha}{\sqrt{2}Lt} \tag{12.13}$$

As an approximation, a triangular stress distribution at the contact between steel and concrete may be assumed as indicated in Fig. 12.6. With this assumption, the moment arm t becomes equal to 2a/3. The other terms of Eq. 12.13 were determined by the tests performed with square bars (n = 4, G = 11.5×10^6 psi, a = 5/16 in., and L = 9 in., where L was the free length between the strand grip and the bonded length).

The spring constant k for 5/16-in. square bars, determined with the assumptions above, is plotted versus the twist angle α of the bar in Fig. 12.7.

Knowing the spring constant k, the pull-out force P can be calculated for any slip with Eq. 12.6. The friction force $F\mu$ in this equation is determined for every slip value by the bond force-slip relationship of the untwisted bar. Two calculated bond-slip relationships

for 5/16-in. square bars are plotted in Fig. 12.8 versus test results of series QB09-1. Considering the simplified assumptions made with the two-dimensional model and the possible scatter of the test results, the agreement of the theoretical solution with the test results is good. The theoretical bond-slip relation is valid, of course, only as long as the bars untwist themselves through the concrete. As soon as the concrete is crushed under excessive contact stresses caused by the rotational spring force of the bar, the bars are pulled out of the concrete without further rotation, and the bond force necessarily deviates from the predicted relationship.

The large increase in bond strength that is due to the torsional stiffness of the square bars in the case where both the steel bar and the concrete specimen are fixed against rotation is demonstrated effectively by the measured bond-slip relationships shown in Fig. 10.3.

The influence of the torsional stiffness of strand on bond may be derived by a similar method to that used above for twisted square bars. The rotational stiffness of the strand was found by experimental means.

The test setup used to measure the torsional stiffness is shown in Fig. 12.9. A free length of 7/16-in. strand was loaded in tension. While the tensile force was held constant, the strand was rotated by small weights acting over a pulley and a lever arm. The weight needed to rotate the strand and the amount of rotation in degrees were measured.

Figure 12.10 shows the measured relationships between the applied torsional moment and the rotation (and slip) of the strand for different lengths tested. The results of several tests indicated

that the tension force to which the strand was subjected did not influence the torsional stiffness of strand within the range of 500 to 1500 lb that covers the unit bond strength developed by strand.

In order to determine the spring constant k, a resultant force distribution representing the contact stress between strand and concrete due to the untwisting of the strand is assumed as shown in Fig. 12.11. The resulting force couples Qt, where Q is the force acting on each exterior wire perpendicular to the main diameter of the strand, and t is the moment arm, form the torsional moment

$$T = 3Qt \tag{12.14}$$

Since Q is identical to the spring force ks/n acting on the model shown in Fig. 12.5, the spring constant k may be expressed by

$$k = \frac{nT}{3ts} \tag{12.15}$$

With the slip, s, and the angle of rotation, θ, being interrelated by Eq. 12.11, the spring constant k may be determined using the results of Fig. 12.10. Assuming that the moment arm t is approximately 5/6 of the strand diameter, the spring constant k for 7/16-in. strand is found to be 2700 lb/in.

The second part of Eq. 12.6 represents the bond force that is caused by the rotational stiffness of the strand. Consequently, this part determines the additional bond force gained in those tests in which both the concrete specimen and the strand were fixed against rotation. Using the above value of k, a twist angle of $\alpha = 13.3^{\circ}$, and an average

friction coefficient of $\mu = 0.30$ (see Section 11.6), the difference in bond force can be shown to be 24 lb for a slip of 0.01 in. and 240 lb for a slip of 0.1 in.

The actually measured difference in bond force is shown in Fig. 3.7, where average bond-slip curves are compared for both test setups. The order of magnitude and the trend of the difference in bond force to increase in proportion to the slip are comparable with the calculated values.

It may be concluded from the experimental as well as the theoretical investigation that the rotational stiffness of strand, in contrast to that of square bars, has only a very small effect on bond strength. This can be related directly to the small torsional stiffness of strand.

12.4 Lack of Fit

The results of Eq. 12.6 and the statements made in the last paragraph of the foregoing section lead to the conclusion that the bond characteristics of strand should be directly comparable with those of plain wire. However, a comparison of typical bond-slip relationships developed by strand with a typical bond-slip relation developed by plain wire indicates that this conclusion is apparently not true (Fig. 12.12). Consequently, Eq. 12.6 does not include all the sources contributing to the bond strength of strand.

With respect to the above problem, the following observations may be deduced from Fig. 12.12:

(1) The bond characteristics may vary significantly from one lot of strand to another.

(2) A sudden drop in bond strength comparable to that observed with plain wire was measured for 7/16-in. strand of coil II immediately after the initial bond strength had been exceeded.

(3) The bond force of strand increased with slip either immediately after the initial shear failure had taken place or after a slip of approximately 0.01 in. had developed. In contrast to that, the bond strength of plain wire decreased with increasing slip approaching an approximately constant value.

From the second observation, it may be concluded that, at small slips, at least some strands tend to show the same bond characteristics as plain wire. However with increasing slip, a new source of bond strength seems to be activated that accounts for the increase of the bond force of strand at slips larger than 0.01 in.

The new bond source may be explained on the basis of the following hypothesis. Assume that the shape of the strand is not perfect, i.e. that the diameter, the pitch, or the angle of twist vary slightly along the axis of the strand. In that case, the strand would tend to wedge as soon as it starts slipping through the presumably rigid concrete embedment because of a certain lack of fit between the cross sections of the strand displaced through slip and the stationary concrete channel. As a result, strand would develop bond characteristics that are similar to those of deformed bars.

It is not very difficult to show that irregularities in the geometry of strand exist. Figure 12.13 and 12.14, for instance, show the

cross sections of a piece of strand cast in concrete which were located at a distance of one in. from one another. The slices were made from a random specimen with a bonded length larger than one in. (Series SA09-18). The different spacing of the exterior wires indicates that the diameter and the angle of twist must have varied from one cross section to the other.

Another attempt to show the nonuniformity of strand was made by measuring the diameter of two 7/16-in. strands at five different locations within a length of one in. (equal to the standard length of the pull-out specimens). At each location, the diameter was measured over the three sets of exterior wires. The measurement was accomplished with a dial indicator having a reading sensitivity of 0.0001 in. Figure 12.15 shows the relative variation of the strand diameter. It was in the order of 0.01 in.

The nonuniformity of the strand may account for the difference in bond characteristics between strand and plain wire as follows:

(a) Theoretically, it may be shown that a small variation of the strand diameter is enough to explain the difference in the relative bond forces. According to the bond-slip relations plotted in Fig. 12.12, plain wire would develop a bond force of roughly 200 lb at a slip of 0.10 in. if it had the same surface area as strand. Strand developed a bond force of approximately 900 lb at the same slip. Thus, a bond force of approximately 700 lb would have to be attributed to the lack of fit of strand if the small effects of the inclined plane and the torsional stiffness of strand were neglected (denominator = 1, k = 0 in Eq. 12.6).

Using a friction coefficient of 0.30, as determined in Section 11.6, a contact stress of approximately 1260 psi would be required to develop a bond force of 700 lb due to wedging of the strand. According to Eq. C.6 of Appendix C, an increase of the diameter of the strand by 0.00016in. over a distance of 0.10 in. would suffice to generate a contact stress of the above magnitude. This required variation of the strand diameter is less than the measured variation shown in Fig. 12.15.

It should be noted that the contact stresses mentioned above may lead to circumferential tensile stresses of such magnitude that radial cracking immediately around the strand will take place.

(b) Practically, it was shown that "straight" (nontwisted) strand which was fabricated in the laboratory as described in Section 10.3 (Series UA09-1) displayed almost the same bond characteristics as the twisted strand (Fig. 10.5 and 10.7). An explanation for the difference in bond characteristics between a single wire and a group of three or seven parallel wires is offered by the hypothesis about the lack of fit. If all the individual wires are not perfectly parallel, "straight" strand will show bond properties of a slightly deformed bar. Because of the tack welding necessary to keep the wires in touch (Section 10.3), it was indeed not possible to produce a perfectly parallel strand.

The few tests performed with "straight" strand indicate that the imperfection in the shape rather than the twist of the strand lead to the relatively good bond characteristics of strand.

An appreciable difference was observed between the shapes of bond-slip curves (Fig. 12.12) for strand acquired at different times.

It is pertinent to discuss the observed difference in the light of the bond mechanisms described.

Figure 12.12 shows that the bond force developed by 7/16-in. strand of coil I increased immediately after the initial shear failure of the interlocking concrete keys had taken place. In contrast, the bond force developed by 7/16-in. strand of coil II dropped after exceeding the initial bond strength. After a slip of approximately 0.01 in., it also started to increase. It should be noted that the average initial bond force was exactly identical, and that the bond force at a slip of 0.15 in. was nearly the same for both strands again.

The only difference between the two strands that could be detected was that the surface of the strand had a dull, dry appearance for coil I and a shiny, oily appearance for coil II. This seems to indicate that the surface of the strand of coil I, which had been stored in the laboratory for a much longer time than coil II, was oxidized to a greater extent.

A similar observation was made for strands of other diameters. The surface of 3/8-in. strand resembled very closely that of the 7/16-in. strand of coil II, while the 1/4-in. and 1/2-in. strand had the dull surface of the 7/16-in. strand of coil I. The 1/4-in. and 1/2-in. strand displayed bond characteristics comparable to those of 7/16-in. strand of coil I. The 3/8-in. strand, however, developed a drop in bond force at very small slips that was typical for 7/16-in. strand of coil II (Fig. 5.1). The decrease of the bond force for the 3/8-in. strand did not occur immediately after the initial shear failure but at a slip of roughly 0.001 in.

The apparent influence of the surface properties on the bond characteristics of steel could also be observed in tests performed by Rehm (1961). The bond strength of round steel bars tested by Rehm with a surface showing indentations of a depth of 0.003 to 0.004 in. increased immediately after the initial shear failure at a much faster rate than the bond force of bars having surface indentations of only 0.001 to 0.003 in.

It may be concluded from the above observations that the bond characteristics of strand are affected by the surface roughness. Consider therefore two contact surfaces between steel and concrete (Fig. 12.16): (a) a contact showing a rough steel surface, characterizing 7/16-in. strand of coil I, and (b) a contact showing a "smooth" surface, characterizing 7/16-in. strand of coil II.

With respect to the initial bond strength determined by shear failure along the peaks of the steel surface, there should be no significant difference between case (a) and case (b) because the shear area is approximately the same for both cases. This conclusion was confirmed by the tests (Fig. 12.12).

With respect to sliding, there may be a difference between case (a) and case (b) at small slips. In view of the wider indentations, it is likely that the initial roughness of the failure surfaces is greater for case (a) than for case (b). Consequently, higher contact stresses and additional shear stresses necessary to shear off "rough spots" will cause initially a larger friction force in case (a). After some slip, the degree of smoothness, and therefore the magnitude of the

contact stress, will assume similar values for both cases. With the assumption that the effect of the lack of fit is comparable for both strands, the friction force will tend to approach the same magnitude after a certain slip (Fig. 12.12).

The effect on bond of strand related to the lack of fit may be summarized as follows:

Ideally, strand with a perfect geometric shape (if every cross section along the length of the strand is identical) will develop a bond-slip relationship similar to one obtained with plain wire. This has been verified for some of the test specimens at small slips (strand of coil II, Fig. 12.12).

With increasing slip, however, a deformed-bar effect develops which causes the bond strength to increase with slip. This effect is due to irregularities in the shape of the strand. The irregularities lead to a lack of fit between the strand and the concrete, thus increasing the lateral confining stresses.

A second effect influencing the bond-slip relationship of strand at very small slips is due to the surface roughness of the steel. This effect may be understood in the light of the following considerations. Because of bearing under the lugs, the bond force of deformed bars increases immediately after the interlocking shear keys of the "plain" part of the bar have failed. On the other hand, the bond force of plain bars with very smooth surfaces will drop immediately after the initial shear failure has taken place. Consequently, it may be assumed that bars with rough surfaces will develop bond-slip relations which,

immediately after the initial shear failure, will range somewhere between the two extreme cases.

12.5 Concluding Remarks

With the conceptual model developed in this chapter to explain bond of strand, it was possible to predict the initial bond strength of strand on the basis of test results obtained with plain wire. It was shown that the inclined-plane effect due to the twisted shape of strand had little influence on the initial bond strength because of the small twist angle α of strand. It was also possible to determine the influence of the lateral pressure on the initial bond strength using the conceptual model.

With respect to sliding-bond strength of strand, it was possible to show that the inclined plane effect and the torsional stiffness of strand had little influence. This led to the conclusion that a perfectly shaped strand would exhibit bond characteristics similar to those developed by plain wire. It was not possible, however, to predict the bond force developed during the sliding phase of the bond-slip relationship theoretically because of the difficulties involved in making deterministic assumptions concerning the irregularities in the shape of the strand.

The disadvantage of not being able to predict the bond force of strand beyond the initial bond strength is not very important considering the fact that the sliding-bond strength of strand remains approximately constant with increasing slip (Fig. 5.1).

13. THE APPLICATION TO PRACTICAL PROBLEMS OF DATA FROM ONE-in. PULL-OUT TESTS

13.1 Introductory Remarks

Short-length pull-out tests provide a valuable means to study the effect of various parameters influencing the bond properties of reinforcing steel. The results are very informative with respect to the fundamental bond-slip relation between steel and concrete. However, short-length pull-out tests can be useful for practice only if the results can be projected directly to problems such as determining the bond force developed over a given bonded length or the anchorage length for a given bond force.

In the following sections, the applicability of a theoretical method is discussed to solve the above problems by using results from one-in. pull-out tests. The theoretical results are compared with actual test values.

13.2 Theoretical Determination of the Bond Force-Slip Relationship for a Given Bonded Length

Theoretically, it is possible to calculate, by an iterative method, the bond force-slip relation for any bonded length of strand if the unit bond force-slip relationship and the stress-strain curve of the strand are known.

The analytical method is based on the following assumptions:

(1) The change in slip over a given bonded length is equal to the change in length of the steel. With this assumption, the deformation of the concrete is neglected. The error is negligibly small because

the deformation of the concrete is usually very small compared to that of the steel. Because of the uncertainties involved in the assumptions concerning the concrete deformations, it does not seem reasonable to include the concrete deformations in the calculation.

(2) The change in steel force over a given bonded length is equal to the bond force transferred to the concrete.

(3) The unit bond force-slip relation measured in the one-in. pull-out tests represents the actual bond-slip relation between strand and concrete.

Consider now a pull-out specimen with a given bonded length. The steel stress at the trail end of the specimen is equal to zero. For a given trail-end slip, the bond force and the slip distribution along the bonded length are to be determined using the bond-slip relationship indicated by the one-in. pull-out test. The bond force and the slip are determined iteratively at small intervals of the bonded length progressing from the trail end of the specimen to the attack end. A detailed description of the calculation, which was performed with the aid of a digital computer is given in Appendix E.1.

Using an average unit bond force-slip relationship of 7/16-in. strand obtained from one-in. pull-out tests and a modulus of elasticity for strand of 28×10^6 psi, slip distributions along the bonded length were calculated for various trail-end slips as shown in Fig. 13.1. Simultaneously, the bond force developed by the strand was calculated as a function of the bonded length (Fig. 13.2).

After calculating the relationships of the bond force and the slip versus the bonded length for several trail-end slips, it was

possible to construct complete bond-slip curves for any given bonded length both for the trail-end and for the attack-end slip. Relationships obtained in this manner are plotted in Fig. 13.3 and 13.4 versus actually measured test curves from series SA09-18.

The agreement between calculated and measured results is favorable. The bond-slip relationships shown in Fig. 13.3 indicate that the bond force at which the trail end started to slip could be calculated almost exactly on the basis of the one-in. pull-out tests. However, at trail-end slips ranging from 0.001 in. to 0.1 in., the calculated bond force was constantly lower than the measured bond force. The difference increased with the bonded length. This discrepancy is understandable in the light of the bond stress-slip relations of series SA09-18 plotted in Fig. 3.5. The bond-slip curve of the one-in. tests on which the calculation was based dropped immediately after the initial bond strength was exceeded and increased only after a slip of approximately 0.03 in. had developed. Tests with larger bonded lengths did not exhibit this marked drop in bond force. Since the calculation was based on the bond values of one-in. tests, all theoretical bond-slip relations reflect this drop.

The difference in the shape of the unit bond-slip curves in Fig. 3.5 may be explained with the help of the lack-of-fit hypothesis. Consider an infinitesimally small bonded length of strand. This length would not develop any effects due to lack of fit if pulled out of the concrete. Consequently, the bond force would drop immediately after the interlocking concrete keys have sheared off. In contrast,

a large embedment length would develop a substantial differential slip between trail end and attack end. Therefore, the slip developed at the attack end will be so large by the time shear failure takes place at the trail end that the strand near the attack end wedges because of lack of fit. As a result, it is not likely that the entire bonded length slips suddenly after the initial bond strength is exceeded at the trail end. Consequently, the drop in bond force observed in the short-length pull-out tests does not occur. It appears that one-in. specimens approach the bond characteristics of an infinitesimally short length while specimens with bonded lengths equal to or larger than three in. exhibit the bond characteristics of large bonded lengths.

The difference between the calculated and the measured bond force related to the attack-end slip observed immediately after the trail end has started to slip (Fig. 13.4) may be explained in a similar manner as above. The pronounced drop of the calculated bond force was caused by the fact that the calculation was based on one-in. pull-out tests.

The difference between the calculated and the measured bond force related to the attack-end slip observed before the trail end has slipped may be attributed partly to the fact that in the calculation the deformation of the concrete was not taken into account. On the other hand, the "measured" relationships shown in Fig. 13.4 may not be absolutely correct because the measurements of the attack-end slip had to be corrected for the deformations of the strand and the concrete specimen, which required several assumptions (Section A.6)

In view of the fact that the calculated bond forces related to the trail-end as well as the attack-end slip (after the trail end has slipped) were always smaller than the measured bond forces, it may be concluded that the method of calculating bond-slip relationships on the basis of results obtained from one-in. pull-out tests leads to safe and satisfactory results.

13.3 Theoretical Determination of the Anchorage Length in Prestressed Members

The anchorage length of strand in a pretensioned prestressed member can be determined in a similar manner to that described in Section 13.2 for any level of prestress on the basis of results obtained from one-in. pull-out tests. Required for the calculation are the stress-strain curve of strand and a unit bond force-slip relationship which is characteristic both for the strand and the concrete used. The assumptions on which the calculation is based are identical to those of Section 13.2.

The anchorage length is defined as the length of strand necessary to transfer the entire effective prestressing force of the pretensioned strand to the concrete by bond. The effective prestressing force is that force that acts on the concrete member immediately after the release of the prestress (i.e. the prestressing force minus the force lost by the instantaneous deformation of the strand and the concrete).

Because of the definition of the anchorage length, the following boundary conditions are known: (a) At the end of the prestressed member, the steel stress is equal to zero. (b) At the end

of the anchorage length (in the interior of the beam) the steel stress is equal to the effective prestress while the slip is equal to zero (it is assumed in the calculations that any bond stress, no matter how low, causes a relative movement between the steel and the concrete). Since the end conditions are known both for the steel stress and the slip at the end of the anchorage length in the interior of the beam, the calculation, consisting of a simple iteration procedure, is started at this end following a similar method as that described in Section 13.2.

It is known that the prestressing force of the strand diminishes towards the end of the prestressing member while the slip between the strand and the concrete increases. The iteration process, in which the steel stress and the slip are determined at small intervals progressing from the end of the anchorage length towards the end of the prestressed member, is terminated by the condition that the steel stress in the strand becomes zero. The anchorage length is determined by the sum of the iteration intervals required. A detailed description of the calculation procedure is given in Appendix E.2.

Using a typical unit bond force-slip relation (the average of the results of the nine pull-out tests (Fig. F.13 and F.14) prepared together with the prestressed beams described in Appendix F), a modulus of elasticity for strand of 28×10^6 psi, and an effective prestress of 160 ksi, the calculation yielded slip and steel stress distributions within the anchorage zone as indicated in Fig. 13.5 and 13.6. The nearly linear curve in Fig. 13.5 shows that an average bond stress could have been used without the iteration procedure to obtain approximately

the same result. This is due to the approximately flat bond response for strand with increasing slip.

The calculated anchorage length plotted as a function of the effective prestress is shown in Fig. 13.7. The curve in this figure could also have been obtained by a simple calculation using an average constant bond stress.

In order to check the applicability of the calculation method based on results of one-in. pull-out tests, five pretensioned prestressed beams were tested as described in Appendix F. The reinforcement in the beams consisted of two 7/16-in. strands. In three beams, the strands were placed 2 in. above the bottom, in two beams 10 in. above the bottom. The effective prestress immediately after transfer of the prestressing force into the beam was approximately 160 ksi. The anchorage length was determined by measuring the strain distribution of the concrete at the level of the reinforcement.

For reasons stated in Appendix F, the length of strand required to transfer 90 percent of the effective prestressing force was measured and called L(90). This value was compared with the calculated results.

Table 13.1 shows the calculated and the measured data for the three beams in which the strand was placed two in. from the bottom of the beam. The calculation was based on the average bond-slip curve of the nine pull-out tests that were performed together with the above beams (Appendix F, Fig. F.14).

Before comparing the calculated with the measured data, it should be noted that the scatter of the measured individual values was

considerable, although the effective prestress and the concrete strength were within three percent for the three beams. The scatter was comparable to that encountered in pull-out tests and is credible in view of the fact that it is more difficult to achieve uniformity in curing and settlement conditions for large beams than for small pull-out specimens. The large influence on bond of curing and settlement was discussed in Chapters 6 and 7.

The calculated lengths L(90) were within +9, +25, and -1 percent of the measured average length L(90) for each beam. The calculated slip was within +9, +12, and 0 percent of the measured average end slip. As far as conclusions may be drawn from three tests, it appears that the calculation based on one-in. pull-out tests using non-pretensioned strand provided a reasonably safe estimate both for the anchorage length and the end slip. This is consistent with the results found in Section 13.2 which indicated that the average bond force developed by a given length of nonprestressed strand was a little higher than the calculated values because the bond characteristics of one-in. specimens differed slightly from those of specimens with longer bonded lengths.

Considering the above results, it may be concluded that the bond characteristics of a nonprestressed strand subjected to "pull-out" forces do not differ significantly from those of a pretensioned strand subjected to "pull-in" forces. Theoretically, the state of the contact stresses between the strand and the concrete is different for both cases. If a nonprestressed strand is subjected to pull-out forces, the strand

diameter tends to contract due to the axial tension. Consequently, there should be a reduction of the compressive stress between the strand and the concrete. On the other hand, if a prestressed strand is pulled into the concrete after the release of the external pretensioning force, the diameter of the strand will tend to expand due to the elastic shortening of the strand and cause the strand to wedge within the concrete channel ("Hoyer Effect"). The resulting radial contact pressures for full prestress may be on the order of several thousand psi if elastic behavior of the concrete and perfect contact is assumed.

In practice, the contact stresses due to the Hoyer Effect appear to be, at least for strand, considerably smaller than assumed on a theoretical basis. Concluding from the reasonably good agreement of the calculated and the measured anchorage length of the pretensioned strand as well as the calculated and the measured bond-slip relation of the nonprestressed strand, the effect of the wedging of the strand in a pull-in case may apparently be neglected in practice. This assumption agrees with test results reported by Keuning (1962) who found that the difference between the bond strength of strand developed in a pull-in test and a pull-out test was not significant. It should also be noted that the steel tensile stress reached in the one-in. pull-out tests was less than 15,000 psi. Although the Hoyer Effect would not have been registered in the test results, neither would the "negative Hoyer Effect".

Since the anchorage length and the end slip could be predicted satisfactorily by the iteration technique described above, it may be

assumed that the calculated slip- and steel-stress distribution (Fig. 13.5, 13.6) are fairly reliable, too. Consequently, it may be derived from the analytical results that the full anchorage length of strand, L, is on the average

$$L = 1.12 \times L(90) \qquad (13.1)$$

For the two beams with the reinforcement near the top surface, no directly comparable results from pull-out tests were available to confirm the measured data by computed values. However, the ratio of the anchorage lengths and the end slips between the two types of beams with different depths of concrete under the strand showed exactly the same trend as the pull-out tests described in Chapter 7. Figure 7.2, for instance, shows that, for a slip of 0.5 in., specimens with a 10-in. depth of concrete under the strand developed, on the average, only 75 percent of the bond strength of specimens with a depth of 2 in. Compared with this, the anchorage lengths developed by the beams with the strand near the top surface were, on the average, 28 percent higher than those of the beams with the strand near the bottom.

13.4 Concluding Remarks

It was shown that the entire bond-slip relation for any bonded length of a nonprestressed strand could be calculated by using the results of one-in. pull-out tests. It was also possible to predict, on the basis of one-in. pull-out tests, the anchorage length and the end slip of strand in a pretensioned prestressed member.

It appeared that the calculated values provided a lower bound to the test results. This was caused by the fact that pull-out specimens with a bonded length of one in. have bond characteristics that differ slightly from those of specimens with larger embedment lengths. The difference was explained with the effect of the "lack of fit". To use a unit bond force-slip relation based on a larger bonded length would, in general, not yield any advantage because the magnitude of the unit bond force deviates from the true unit bond force with increasing bonded length. The degree of deviation depends on the slope of the actual unit bond force-slip relationship (see Chapter 3).

For practical purposes, the theoretical determination of the anchorage length and the end slip in a prestressed member, based on results from one-in. pull-out tests, appears to be adequate. Therefore, it may be concluded that one-in. pull-out tests provide data that are applicable directly to practical problems. Furthermore, if the bond-slip curve from the one-in. test is nearly flat in the range of slips expected for the case under consideration, the average bond stress from the one-in. test can be used directly to determine anchorage length and slip.

14. RECOMMENDATIONS FOR DESIGN

14.1 Introductory Remarks

In the design of pretensioned prestressed concrete members, it is desirable to know the anchorage length of the prestressing reinforcement as well as the build-up of the steel stresses within the anchorage zone in order to be able (a) to calculate the shear stresses near the end of the member, (b) to determine the distribution of the anchorage-zone stresses perpendicular to the prestressing reinforcement, and (c) in short members, to establish that part of the member for which full prestress is available.

In the following section, recommendations are made concerning the anchorage length of seven-wire (round wire) strand. These recommendations are based on the results of 486 pull-out tests and five prestressed-beam tests described in this investigation as well as the results of several investigations carried out at other research institutions reviewed in Chapter 1.

14.2 Basic Anchorage Length

The anchorage length is defined as the length required to transfer the full effective prestressing force to the concrete by bond. The critical steel stress is the effective prestress immediately after release of the prestressing force and is less than the pretensioning stress existing in the prestressing bed.

In design practice, it is tacitly assumed that there is a unique value for the anchorage length of a given strand at a specified prestress. Actually this value can vary over a considerable range

depending on factors such as condition and position of the strand and workmanship. In order to discuss the effects of the pertinent variables, it is necessary to define a "basic anchorage length" for a set of specified conditions as follows:

(a) The effective prestress immediately after release of the prestressing force is 175 ksi. This value is the maximum allowable steel stress for strand with a tensile strength of 250 ksi according to the Building Code Requirements for Reinforced Concrete (ACI 318-63, paragraph 2606 (a)2.).

(b) The prestressing force is released gradually into the concrete member.

(c) The strand is clean, and free of oil, grease, or severe corrosion.

(d) The concrete strength at the time of release is 4000 psi.

(e) The strand is placed in a horizontal position such that the depth of concrete below the strand is no more than 2 in.

For the above conditions, the average anchorage length may be assumed to be

$$L = CD \qquad (14.1)$$

where L = anchorage length, C = coefficient reflecting the surface conditions of the strand, and D = nominal diameter of the strand.

Results from pull-out tests performed with strand have indicated that C may vary for different lots of strand despite the specified conditions described under (c) above.

Figure 14.1 shows two distributions for the anchorage lengths determined on the basis of individual results from pull-out tests:

(1) The distribution indicated by the heavy line represents the results from 153 pull-out tests including four strand sizes (1/4, 3/8, 7/16, and 1/2-in. strand). The strand had been stored in the laboratory for periods ranging from three to five years. The surface had a dull, dry appearance although it could not be described as rusty.

(2) The distribution indicated by the shaded area represents the results from 30 pull-out tests with 7/16-in. strand (coil II) which had been stored in the laboratory for less than one half year. Its surface was very clean and shiny.

The distributions are shown for concrete of mix A (average compressive strength = 5400 psi). The anchorage lengths determined from tests with different concrete strengths were normalized to a concrete strength of 5400 psi using the relationship between concrete strength and anchorage length indicated in Fig. 14.2 and 14.3.

Distribution (1) yields a mean anchorage length of 49 strand diameters, or normalized to a concrete strength of 4000 psi (Fig. 14.3),55 strand diameters. The <u>average</u> basic anchorage length for that type of strand would therefore be

$$L = 55\ D \qquad (14.2)$$

The variation of individual anchorage lengths expressed in terms of the mean plus and minus two standard deviations ranged from

33 to 65 strand diameters, or normalized to a concrete strength of 4000 psi, from 39 to 71 strand diameters.

Distribution (2) yields a mean anchorage of 69 strand diameters, or for a concrete strength of 4000 psi, a mean value of 77 strand diameters.

The average basic anchorage length for that type of strand would therefore be

$$L = 77\ D \qquad (14.3)$$

The mean plus minus two standard deviations ranged from 43 to 96 strand diameters, or for a concrete strength of 4000 psi, from 51 to 103 strand diameters.

A direct comparison of anchorage lengths determined on the basis of results from pull-out tests using only concrete of mix A (average concrete strength = 5400 psi) and 7/16-in. strand from coil I and coil II (Table A.2) is presented in Fig. 14.4.

If the individual anchorage lengths of 7/16-in. strand from coil II measured in three prestressed test beams, as described in Appendix F, are normalized to an effective prestress of 175 ksi and a concrete strength of 4000 psi, the average anchorage length is found to be 69 strand diameters, with the individual values varying from 56 to 90 diameters. The "measured" anchorage lengths are thus within the range predicted on the basis of the pull-out tests represented by distribution (2).

As demonstrated by the data in Fig. 14.4, two strands of presumably the same type and diameter may have different bond

characteristics depending on the surface conditions, even if both strands are termed "free of corrosion".

The basic value of the anchorage length for the conditions described above may be affected by several variables. Their influences will be discussed in the following sections.

14.3 Effect of Strand Properties

14.3.1 Prestress Level

It may be assumed that the anchorage length increases approximately in linear proportion to the effective prestress. This assumption was confirmed by tests (Kaar, 1963) and computations based on bond-slip relationships from pull-out tests (Section 13.3, Fig. 13.7).

14.3.2 Strand Size

As expressed by Eq. 14.1, it may be assumed that the anchorage length varies approximately linearly with the strand diameter. This reflects simply the fact that the anchorage length varies in proportion to the bonded area. Anchorage lengths measured by Kaar (1963) as well as results from pull-out tests (Chapter 5, Fig. 5.7, Fig. 14.3) confirm the above assumption.

14.3.3 Surface Conditions

The surface conditions of the strand may have a significant influence on the anchorage length.

(a) Rusted strands were found to have better bond characteristics than clean strand. Depending on the extent of the corrosion, the anchorage length for rusted strand may be up to 30 percent shorter than that for clean strand (Preston, 1963; Hanson, N. W.,1969).

(b) Surface films of grease, oil, or dirt which may be deposited on the strand during handling in the prestressing plant are known to reduce the bond strength significantly. As a result, the anchorage length will be larger than that for clean strand.

14.4 Effect of Concrete Properties

14.4.1 Concrete Strength

Conclusions and test results concerning the effect of the concrete strength on the anchorage length are not quite consistent (see Section F.8.7 and Table F.4). The anchorage lengths predicted on the basis of bond-slip relationships from pull-out tests indicate that the anchorage length decreases with increasing concrete strength (Fig. 14.2, 14.3). Kaar (1963), on the other hand, found on the basis of a large number of beam tests that the concrete strength ranging from 1600 to 5500 psi had no significant influence on the anchorage length.

In practice, the variation of the concrete strength will be relatively small since the prestress will be released as early as possible in most cases. The minimum allowable concrete strength at release of the prestress is according to the Building Code Requirements for Reinforced Concrete (ACI 318-63, paragraph 2618(b)) 3000 psi for strand with diameters equal to or smaller than 3/8 in., and 3500 psi for larger strands. The Standard Specifications for Highway Bridges, AASHO, (Section 1.6.18), requires a minimum concrete strength at the time of the release of prestress of 4000 psi.

In view of the above, it appears advisable to neglect the influence of the concrete strength on the anchorage length and to assume the basic value for the anchorage length as discussed in Section 13.2.

14.4.2 Shrinkage

Results from many pull-out tests have indicated that the bond strength is affected by all variables related to shrinkage such as curing conditions, consistency, and age of the concrete (Chapter 6). This is caused by the fact that the reduction of the concrete volume due to shrinkage initiates lateral pressures at the contact face between strand and concrete. These stresses result in an increase of initial bond strength (see Chapter 8).

Despite the significant influence of shrinkage on the anchorage length, it is not possible to take its effect into account explicitly for practical purposes. However, special bond tests should be made in case expansive or shrinkage-compensating cements are used.

14.4.3 Age of Concrete

The bond strength between strand and concrete was found to increase with the age of the concrete at which the load was applied (Section 6.5). Part of the increase is due to the increase in concrete strength. The greater part is attributable to shrinkage, an effect which appears to be dissipated over a long period of time, possibly because of relief of shrinkage stresses.

For practical purposes, the influence of the age of the concrete on the anchorage length may be neglected, since the time at which the prestress is released in practice varies at the most by a few days. According to the results described in Section 6.5, the effect of the age on the bond strength is hardly noticeable over such a short period of time.

14.5 Effect of Settlement of Concrete

Aggregates and water segregate in the early phases of the fresh concrete due to differences in their specific gravities. If strand is held rigidly with respect to the formwork during the hardening process of the concrete, the solid parts of the concrete mix tend to settle away from the strand in the direction of gravity while the water tends to rise towards the top of the concrete member. This may lead to a reduced area and quality of concrete on that side of the strand that faces into the direction of the gravity forces. The resulting loss of bond strength will depend on the amount of settlement.

Settlement of concrete is affected by many parameters (see Chapter 7). The most significant parameter is the depth of concrete that settles. Results from pull-out tests (Chapter 7) and beam tests (Appendix F) indicated that the bond strength is reduced markedly for depths exceeding two in. of concrete below a horizontally placed strand.

Based on the results of Fig. 7.2 and Table F.2, the following percentages of the basic value of the anchorage length are recommended with respect to the depth of concrete below the strand (Fig. 14.5)

(1) Depth $\leq$ 2 in. 100% of basic value

(2) Depth $\geq$ 12 in. 140% of basic value

For depths ranging from 2 to 12 in., values for the required anchorage lengths may be obtained by a linear interpolation.

Draped strands may be treated as horizontal strands. An average depth of concrete may be assumed within the anchorage zone.

For strands prestressed in the vertical direction, no test data are available. Concluding from results obtained with deformed bars, an increase of the basic value of the anchorage length by at least 40 percent seems to be advisable.

14.6 Effect of Lateral Pressure

Lateral compressive stresses acting perpendicular to the contact face between strand and concrete were found to have a significant influence on the bond strength (Chapter 8). Although no direct results concerning the anchorage length are available, it may be expected that the anchorage length is influenced to the same extent by lateral pressure as the bond-slip relationships developed in pull-out tests.

In practice, lateral compressive stresses perpendicular to the strand in the anchorage zone may be caused by various sources such as support reactions, lateral prestressing forces, or shrinkage deformations. Since it is difficult to predict the stress conditions at the contact between strand and concrete, the consideration of the beneficial influence of lateral stresses on the anchorage length does not seem to be justified unless tests under similar stress conditions show otherwise.

14.7 Effect of Time

Bond between strand and concrete is provided by two mechanisms: (a) mechanical interlocking between the microscopically rough strand surface and the concrete which does not permit any measurable slip, and (b) a friction mechanism between two sliding contact surfaces

after the interlocks have sheared off (see Chapter 11 and 12). During the frictional phase, the strand must wind or twist itself through a rigid predetermined concrete channel. Although the torsional stiffness of the strand is too small to cause a significant increase of contact pressure between the strand and the concrete to increase the bond strength, it was found that slight variations of the pitch or the diameter of the strand along its axis causes wedging of the strand. This lack-of-fit effect, which increases with the slip, causes the bond strength to increase after the interlocks have sheared off. In contrast to that, the bond stress of plain wire drops immediately after the shear failure of the interlocking keys because wire does not exhibit this lack-of-fit effect. Typical bond-slip relations for strand and plain wire are shown in Fig. B.1.

Pull-out tests subjected to sustained loading over a period of 15 months have implied that the initial interlocking bond strength may decay with time. In series SBL12-1, the strand started to slip after a period of one half year. This may have been due to a gradual reduction of contact stresses between strand and concrete due to creep and the formation of shrinkage cracks. The reduction may be as large as 20 to 30 percent.

The frictional bond of strand at large slips appears to be less sensitive to time under sustained loading than the initial bond because the lack-of-fit effect which is responsible for the relatively high bond strength at large slips depends more on geometric conditions and less on the state of lateral stresses. Pull-out specimens that

have slipped under sustained loading seemed to reach a state of equilibrium at a slip of approximately 0.1 in.

The end slip of strand caused by the transfer of the prestress is on the order of 0.05 to 0.1 in. depending on variables such as level of prestress, size of strand, or type of release. With the assumption that the bond strength due to sustained loading is reduced by 5 percent at a slip of 0.1 in. and by 20 to 30 percent at a slip of 0.0001 in., the average bond strength affecting the anchorage length may be assumed to be reduced by 10 to 15 percent if the slip distribution within the anchorage zone is taken into consideration. Accordingly, the anchorage length of strand may possibly increase under sustained loading by 10 to 15 percent.

A definite increase of the anchorage length of strand with time has not been observed over periods up to one year (Rüsch, 1963; Kaar, 1963; Appendix F). It must be noted, however, that in the tests the prestress decreased with time due to shrinkage and creep of the concrete and relaxation losses in the strand. This loss of prestress may balance the reduction of the bond strength. Kaar (1963) adjusted the anchorage lengths measured at certain time intervals to the original prestress and found that the average increase of the anchorage length would be approximately 6 percent, the maximum increase 19 percent. These values, however, were not observed actually.

The influence of time on the anchorage length of plain prestressing wire may be more significant than that for strand. As pointed out above, frictional bond of plain wire is not improved by

the lack-of-fit effect. Consequently, the bond stresses depend on lateral stresses throughout the whole range of slip. The reduction of the bond stress, or the increase of the anchorage length, may therefore be expected to be possibly as much as 20 to 30 percent if the same assumptions are made as for strand.

Test results reported in literature vary considerably. Roŝ (1946) reported that the anchorage length of 2- and 3-mm wires doubled with time. Marshall (1949), and Evans (1955) found an approximately 100-percent increase in the anchorage length of plain 0.08-in. wire over a period of one year. On the other hand, Base (1957) reported that the anchorage length of plain 0.2-in. wire increased very little over a period of one half year. Rüsch (1963) found no increase in the anchorage length of plain 2-mm wire over a period of three months.

On the basis of the understanding of the bond mechanism developed in this investigation and the evidence provided by Roŝ (1946), Marshall (1949), and Evans (1955), it would not be unreasonably conservative to assume that the anchorage length for wire would increase with time by as much as 100 percent.

14.8 Effect of Workmanship

14.8.1 Vibration

Bond-slip relationships from pull-out tests indicated that omitting vibration of the concrete may lead to a reduction of the bond strength by as much as 40 percent (Fig. 7.2). In order to ensure a short anchorage length, the vibration of the concrete in the anchorage zone should be carried out with special care.

14.8.2 Release of Prestress

The anchorage length was found to be sensitive to the manner of release of the prestressing force by several investigators (Kaar, 1963; Rüsch, 1963; Hanson, N. W.,1969). Releasing the prestress gradually resulted in the shortest anchorage length. Cutting the strand increased the anchorage length to a maximum. The difference was found to be as high as 20 percent for strands up to 1/2-in. diameter, and as high as 30 percent for 6/10-in. strand (Kaar, 1963).

14.9 Concluding Remarks

Although the anchorage length depends on many parameters which cannot be controlled by the designer, a knowledge of the range of the anchorage length that may be expected under certain circumstances is required in design of pretensioned prestressed structures.

The average anchorage length may be estimated by the following expression.

$$L = A\ B\ C\ D\ \frac{f_{se}}{175} \qquad (14.4)$$

where L = anchorage length in in.

A = Factor reflecting the depth of concrete below the strand (Section 14.5). This factor may range from 1.0 to 1.4.

B = Factor reflecting the type of release of the prestress (Section 14.8.2). This factor may vary between 1.0 and 1.3. Assuming that the strand is cut after careful preheating of the strand, an average value of 1.1 may be assumed.

C = Factor reflecting the surface roughness of the steel. Its value is discussed in Section 14.2.

D = nominal strand diameter in in.

f_{se} = effective prestress in the strand immediately after release of the prestress in ksi.

Other factors than those given in Eq. 14.4 are more difficult to quantify. It is possible, however, since the quality of the workmanship is of great significance for a short anchorage length, to demand a tight control over it by the manufacturer.

In general, the designer does not know the surface conditions of the strand which is going to be used in the structure. Consequently, he has to use a safe value for the coefficient C. On the basis of the results described in Section 14.2 and anchorage lengths measured in beams (Table F.4), a value of C = 70 appears to be adequate. Thus, the anchorage length may be estimated by the expression

$$L = 70\ A\ B\ D\ \frac{f_{se}}{175} \qquad (14.5)$$

It should be emphasized that this equation refers to an average value. In choosing an anchorage length, the designer should consider the significance of an overestimate of the bond strength on the safety and serviceability of the structure. In investigating shear stresses near the supports, it would not be overconservative to increase the value given by Eq. 14.5 by 50 percent. On the other hand, in investigating anchorage-zone stresses, the value given by Eq. 14.5 should be reduced by 50 percent.

In case the information concerning the anchorage length of prestressing strand under a given set of conditions is not sufficient, it is advisable to perform a series of pull-out tests as described in Appendix A under the conditions for which the information is required and use the average bond-slip relationship to estimate the anchorage length. Since the bond-slip relationship of strand is generally a fairly flat curve, a good estimate of the anchorage length may be obtained by using an average unit bond force.

15. SUMMARY

The main objective of this investigation was to develop a fundamental understanding of the nature of bond between strand and concrete and to establish the effects of various parameters on the anchorage length for prestressing strand.

The experimental part of this investigation consisted of 486 pull-out tests and five prestressed-beam tests. With a few exceptions, the pull-out tests had an embedment length of one in. in order to obtain bond-slip relationships that were nearly independent of the bonded length and characteristic for the strand used.

A hypothesis was developed to describe the nature of bond between strand and concrete. It was shown that the test results of the one-in. pull-out tests could be applied directly to practical design problems. Recommendations for the anchorage length of strand in pre-tensioned prestressed beams are made on the basis of data from pull-out tests as well as beam tests.

The hypothesis on the nature of bond between strand and concrete may be summarized as follows:

(1) Bond between strand and concrete is provided by two mechanisms: (a) a physical interlocking between the microscopically rough steel surface and the surrounding concrete and (b) a frictional mechanism between two sliding contact surfaces after the original interlocks have sheared off. No significant slip (less than 0.0001 in.) takes place during the initial interlocking phase.

(2) During the frictional phase, the strand slips. Because of the helical arrangement of the exterior wires, strand rotates while slipping through the concrete channel. The maximum torsional moment created by this rotation was found to produce contact pressures between the strand and the concrete that were too small to cause a significant increase in bond.

(3) Ideally, the bond characteristics of a perfectly made strand (if every cross section along the length of the strand is identical) should be similar to those of plain wire. However, slight irregularities in the arrangement of the exterior wires result in wedging of the strand in the concrete channel. This deformed-bar effect acts only during the frictional phase and increases with the slip.

The bond-slip characteristics of strand as measured in the pull-out tests were found to be influenced by the following variables:

(4) Strand diameter: The bond strength per unit length of strand increased approximately in linear proportion to the strand diameter which was varied in this investigation from 1/4 to 1/2 in.

(5) Concrete strength: The bond strength of strand increased by approximately ten percent per 1000 psi of concrete compressive strength. The range of concrete strengths in the tests varied from 2400 to 7600 psi.

(6) Shrinkage: The lateral pressure due to shrinkage acting normal to the surface of the embedded strand increased

the bond strength markedly. Therefore, all parameters investigated that varied with shrinkage were found to affect the bond strength. Such variables were consistency, curing conditions, and age of the concrete.

(7) Settlement of Concrete: The bond strength of strand held in a horizontal position during casting decreased rapidly with increasing depth of concrete below the strand due to settlement of the fresh concrete. A depth of concrete of six in. below the strand caused the bond strength to drop by as much as 30 percent with respect to that obtained for a concrete depth of two in. Beyond a concrete depth of ten in., the bond strength tended to approach a constant value. The maximum observed reduction of the bond strength was approximately 35 percent with respect to the average bond strength developed for a depth of two in.

(8) Lateral pressure: Results from pull-out specimens subjected to externally applied lateral pressures ranging from zero to 2500 psi indicated a linear increase of the bond strength of strand with the lateral pressure. The effect was greater for the initial bond strength (interlocking phase) than for the frictional phase.

(9) Time effects: (a) The effect of the age of the concrete was not investigated systematically. However, the available test data indicate that the initial bond strength may increase during the first 20 to 50 days and then decrease

again. At a concrete age of 15 months, the initial bond strength was almost identical to that developed at an age of eight days. (b) Under sustained loading, the initial bond strength appeared to decay. The reduction of the initial bond strength which may take place as late as one half year after the application of the load may possibly be as high as 30 percent. The bond strength at large slips (0.1 in.) was less sensitive to sustained loading.

A major objective of this investigation was to apply the results from the pull-out tests directly to practical problems.

(10) With the aid of a simple iteration procedure and the results from one-in. pull-out tests, it was possible to predict the measured bond-slip relationship, both for the attack-end and the trail-end slip, for any given bonded length of strand subjected to pull-out forces.

Using the same procedure it was possible to calculate the anchorage length of strand in a pretensioned prestressed beam for any given prestress. The results demonstrated that data from one-in. pull-out tests with nonprestressed strand can be used directly to determine the anchorage length of a prestressed strand.

On the basis of results from pull-out tests, and prestressed beam tests conducted during this investigation and in other laboratories, the following recommendations may be made with respect to the anchorage length of strand:

(11) The anchorage length is a direct function of the strand diameter and the prestress. The average anchorage length, L, may be expressed as

$$L = 70\ A\ B\ D\ \frac{f_{se}}{175} \qquad (15.1)$$

where A = coefficient reflecting the settlement of the concrete (range: 1.0 to 1.4, depending on the depth of the concrete below the strand); B = coefficient reflecting the type of release of the prestress (range: 1.0 to 1.3); D = nominal strand diameter, f_{se} = effective prestress (in ksi) immediately after release of the prestressing force.

Equation 15.1 represents an average value based on laboratory tests without representing factors such as surface conditions of the strand, concrete properties, and quality of workmanship. According to observations made with pull-out tests, the average anchorage length may vary under field or plant conditions from values 50 percent smaller to 50 percent higher than that suggested by Eq. 15.1.

LIST OF REFERENCES

1. Abrams, D. A., "Tests of Bond Between Concrete and Steel", Engineering Experiment Station, University of Illinois, Bulletin No. 71, Urbana, December 1913.

2. ACI Committee 408, "Bond Stress - The State of the Art", Journal of the American Concrete Institute, Proceedings, Vol. 63, No. 11, November 1966, pp. 1161-1190.

3. Anderson, W. R., "Steel for Prestressed Concrete", Journal of the Prestressed Concrete Institute, Vol. 9, No. 2, April 1964, pp. 108-116.

4. Archard, I. F., "Elastic Deformation and the Laws of Friction", Proceedings of the Royal Society, Ser. A, Vol. 243, London, 1957, pp. 190-205.

5. Base, G. D., "Some Tests on the Effect of Time On Transmission Length in Pretensioned Concrete", Magazine of Concrete Research, Vol. 9, No. 26, August 1957, pp. 73-83.

6. Base, G. D., "An Investigation of Transmission Length in Pre-Tensioned Concrete", III. Congress of the Fédération Internationale de la Précontrainte, Session III, Paper No. 9, Berlin, 1958, pp. 603-623.

7. Bowden, F. P., and G. W. Rowe, "The Adhesion of Clean Metals", Proceedings of the Royal Society, Ser. A, Vol. 233, London, 1956, pp. 429-442.

8. Bowden, F. P., and D. Tabor, "The Friction and Lubrication of Solids", Part I and Part II, Clarendon Press, Oxford, 1964.

9. Brown, C. B. "Bond Failure Between Steel and Concrete", Journal of the Franklin Institute, Vol. 282, No. 5, 1966, pp. 271-290.

10. Brown, C. B., and Z. S. Szabo, "A Study of Bond Between Steel and Restrained Expanding Concrete", Magazine of Concrete Research, Vol. 20, No. 62, March 1968, pp. 3-12.

11. "Building Code Requirements for Reinforced Concrete (ACI 318-63)", American Concrete Institute, Detroit, Michigan, June 1963.

12. Clark, A. P. "Comparative Bond Efficiency of Deformed Concrete Reinforcing Bars", Journal of the American Concrete Institute, Proceedings, Vol. 43, No. 4, December 1946, pp. 381-400.

13. Debly, L. J. "Static Tests on Prestressed Concrete Beams Using 7/16-in. Strands", Lehigh University, Fritz Engineering Laboratory, Progress Report No. 13 on Prestressed Concrete Bridge Members, November 1956.

14. Dinsmore, G. A., P. L. Deutsch, and J. L. Montemayor, "Anchorage and Bond in Pretensioned Prestressed Concrete Members", Lehigh University, Fritz Engineering Laboratory Report 223-19, December 1958.

15. Dokos, S. J., "Sliding Friction Under Extreme Pressures", Journal of Applied Mechanics, Vol. 13, No. 2, June 1946, pp. 148-156.

16. Evans, R. H., and G. W. Robinson, "Bond Stresses in Prestressed Concrete from X-Ray Photographs", Proceedings of the Institution of Civil Engineers, Part I, Vol. 4, No. 2, March 1955, pp. 212-235.

17. Evans, R. H., and A. Williams, "The Use of X-Rays in Measuring Bond Stresses in Prestressed Concrete", World Conference on Prestressed Concrete, San Francisco, July/August 1957.

18. Evans, R. H., "Research and Development in Prestressing", Journal of the Institution of Civil Engineers, Vol. 35, No. 4, February 1961, pp. 231-261.

19. Ferguson, P. M., and J. N. Thompson, "Development Length of High Strength Reinforcing Bars in Bond", Journal of the American Concrete Institute, Proceedings, Vol. 59, No. 7, July 1962, pp. 887-922.

20. Fumagalli, E., "Caratteristiche di resistenza dei conglomerati cementizi per stati di compressione pluriassiali," (Characteristics of the Strength of Concrete Under Multiaxial Compression), Instituto Sperimentale Modelli e Strutture (I.S.M.E.S.), Bergamo, Bulletin No. 30, October 1965.

21. Gemant, A., "Frictional Phenomena", Chemical Publishing Company, Inc., Brooklyn, N. Y., 1950.

22. Gilkey, H. I., S. I. Chamberlin, and R. W. Beal, "The Bond Between Concrete and Steel," Journal of the American Concrete Institute, Proceedings, Vol. 35, No. 1, September 1938, pp. 1-20.

23. Hajnal-Konyi, K., "Bond Between Concrete and Steel", Structural Concrete, Vol. 1, No. 9, May/June 1963, pp. 373-390.

24. Hanson, J. M., and C. L. Hulsbos, "Overload Behavior of Pretensioned Prestressed Concrete I-Beams With Web Reinforcement", Highway Research Record, No. 76, 1965, pp. 1-31.

25. Hanson, N. W., and P. H. Kaar, "Flexural Bond Tests of Pre-Tensioned Prestressed Beams", Journal of the American Concrete Institute, Proceedings, Vol. 55, No. 7, January 1959, pp. 783-802

26. Hanson, N. W. "Influence of Surface Roughness of Prestressing Strand on Bond Performance", Journal of the Prestressed Concrete Institute, Vol. 14, No. 1, February 1969, pp. 32-45.

27. Hognestad, H., N. W. Hanson, and D. McHenry, "Concrete Stress Distribution in Ultimate Strength Design," Journal of the American Concrete Institute, Proceedings, Vol. 52, No. 4, December 1955, pp. 455-480.

28. Ishlinski, A. Y. and I. V. Kraghelskii,"On Stick-Slip in Friction" (in Russian), Journal of Technical Physics, (Zhur. Tekhn. Fiz.), No. 14, 1944, pp. 276-282.

29. Janney, J. R., "Nature of Bond in Pre-Tensioned Prestressed Concrete", Journal of the American Concrete Institute, Proceedings, Vol. 50, No. 9, May 1954, pp. 717-736.

30. Kaar, P.H., R. W. LaFraugh, and M. A. Mass, "Influence of Concrete Strength on Strand Transfer Length", Journal of the Prestressed Concrete Institute, Vol. 8, No. 5, October 1963, pp. 47-67.

31. Keuning, R. W., M. A. Sozen, and C. P. Siess, "A Study of Anchorage Bond in Prestressed Concrete", University of Illinois, Civil Engineering Studies, Structural Research Series No. 251, June 1962.

32. Kraghelskii, I. V., "Friction and Wear", Butterworths, London 1965.

33. Leonhardt, F. "Prestressed Concrete, Design and Construction", Second Edition, Wilhelm Ernst & Sohn, Berlin 1964.

34. Leonhardt, F., "On The Need to Consider the Influence of Lateral Stresses on Bond", Proceedings, Symbosium on Bond and Crack Formation in Reinforced Concrete", (Stockholm 1957), Vol. 1, RILEM, Paris, (published by Tekniska Högskolans Rotaprinttryckery, Stockholm, 1958).

35. Lin, T. Y., "Design of Prestressed Concrete Structures", Second Edition, John Wiley & Sons, Inc., New York 1963.

36, Linger, D. A., and S. R. Bhonsle, "An Investigation of Transfer Length in Pretensioned Concrete Using Photoelasticity", Journal of the Prestressed Concrete Institute, Vol. 8, No. 4, August 1963, pp. 13-30.

37. Marshall, G. "End Anchorage and Bond Stresses in Prestressed Concrete", Magazine of Concrete Research, No. 3, December 1949, pp. 123-127.

38. Martin, H., "Die Haftung der Bewehrung im Stahlbeton", (Bond of Reinforcement in Reinforced Concrete), RADEX-RUNDSCHAU, No. 2, April 1967, pp. 486-509.

39. McFarlane, J. S., and D. Tabor, "Adhesion of Solids and the Effect of Surface Films", Proceedings of the Royal Society, Ser. A, Vol. 202, 1950, pp. 224-243.

40. Menzel, C. A., "Effect of Settlement of Concrete on Results of Pull-Out Bond Tests", Research Department Bulletin No. 41, Research and Development Laboratories, Portland Cement Association, November 1952.

41. Menzel, C. A., and W. M. Woods, "An Investigation of Bond, Anchorage and Related Factors in Reinforced Concrete Beams", Research Department Bulletin No. 42, Research and Development Laboratories, Portland Cement Association, November 1952.

42. Over, R. S., and T. Au, "Prestress Transfer Bond of Pretensioned Strands in Concrete", Journal of the American Concrete Institute, Proceedings, Vol. 62, No. 11, November 1965, pp. 1451-1460.

43. Peattie, K. R. and J. A. Pope, "Effect of Age of Concrete on Bond Resistance", Journal of the American Concrete Institute, Proceedings, Vol. 52, No. 6, February 1956, pp. 661-672.

44. Pecknold D. A., and W. C. Schnobrich, "Finite Element Analysis of Skewed Shallow Shells", Journal of the Structural Division, ASCE, Vol. 95, No. ST4, April 1969, pp. 715-744.

45. Picket, G., "Effect of Aggregate on Shrinkage of Concrete and a Hypothesis Concerning Shrinkage", Journal of the American Concrete Institute, Proceedings, Vol. 52, January 1956, pp. 581-590.

46. Plowman, J. M., "The Measurement of Bond Strength", Proceedings, Symbosium on Bond and Crack Formation in Reinforced Concrete, (Stockholm 1957), RILEM, Paris (published by Tekniska Högskolans Rotaprinttryckery, Stockholm 1958).

47. Plowman, J. M., "Bond Between Concrete and Steel", Structural Concrete, Vol. 1, No. 9, May/June 1963, pp. 391-401.

48. Podolny, W., "Understanding the Steel in Prestressing", Journal of the Prestressed Concrete Institute, Vol. 12, No. 5, October 1967, pp. 54-66.

49. Preston, H. K., "Characteristics of 15% Stronger Seven-Wire Strand", Journal of the Prestressed Concrete Institute, Vol. 8, No. 1, February 1963, pp. 39-45.

50. Rabinowicz, E., "Friction and Wear of Materials", John Wiley and Sons, Inc., New York, 1965.

51. Ratz, E. H., M. M. Holmjanski, and V. M. Kolner, "The Transmission of Prestress to Concrete by Bond", III. Congress of the Federation Internationale de la Precontrainte, Session III, Paper No. 10, Berlin 1958, pp. 624-640.

52. Rehm, G., "Über die Grundlagen des Verbundes zwischen Stahl und Beton", (On the Fundamentals of Bond Between Steel and Concrete), Deutscher Ausschuss für Stahlbeton, Heft 138, Berlin, 1961.

53. Roš, M., "Vorgespannter Beton", (Prestressed Concrete), Eidgenössische Materialpfrüfungs und Versuchsanstalt für Industrie, Bauwesen und Gewerbe, E.M.P.A. Report No. 155, Zürich, March 1946.

54. Rüsch, H., and G. Rehm, "Versuche zur Bestimmung der Übertragungslänge von Spannstählen", (Tests for the Determination of Transfer Lengths of Prestressing Steels), Deutscher Ausschuss fur Stahlbeton, Heft 147, Berlin, 1963, pp. 1-38.

55. Sampson, J. B., F. Morgan, D. W. Reed, and M. Muskat, "Friction Behavior During the Slip Portion of the Stick-Slip Process", Journal of Applied Physics, Vol. 14, No. 12, December 1943, pp. 689-700.

56. Schmidt, A. O., and E. J. Weiter, "Coefficients of Flat-Surface Friction", Mechanical Engineering, Vol. 79, No. 12, December 1957, pp. 1130-1136.

57. Standard Specifications for Highway Bridges, AASHO, Nineth Edition, 1965.

58. Thorsen, N., "Use of Large Tendons in Pre-Tensioned Concrete", Journal of the American Concrete Institute, Proceedings, Vol. 52, No. 6, February 1956, pp. 649-660.

59. Timoshenko, S. and J. N. Goodier, "Theory of Elasticity", Second Edition, McGraw Hill Book Company, Inc. New York 1951.

60. Timoshenko, S., "Strength of Materials," Part I, Third Edition, Van Nostrand Comp., Inc., New York, 1955.

61. Untrauer, R. E., and R. L. Henry, "Influence of Normal Pressure on Bond Strength", Journal of the American Concrete Institute, Proceedings, Vol. 62, No. 5, May 1965, pp. 577-585.

62. Walker, S., and D. L. Bloem, "Effects of Aggregate Size on Properties of Concrete", Journal of the American Concrete Institute, Proceedings, Vol. 57, September 1960, pp. 283-298.

63. Warner, R. F., and C. L. Hulsbos, "Fatigue Properties of Prestressing Strand", Journal of the Prestressed Concrete Institute, Vol. 11, No. 1, February 1966, pp. 32-52.

64. Watanabe, A., "Studies on the Friction Coefficient of Prestressing Wire of Pretensioned Prestressed Concrete and its Measuring Method", (in Japanese), Transactions of the Japan Society of Civil Engineers, No. 135, November 1966, pp. 32-42.

65. Welch, G. B., and B. J. F. Patten, "Factors Affecting Bond Between Concrete and Reinforcement", Constructional Review, Vol. 34, No. 2, Sidney, Australia, February 1961, pp. 31-39.

66. Welch, G. B. and B. J. F. Patten, "Bond Strength of Reinforcement Affected by Concrete Sedimentation", Journal of the American Concrete Institute, Proceedings Vol. 62, No. 2, February 1965, pp. 251-264.

Table 13.1

COMPARISON OF EXPERIMENTAL AND CALCULATED DATA FOR PRESTRESSED BEAMS

		Beam PBB-1	PBB-2	PBB-3
Prestress before Release (ksi)		169.7	168.7	165.7
Effective Prestress (ksi)		161.4	160.8	157.5
L(90) measured	South	22	20	23.5
at Release End (in.)	North	21	20.5	20.5
L(90) measured	South	24	19	24
at Fixed End (in.)	North	22	18	28
Measured Average L(90) (in.)		22.5	19.4	24.0
Calculated L(90) (in.)		24.6	24.3	23.8
End Slip measured	South	0.068	0.051	0.076
at Release End (in.)	North	0.064	0.067	0.064
End Slip measured	South	0.071	0.075	0.071
at Fixed End (in.)	North	0.073	0.062	0.070
Measured Average End Slip (in.)		0.069	0.064	0.070
Calculated End Slip (in.)		0.075	0.072	0.070

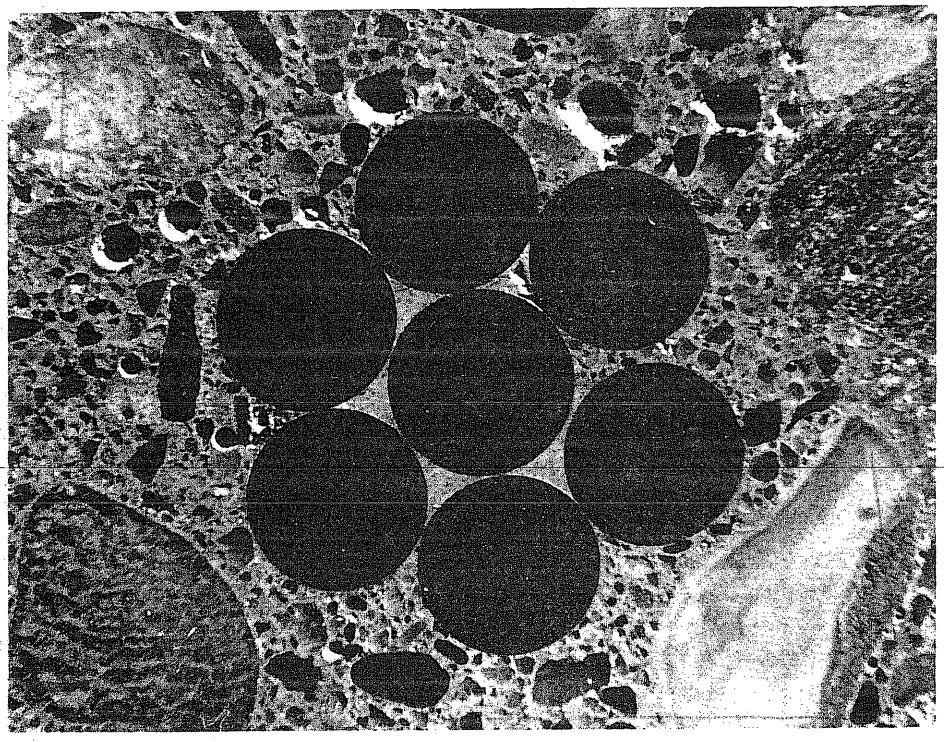

FIG. 1.1 CROSS SECTION OF STRAND CAST IN CONCRETE

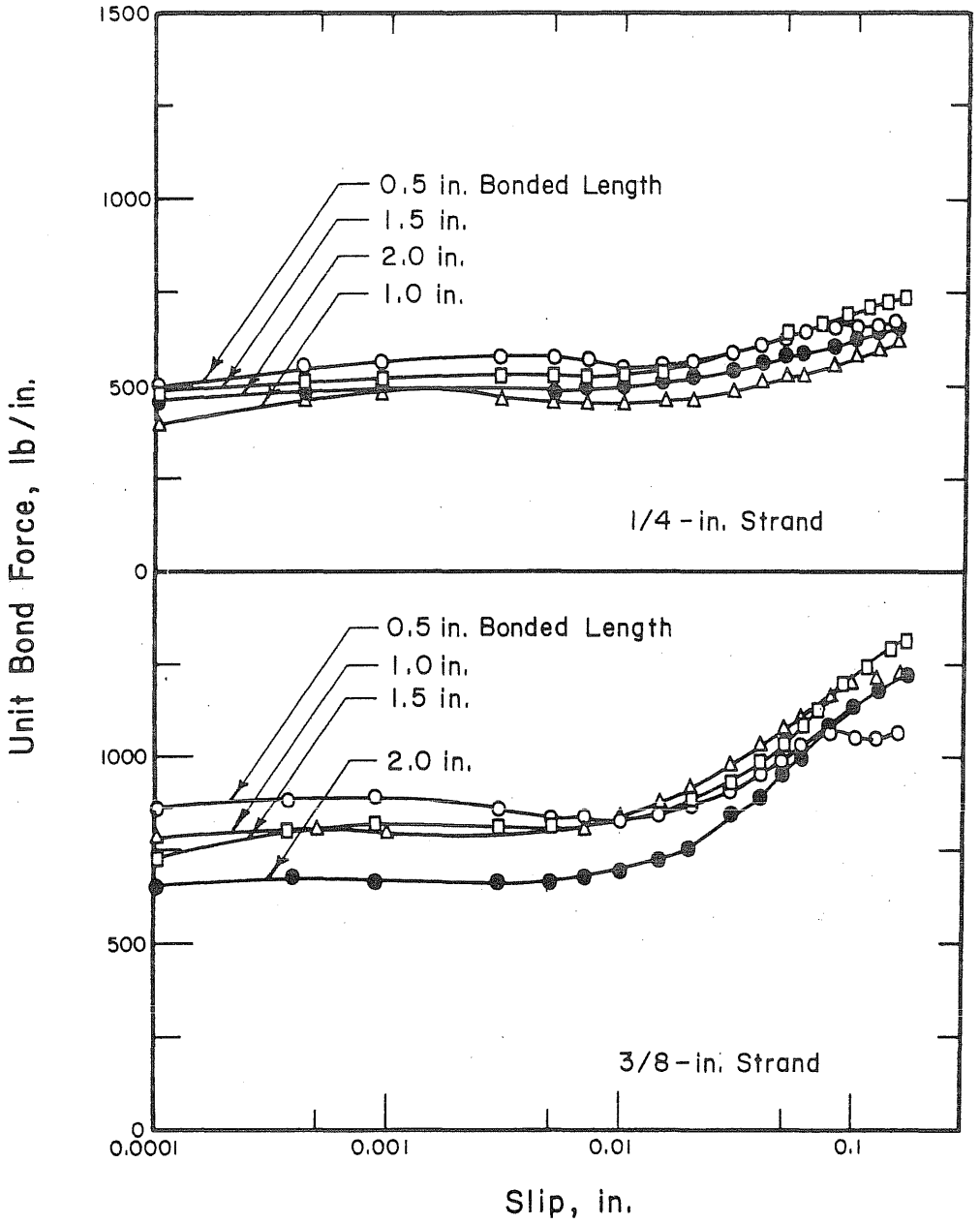

FIG. 3.1 AVERAGE UNIT BOND FORCE-SLIP RELATIONSHIPS OF STRAND FOR VARIOUS BONDED LENGTHS, SERIES: SA09-1, SA09-2

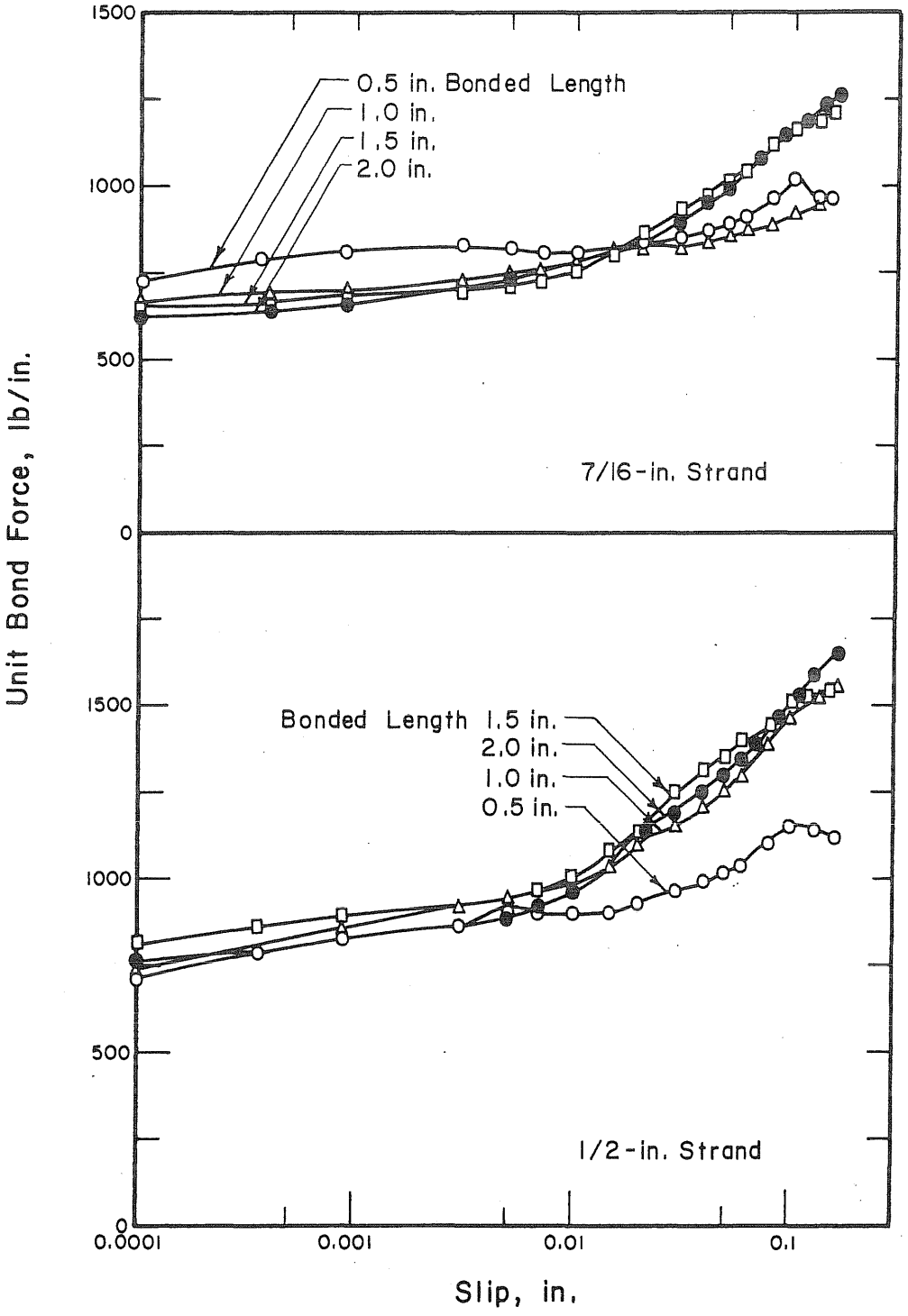

FIG. 3.2 AVERAGE UNIT BOND FORCE-SLIP RELATIONSHIPS OF STRAND FOR VARIOUS BONDED LENGTHS, SERIES: SA08-3, SA09-4

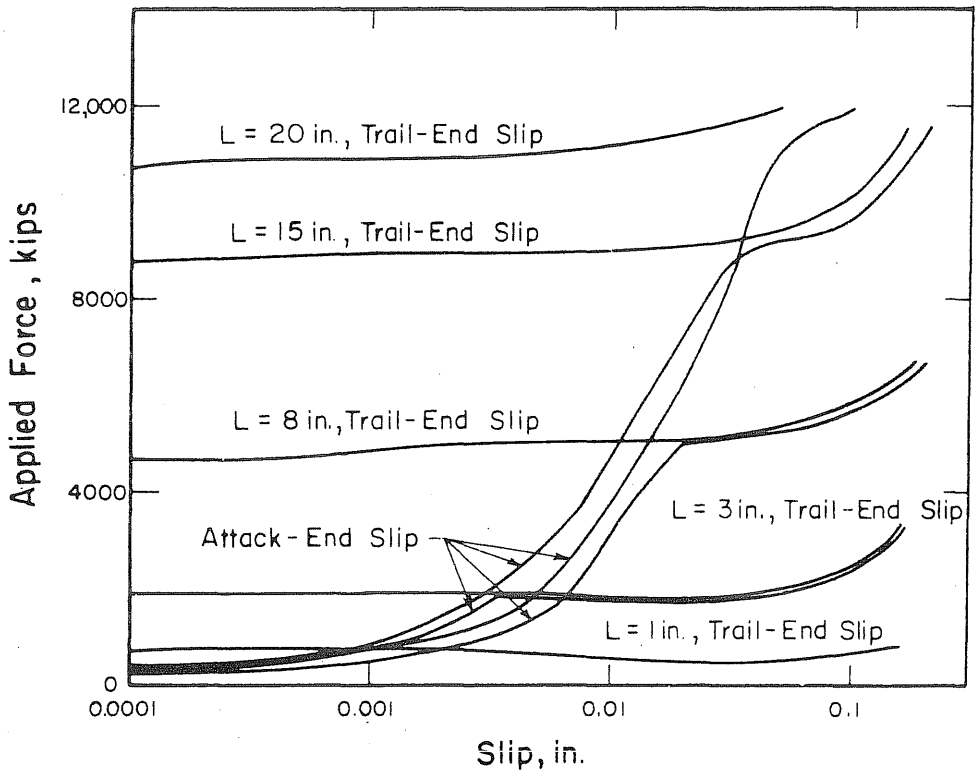

FIG. 3.3 AVERAGE FORCE-SLIP RELATIONSHIPS OF 7/16-In. STRAND FOR VARIOUS BONDED LENGTHS, SERIES:SA09-18

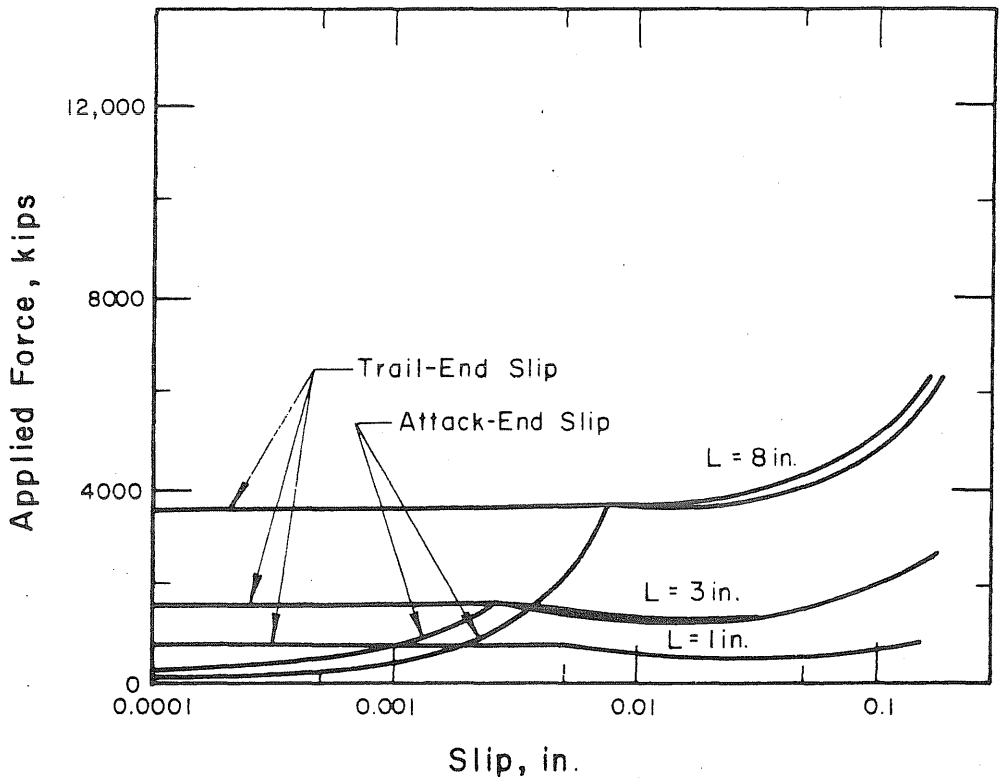

FIG. 3.4 AVERAGE FORCE-SLIP RELATIONSHIPS OF 7/16-in. STRAND FOR VARIOUS BONDED LENGTHS, SERIES: SA10-19

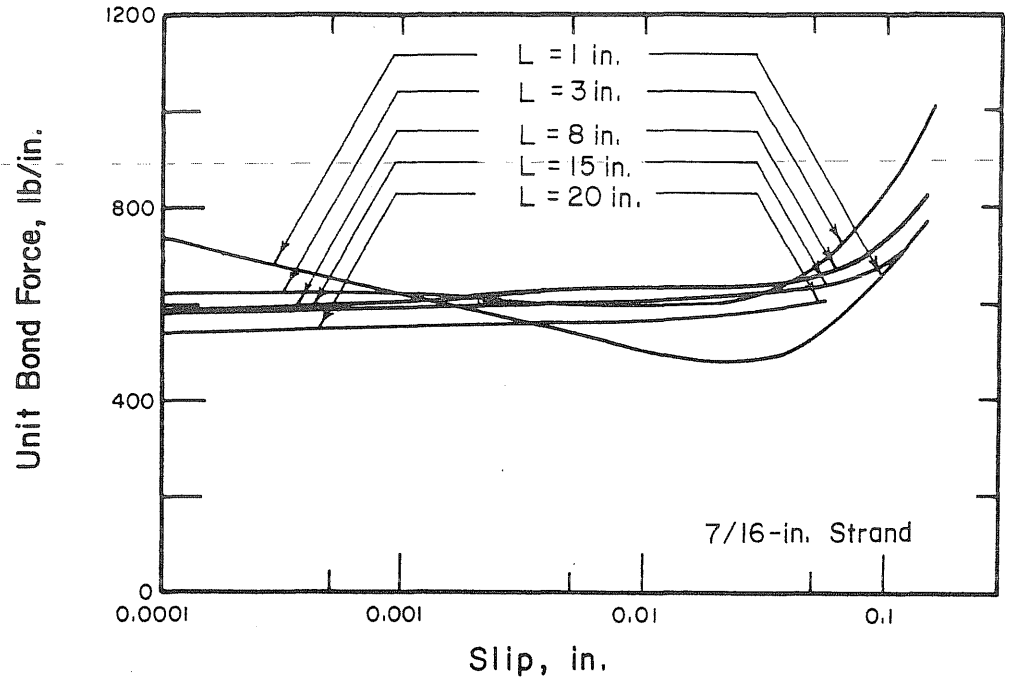

FIG. 3.5 AVERAGE UNIT BOND FORCE vs. TRAIL-END SLIP RELATIONSHIPS FOR DIFFERENT BONDED LENGTHS, SERIES: SA09-18

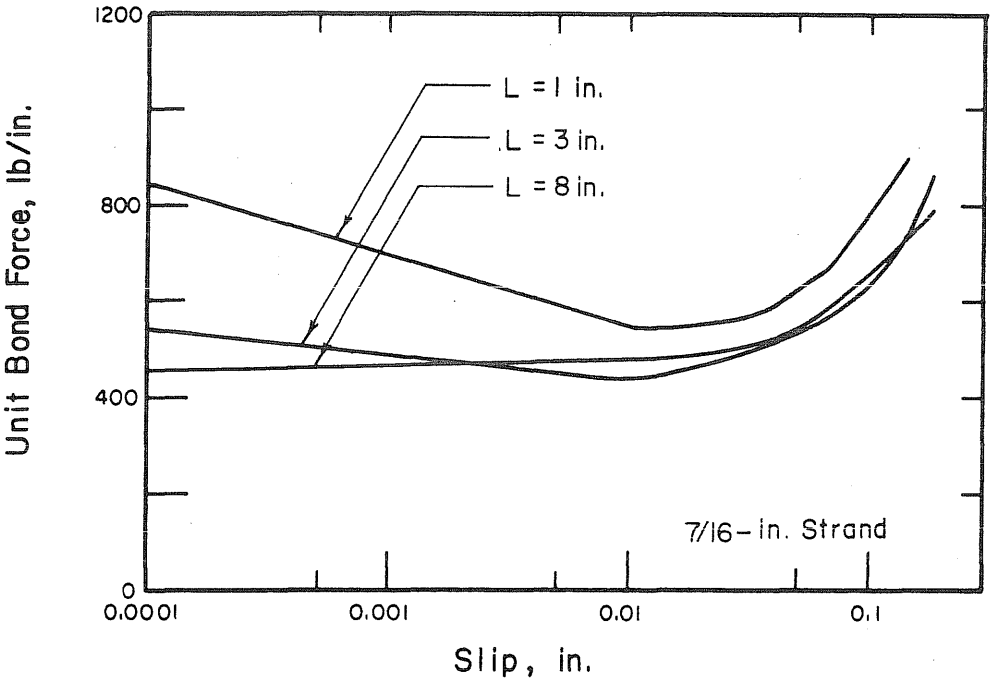

FIG. 3.6 AVERAGE UNIT BOND FORCE vs. TRAIL-END SLIP RELATIONSHIPS FOR DIFFERENT BONDED LENGTHS, SERIES: SA10-19

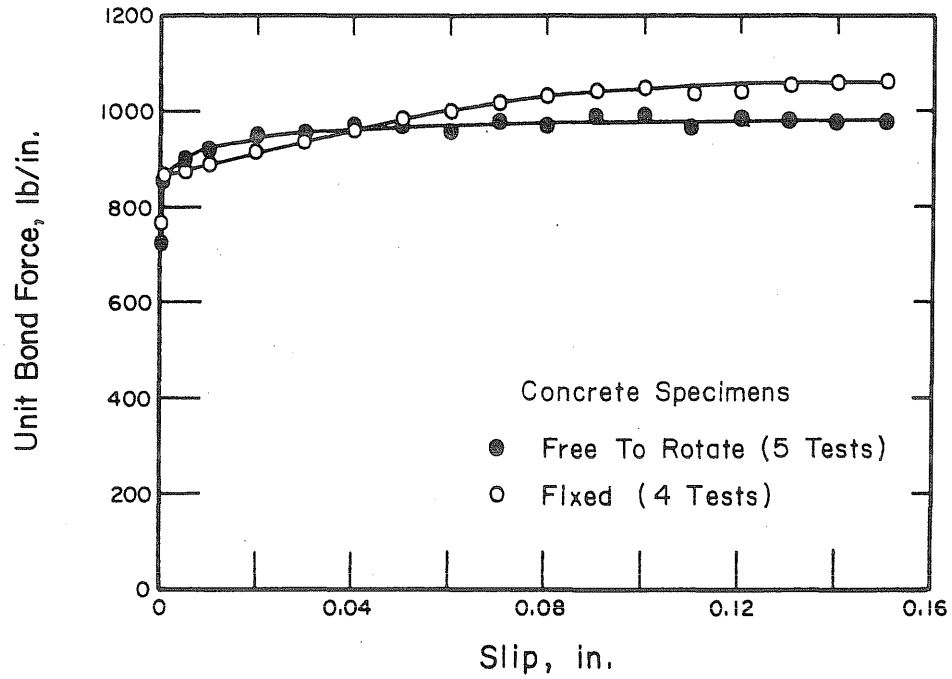

FIG. 3.7 AVERAGE UNIT BOND FORCE-SLIP RELATIONSHIPS OF 7/16-in. STRAND FOR DIFFERENT TEST SETUPS, SERIES: SA08-5

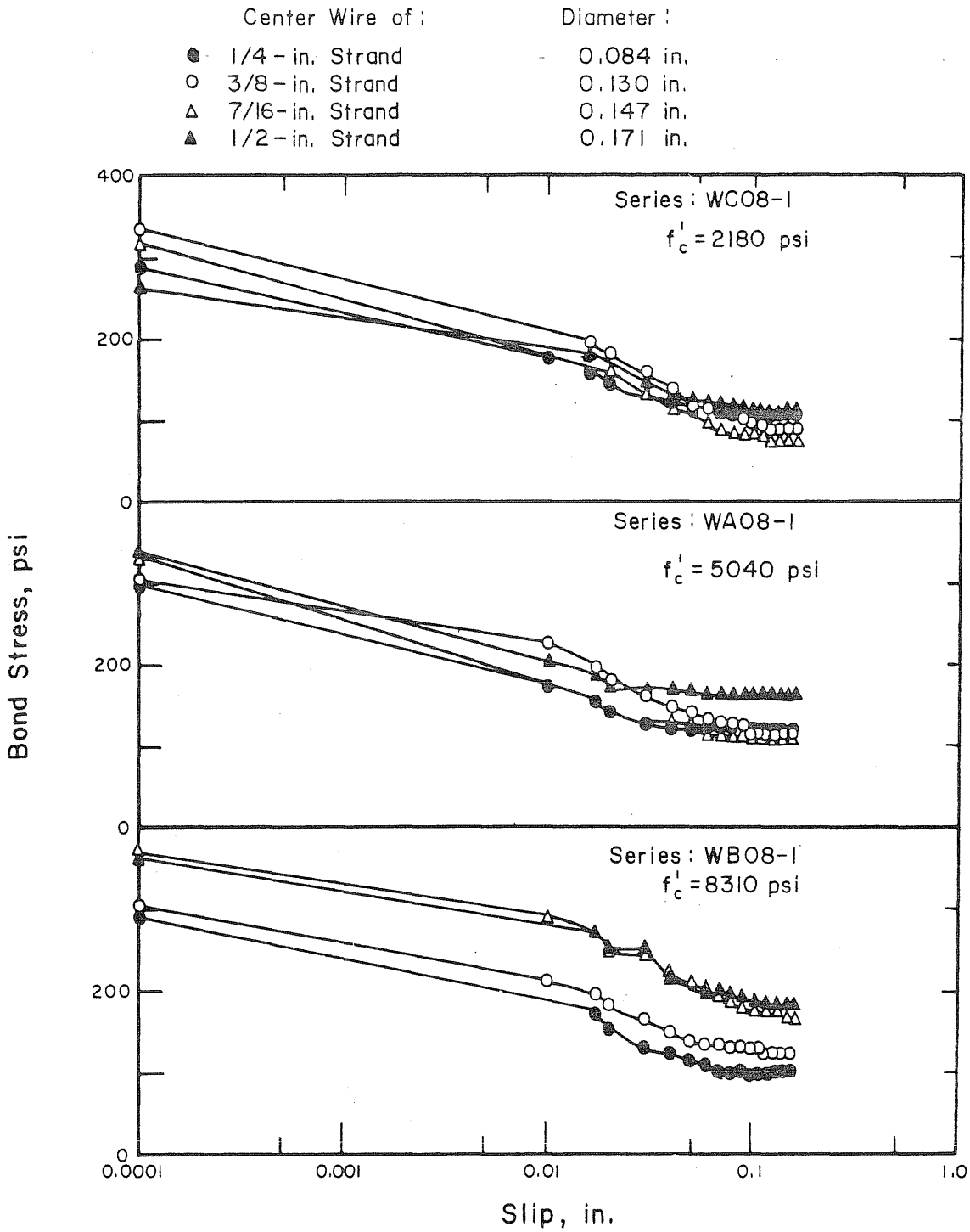

FIG. 4.1 AVERAGE BOND STRESS-SLIP RELATIONSHIPS FOR CENTER WIRES OF DIFFERENT STRAND SIZES, SERIES WC08-1, WA08-1, WB08-1

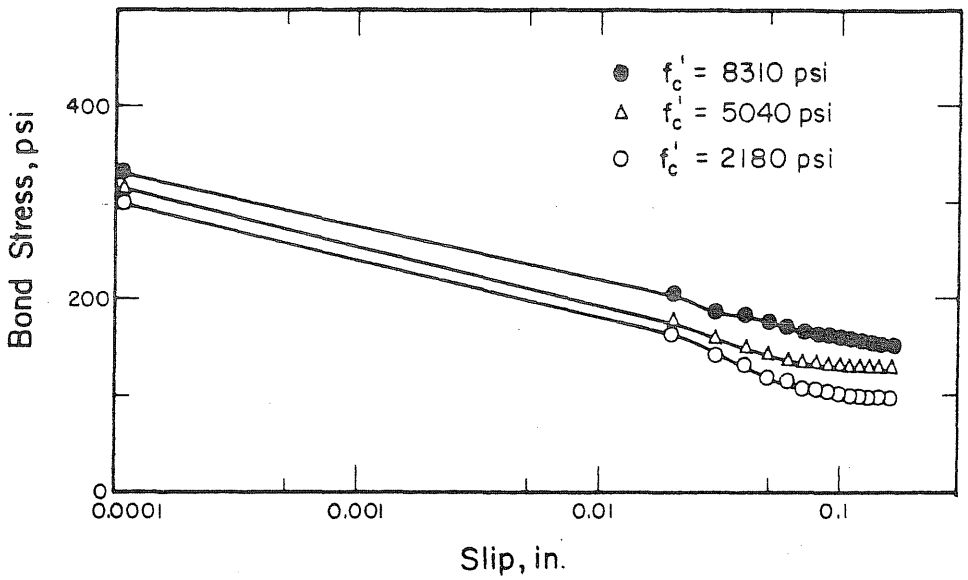

FIG. 4.2 AVERAGE BOND STRESS-SLIP RELATIONSHIPS OF PLAIN WIRE FOR DIFFERENT CONCRETE STRENGTHS, SERIES: WA08-1, WB08-1, WC08-1

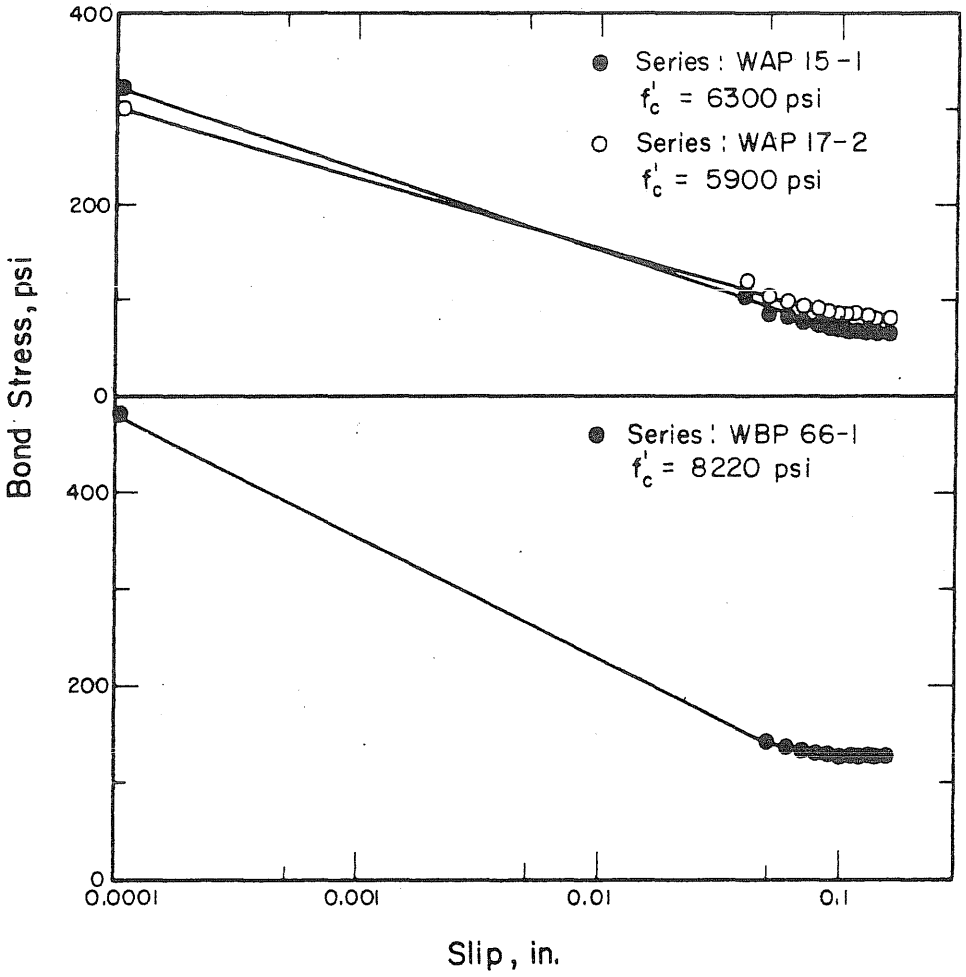

FIG. 4.3 AVERAGE BOND STRESS-SLIP RELATIONSHIPS FOR CENTER WIRES OF 7/16-in. STRAND, SERIES: WAP15-1, WAP17-2, WBP66-1

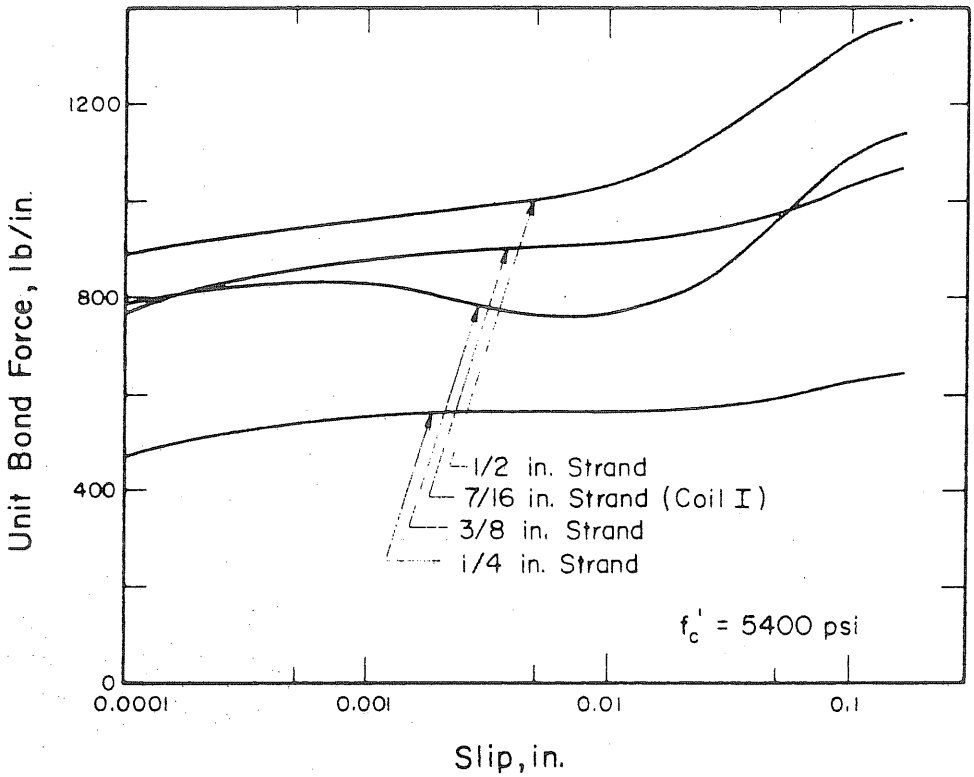

FIG. 5.1 AVERAGE UNIT BOND FORCE-SLIP RELATIONSHIPS FOR STRANDS OF DIFFERENT DIAMETERS

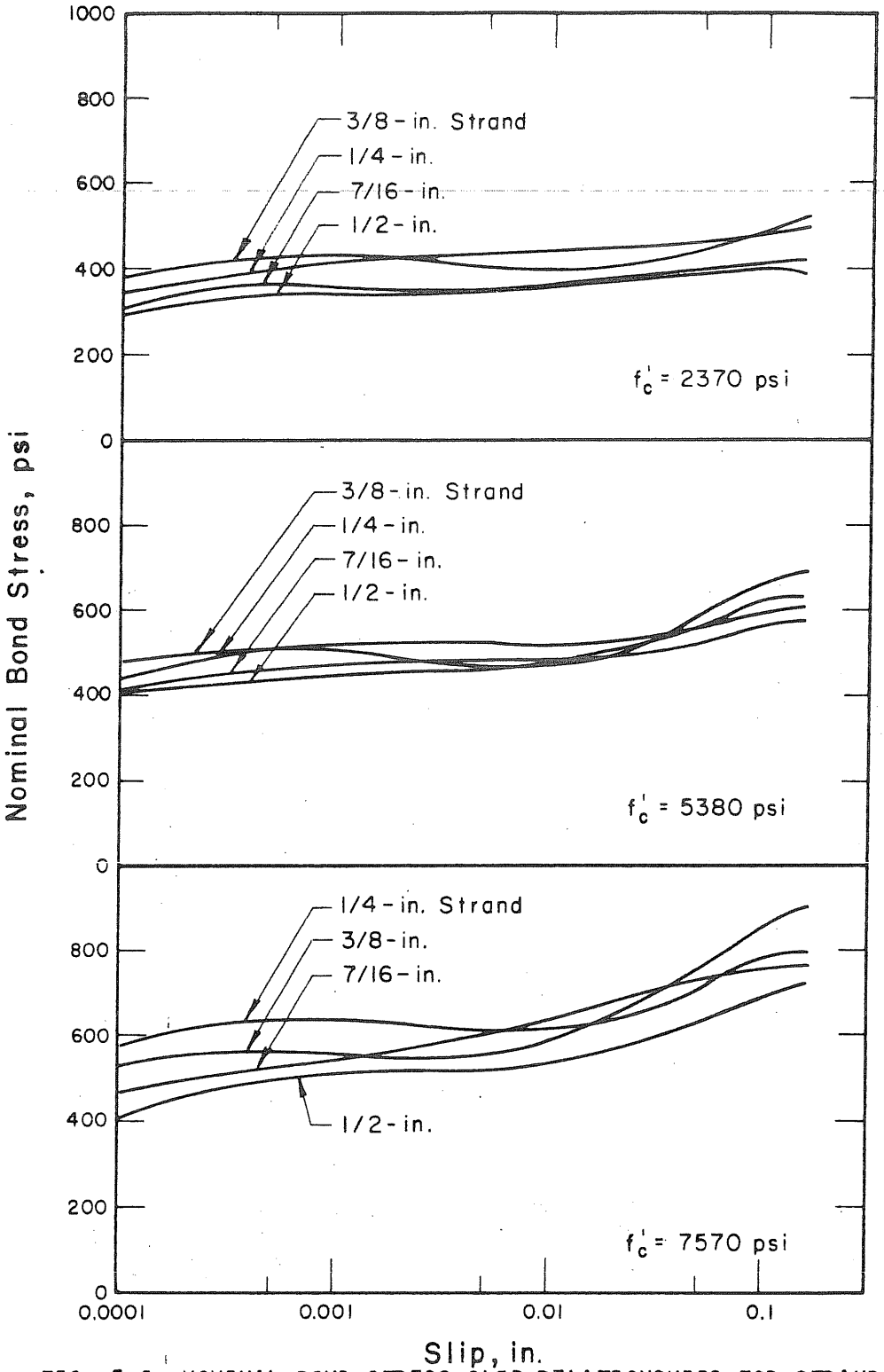

FIG. 5.2 NOMINAL BOND STRESS-SLIP RELATIONSHIPS FOR STRANDS OF DIFFERENT DIAMETERS

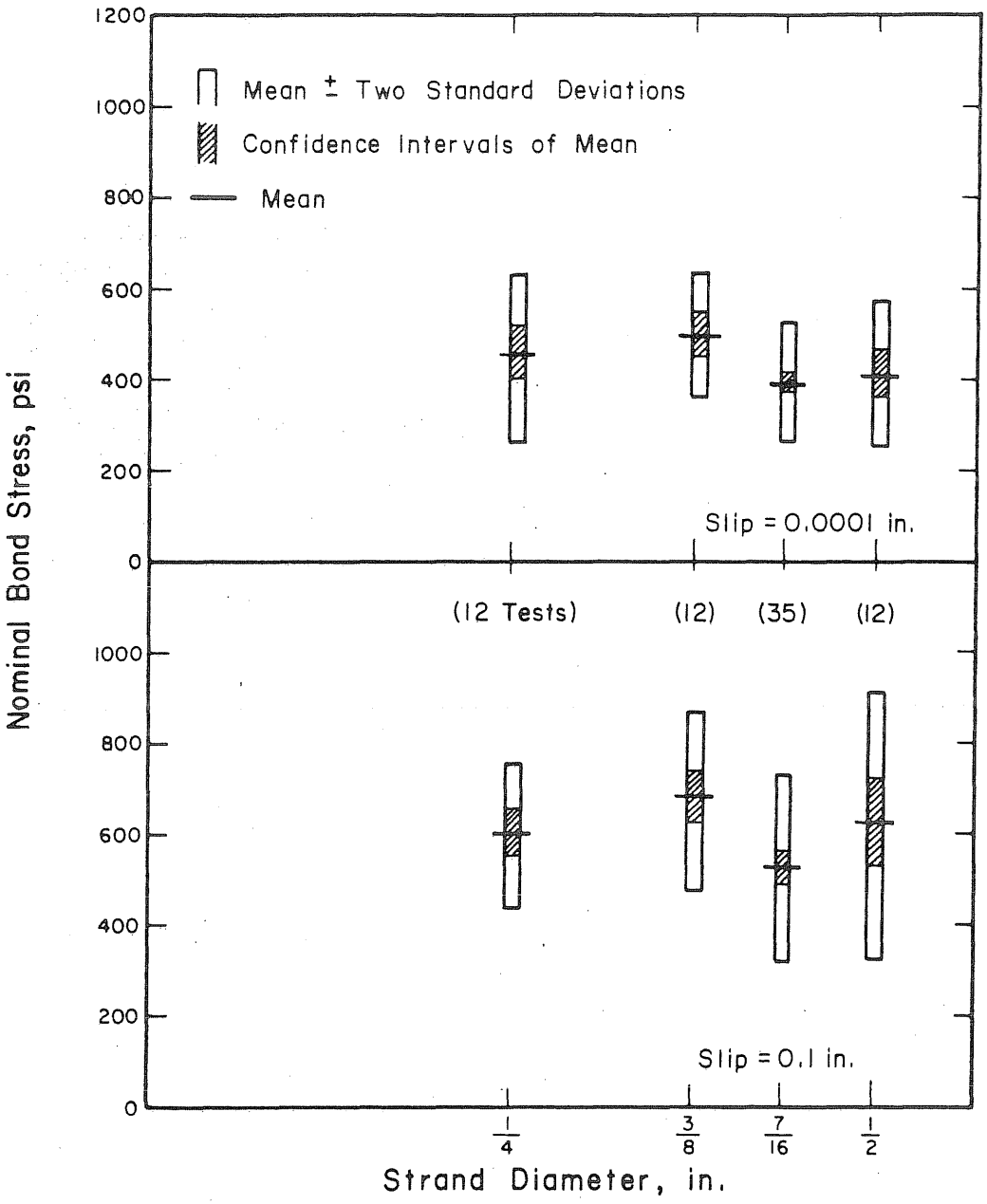

FIG. 5.3 VARIATION OF MEAN, CONFIDENCE INTERVALS OF MEAN, AND MEAN ± TWO STANDARD DEVIATIONS WITH STRAND SIZE FOR TESTS WITH CONCRETE MIX A (Avg. f'_c = 5380 psi)

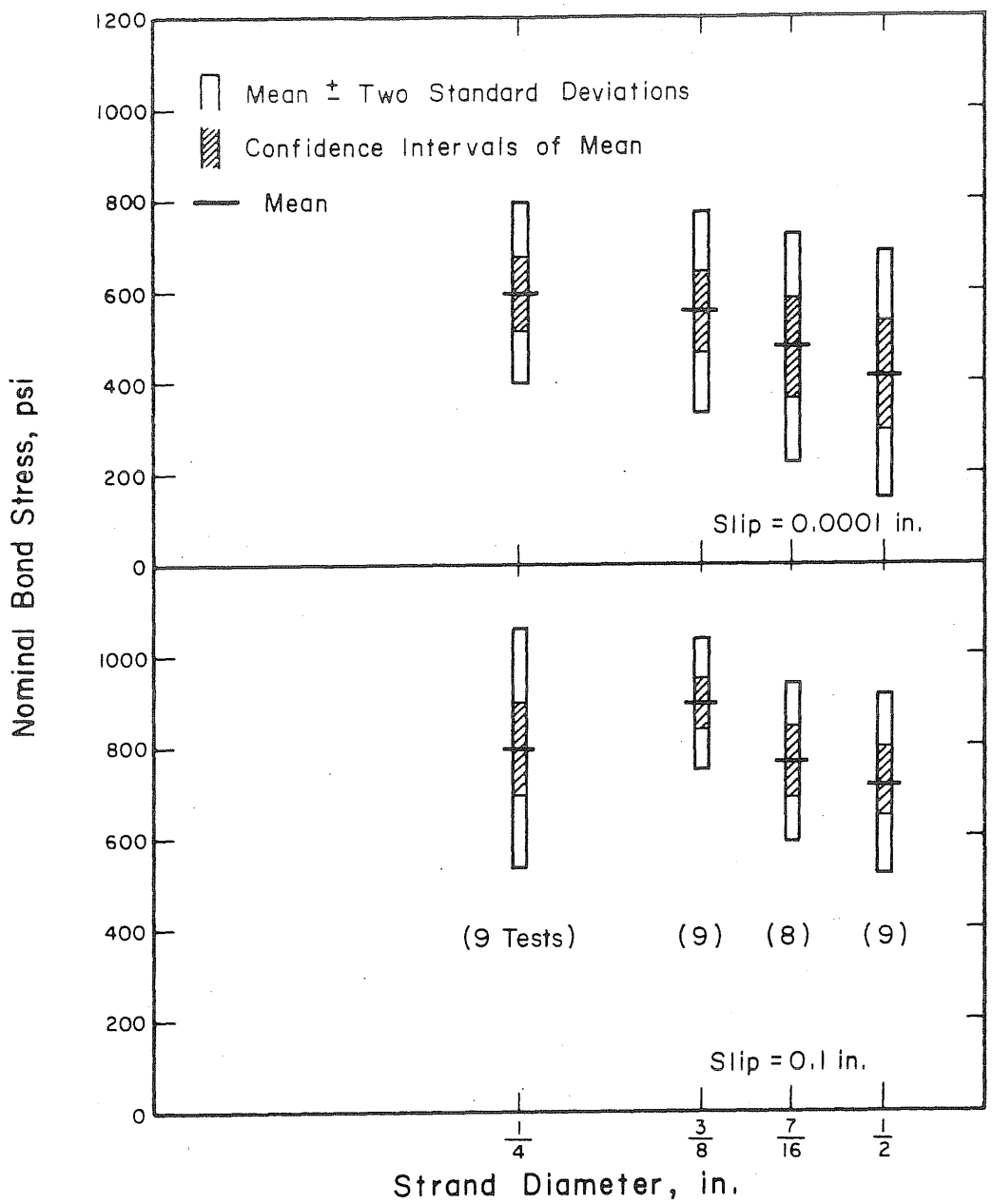

FIG. 5.4 VARIATION OF MEAN, CONFIDENCE INTERVALS OF MEAN AND MEAN ± TWO STANDARD DEVIATIONS WITH STRAND SIZE FOR TESTS WITH CONCRETE MIX B (Avg. f'_c = 7570 psi)

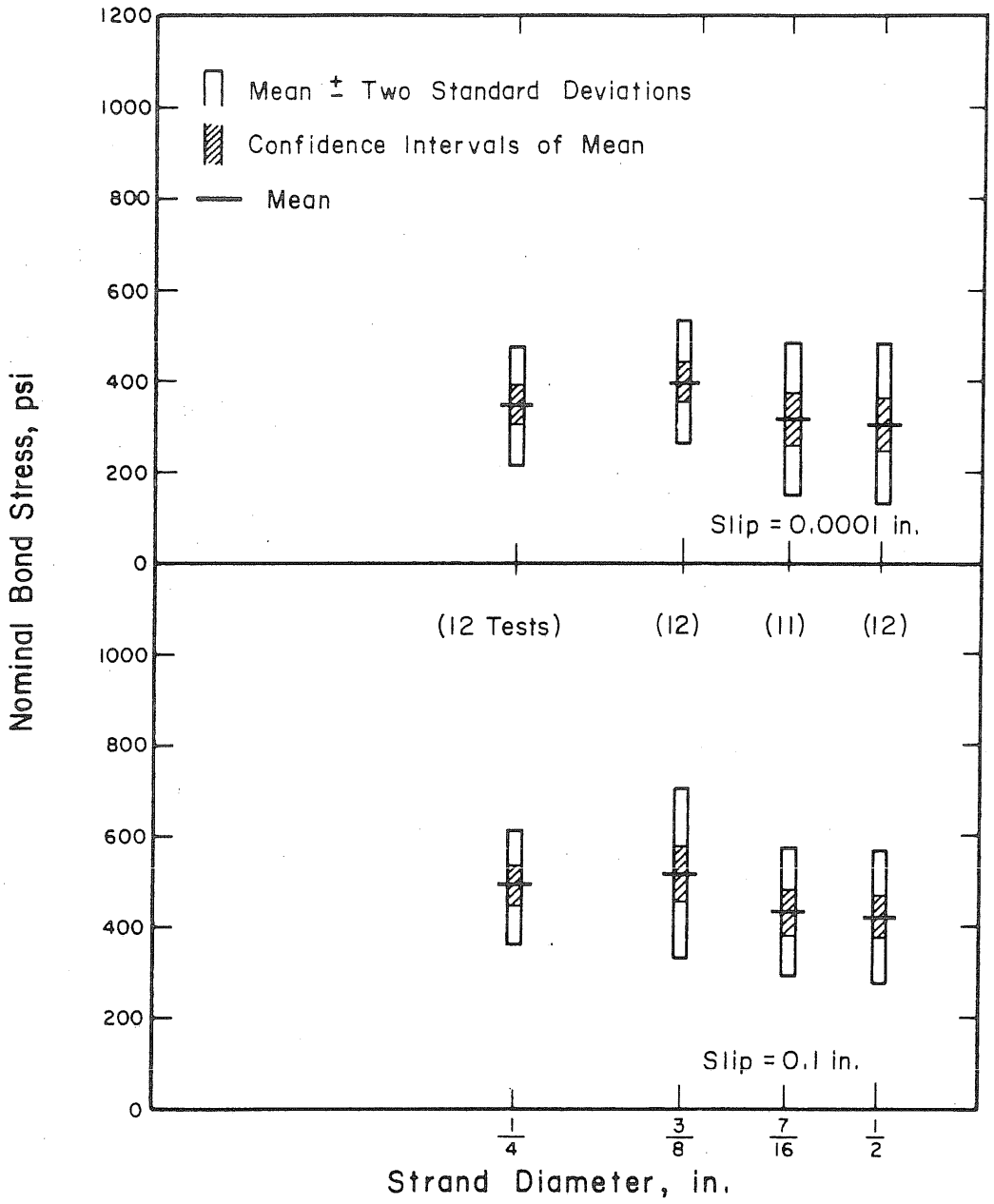

FIG. 5.5 VARIATION OF MEAN, CONFIDENCE INTERVALS OF MEAN AND MEAN ± TWO STANDARD DEVIATIONS WITH STRAND SIZE FOR TESTS WITH CONCRETE MIX C (Avg. f'_c = 2370 psi)

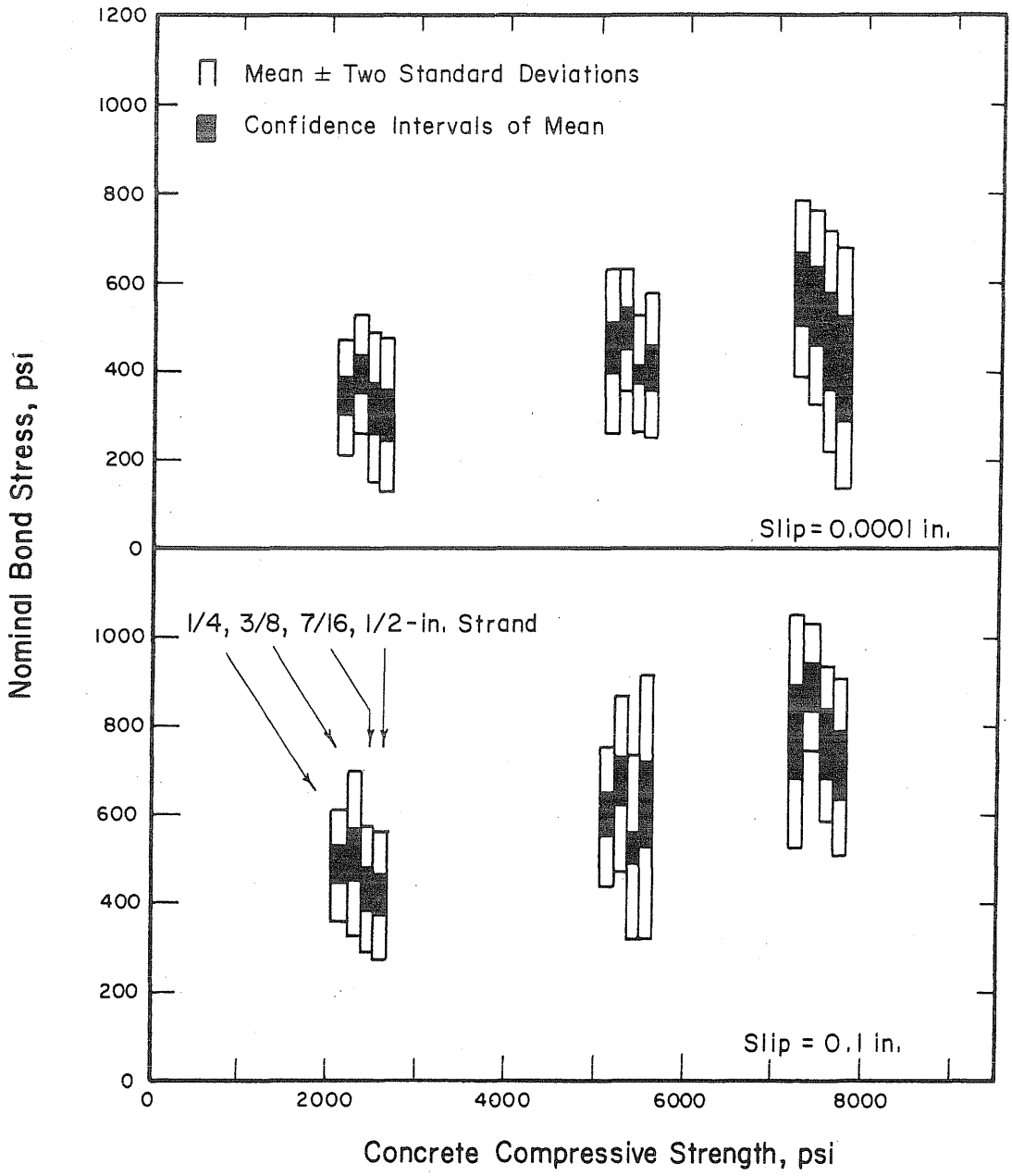

FIG. 5.6 VARIATION OF NOMINAL BOND STRESS WITH STRAND DIAMETER AND CONCRETE STRENGTH

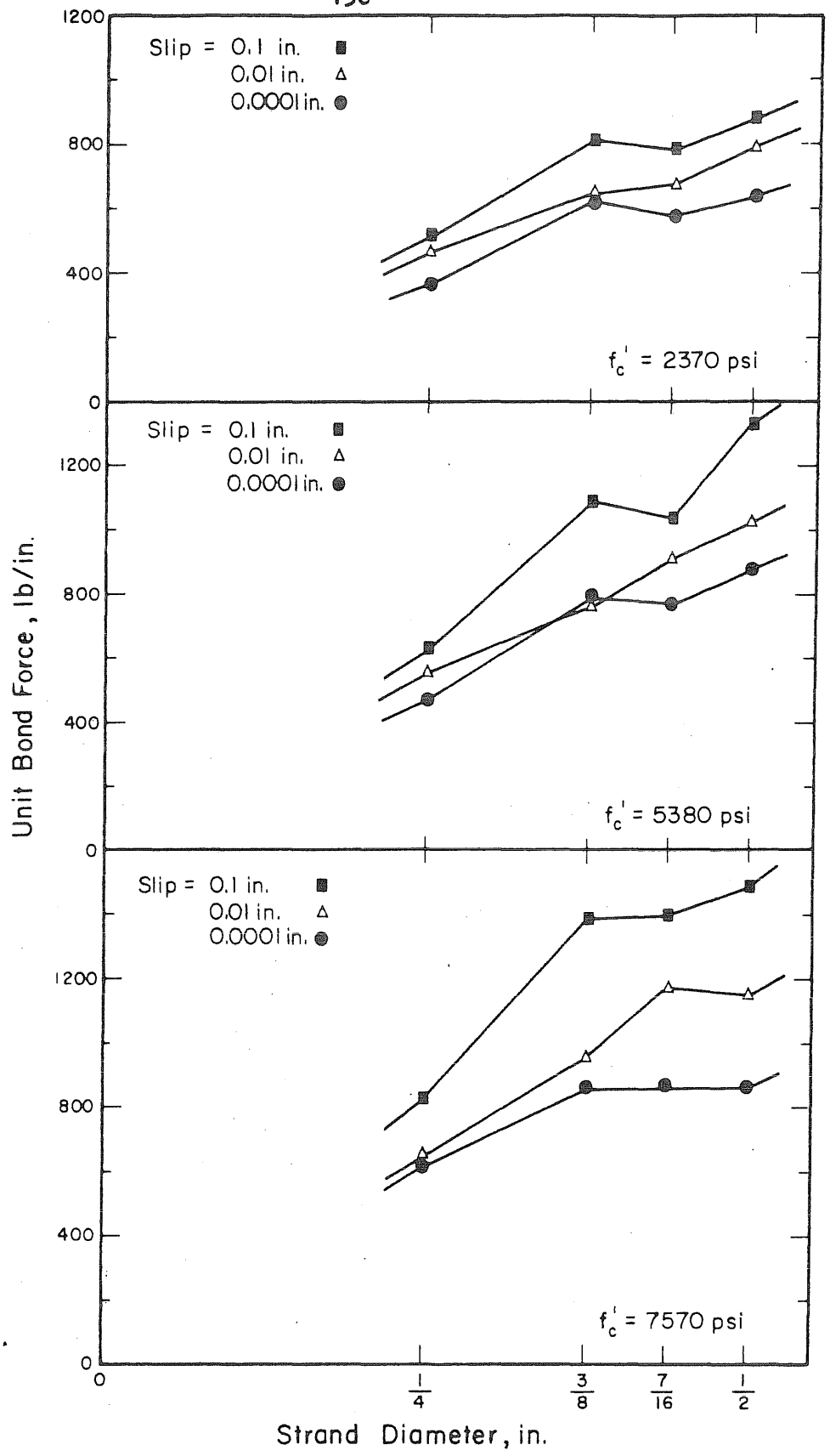

FIG. 5.7 AVERAGE UNIT BOND FORCE vs. STRAND DIAMETER FOR VARIOUS SLIPS AND CONCRETE STRENGTHS

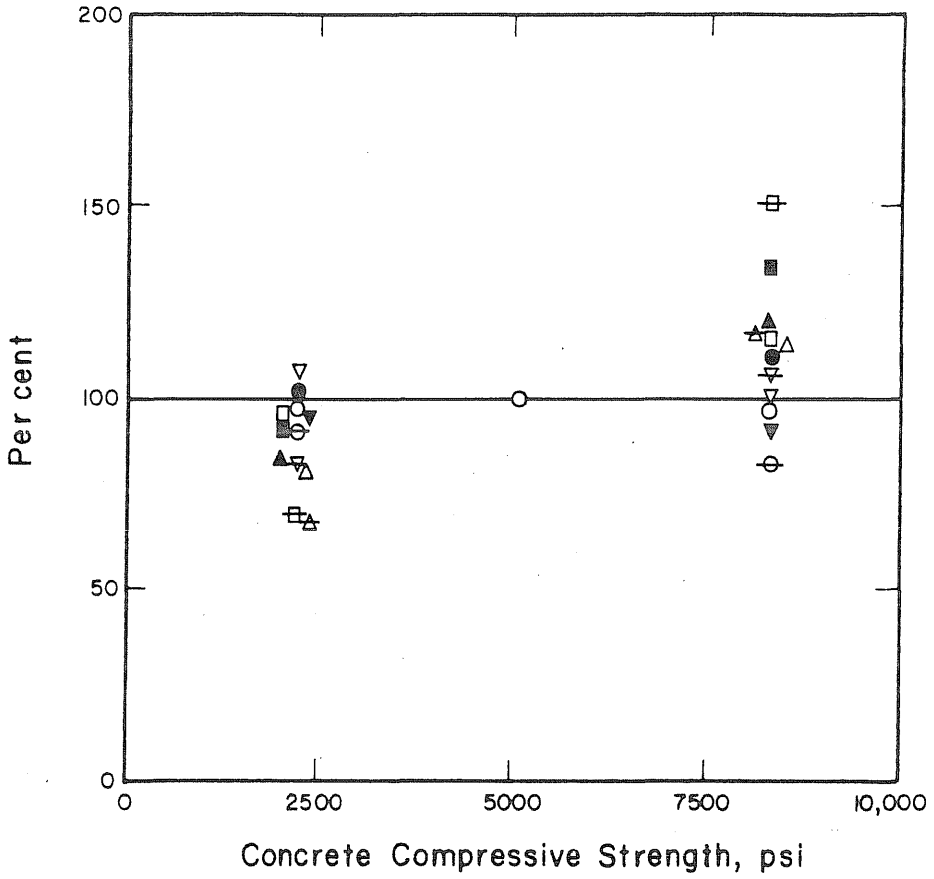

FIG. 6.1 VARIATION OF BOND STRENGTH WITH CONCRETE STRENGTH FOR PLAIN WIRE IN PERCENT OF THE BOND STRESS OBTAINED WITH A CONCRETE STRENGTH OF APPROXIMATELY 5000 psi

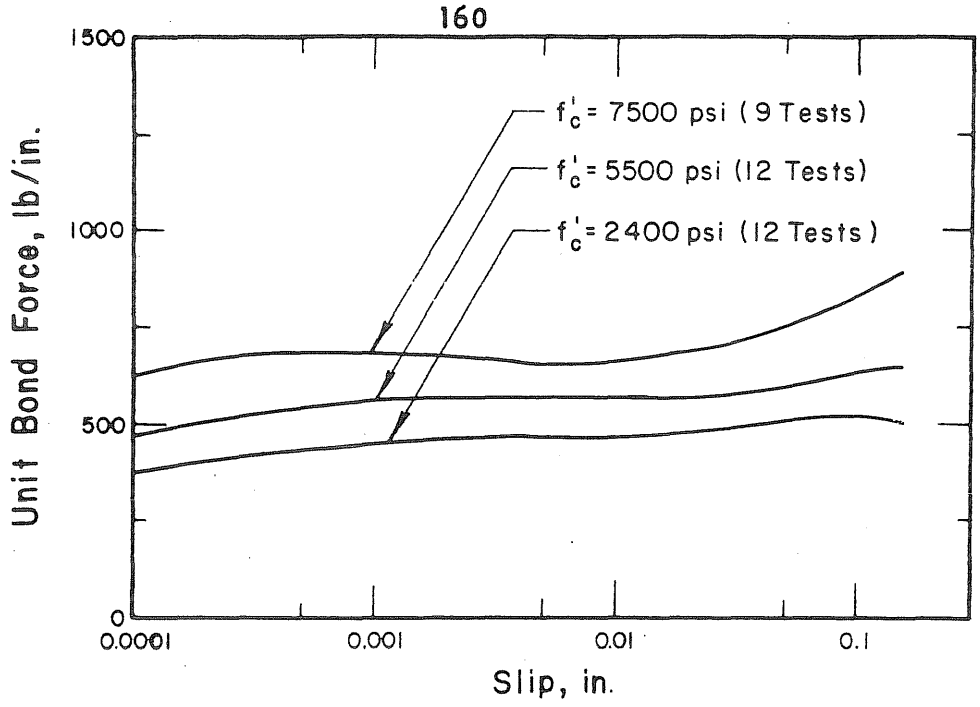

FIG. 6.2 VARIATION OF BOND STRENGTH WITH CONCRETE STRENGTH FOR 1/4-in. STRAND

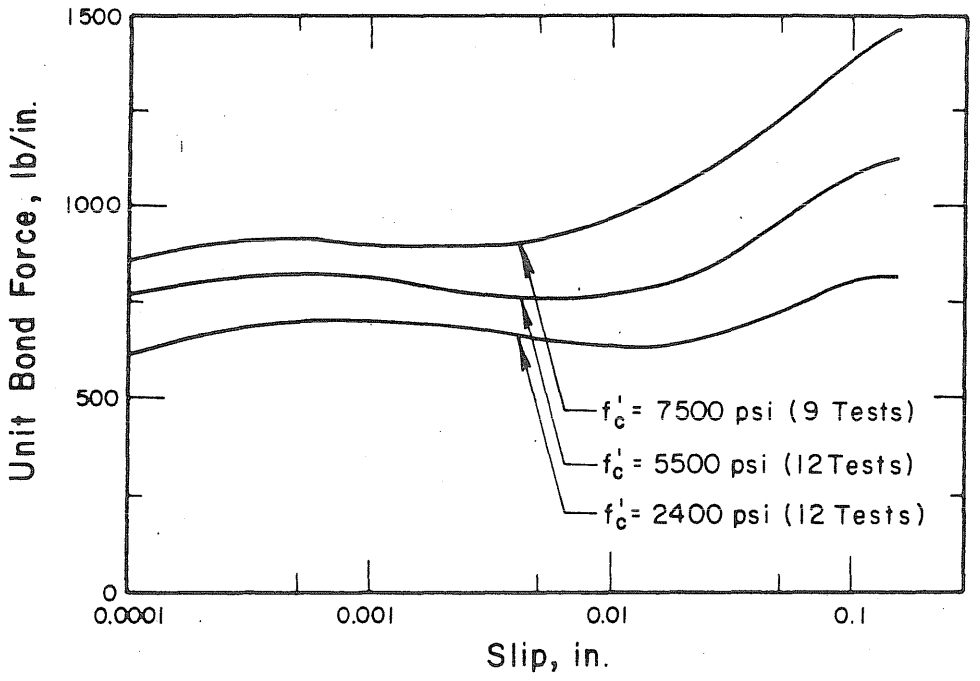

FIG 6.3 VARIATION OF BOND STRENGTH WITH CONCRETE STRENGTH FOR 3/8-in. STRAND

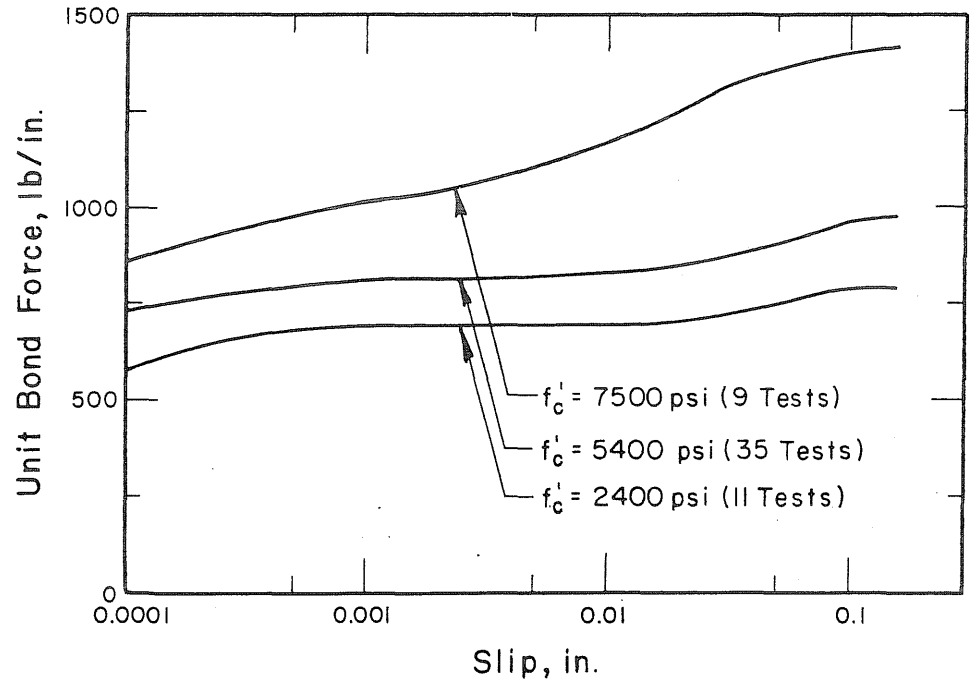

FIG. 6.4 VARIATION OF BOND STRENGTH WITH CONCRETE STRENGTH FOR 7/16-in. STRAND

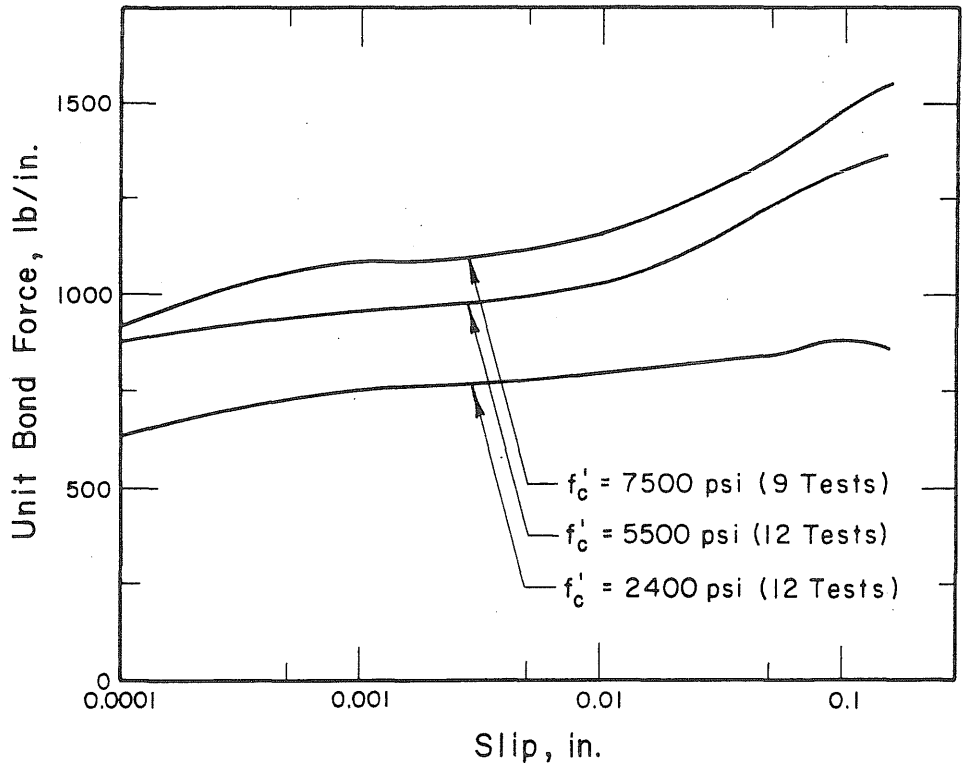

FIG. 6.5 VARIATION OF BOND STRENGTH WITH CONCRETE STRENGTH FOR 1/2-in. STRAND

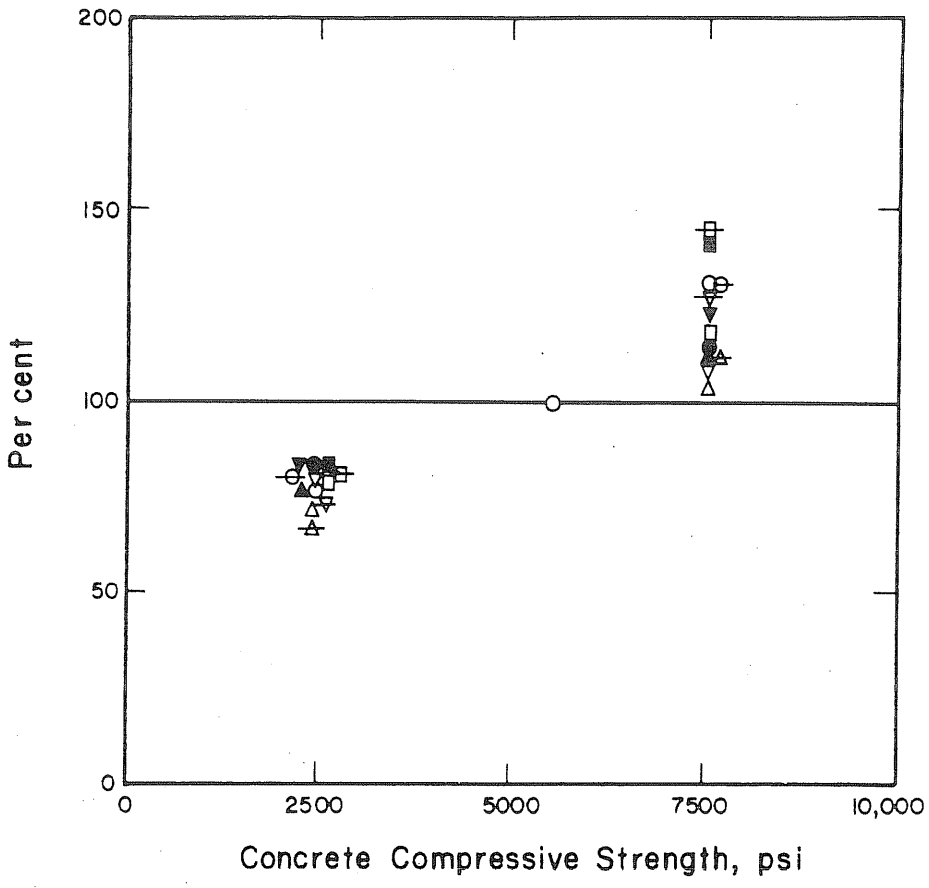

FIG. 6.6 VARIATION OF BOND STRENGTH WITH CONCRETE STRENGTH FOR STRAND IN PERCENT OF THE BOND STRENGTH OBTAINED WITH A CONCRETE STRENGTH OF APPROXIMATELY 5500 psi

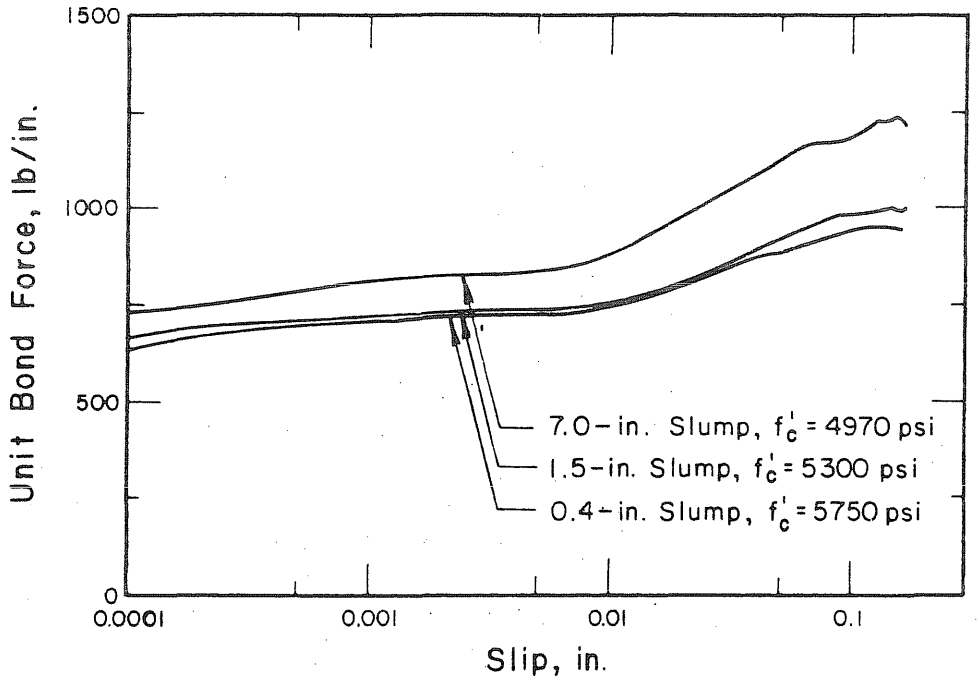

FIG. 6.7 VARIATION OF BOND STRENGTH WITH CONCRETE CONSISTENCY FOR 7/16-in. STRAND

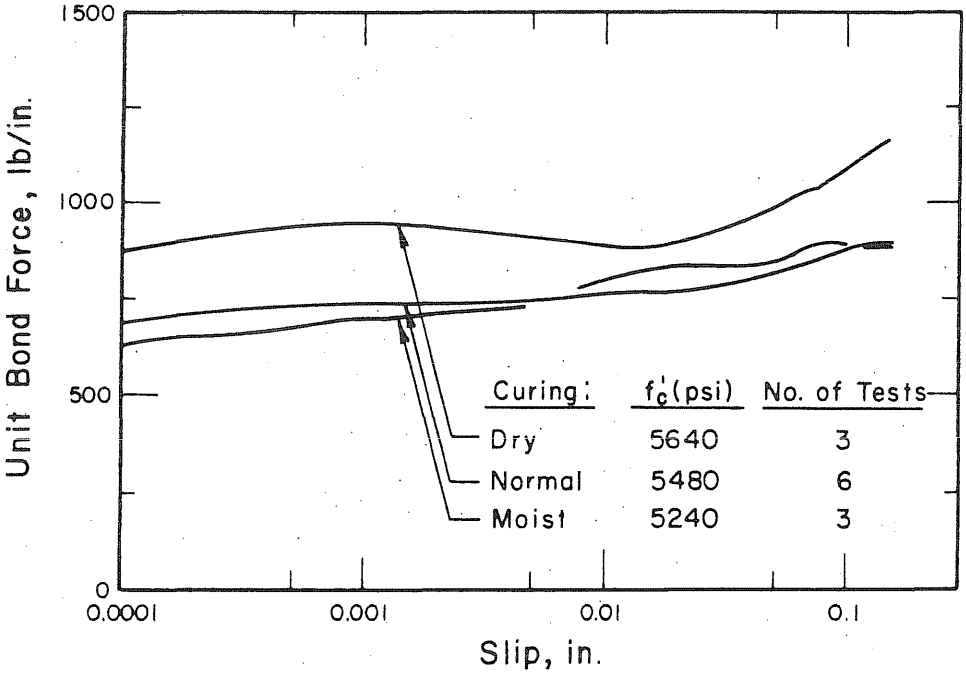

FIG. 6.8 VARIATION OF BOND STRENGTH WITH CURING CONDITIONS OF CONCRETE FOR 7/16-in. STRAND, AGE OF CONCRETE: 8 DAYS, SERIES: SA08-12, SA08-13

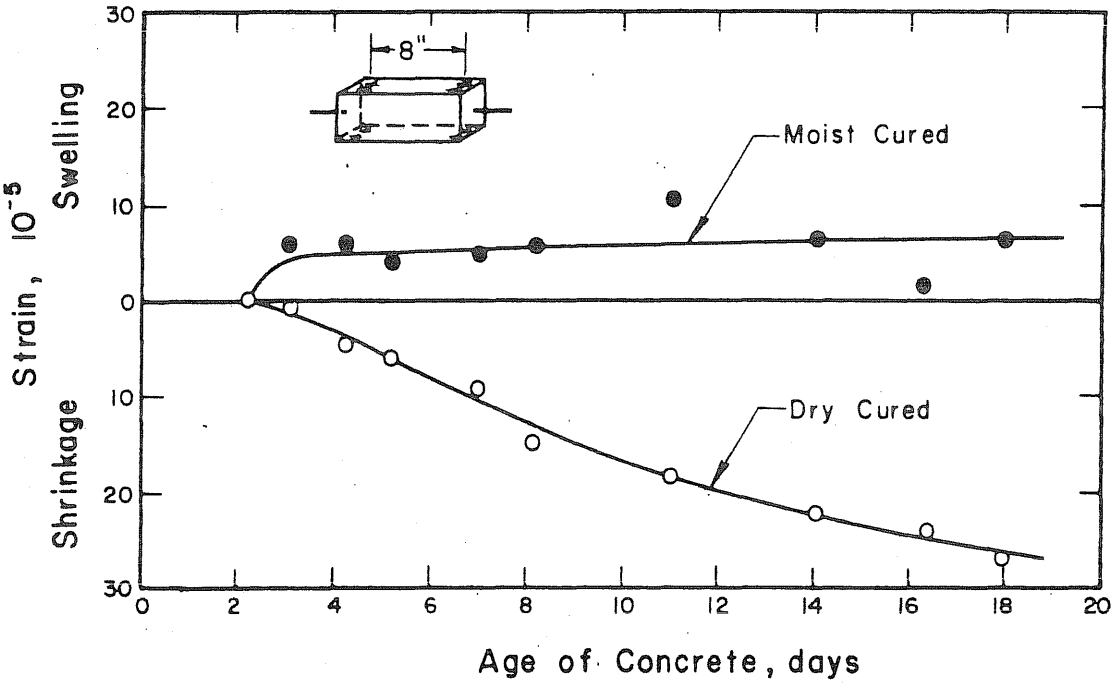

FIG. 6.9 SWELLING AND SHRINKAGE STRAINS OF CONCRETE vs. TIME, SERIES: WB18-2, SB18-4

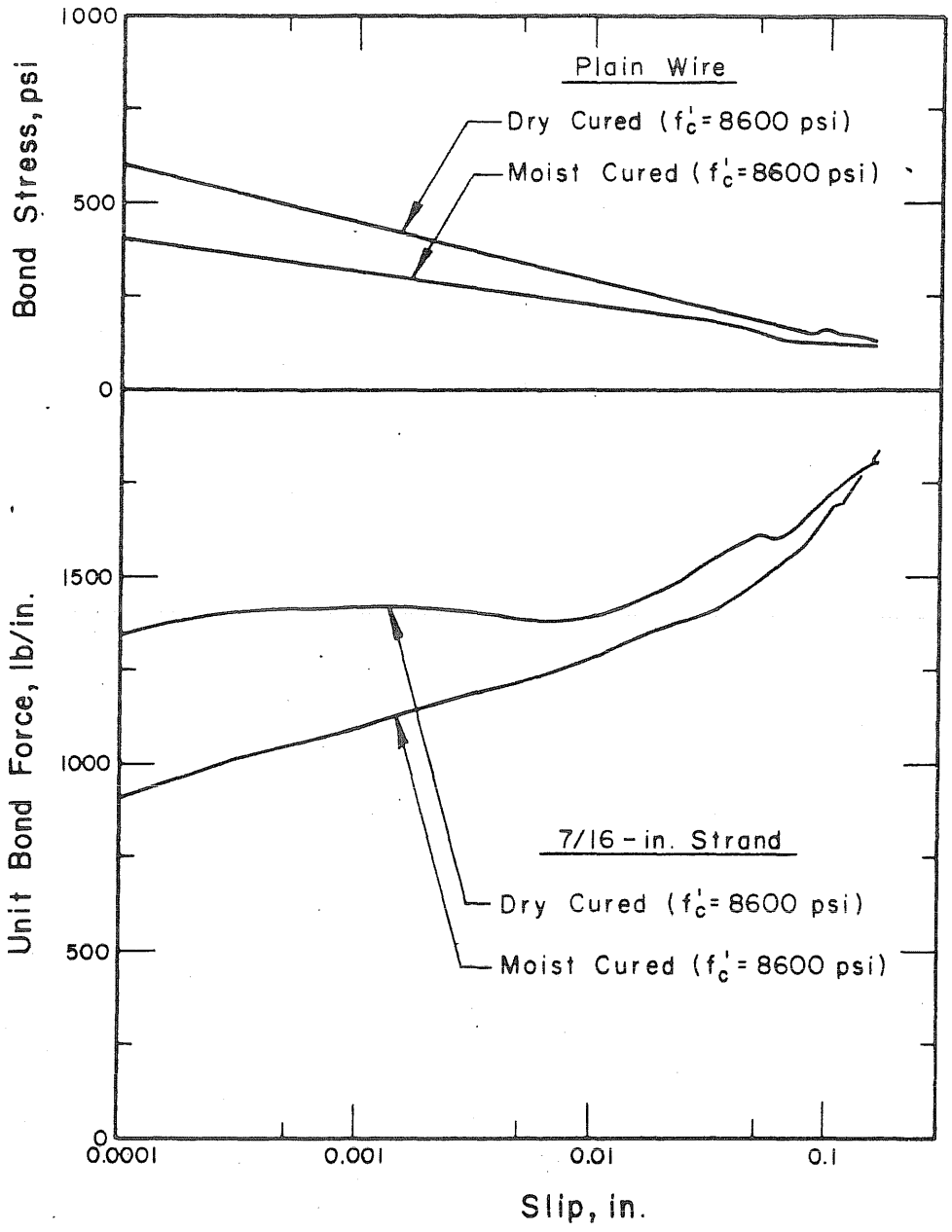

FIG. 6.10 VARIATION OF BOND STRENGTH WITH CURING CONDITIONS OF CONCRETE FOR CENTER WIRE (OF 7/16-In. STRAND) AND 7/16-In. STRAND, AGE OF CONCRETE: 18 DAYS, SERIES: WB18-2, SB18-4
(Each curve represents an average of three tests).

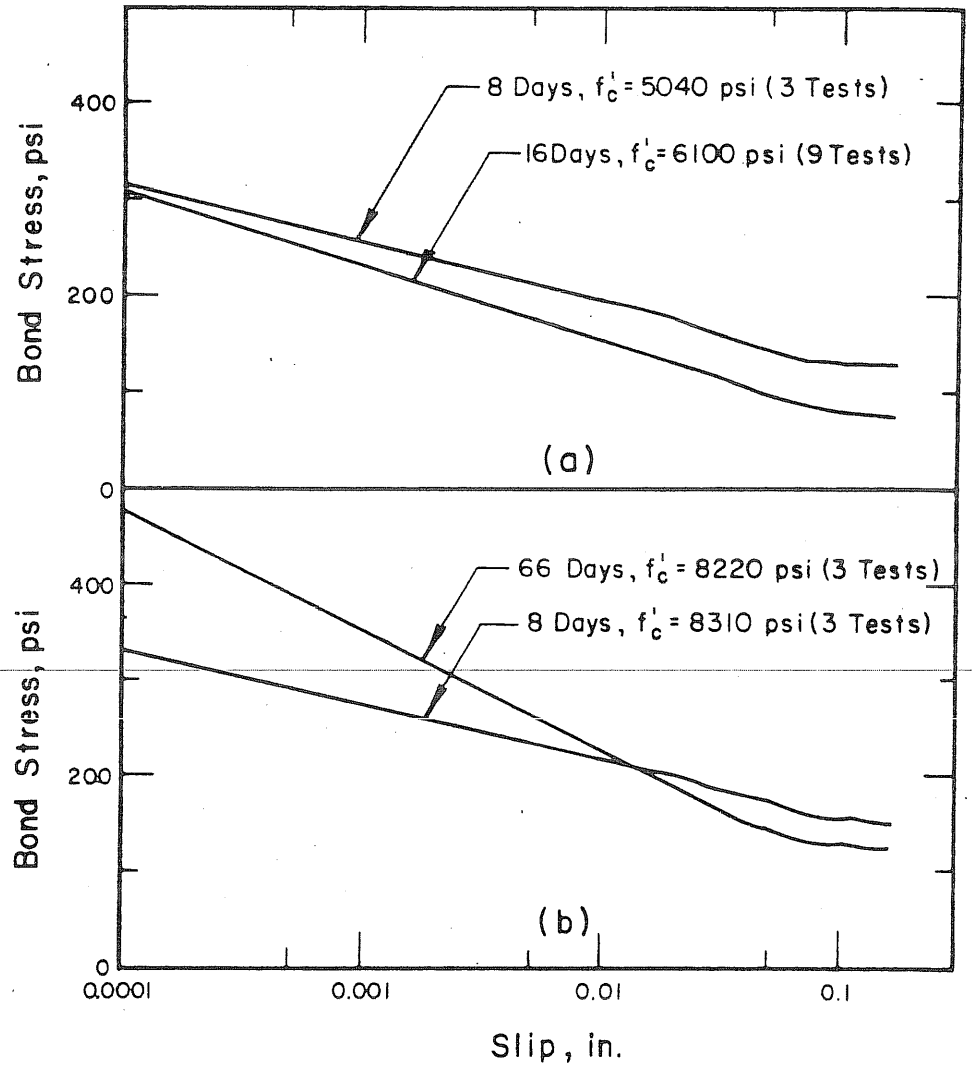

FIG. 6.11 VARIATION OF BOND STRESS WITH AGE OF CONCRETE FOR PLAIN CENTER WIRE OF 7/16-in. STRAND, SERIES: WA08-1, WAP15-1, WAP17-2, WBP66-1, WB08-1

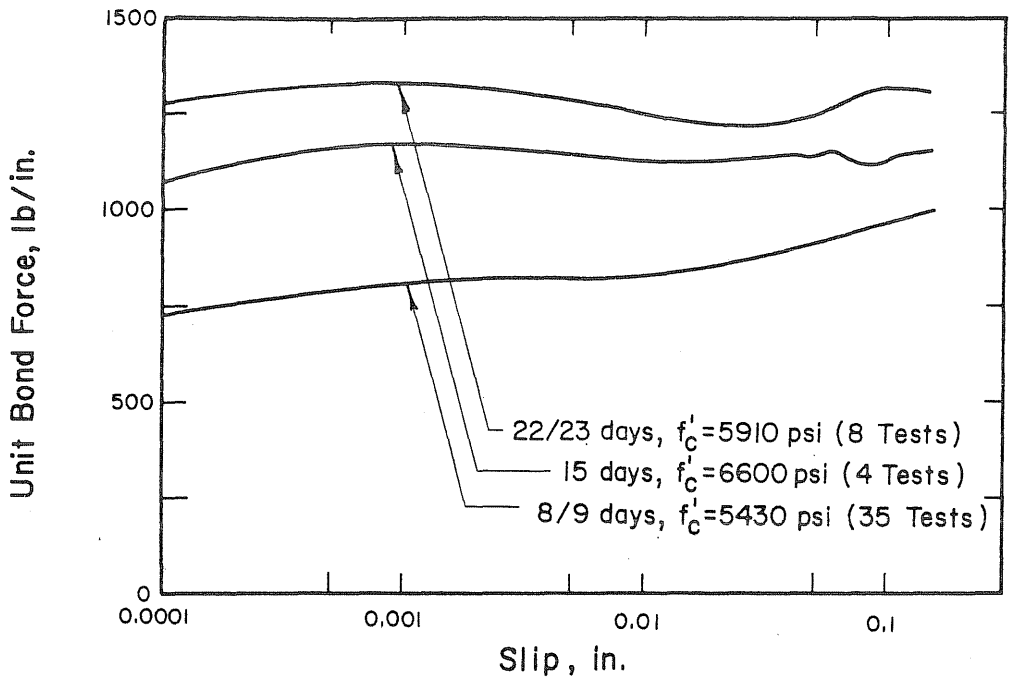

FIG. 6.12 VARIATION OF BOND STRENGTH WITH AGE OF CONCRETE FOR 7/16-in. STRAND (COIL I)

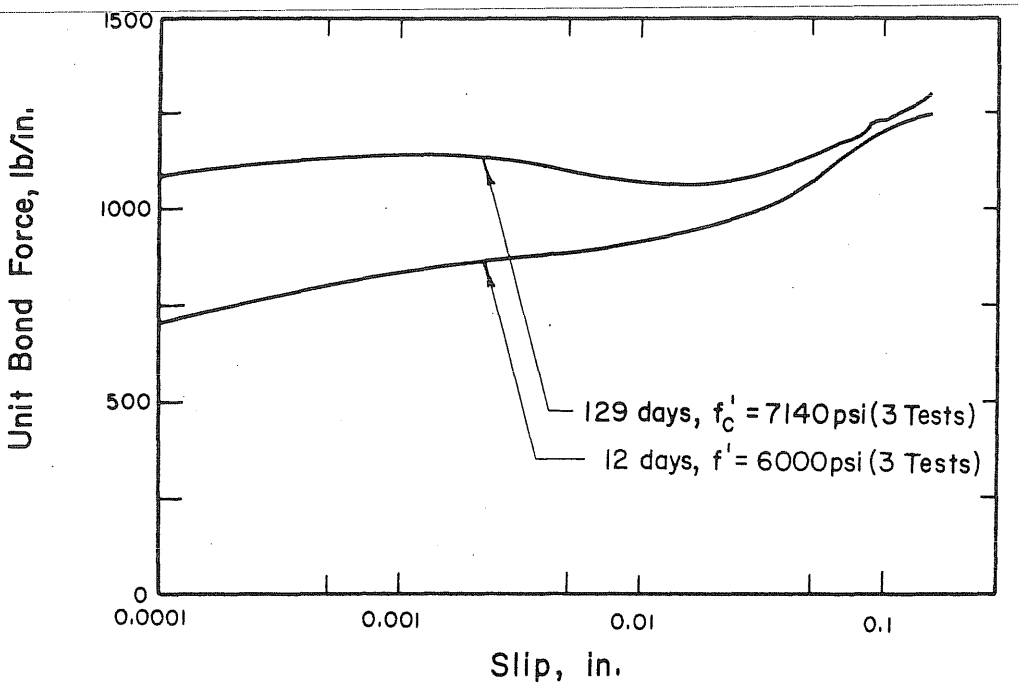

FIG. 6.13 VARIATION OF BOND STRENGTH WITH AGE OF CONCRETE FOR 7/16-in. STRAND (COIL I), SERIES: SAL12-1

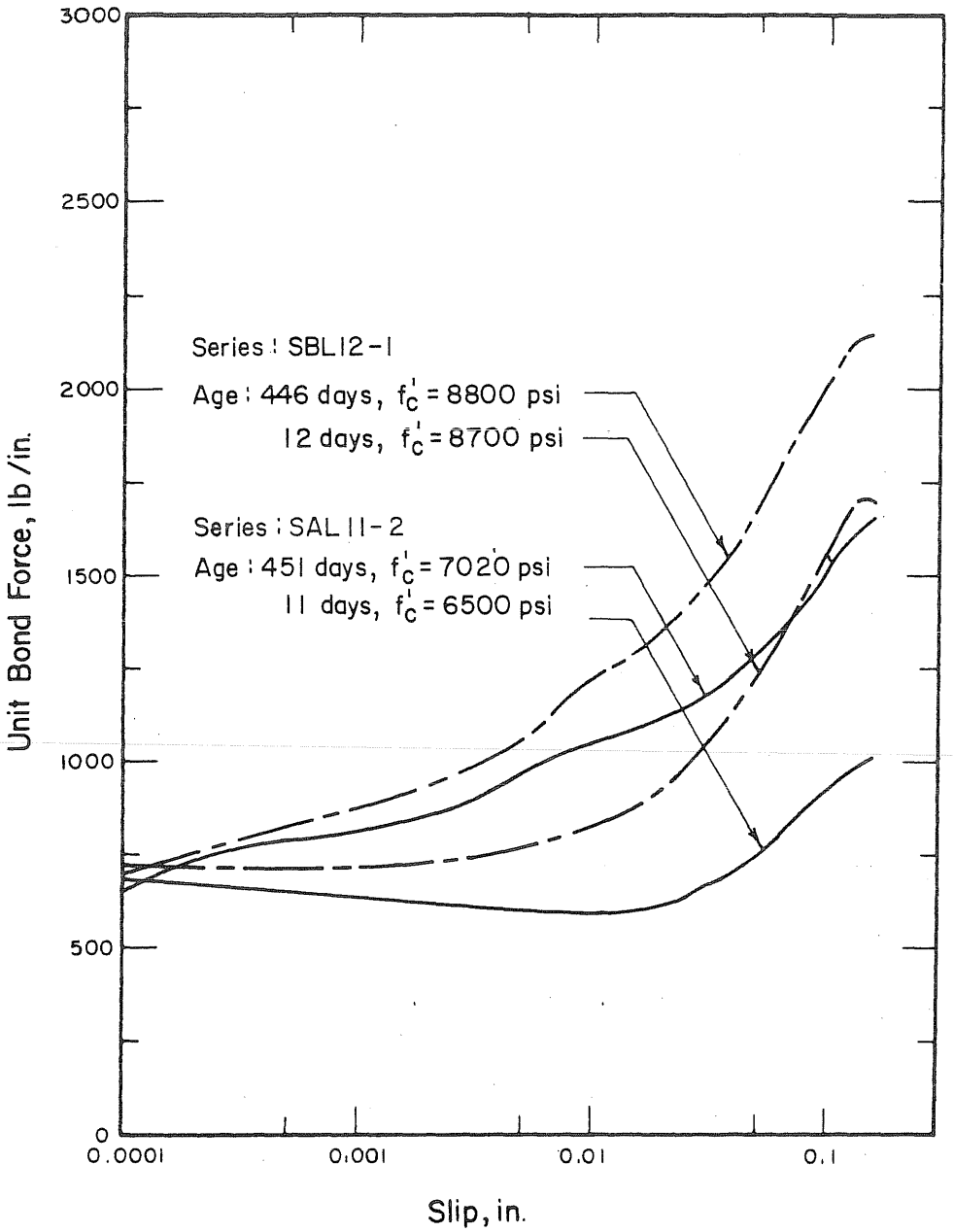

FIG. 6.14 VARIATION OF BOND STRENGTH WITH AGE OF CONCRETE FOR 7/16-in. STRAND (COIL II), SERIES: SAL11-2, SBL12-1

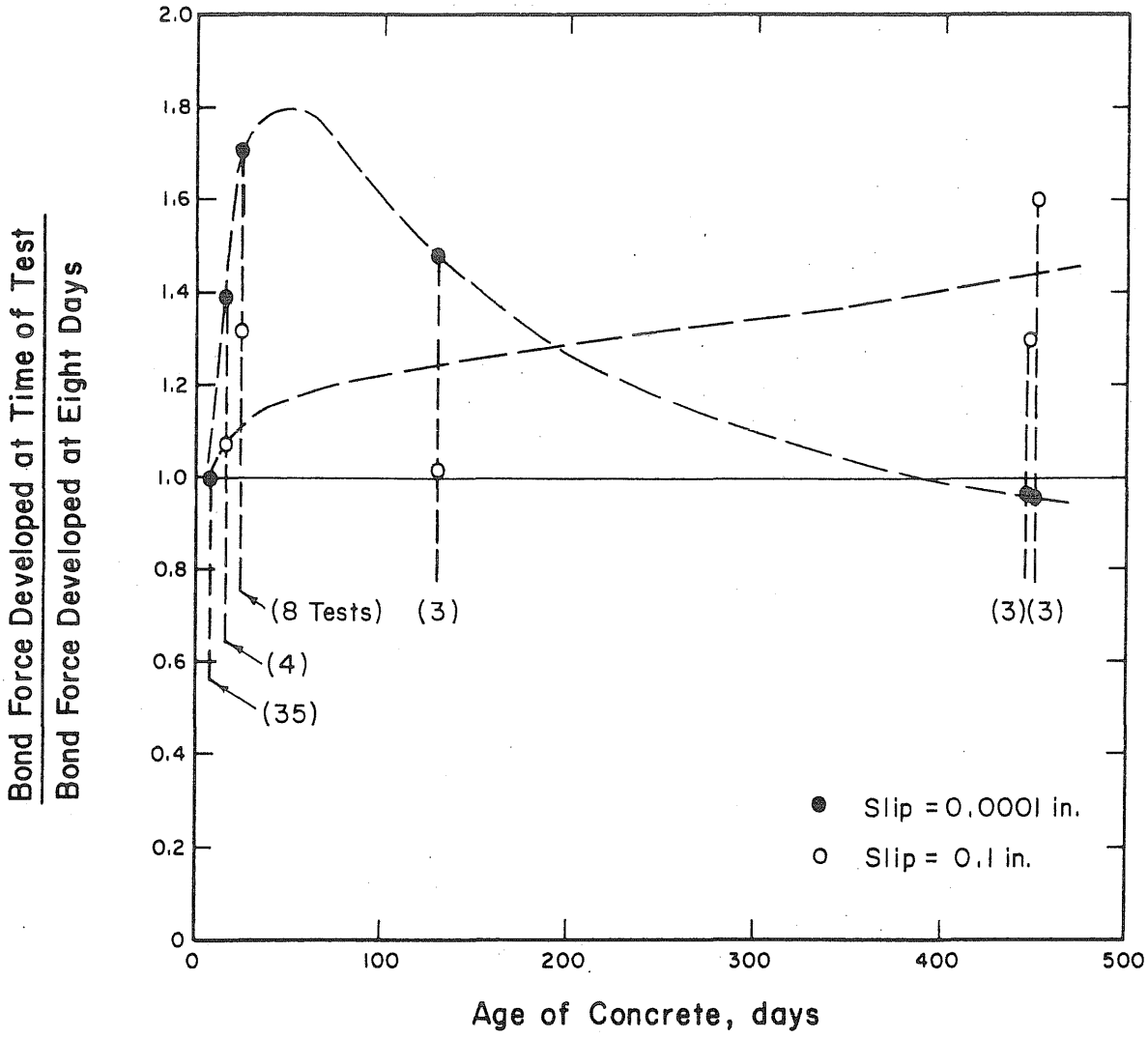

FIG. 6.15 VARIATION OF BOND STRENGTH WITH AGE OF CONCRETE FOR 7/16-in. STRAND

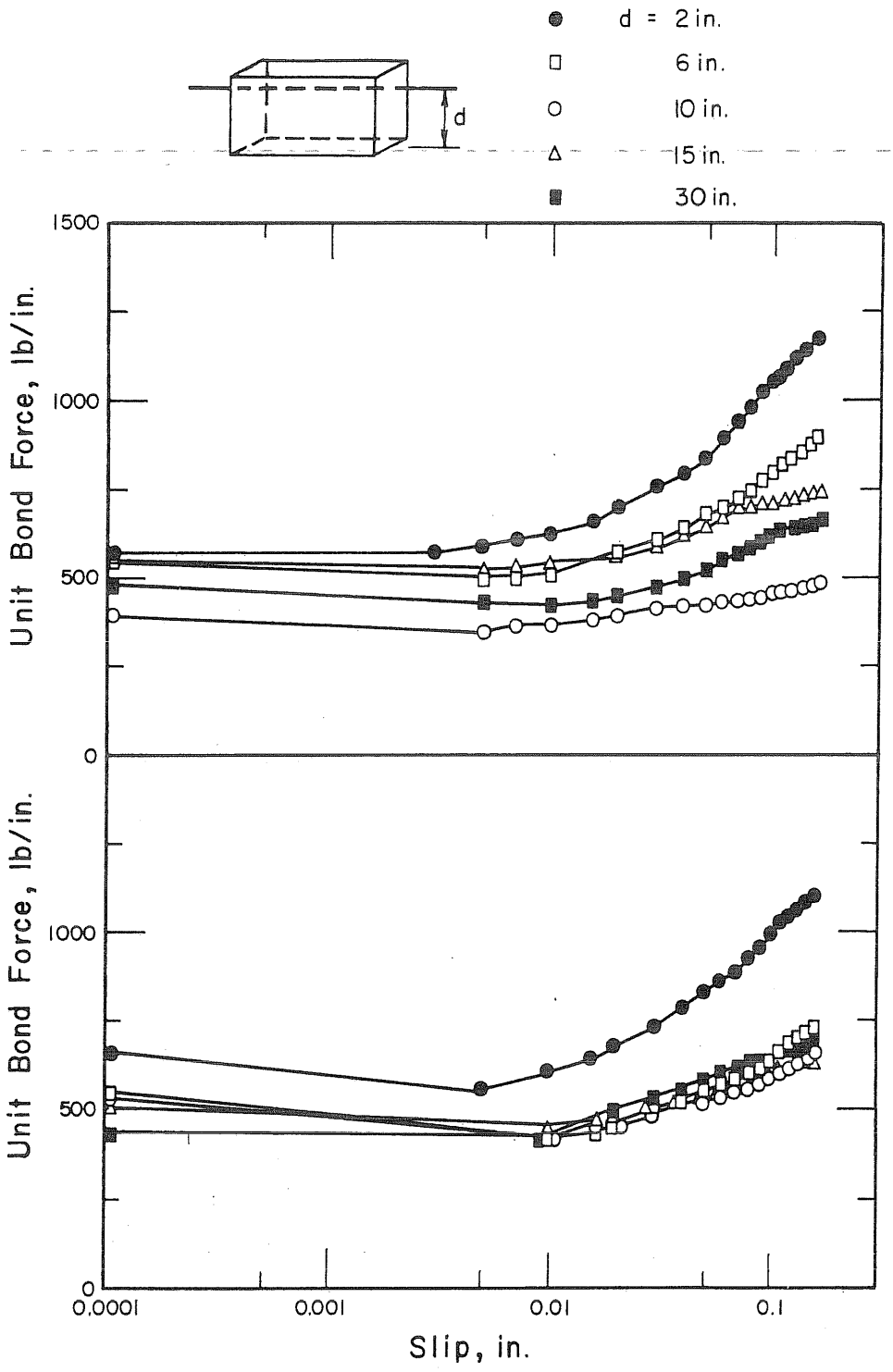

FIG. 7.1 AVERAGE UNIT BOND FORCE-SLIP RELATIONSHIPS OF 7/16-in. STRAND FOR VARIOUS CONCRETE DEPTHS BELOW THE STRAND, SERIES: SA09-15, SA09-16

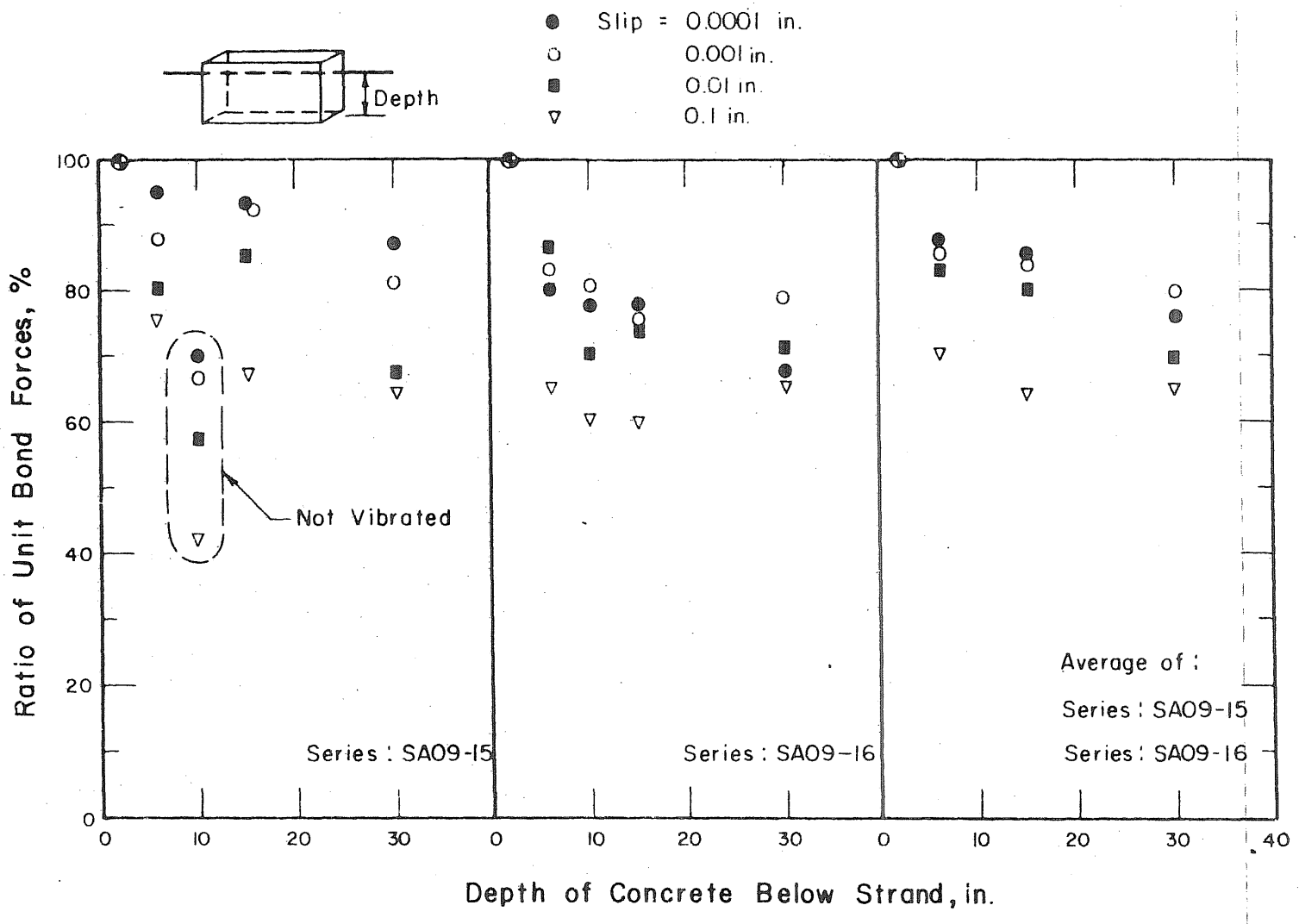

FIG. 7.2 EFFECT OF DEPTH OF CONCRETE BELOW STRAND ON BOND, SERIES: SA09-15, SA09-16

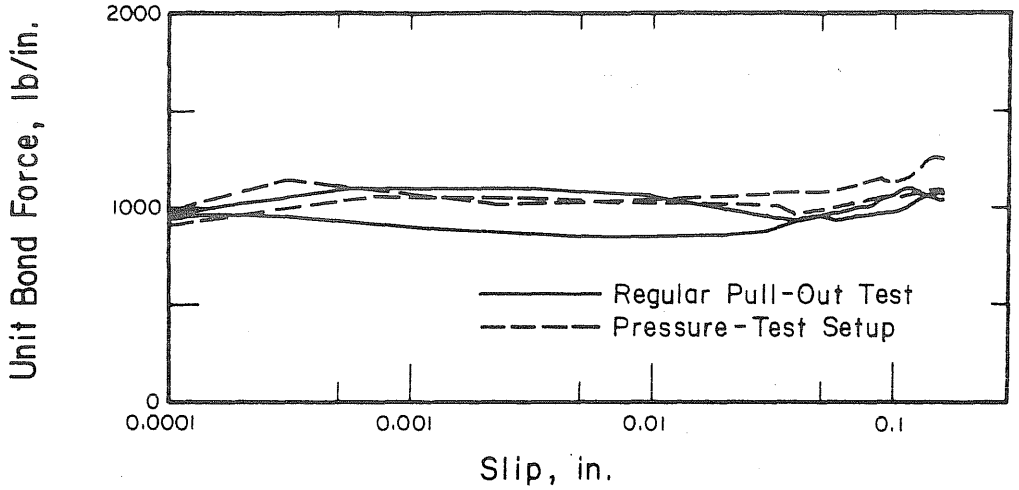

FIG. 8.1 INFLUENCE OF PRESSURE-TEST SETUP ON UNIT BOND FORCE-SLIP RELATIONSHIPS OF 7/16-in. STRAND, SERIES: SA08-14

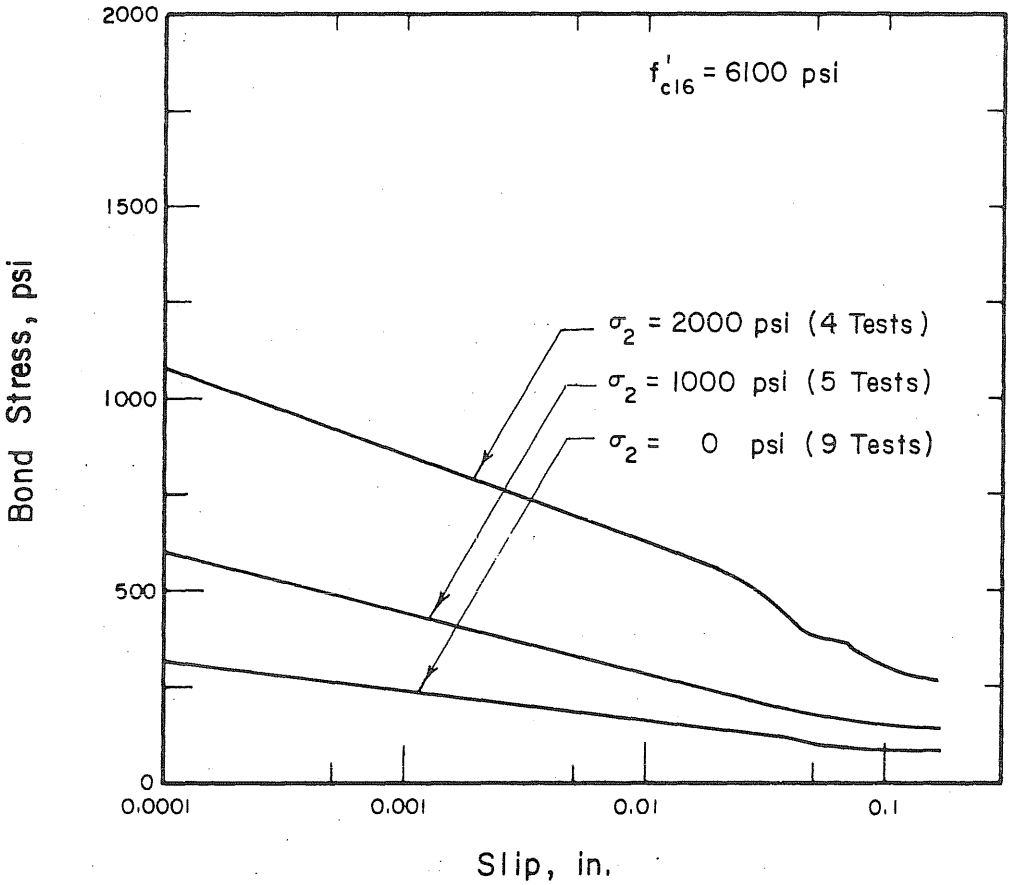

FIG. 8.2 AVERAGE BOND STRESS-SLIP RELATIONSHIPS FOR CENTER WIRE FROM 7/16-in. STRAND UNDER VARIOUS LATERAL PRESSURES, SERIES: WAP15-1, WAP17-2

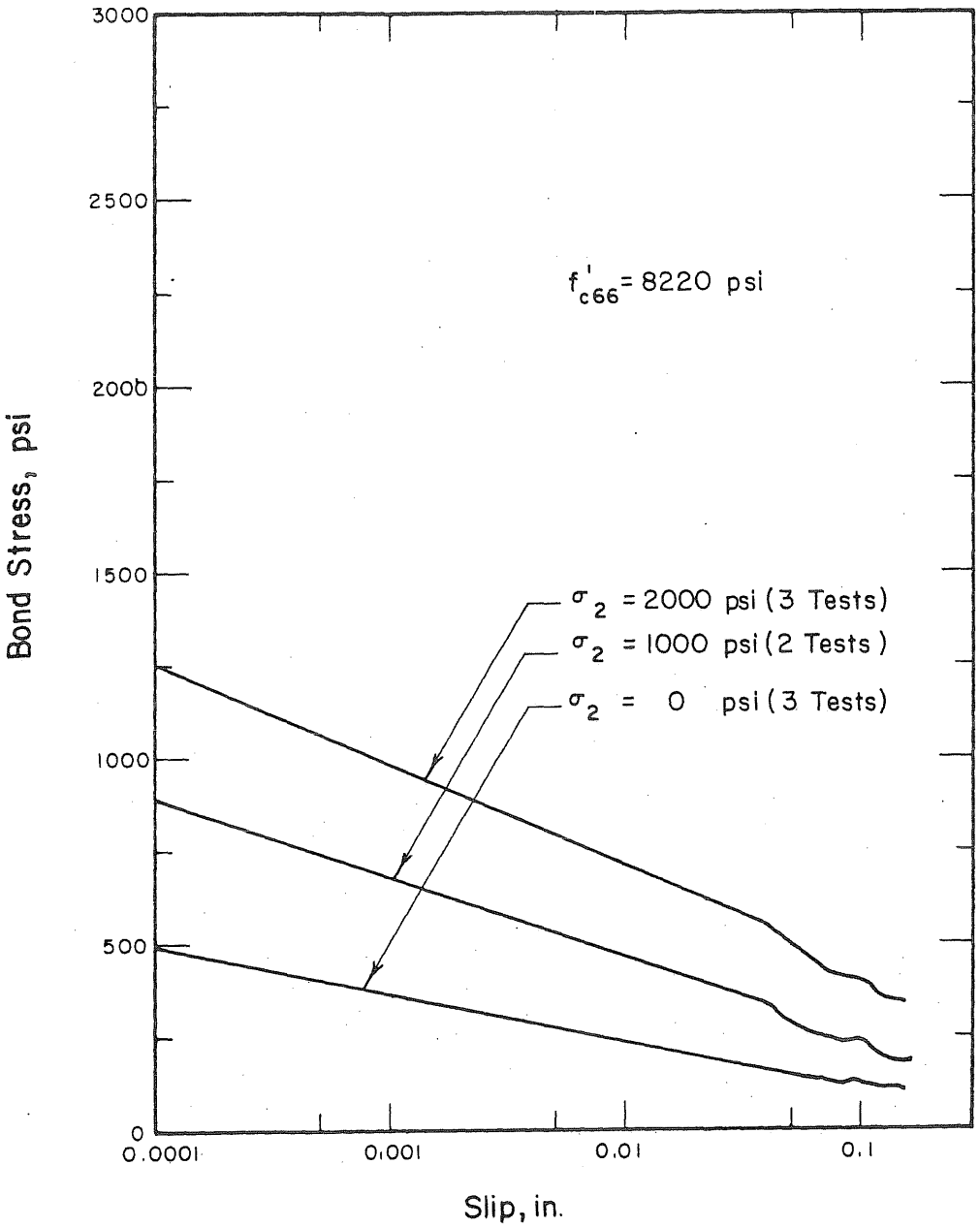

FIG. 8.3 AVERAGE BOND STRESS-SLIP RELATIONSHIPS FOR CENTER WIRE FROM 7/16-in. STRAND UNDER VARIOUS LATERAL PRESSURES, SERIES: WBP66-1

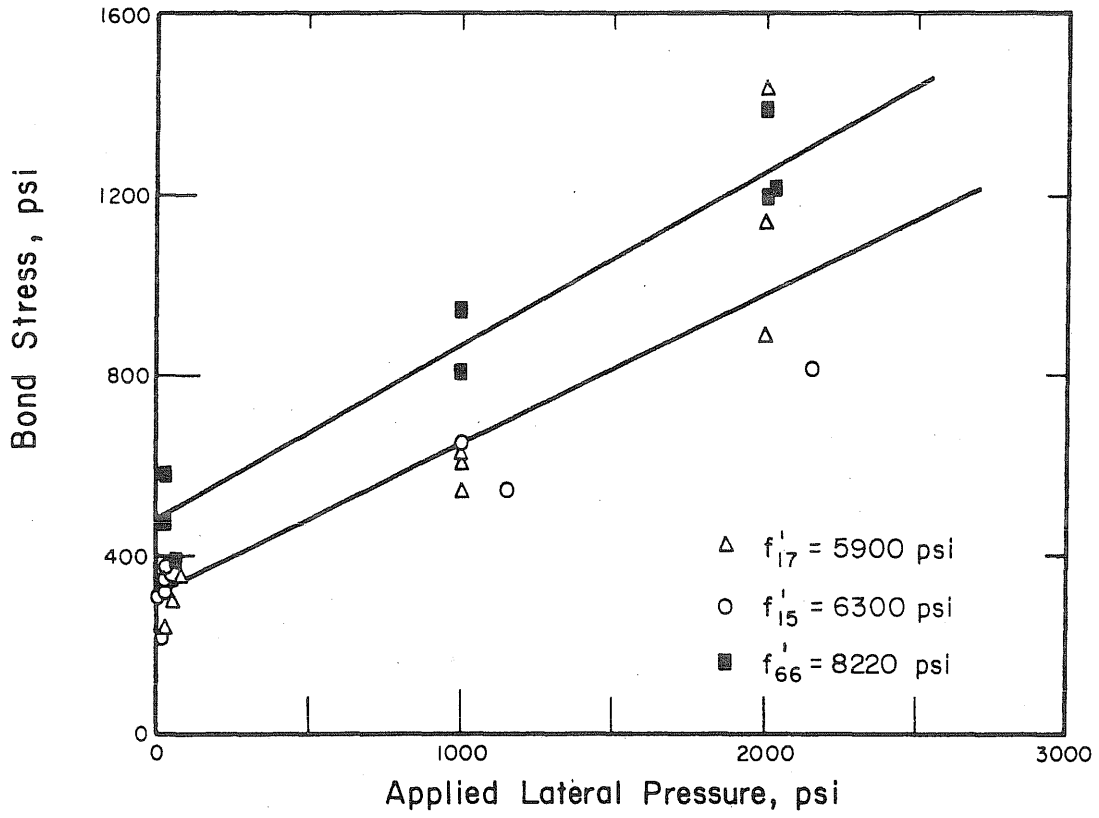

FIG. 8.4 VARIATION OF INITIAL BOND STRESS WITH LATERAL PRESSURE FOR CENTER WIRE FROM 7/16-in. STRAND, SERIES: WAP15-1, WAP17-2, WBP66-1

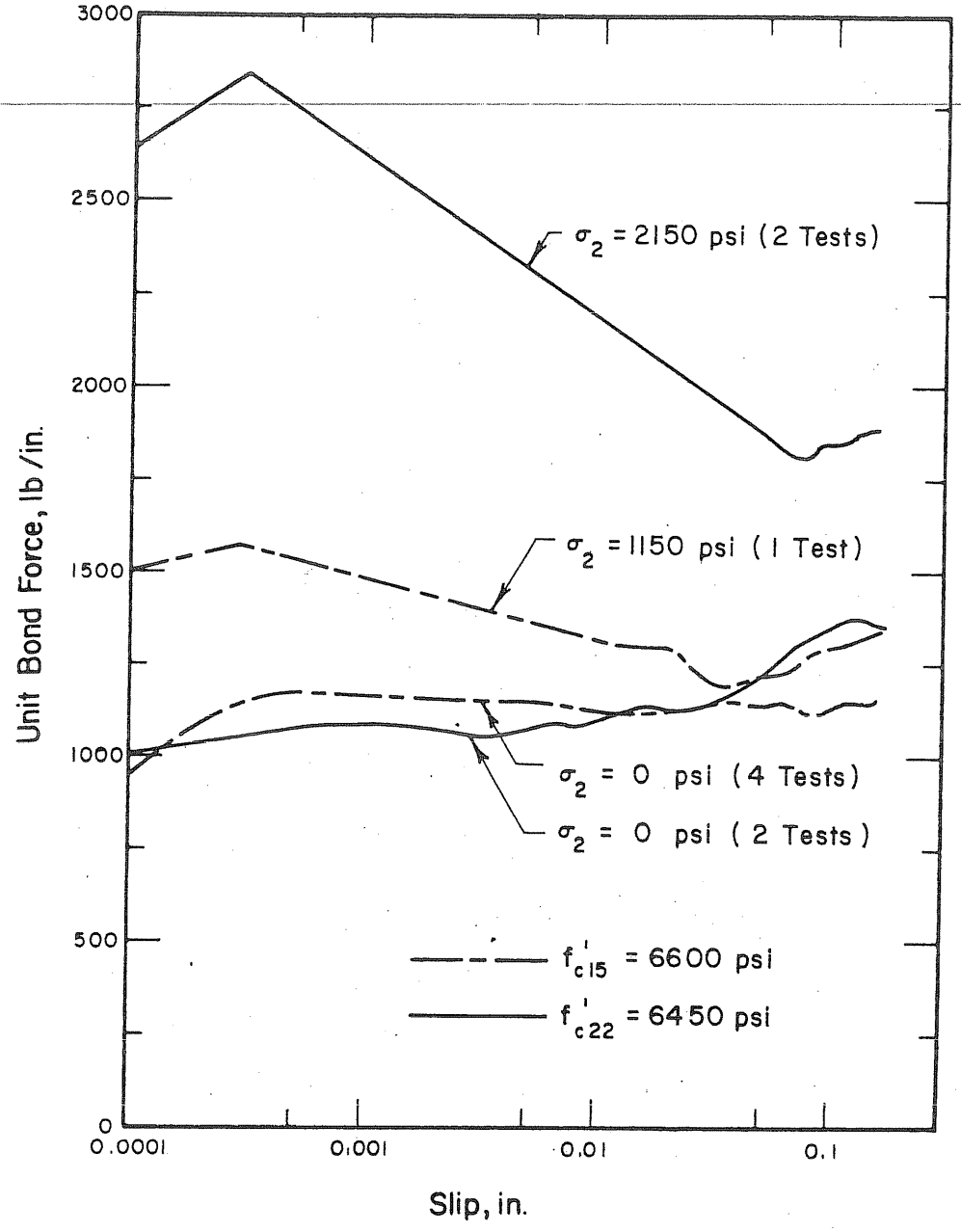

FIG. 8.5 AVERAGE UNIT BOND FORCE-SLIP RELATIONSHIPS OF 7/16-in. STRAND FOR VARIOUS LATERAL PRESSURES, SERIES: SAP15-1, SAP22-2

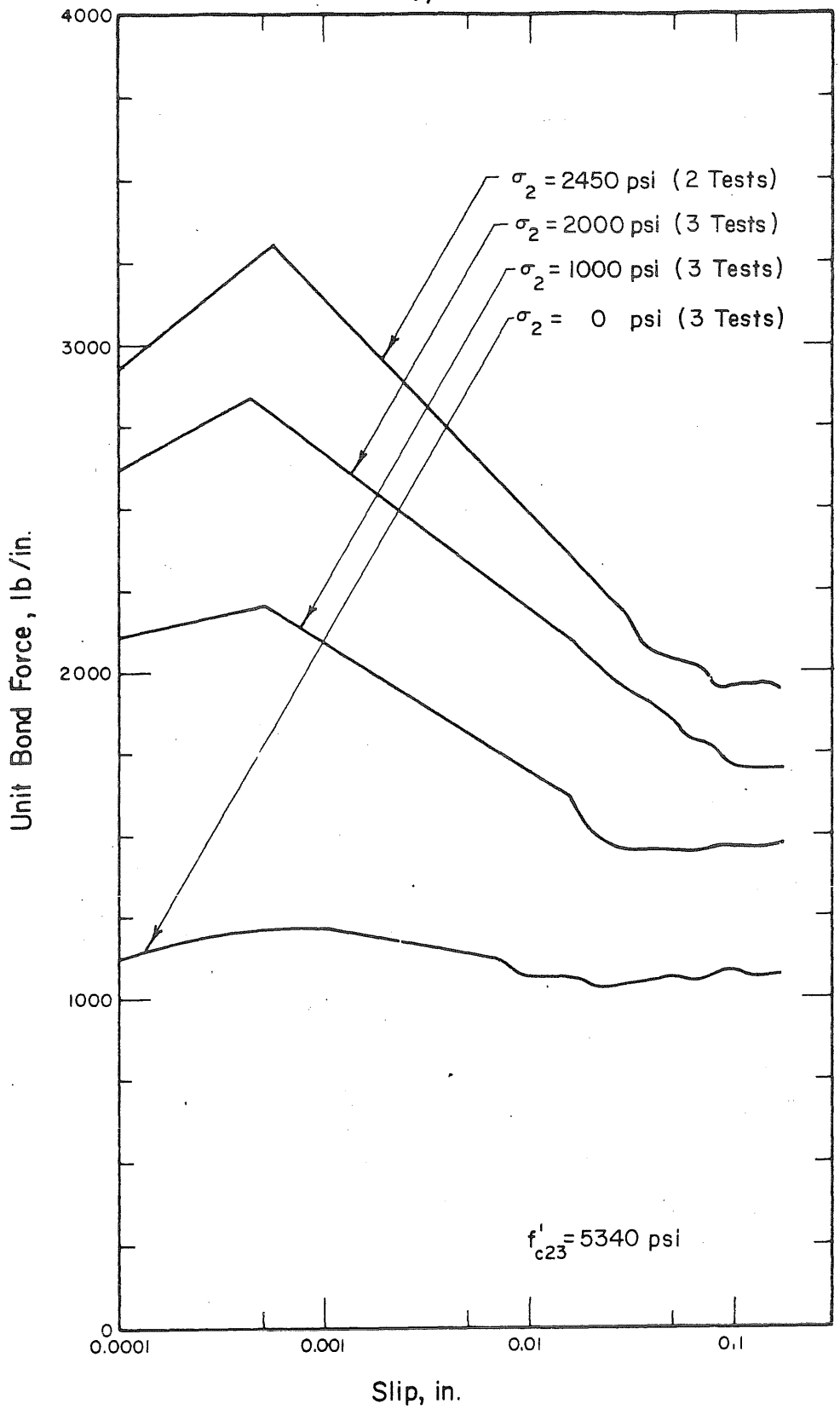

FIG. 8.6 AVERAGE UNIT BOND FORCE-SLIP RELATIONSHIPS OF 7/16-in. STRAND FOR VARIOUS LATERAL PRESSURES, SERIES: SAP23-3

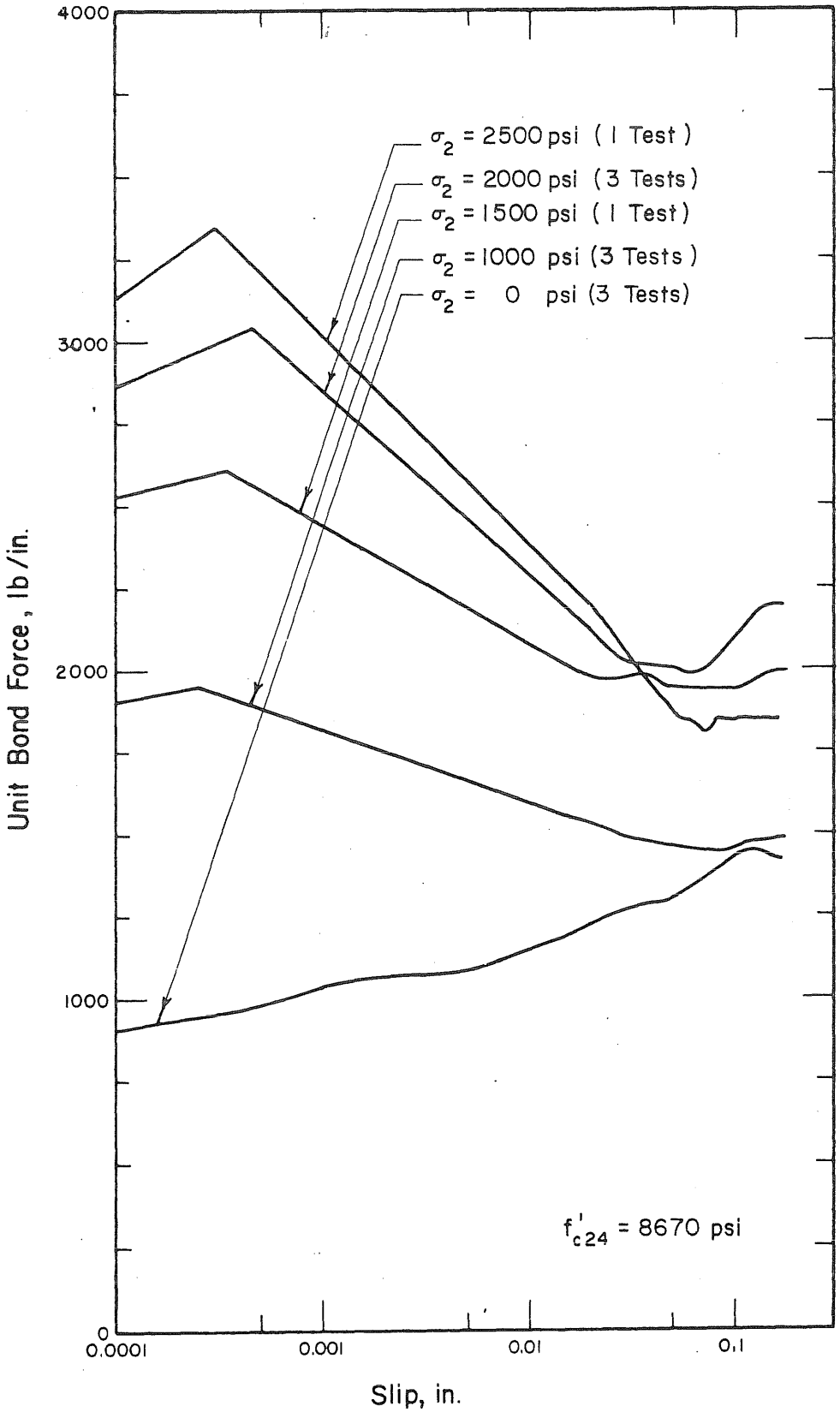

FIG. 8.7 AVERAGE UNIT BOND FORCE-SLIP RELATIONSHIPS OF 7/16-in. STRAND FOR VARIOUS LATERAL PRESSURES, SERIES: SBP24-1

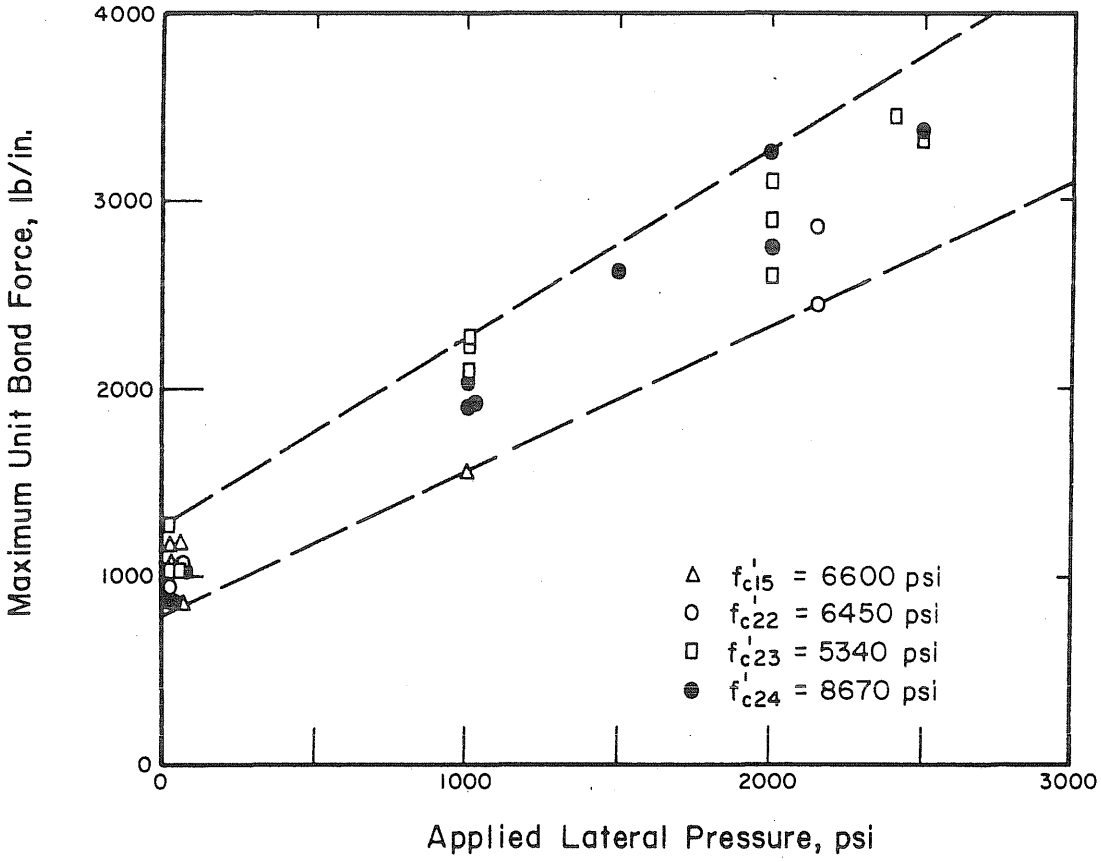

FIG. 8.8 VARIATION OF UNIT BOND FORCE WITH LATERAL PRESSURE FOR 7/16-in. STRAND, SERIES: SAP15-1, SAP22-2, SAP23-3, SAP24-1

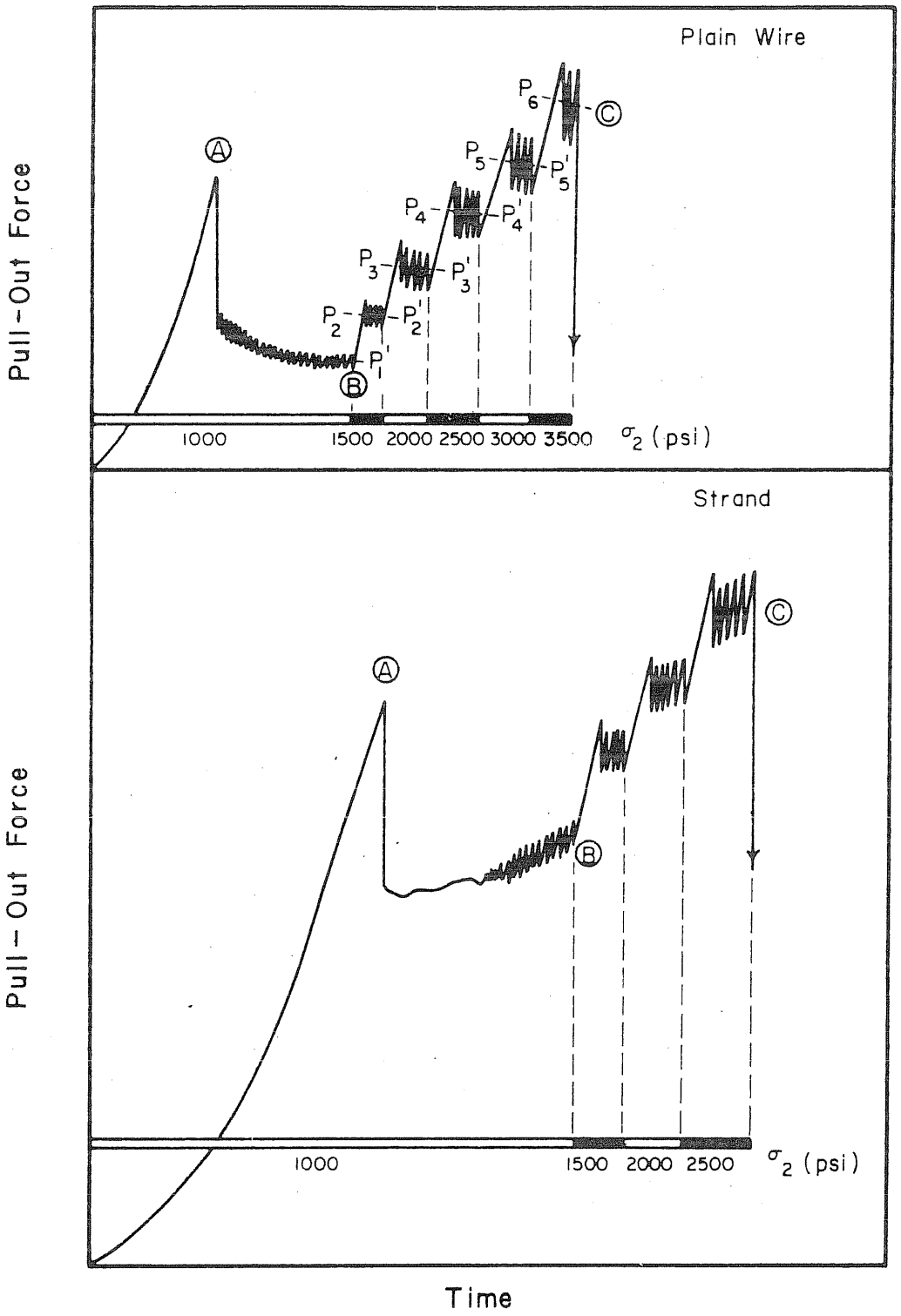

FIG. 8.9 TYPICAL FORCE-TIME CHARTS AS RECORDED BY THE TESTING MACHINE FOR SPECIMENS WITH PLAIN WIRE AND STRAND WHICH WERE SUBJECTED TO LATERAL PRESSURE (σ_2)

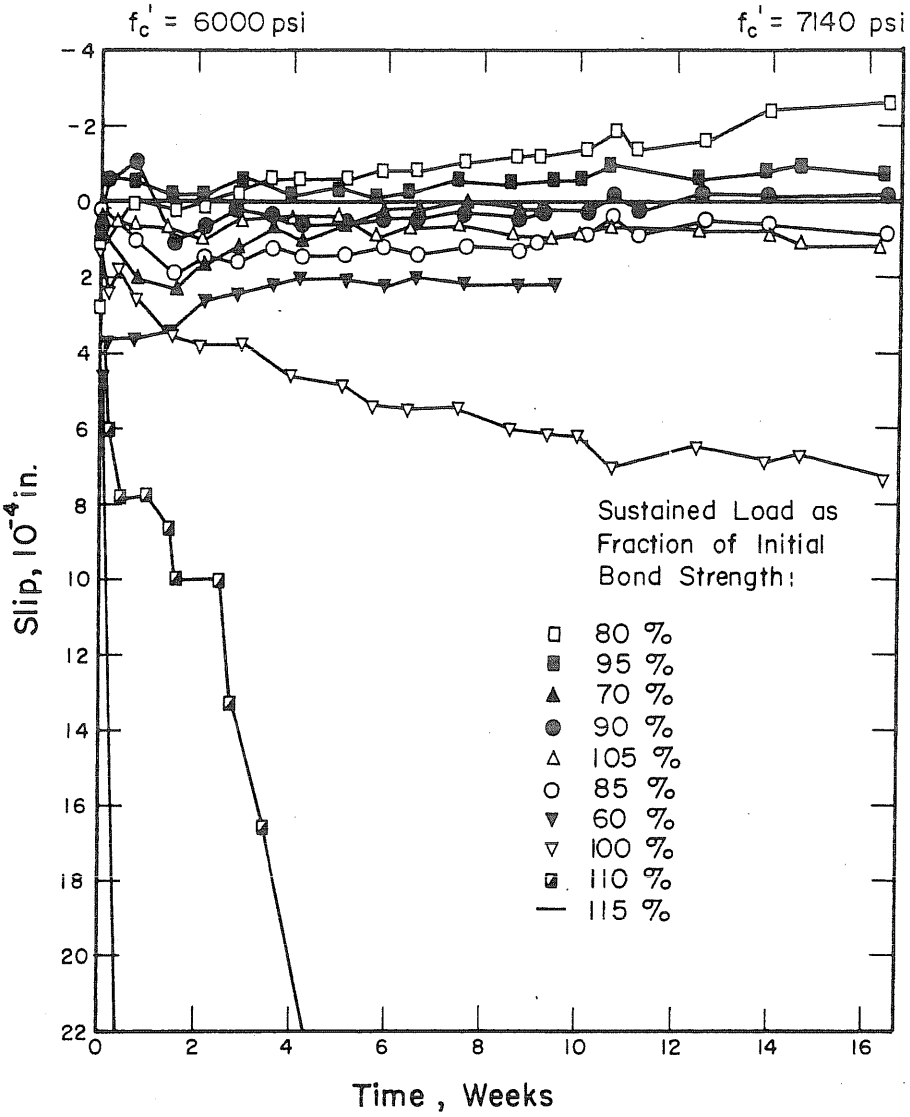

FIG. 9.1 SLIP-TIME RELATIONSHIPS OF 7/16-in. STRAND FOR VARIOUS LOADS, SERIES: SAL12-1

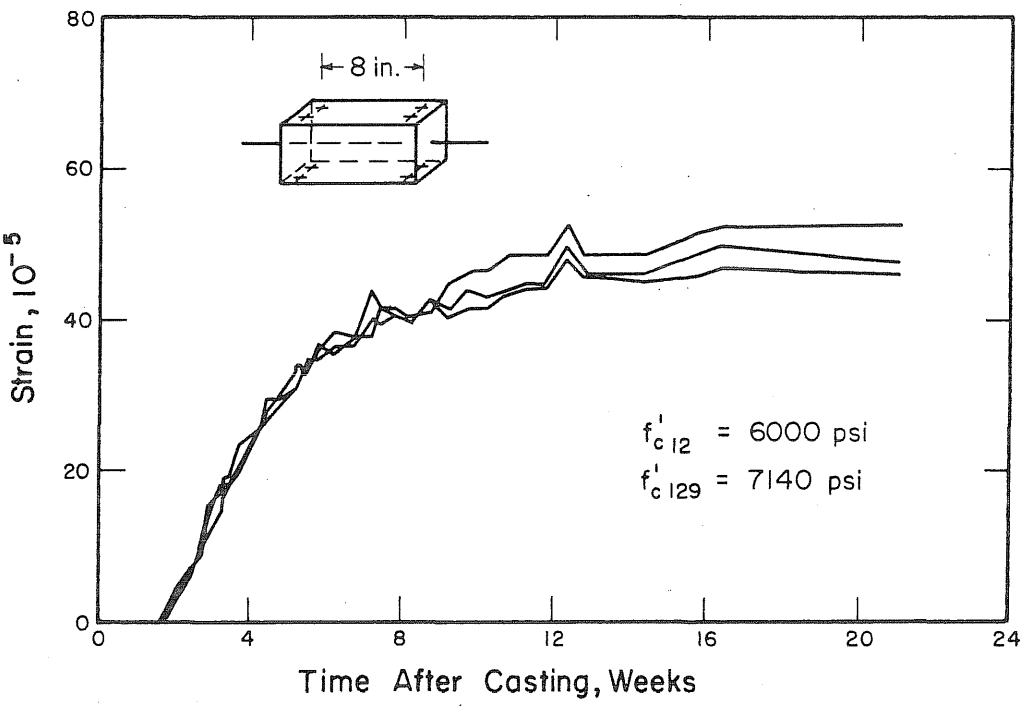

FIG. 9.2 INCREASE IN SHRINKAGE STRAIN DURING SUSTAINED-LOAD TEST, SERIES: SAL12-1

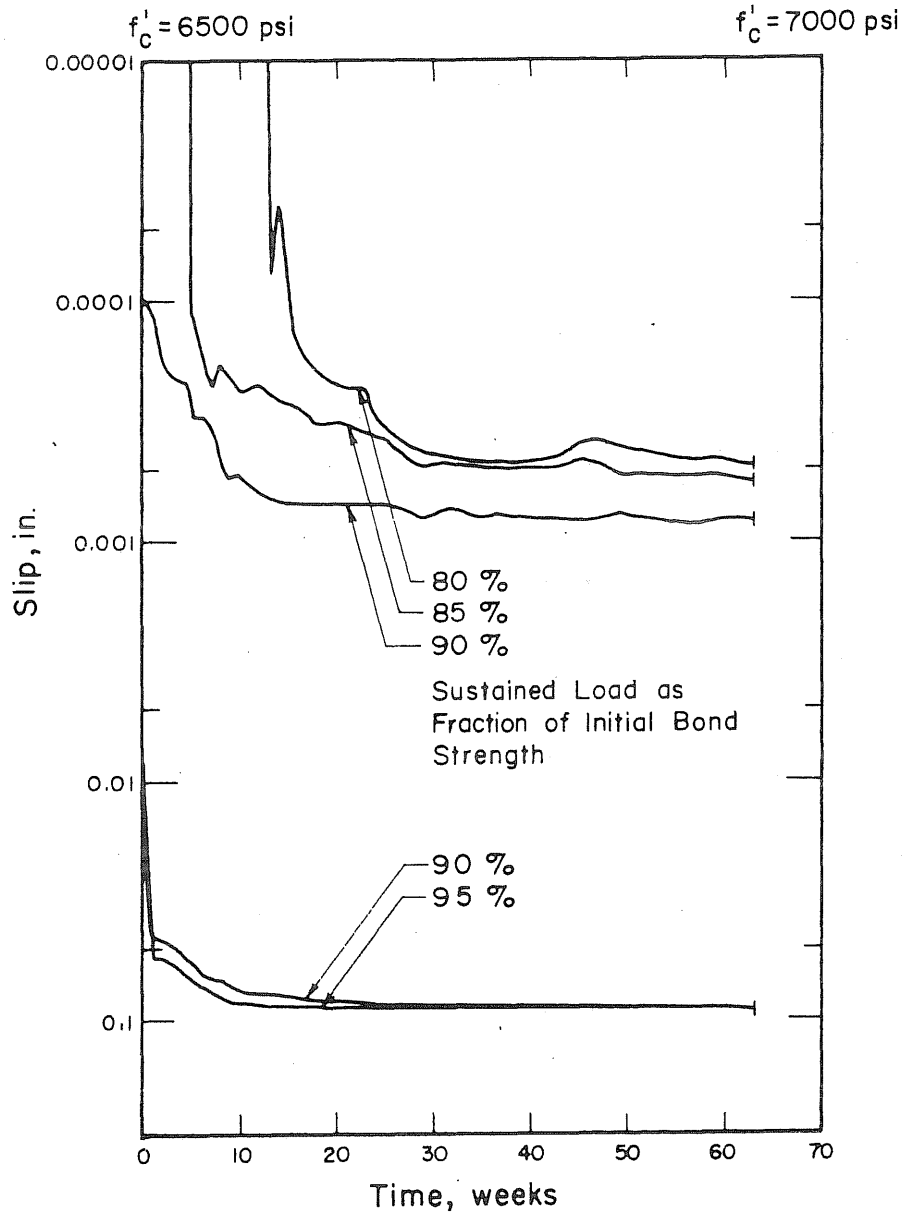

FIG. 9.3 SLIP-TIME RELATIONSHIPS OF 7/16-in. STRAND FOR VARIOUS LOADS, SERIES: SAL11-2

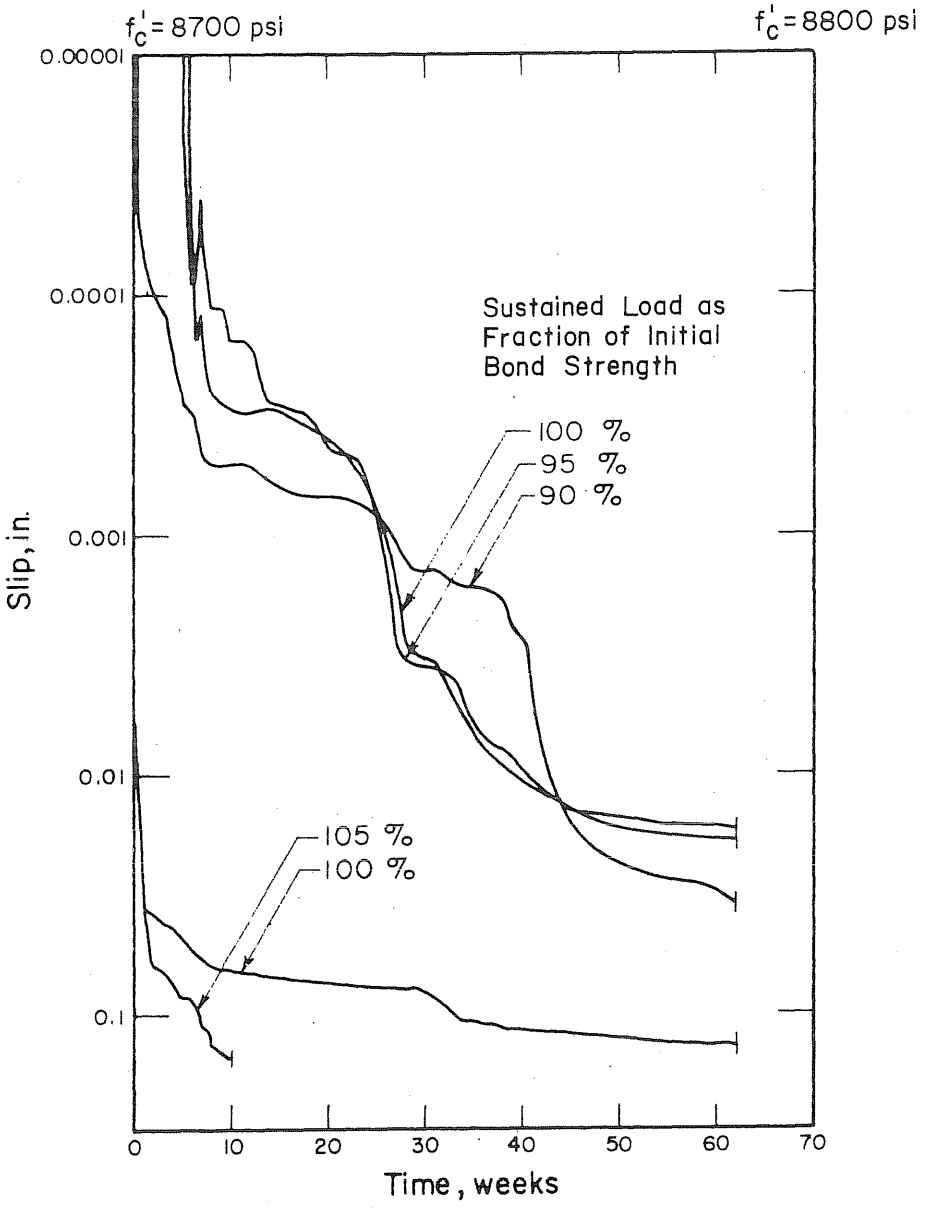

FIG. 9.4 SLIP-TIME RELATIONSHIPS OF 7/16-in. STRAND FOR VARIOUS LOADS, SERIES: SBL12-1

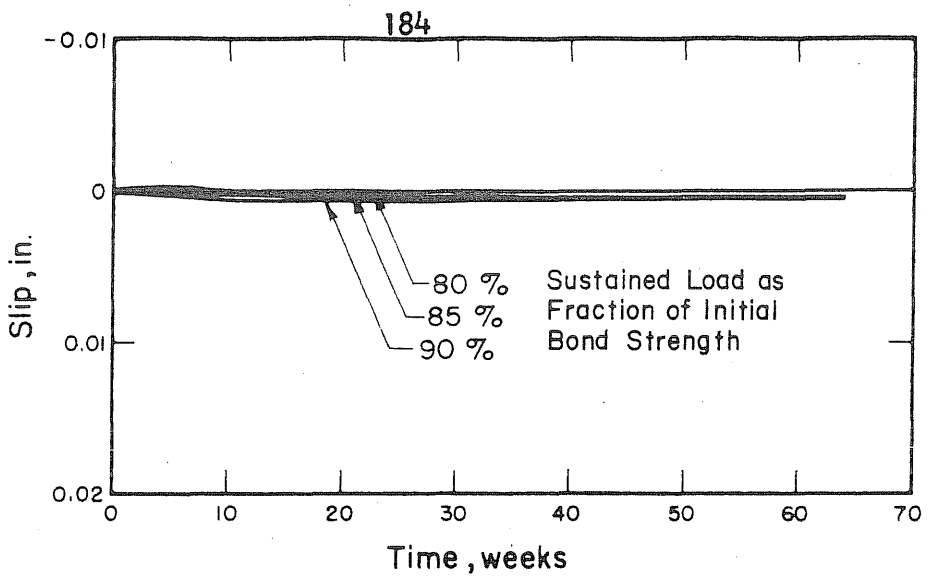

FIG. 9.5 SLIP-TIME RELATIONSHIPS OF 7/16-in. STRAND FOR VARIOUS LOADS, SERIES: SAL11-2

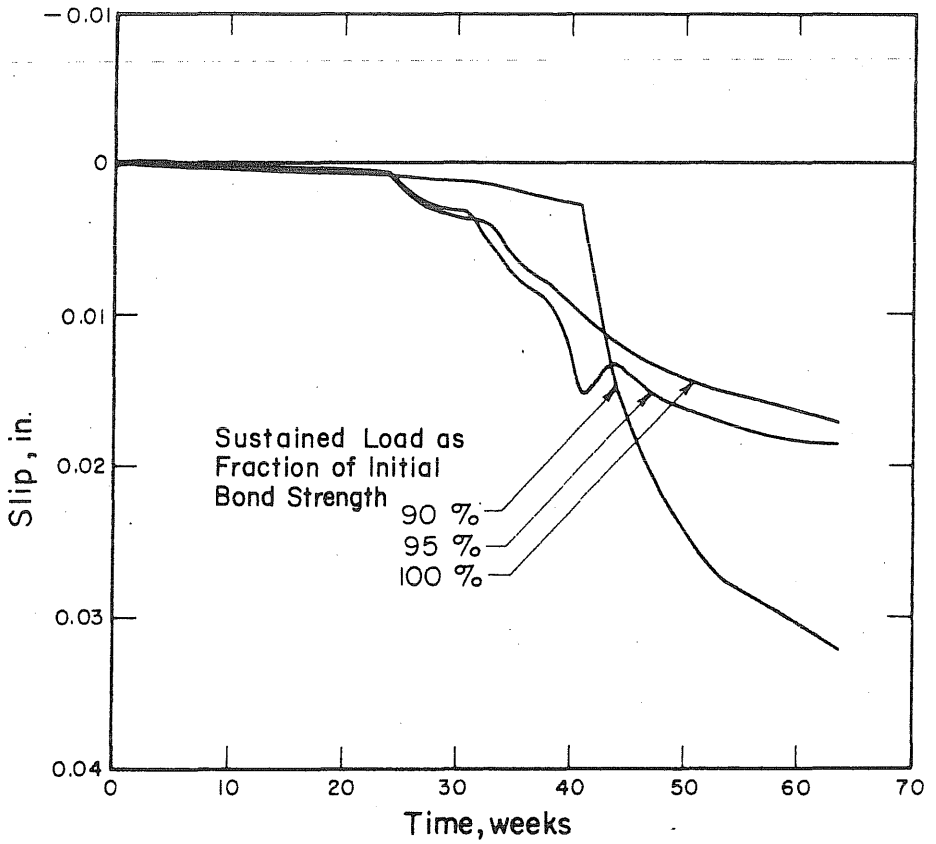

FIG. 9.6 SLIP-TIME RELATIONSHIPS OF 7/16-in. STRAND FOR VARIOUS LOADS, SERIES: SBL12-1

FIG. 9.7 TYPICAL CRACKS ALONG BONDED LENGTH OF SPECIMENS FROM SERIES SAL11-2

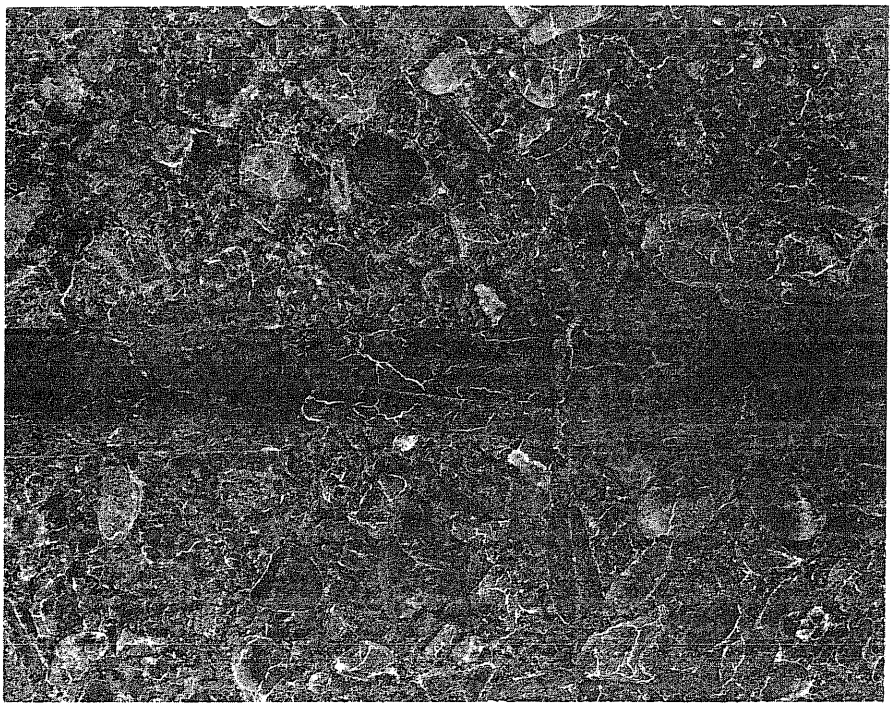

FIG. 9.8 TYPICAL CRACKS ALONG BONDED LENGTH OF SPECIMENS FROM SERIES SBL12-1

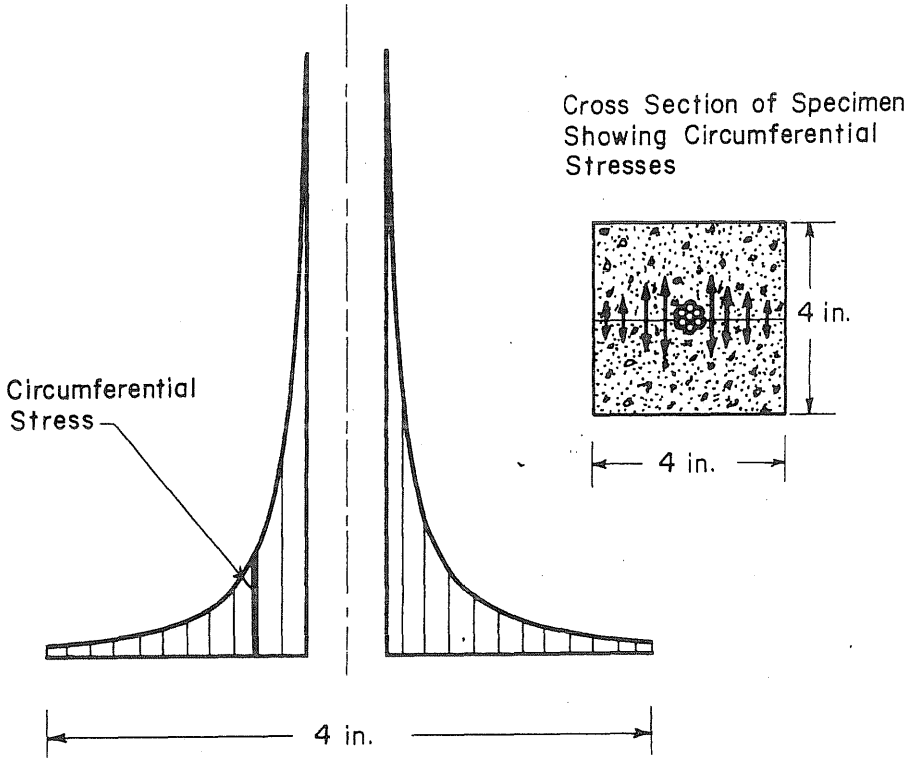

FIG. 9.9 THEORETICAL DISTRIBUTION OF CIRCUMFERENTIAL STRESSES IN THE CONCRETE DUE TO SHRINKAGE

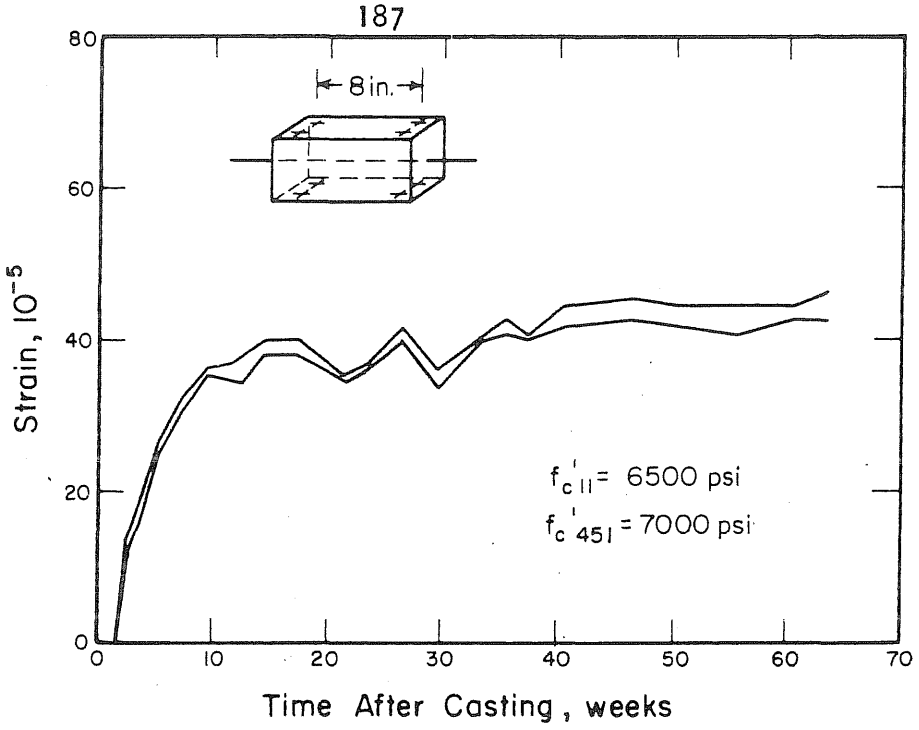

FIG. 9.10 INCREASE IN SHRINKAGE STRAIN DURING SUSTAINED-LOAD TEST, SERIES: SAL11-2

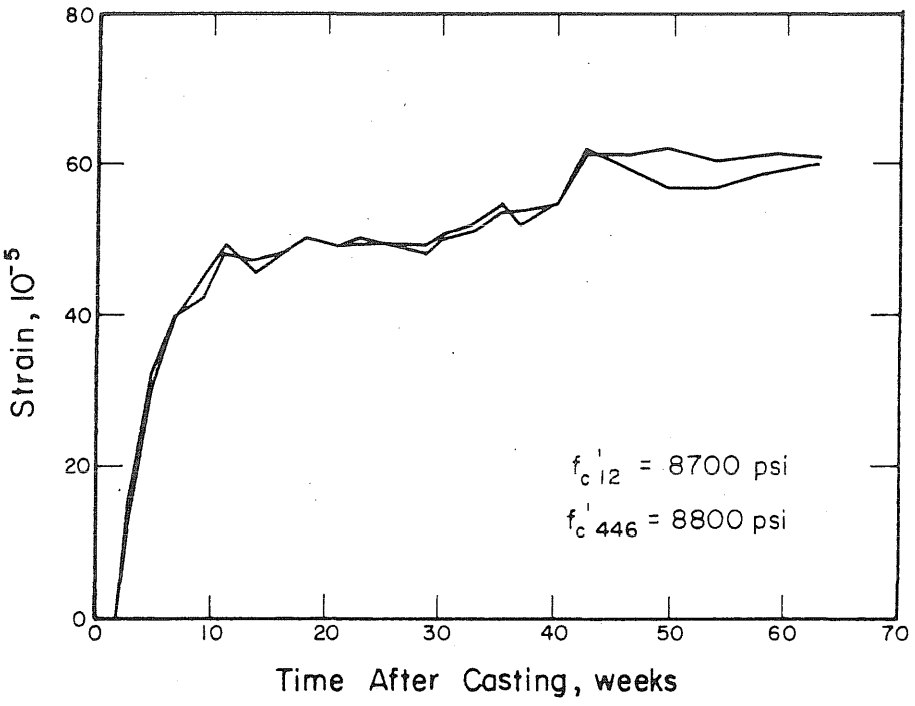

FIG. 9.11 INCREASE IN SHRINKAGE STRAIN DURING SUSTAINED-LOAD TEST, SERIES: SBL12-1

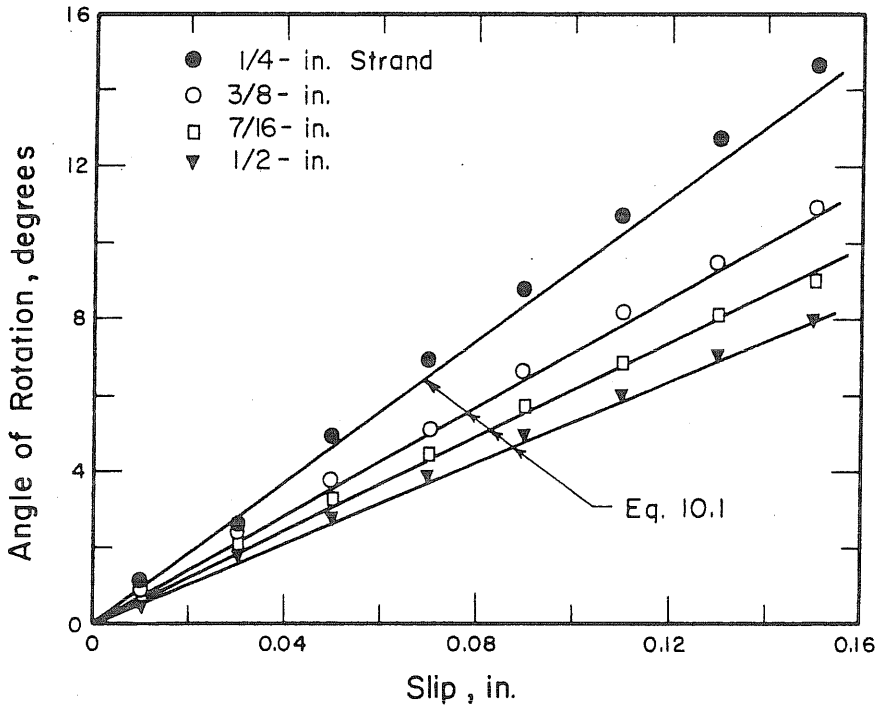

FIG. 10.1 AVERAGE ROTATION-SLIP RELATIONSHIPS FOR DIFFERENT STRAND SIZES

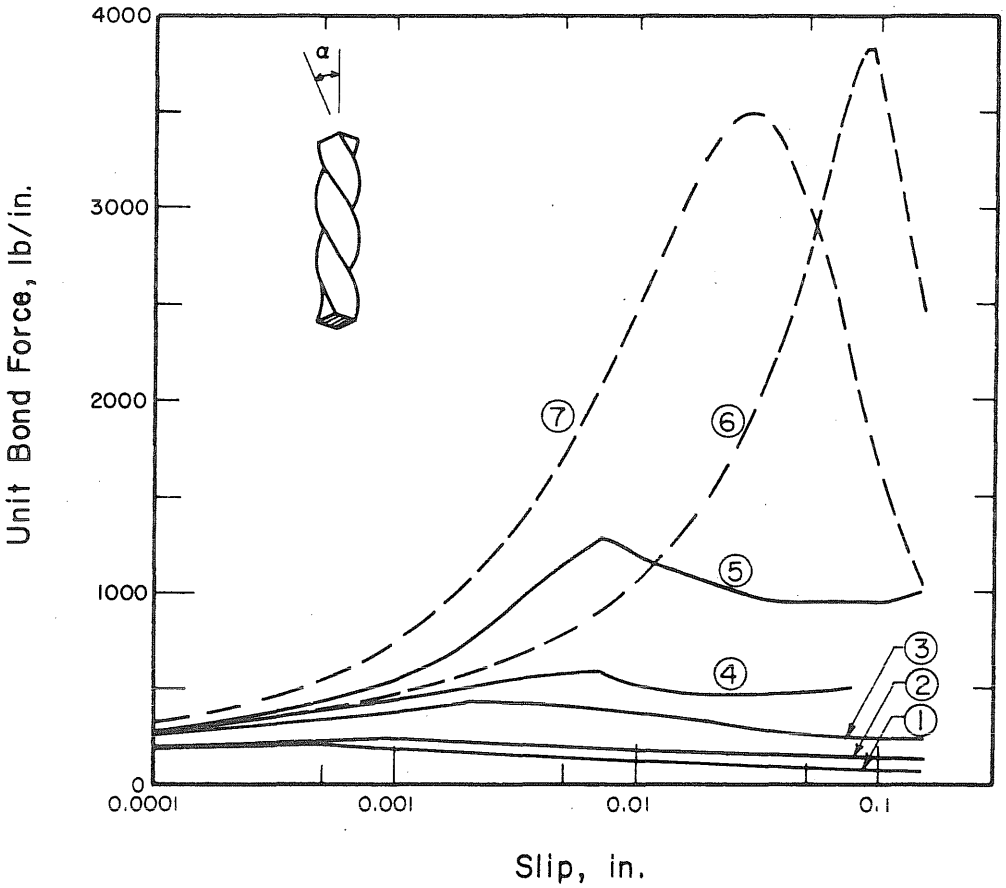

(a) Concrete specimens free to rotate:

(1) $\alpha = 0^{o}$, 3 tests

(2) $\alpha = 11^{o}$, 3 tests

(3) $\alpha = 28^{o}$, 3 tests

(4) $\alpha = 38^{o}$, 4 tests

(5) $\alpha = 44^{o}$, 1 test

(b) Concrete specimens restrained from rotation

(6) $\alpha = 37^{o}$, 2 tests

(7) $\alpha = 46^{o}$, 1 test

FIG. 10.2 AVERAGE UNIT BOND FORCE-SLIP RELATIONSHIPS OF 5/16-in. SQUARE BARS FOR DIFFERENT TEST CONDITIONS, SERIES: QB09-1

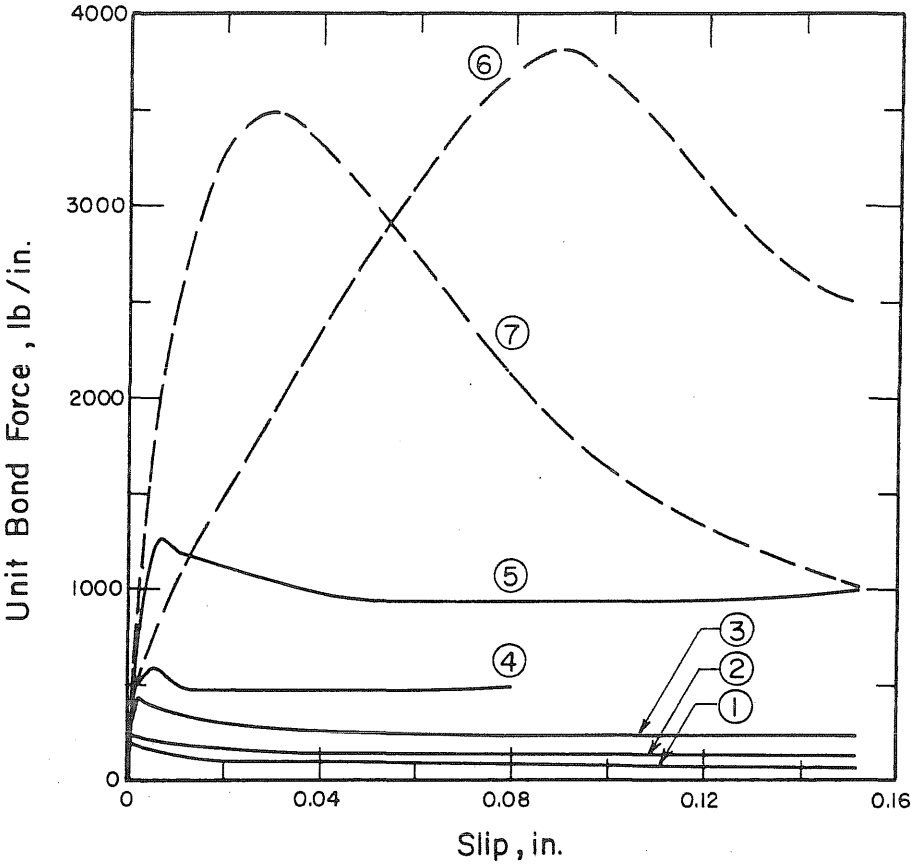

(a) Concrete specimens free to rotate
- (1) $\alpha = 0^{o}$, 3 tests
- (2) $\alpha = 11^{o}$, 3 tests
- (3) $\alpha = 28^{o}$, 3 tests
- (4) $\alpha = 38^{o}$, 4 tests
- (5) $\alpha = 44^{o}$, 1 test

(b) Concrete specimens restrained from rotation:
- (6) $\alpha = 37^{o}$, 2 tests
- (7) $\alpha = 46^{o}$, 1 test

FIG. 10.3 AVERAGE UNIT BOND FORCE-SLIP RELATIONSHIPS OF 5/16-in. SQUARE BARS FOR DIFFERENT TEST CONDITIONS, SERIES: QB09-1

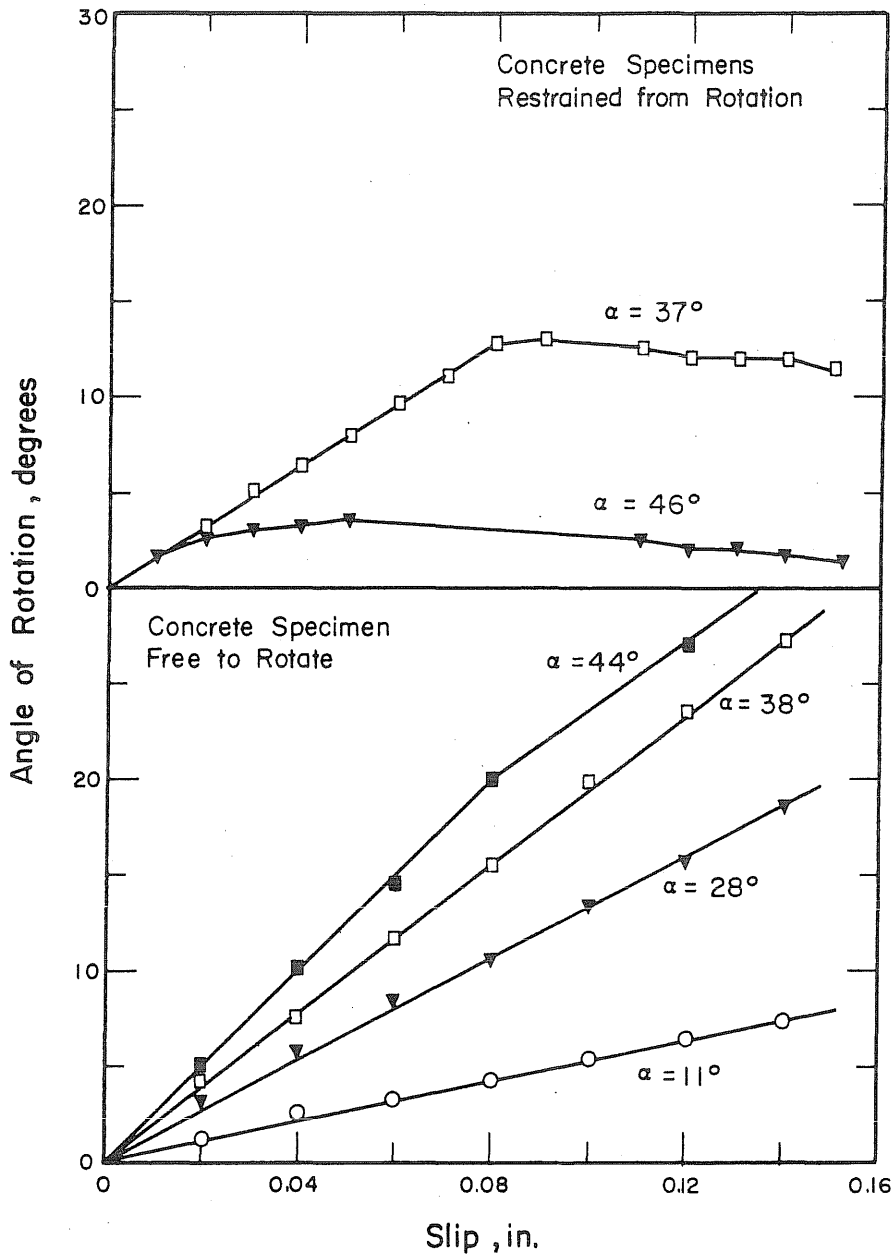

FIG. 10.4 AVERAGE ROTATION-SLIP RELATIONSHIPS OF TWISTED 5/16-in. SQUARE BARS FOR DIFFERENT TEST CONDITIONS, SERIES: QB09-1

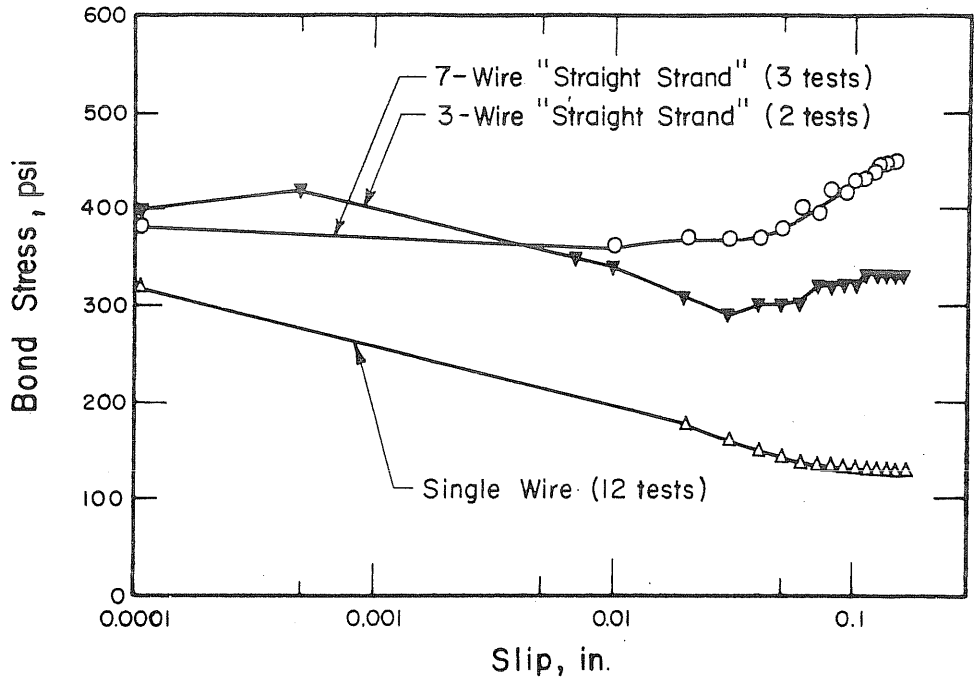

FIG. 10.5 AVERAGE BOND STRESS-SLIP RELATIONSHIPS FOR "STRAIGHT" (NONTWISTED) STRAND AND PLAIN WIRE, SERIES: UA09-1

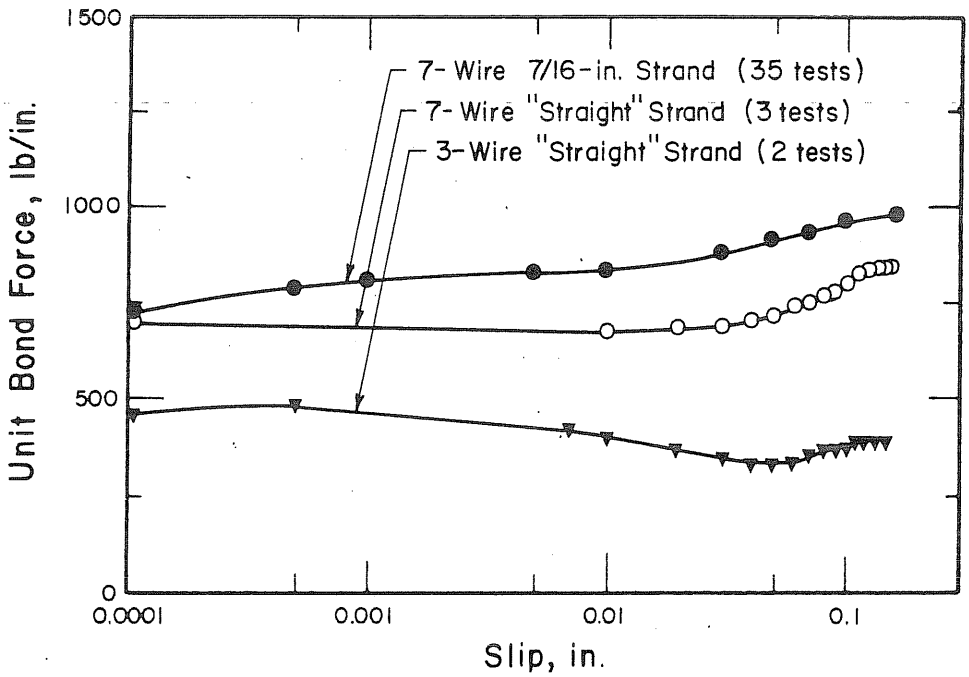

FIG. 10.6 AVERAGE UNIT BOND FORCE-SLIP RELATIONSHIPS FOR "STRAIGHT" (NONTWISTED) STRAND AND REGULAR 7/16-in. STRAND, SERIES: UA09-1

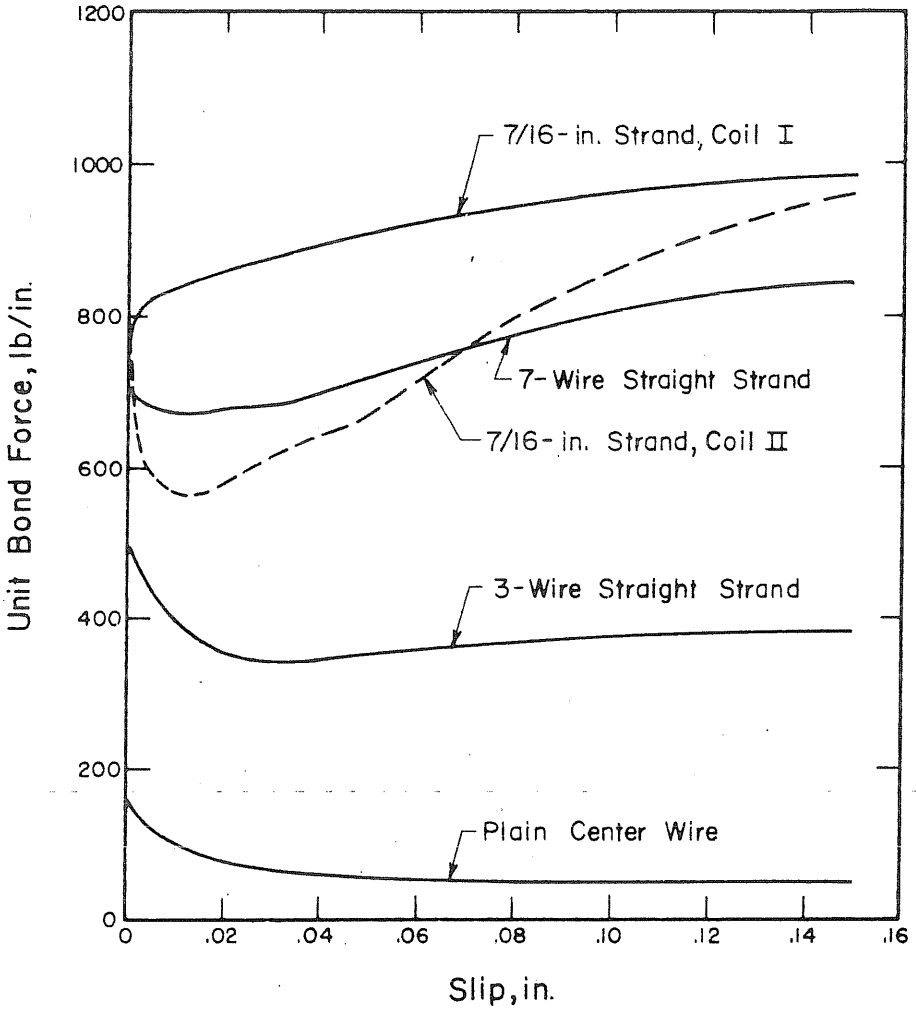

FIG. 10.7 COMPARISON OF UNIT BOND FORCE-SLIP RELATIONSHIPS OF "STRAIGHT" (NONTWISTED) STRAND, REGULAR 7/16-in. STRAND, AND PLAIN CENTER WIRE FROM 7/16-in. STRAND, SERIES: UA09-1

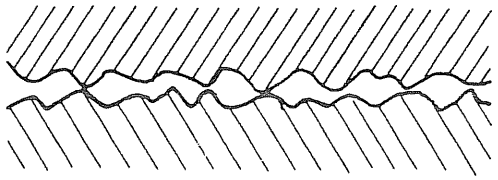

(a) Contact Between Two Solid Bodies

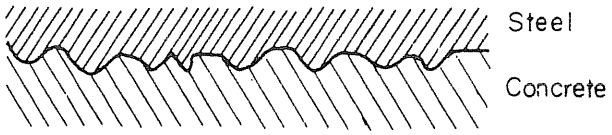

(b) Contact Between Steel and Concrete

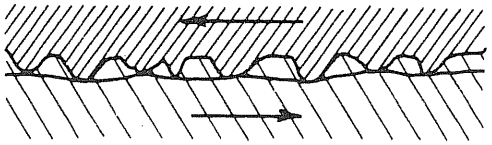

(c) Forming of a Shear Plane in The Concrete

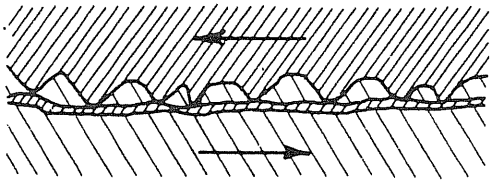

(d) Forming of a Layer of Abrasive Wear Particles

FIG. 11.1 ASSUMED PHASES DURING A BOND FAILURE BETWEEN STEEL AND CONCRETE

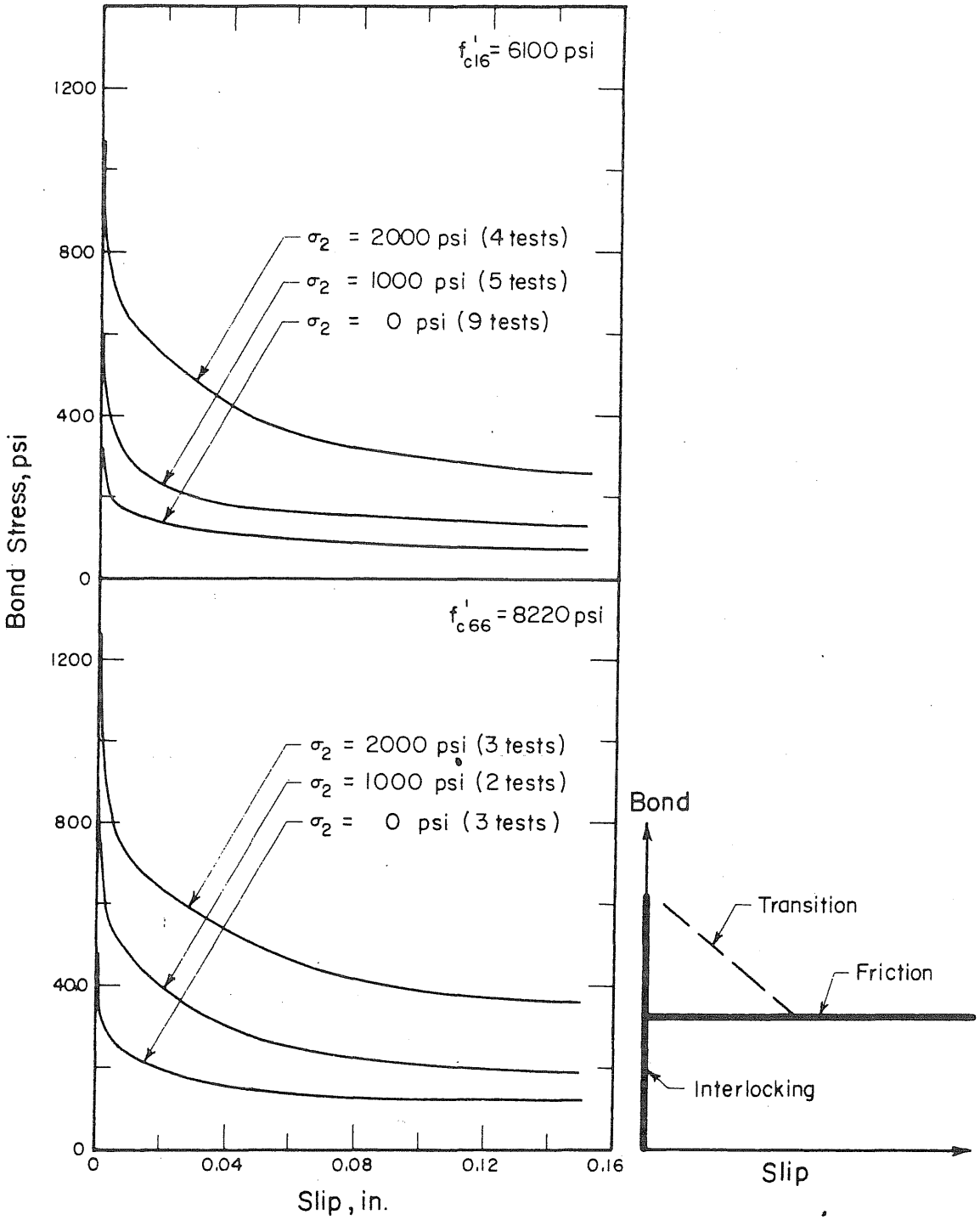

FIG. 11.2 AVERAGE BOND STRESS-SLIP RELATIONSHIPS OF CENTER WIRES FROM 7/16-in. STRAND FOR VARIOUS LEVELS OF LATERAL PRESSURE, SERIES: WAP15-1, WAP17-2, WBP66-1

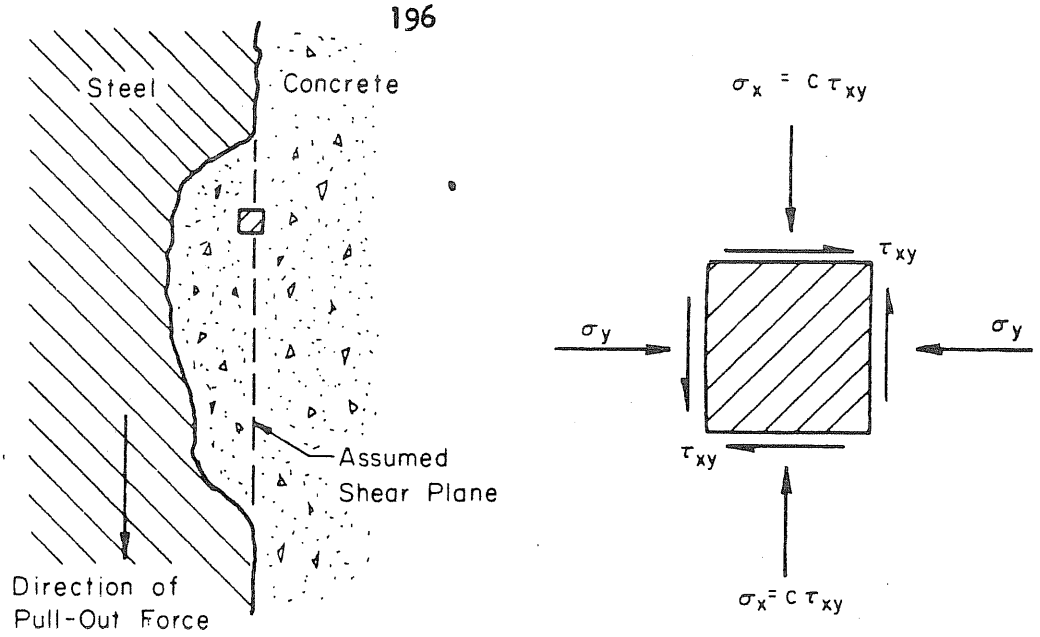

FIG. 11.3 SIMPLIFIED STRESS CONDITIONS IN AN INTERLOCKING CONCRETE SHEAR KEY

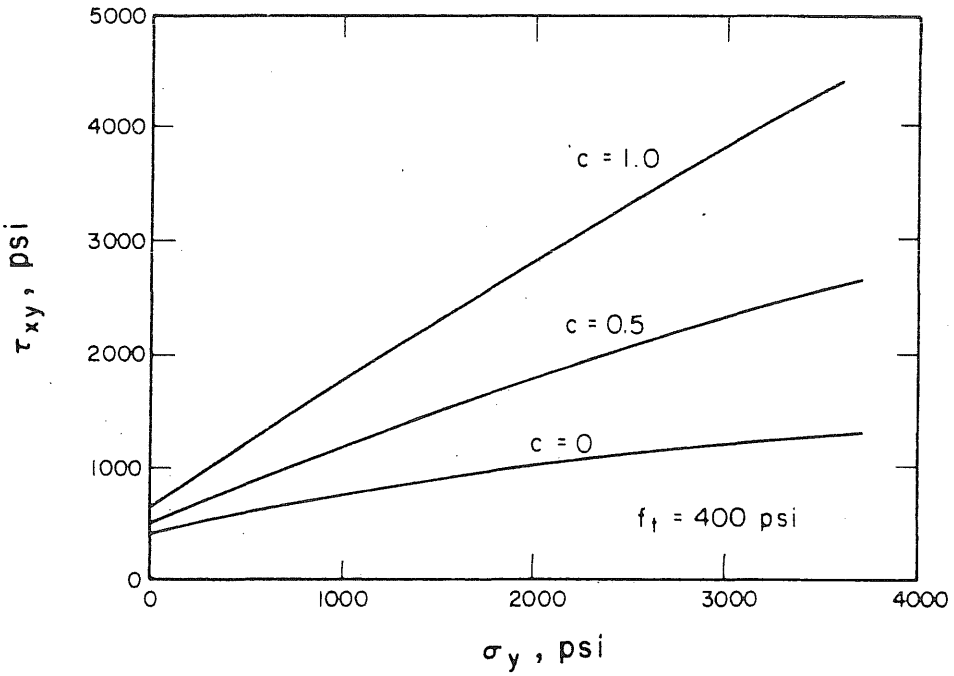

FIG. 11.4 SHEAR STRESS vs. LATERAL PRESSURE FOR DIFFERENT VALUES OF C

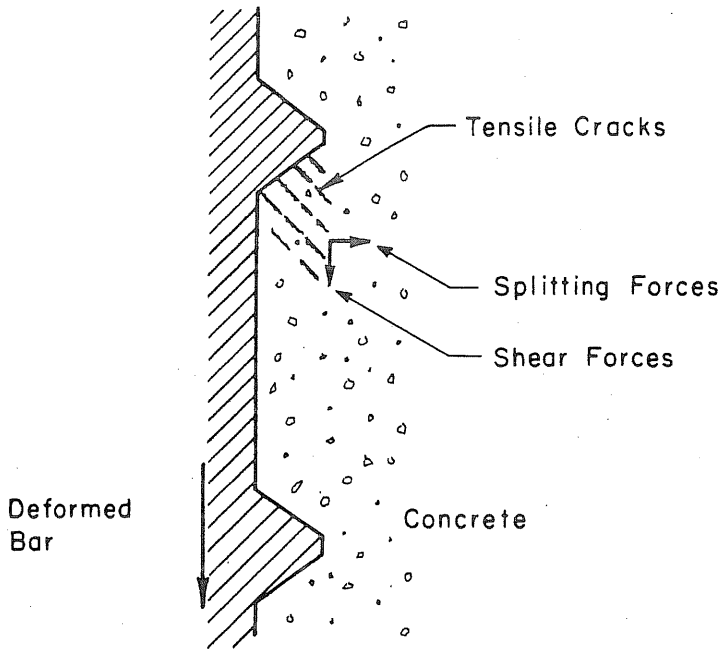

FIG. 11.5 BOND MECHANISM FOR A DEFORMED BAR

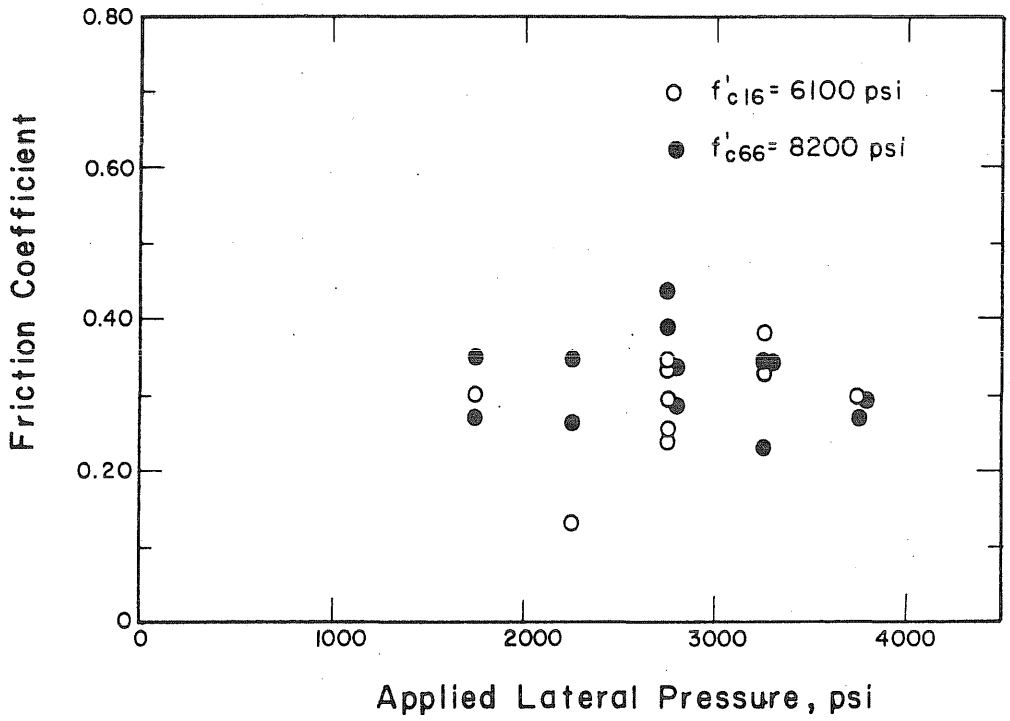

FIG. 11.6 VARIATION OF FRICTION COEFFICIENT WITH LATERAL PRESSURE AFTER A SLIP OF 0.15 in. HAD DEVELOPED

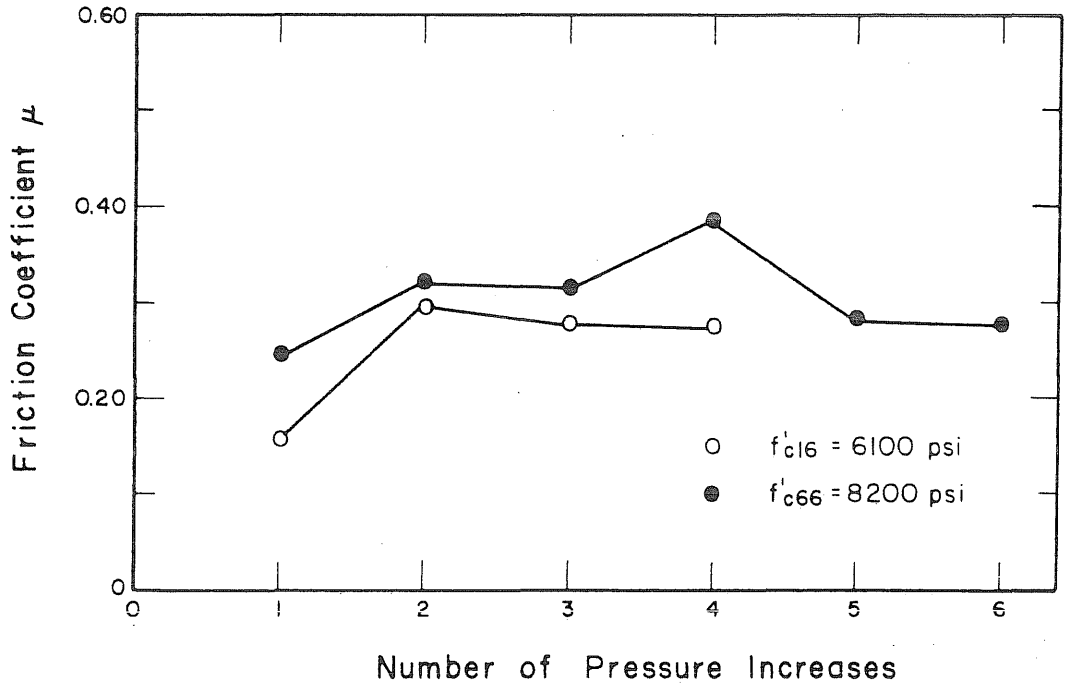

FIG. 11.7 VARIATION OF FRICTION COEFFICIENT WITH THE NUMBER OF PRESSURE INCREASES

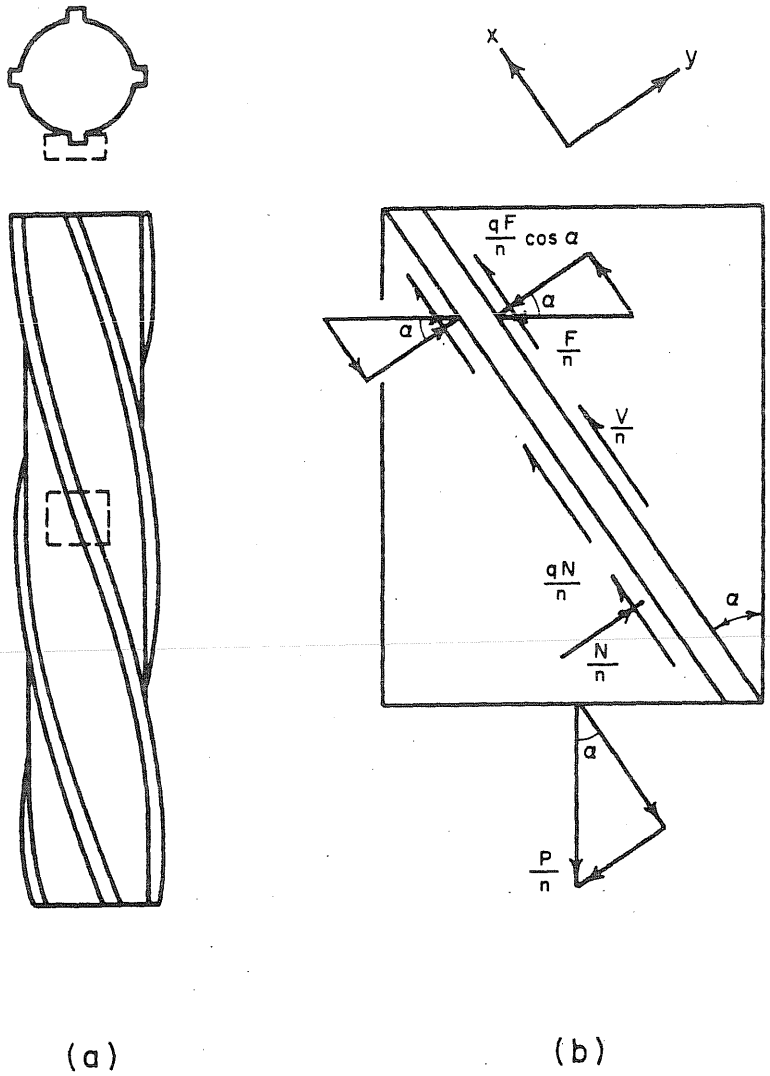

FIG. 12.1 A CONCEPTUAL MODEL FOR INITIAL BOND OF STRAND

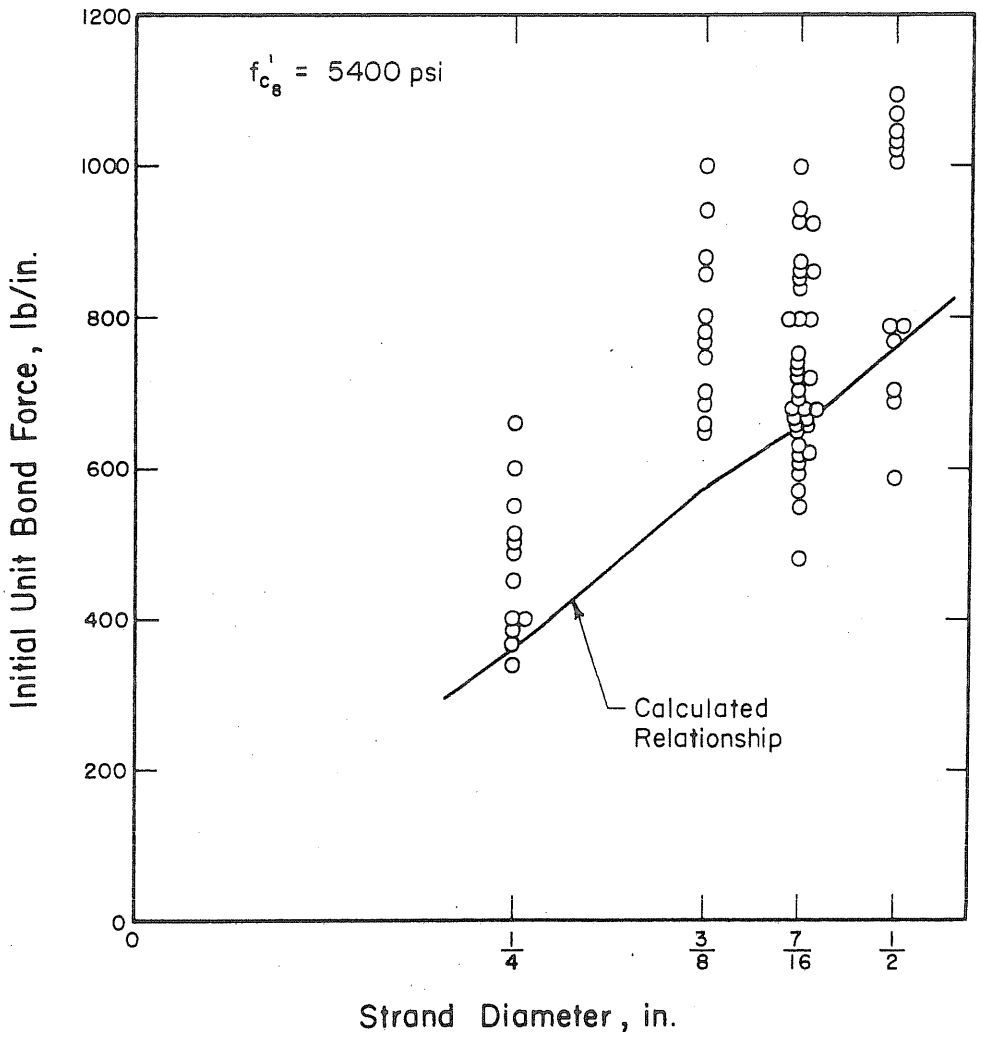

FIG. 12.2 INITIAL UNIT BOND FORCE vs. STRAND DIAMETER

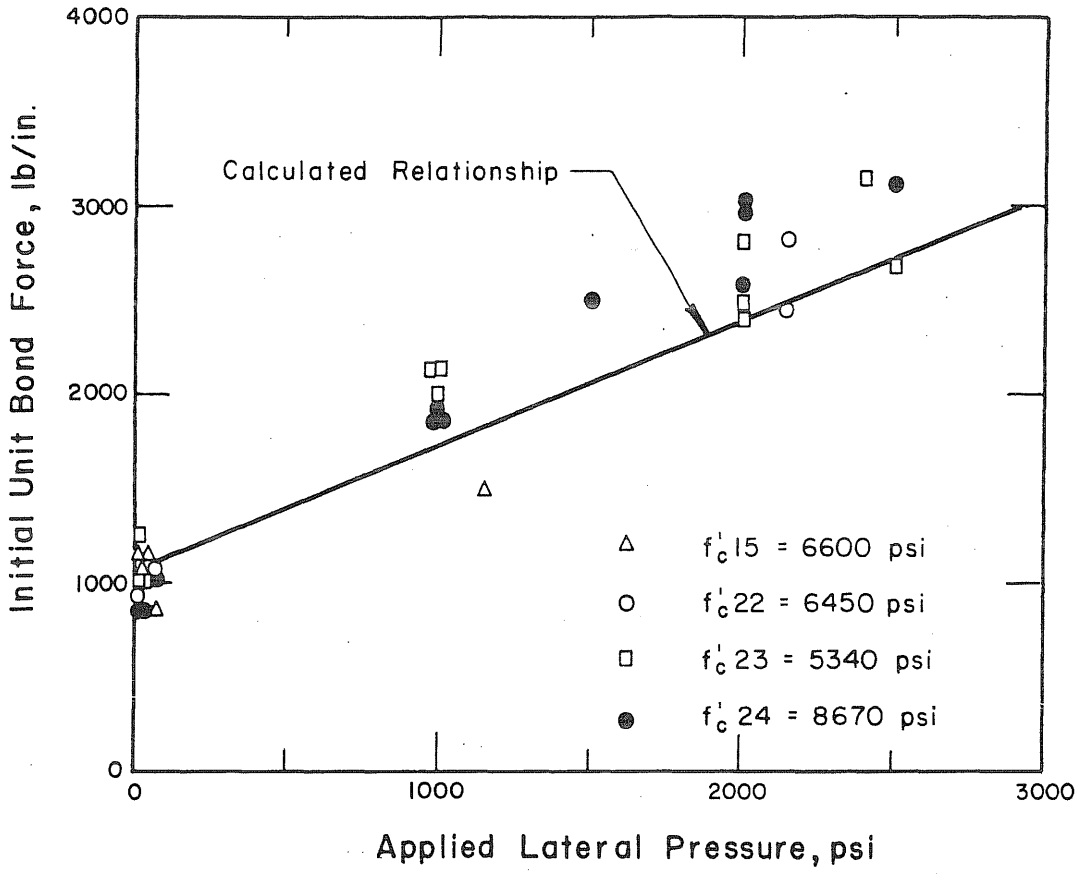

FIG. 12.3 INITIAL UNIT BOND FORCE OF 7/16-in. STRAND vs. APPLIED LATERAL PRESSURE

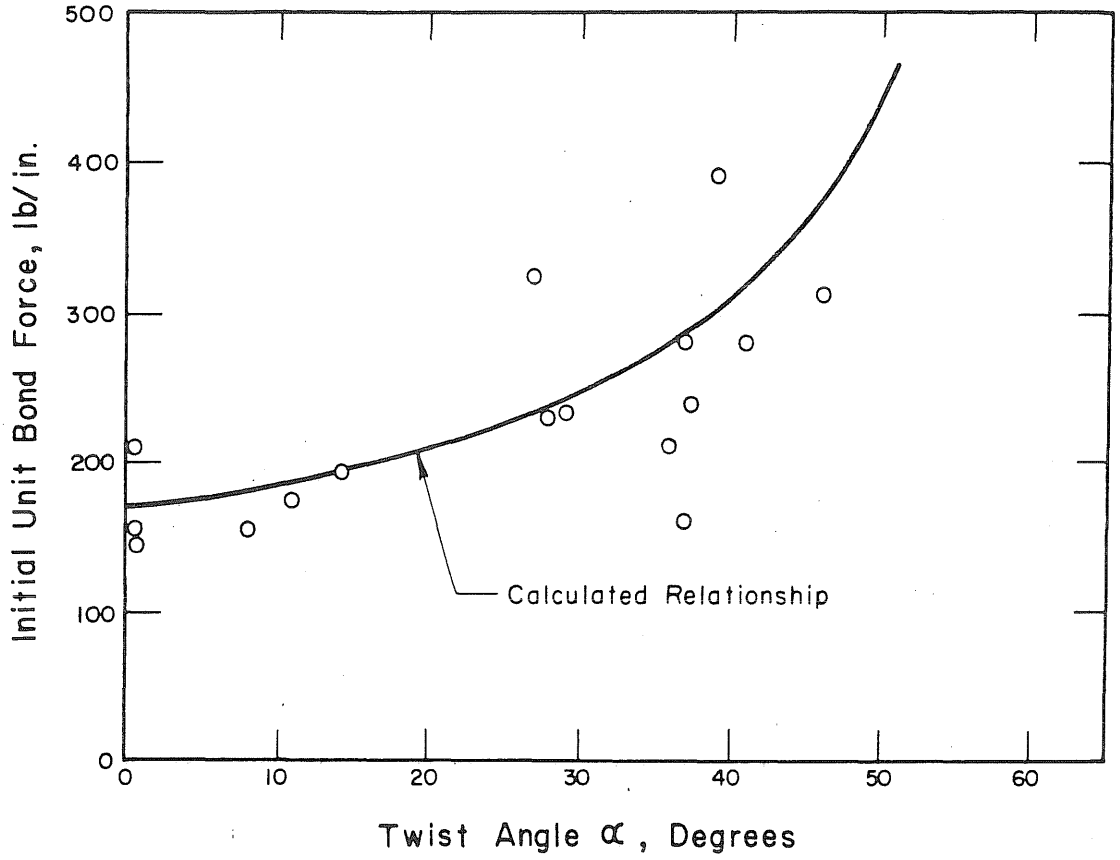

FIG. 12.4 INITIAL UNIT BOND FORCE vs. TWIST ANGLE FOR 5/16-in. SQUARE BARS

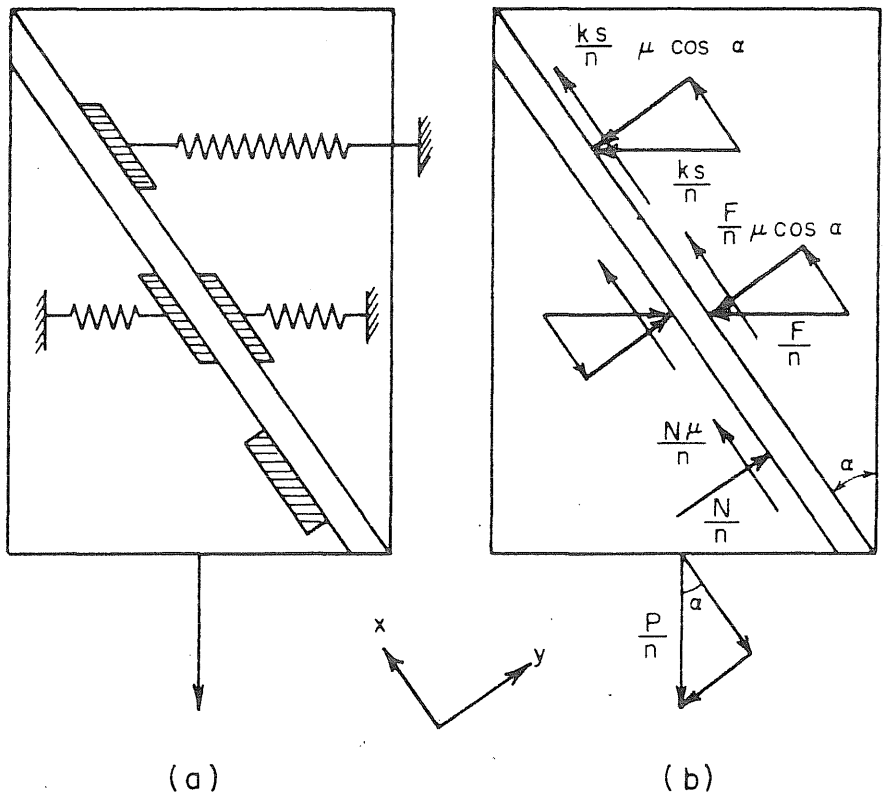

FIG. 12.5 A CONCEPTUAL MODEL FOR SLIDING BOND OF STRAND

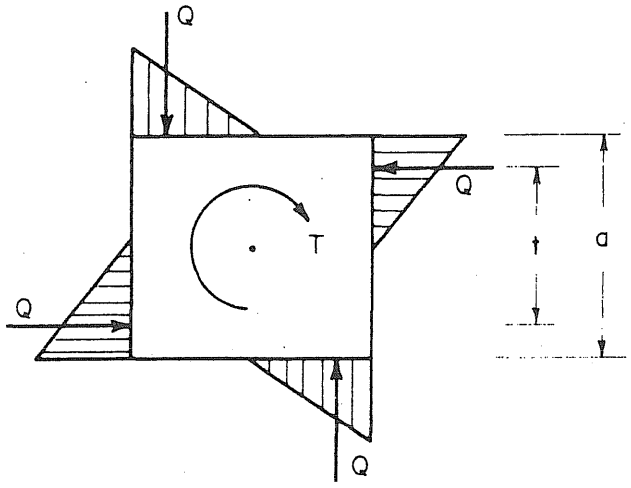

FIG. 12.6 ASSUMED FORCE DISTRIBUTION ON CROSS SECTION OF SQUARE BAR DUE TO UNTWISTING OF THE BAR

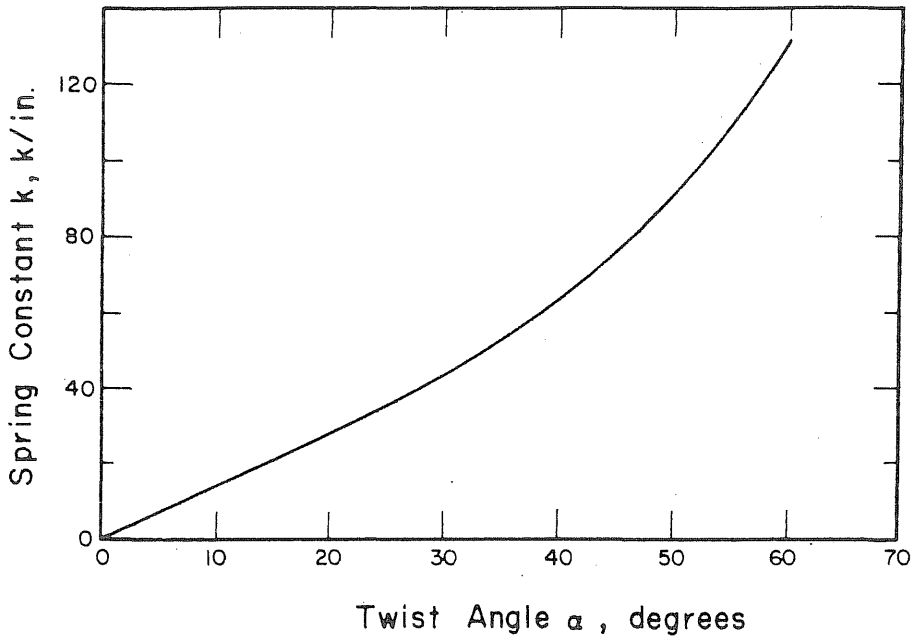

FIG. 12.7 VARIATION OF SPRING CONSTANT k WITH TWIST ANGLE α OF 5/16-in. SQUARE BARS

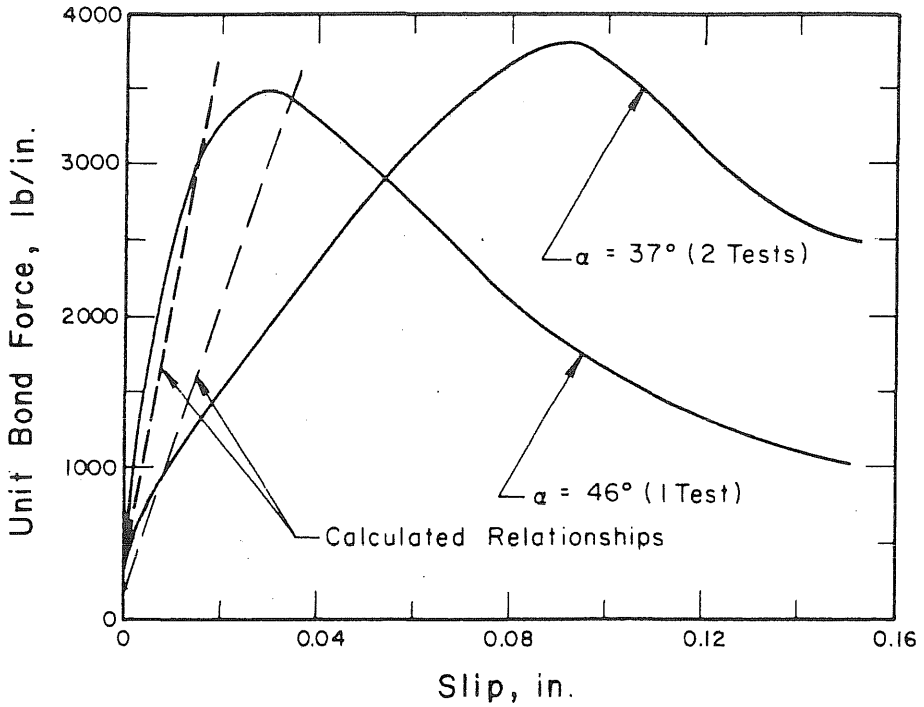

FIG. 12.8 CALCULATED vs. MEASURED BOND-SLIP RELATIONSHIPS OF TWISTED 5/16-in. SQUARE BARS, SERIES: QB09-1

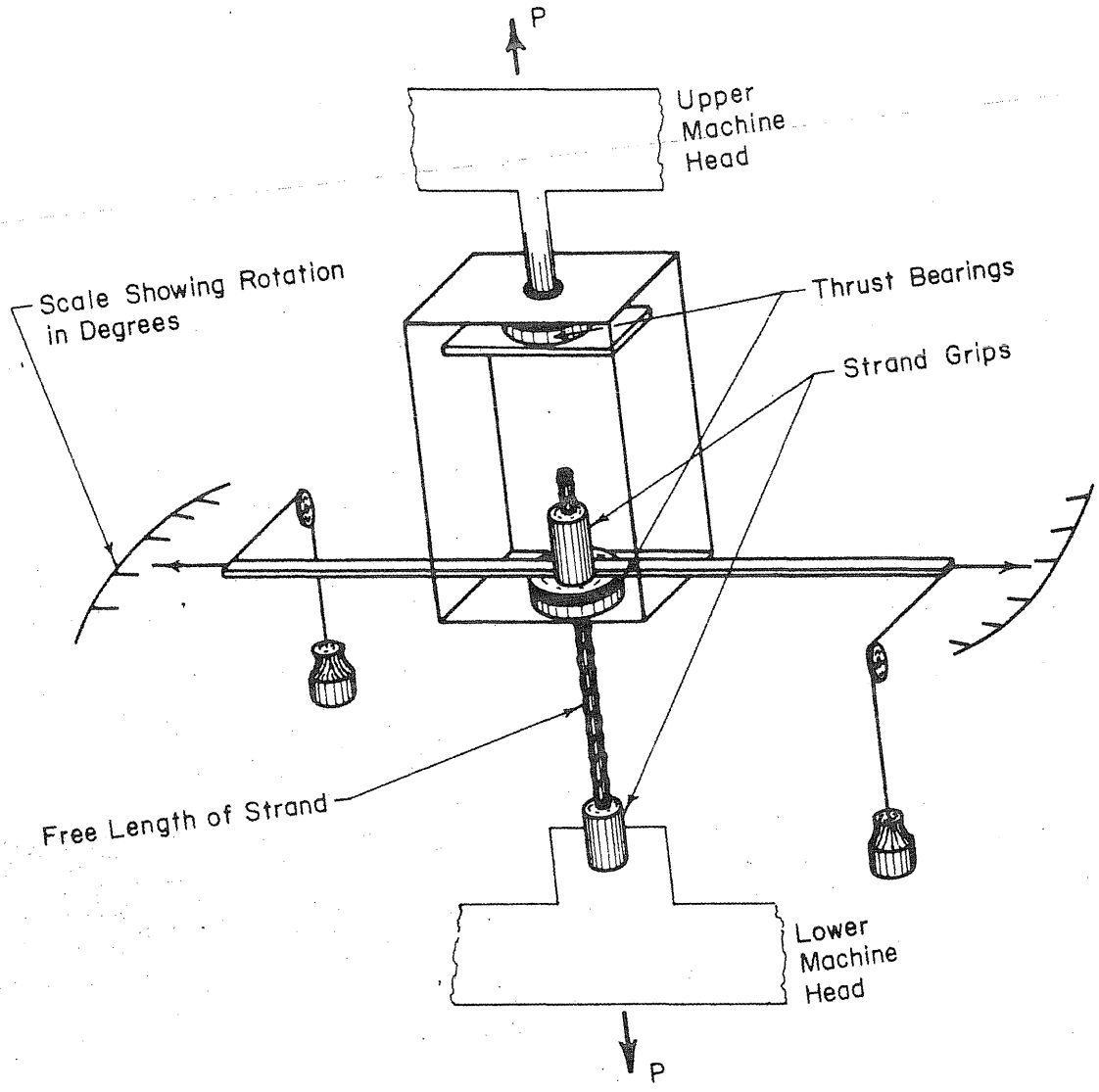

FIG. 12.9 TEST SETUP FOR DETERMINATION OF ROTATIONAL STIFFNESS OF STRAND

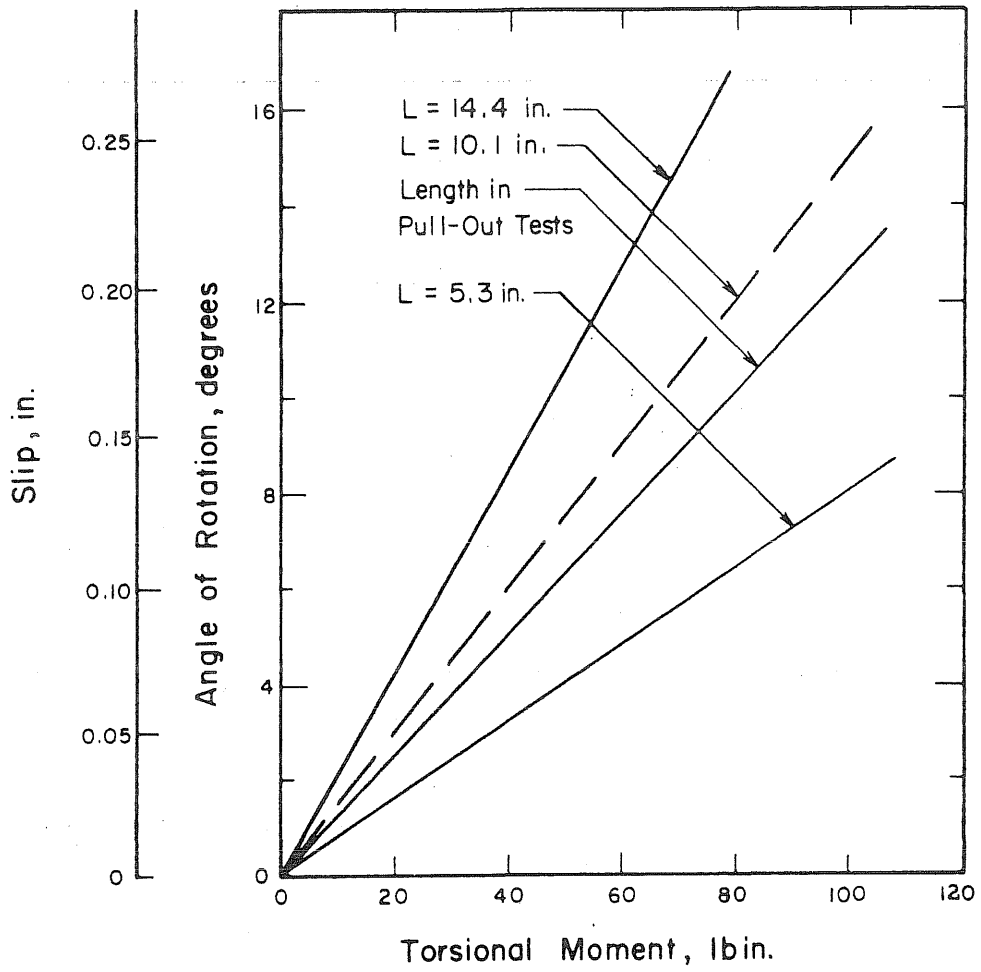

FIG. 12.10 AVERAGE MOMENT-ROTATION RELATIONSHIPS OF 7/16-in. STRAND FOR VARIOUS LENGTHS OF STRAND

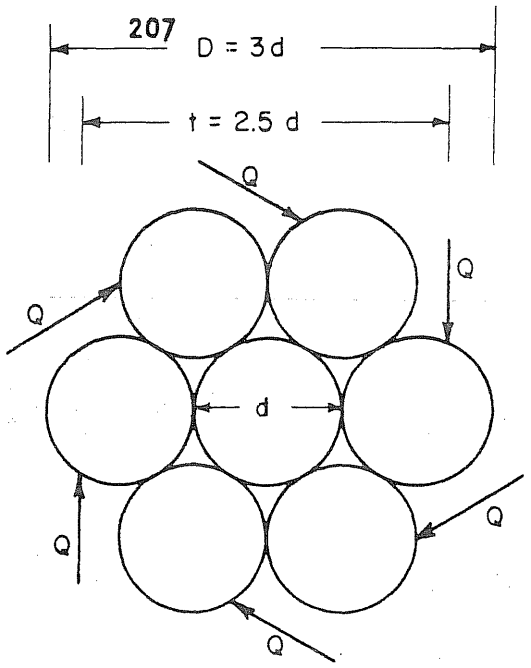

FIG. 12.11 ASSUMED FORCE DISTRIBUTION ON CROSS SECTION DUE TO UNTWISTING OF STRAND

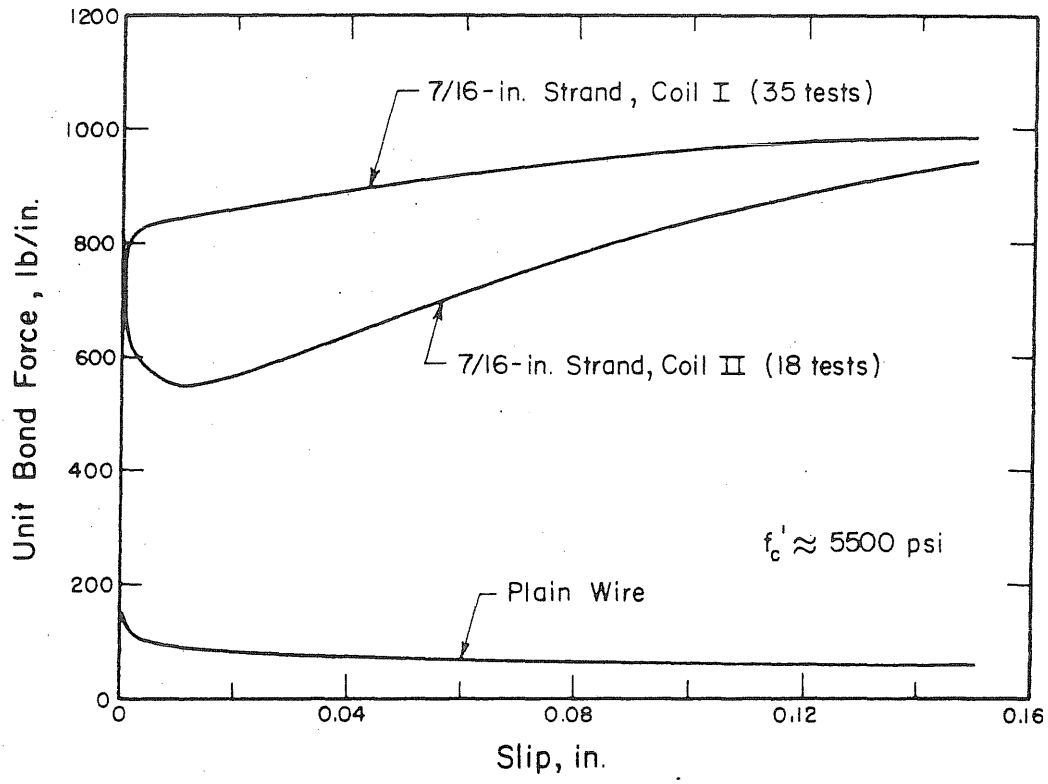

FIG. 12.12 TYPICAL BOND-SLIP RELATIONSHIPS OF 7/16-in. STRAND AND CENTER WIRE FROM THE SAME STRAND

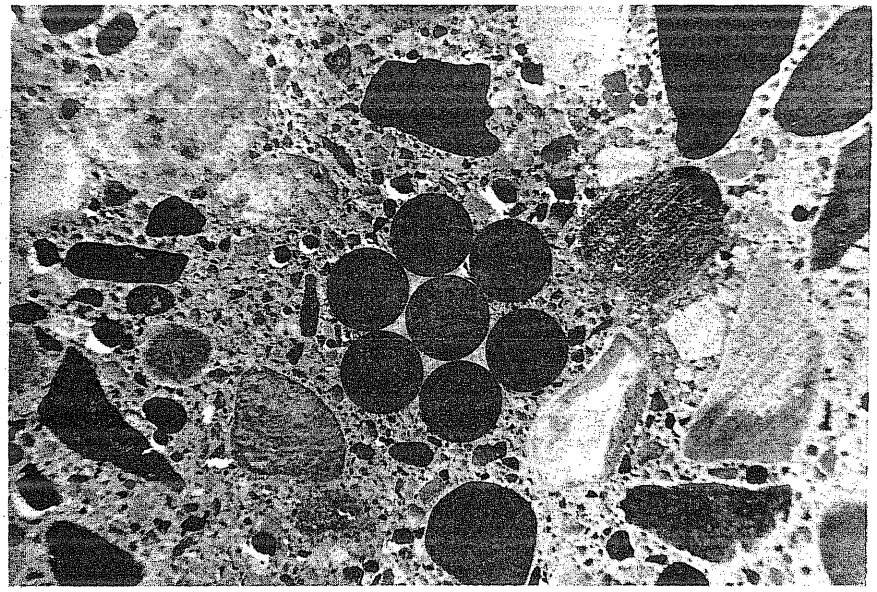

FIG. 12.13 RANDOM CROSS SECTION, A, THROUGH PULL-OUT SPECIMEN OF SERIES SA09-18

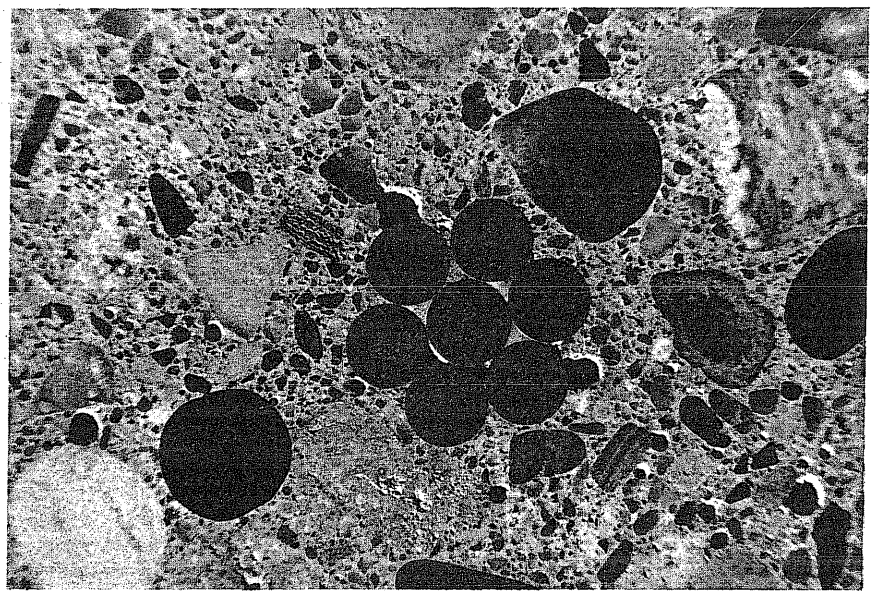

FIG. 12.14 CROSS SECTION THROUGH THE SAME SPECIMEN AS SHOWN IN FIG. 12.13 LOCATED ONE in. FROM CROSS SECTION A

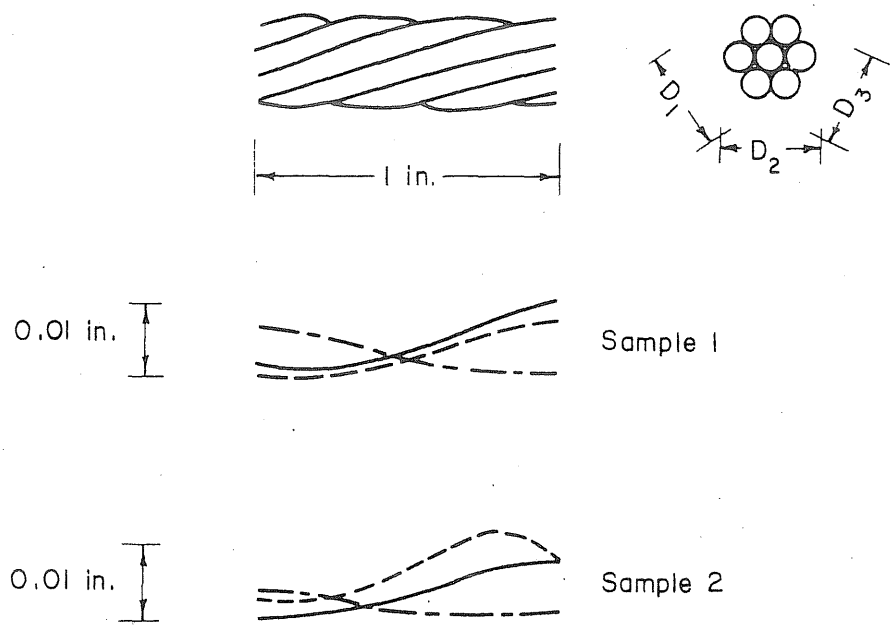

FIG. 12.15 RELATIVE VARIATION OF STRAND DIAMETER

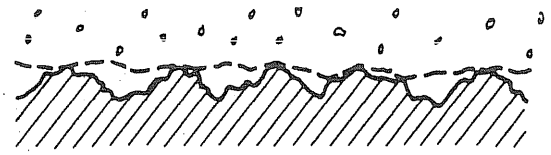

(a)

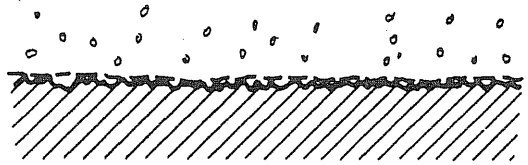

(b)

FIG. 12.16 FAILURE PLANES RELATED TO THE SURFACE ROUGHNESS OF THE STEEL

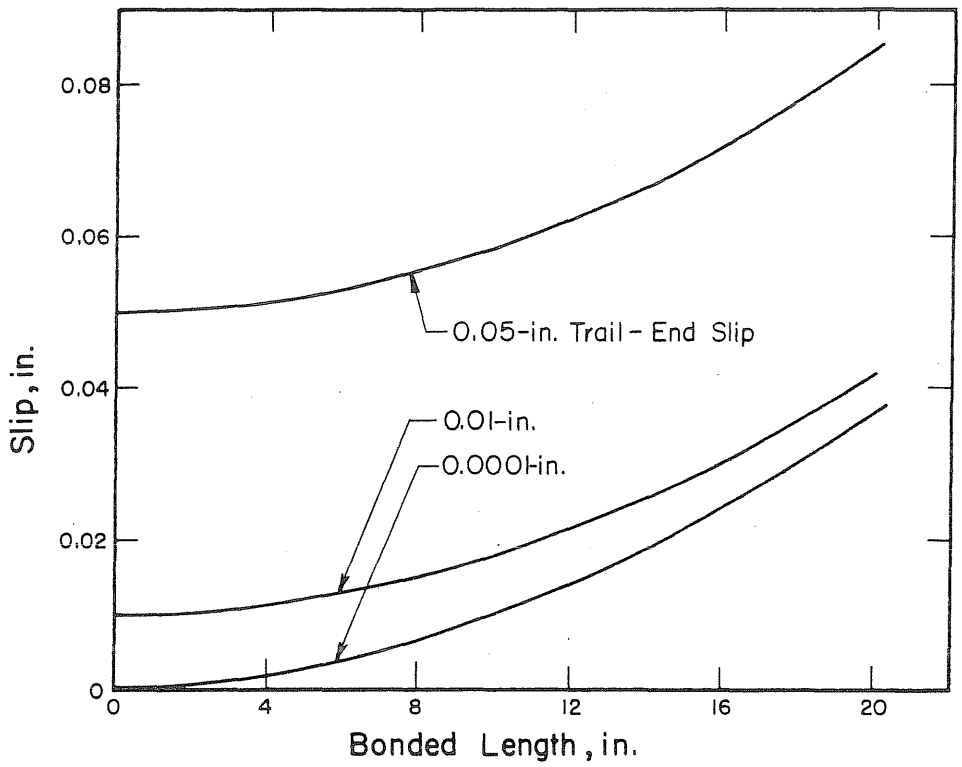

FIG. 13.1 CALCULATED SLIP DISTRIBUTION ALONG BONDED LENGTH FOR VARIOUS TRAIL-END SLIPS

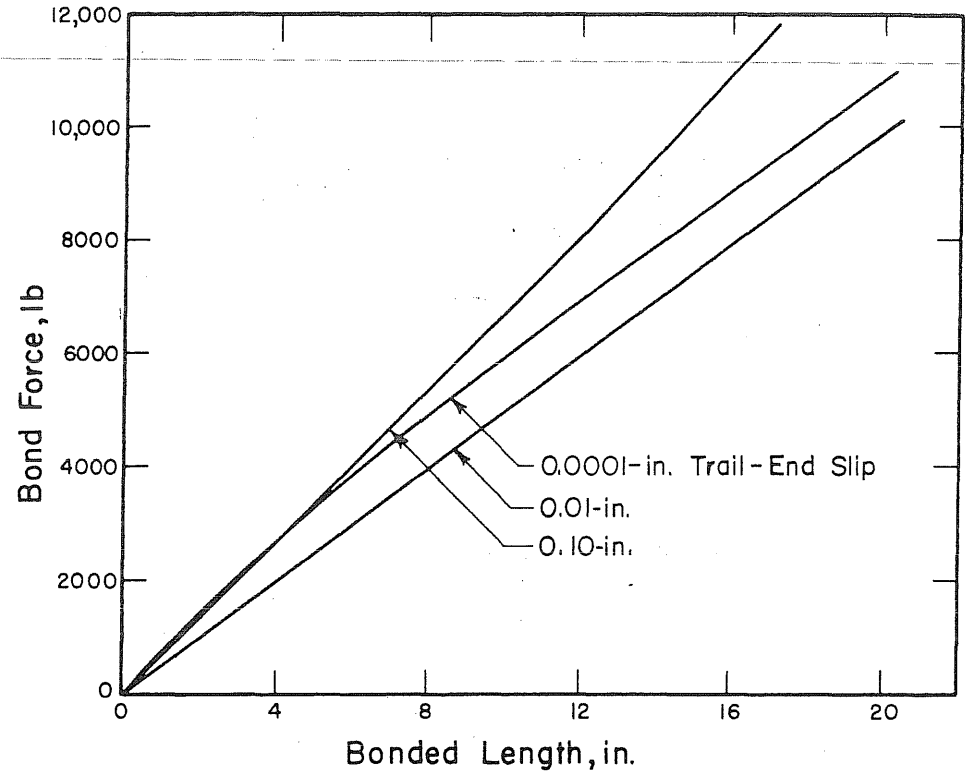

FIG. 13.2 CALCULATED FORCE DISTRIBUTION ALONG BONDED LENGTH FOR VARIOUS TRAIL-END SLIPS

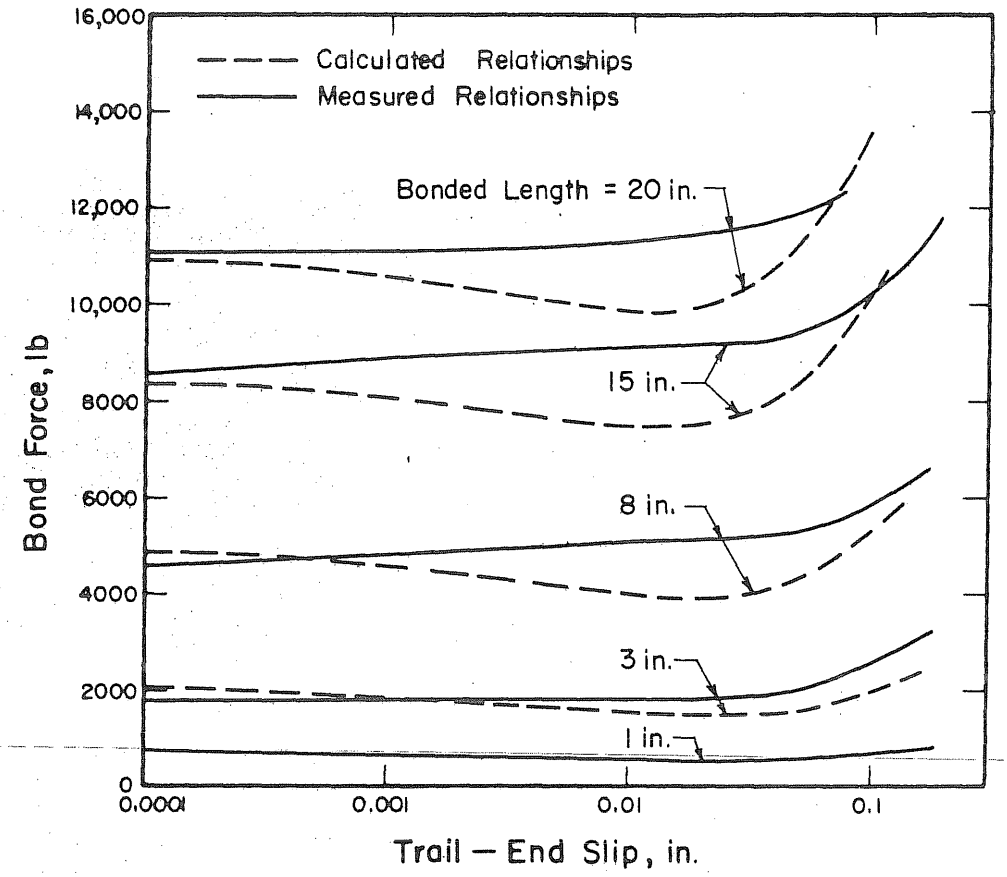

FIG. 13.3 CALCULATED AND MEASURED BOND FORCE vs. TRAIL-END SLIP, SERIES: SA09-18

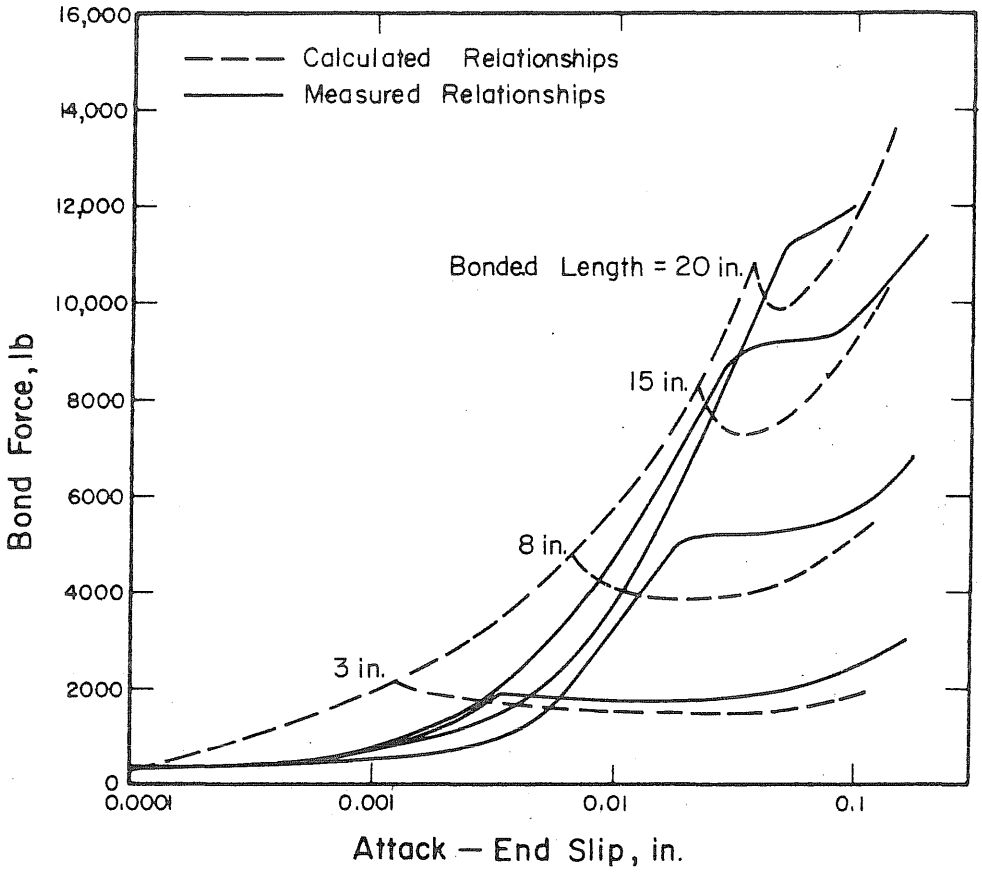

FIG. 13.4 CALCULATED AND MEASURED BOND FORCE vs. ATTACK-END SLIP, SERIES: SA09-18

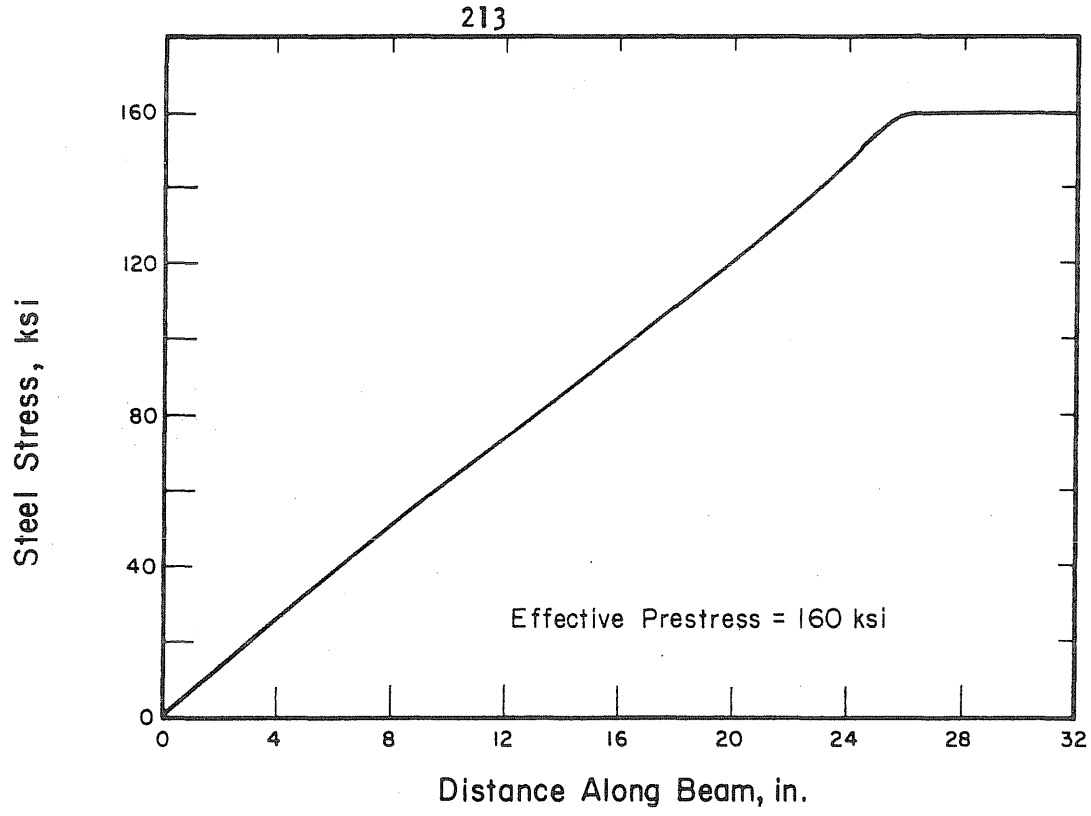

FIG. 13.5 CALCULATED STEEL STRESS DISTRIBUTION FOR 7/16-in. STRAND IN ANCHORAGE ZONE OF PRESTRESSED BEAM

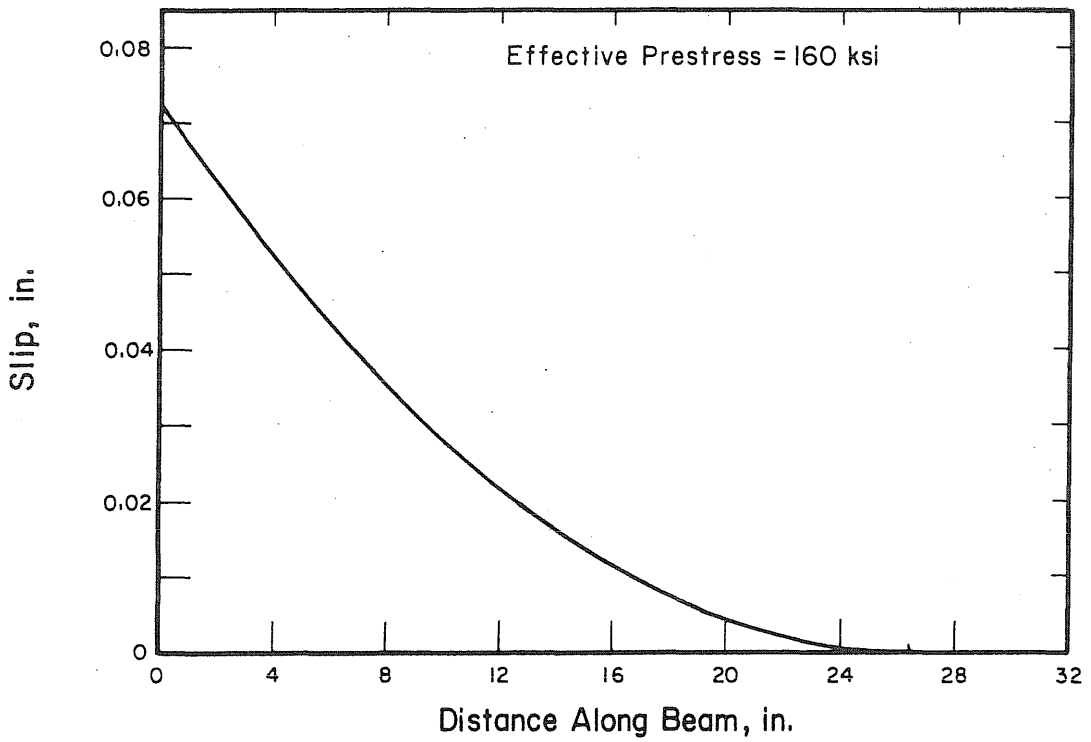

FIG. 13.6 CALCULATED SLIP OF 7/16-in. STRAND IN ANCHORAGE ZONE OF PRESTRESSED BEAM

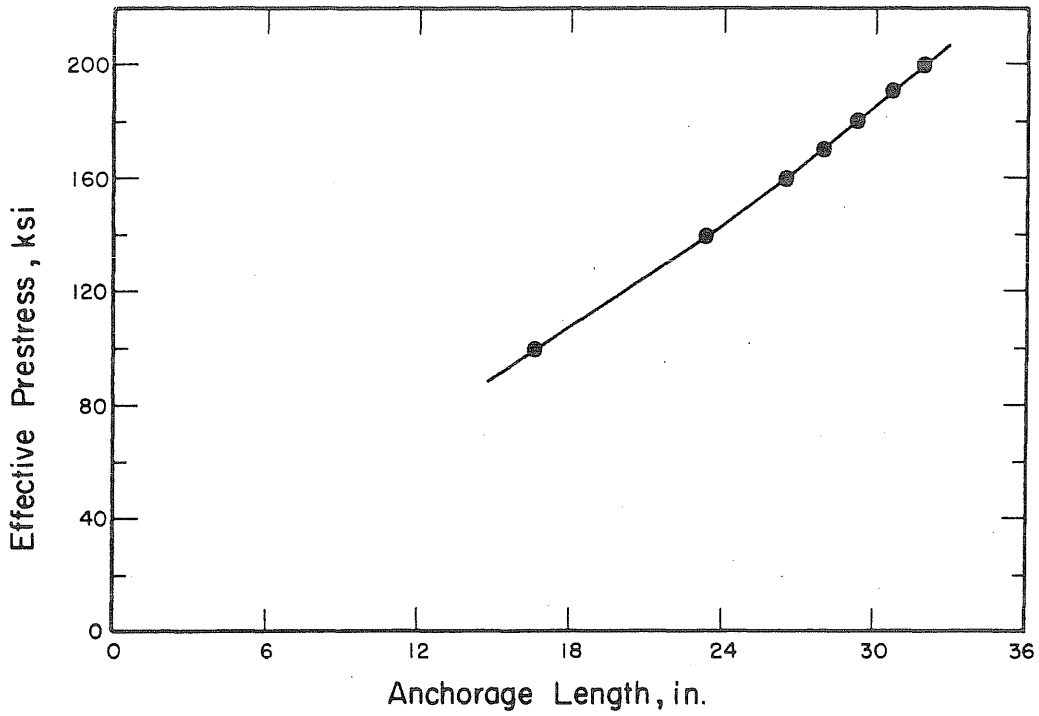

FIG. 13.7 CALCULATED ANCHORAGE LENGTH vs. EFFECTIVE PRESTRESS

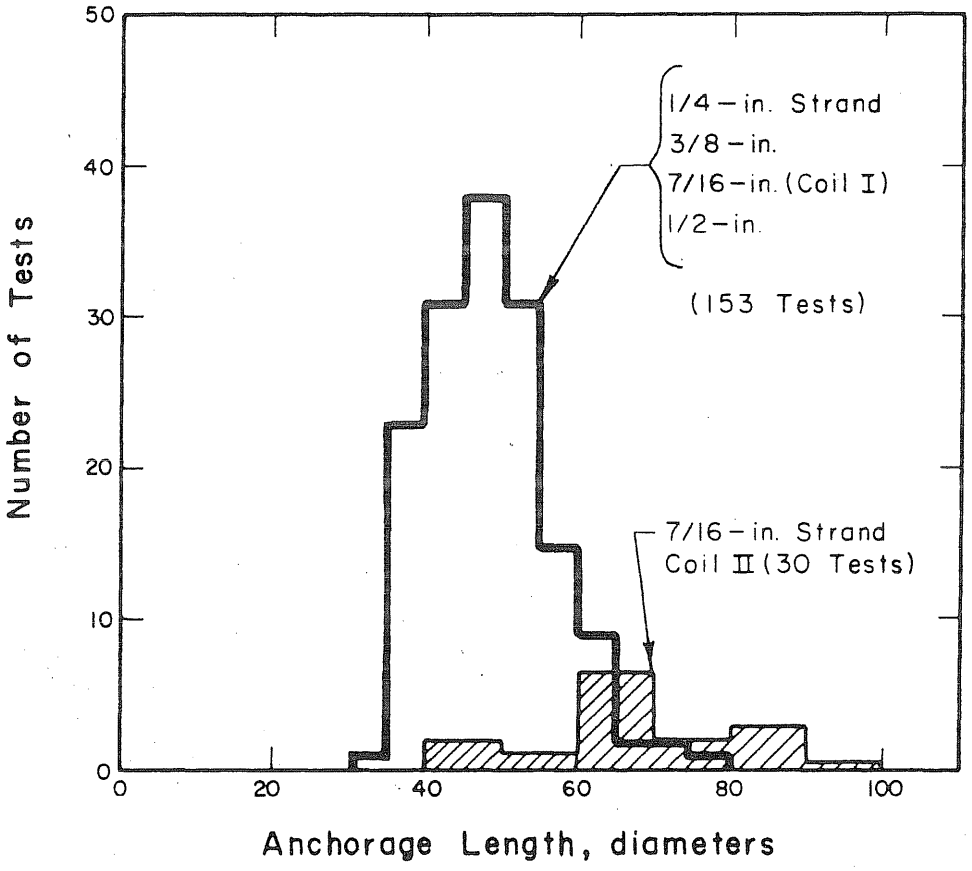

FIG. 14.1 DISTRIBUTION OF ANCHORAGE LENGTHS DETERMINED ON BASIS OF INDIVIDUAL RESULTS FROM PULL-OUT TESTS (EFFECTIVE PRESTRESS AFTER RELEASE = 175 ksi, f'_c = 5400 psi)

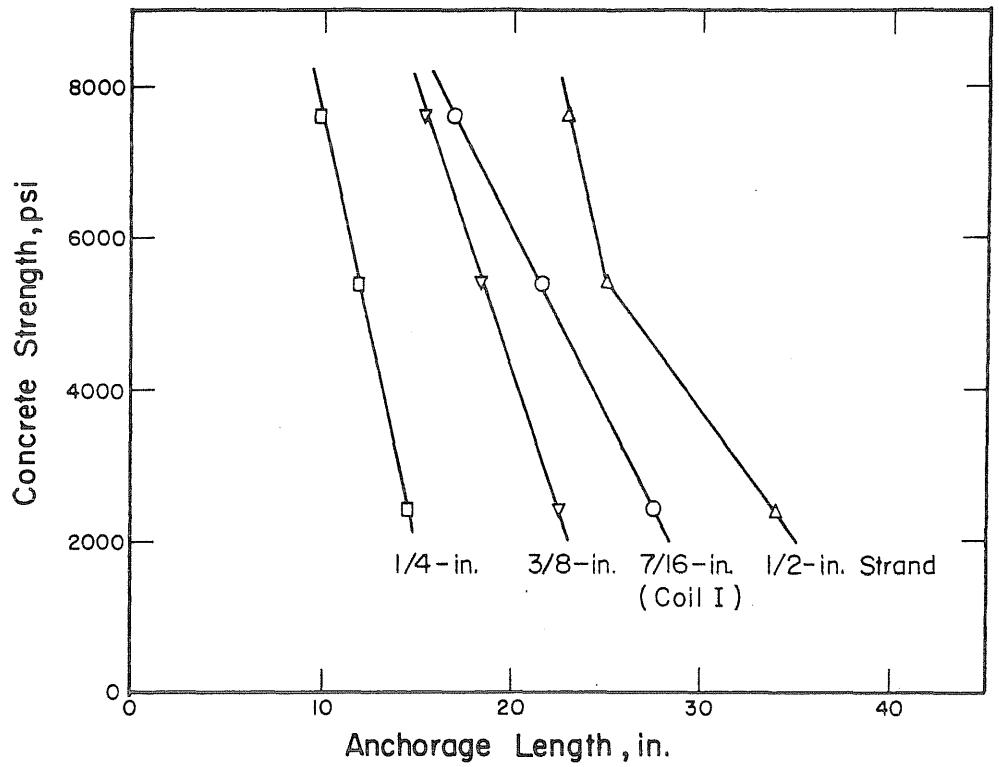

FIG. 14.2 ANCHORAGE LENGTHS DETERMINED ON THE BASIS OF AVERAGE RESULTS FROM PULL-OUT TESTS (EFFECTIVE PRESTRESS AFTER RELEASE = 175 ksi)

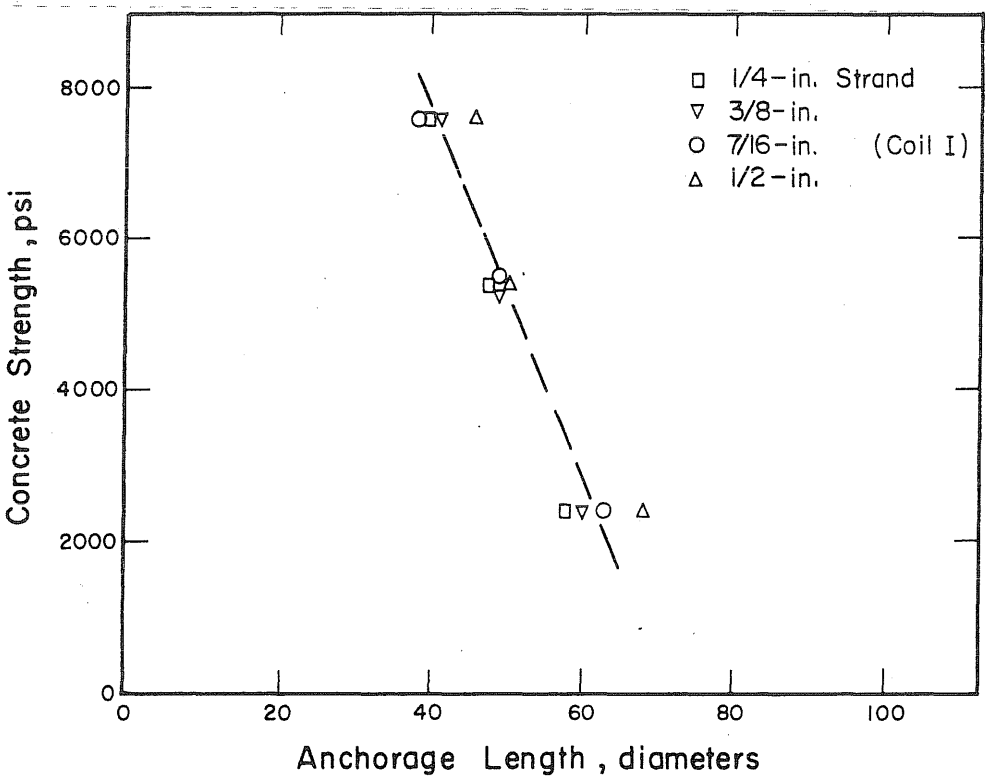

FIG. 14.3 ANCHORAGE LENGTHS DETERMINED ON THE BASIS OF AVERAGE RESULTS FROM PULL-OUT TESTS (EFFECTIVE PRESTRESS AFTER RELEASE = 175 ksi)

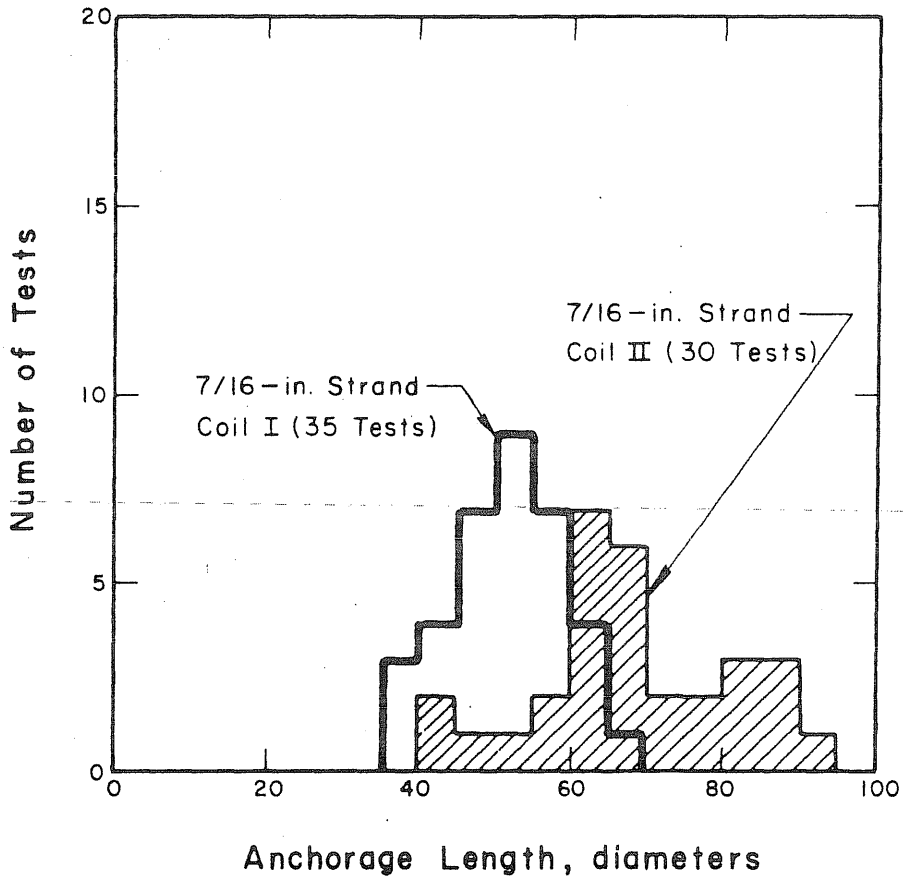

FIG. 14.4 DISTRIBUTION OF ANCHORAGE LENGTHS DETERMINED ON BASIS OF INDIVIDUAL RESULTS FROM PULL-OUT TESTS (EFFECTIVE PRESTRESS AFTER RELEASE = 175 ksi, f'_c = 5400 psi.)

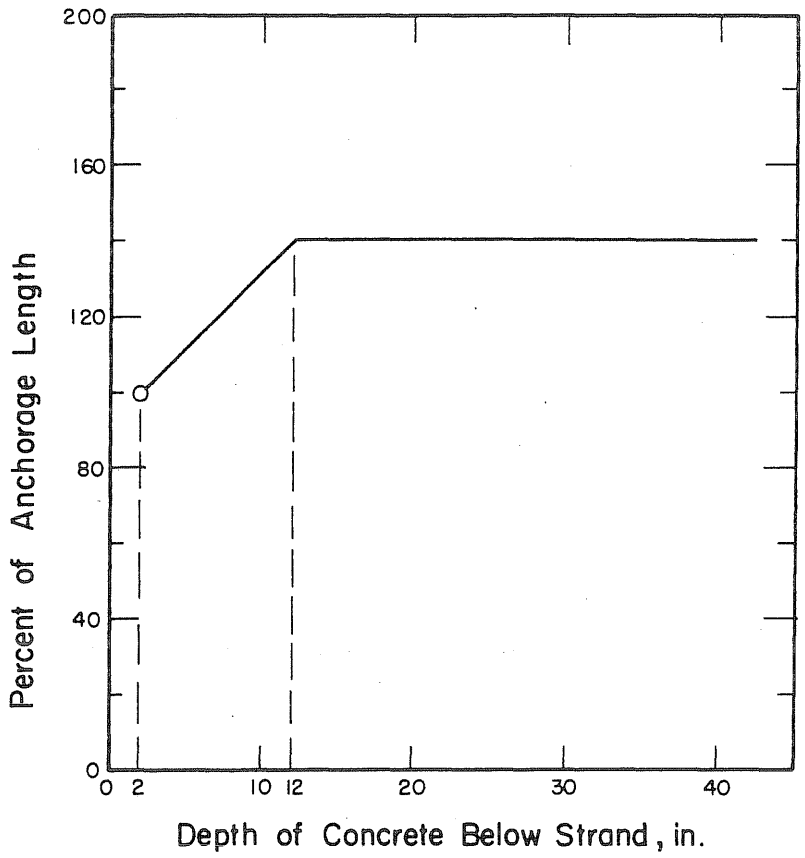

FIG. 14.5 VARIATION OF ANCHORAGE LENGTH WITH DEPTH OF CONCRETE BELOW CENTER OF STRAND

APPENDIX A: DESCRIPTION OF PULL-OUT TESTS

A.1 Introductory Remarks

This appendix presents a description of the materials used, the test specimens, the loading system, the testing procedure, and the measurements.

A.2 Materials

A.2.1 Cement

High-early-strength cement was used for all test specimens (Brand: Universal Atlas, Type III).

A.2.2 Aggregates

Sand and pea gravel from the Wabash River were used in all concrete mixes. The origin of these aggregates is an outwash of the Wisconsin glaciation. The sand consisted mainly of quartz. The major constituents of the gravel were limestone and dolomite. The sand had a fineness modulus of approximately 3.0. The maximum size of the gravel was 3/8 in. A characteristic sieve analysis for both the sand and the gravel is shown in Fig. A.1. The sand and gravel were oven-dried and cooled before mixing.

A.2.3 Concrete Mixes

Six different mix proportions were used during the whole test program. The proportions of the mixes and the average strength characteristics of the resulting concrete are listed in Table A.1. All proportions are given in terms of dry weights. In each mix proportion, the ratio of the volume of cement plus sand to the volume of gravel was kept constant. It was approximately 1.2.

The majority of all test specimens was cast using mixes designated A, B, and C. The average nine-day compressive strengths of these mixes were approximately 5500, 7500, and 2500 psi. It was intended to keep the slump constant at 1.5 in. in all three mixes.

Mixes D and E were designed as variations of mix A. The consistency of the concrete, indicated by the slump, was varied whereas the water-cement ratio was kept unchanged. The mix proportions were chosen in such a way that approximately the same concrete strength as for mix A was obtained. Mix F was used only in one test series.

The concrete properties and the age of the concrete at the time of testing are listed in Table B.1 through B.4 for each individual test series.

The compressive strength of the concrete was determined from tests on three 6 by 12-in. cylinders. The loading speed was 60,000 lb per minute. The splitting strength was found from three 6 by 6-in. cylinders loaded by a compressive force on opposite generators of the cylinder. Strips of stiff fiber board, 1/8 in. thick and 1/2 in. wide, were placed between the heads of the testing machine and the cylinder to distribute the load uniformly along the length of the specimen. The loading speed was 9000 lb per minute.

The average splitting strength of each test series is plotted versus the average compressive strength in Fig. A.2. The following expression approximately satisfies the relationship between

the splitting strength and the compressive strength:

$$f_{sp} = 5.5 \sqrt{f'_c} \qquad (A.1)$$

Both stresses are expressed in psi.

A.2.4 Steel

The reinforcing strand used in this test program consisted of seven-wire (round wire) strand with nominal diameters of 1/4 in., 3/8 in., 7/16 in., and 1/2 in. The 1/4-in., 3/8-in., and 1/2-in. strands were cut from one roll each. Two rolls were used for the 7/16-in. strand. The surface of the strand was clean and not corroded. The measured properties of the strand such as cross sectional area, pitch, angle of twist, and the apparent modulus of elasticity are listed for each strand size in Table A.2. The modulus of elasticity was measured with the strand clamped at both ends of a 25-in. length. The deformation over ten in. was measured with a mechanical gage.

The plain wires used in the tests were cut from the straight center wires of the different strand sizes. The diameters are listed in Table A.2. The surface characteristics of the center wires were approximately identical to those of the exterior wires of the strand.

In a few test series, 5/16-in. square steel bars were used. For reasons stated in Chapter 10, it was required to twist the bars by different amounts. The twisting was accomplished in a lathe without subjecting the bar to any axial force. The torque was applied by rotating one end of the bar about its axis while holding the other

end in a grip that permitted axial motion. Bars with lengths of approximately five ft were twisted in one piece. The center of the bar was supported by a sleeve to prevent buckling. The degree of twisting along the axis of the bar was fairly uniform up to a twist angle of approximately 30°. (The twist angle was formed by the helical edges of the twisted bar and its longitudinal axis). Beyond that, the uniformity decreased rapidly because of local twist concentrations.

A.3 Description of Specimens

The basic pull-out specimen consisted of a 4 by 4 by 9-in. concrete prism. The steel (strand, wire, or square bar) was centered in the middle of the specimen parallel to the long side. The length over which the steel was actually bonded to the concrete was shorter than the length of the concrete prism. The rest of the embedded length was kept free from bond by thin-walled metal pipes that were drawn over the steel. In most cases, the bonded length was only one in., located at midheight of the concrete prism. Figure A.3 shows a typical specimen split in two halves.

Regardless of the bonded length, a length of four in. was left unbonded at the end where the pull-out force was to be applied. For bonded lengths greater than two in., the length of the concrete specimen was extended such that two in. of steel could be left free of bond at the unloaded end of the specimen. Thus, the length of the concrete specimen was equal to the bonded length plus four in. plus two in.

The specimen was cast in such a way that approximately five in. of strand extended from the concrete prism at the end where the load was to be applied, and three in. at the free end where the slip was to be measured.

In some cases the depth of the concrete specimen was varied to study its effect on bond. The steel, however, remained centered for all specimens in the upper cross section of 4 by 4 in. with respect to the direction of pouring.

A.4 Casting and Curing

The length of steel (strand, wire, square bars) that was to be in contact with the concrete was treated with utmost care. First it was brushed with a steel brush to clean it of surface dirt. Then it was carefully washed with acetone and trichloroethylene to remove any grease that might have been deposited on the surface while handling the steel. This treatment may be considered as being unrealistic if compared with common field practice. However it was necessary in order to obtain a maximum of uniformity in the test conditions.

Two steel pipes with a wall thickness of approximately 0.016 in. were pulled over both ends of the steel so far that only the bonded length (mostly one-in. long) was still visible. The inner diameter of the pipes was chosen so that the pipes could slide along the steel with a minimum of clearance between the pipe and the steel. The clearance at the ends near the bonded length was sealed with hot sealing wax. This procedure could be accomplished so that the desired bonded length was obtained with a maximum error of 0.06 in. or 6 percent of a bonded length of one inch.

The steel strand, which was delivered by the manufacturer in rolls, retained a curvature when cut into short pieces, especially in the larger diameters. Therefore, all specimens were cast in steel forms which had clamping devices on the end plates to keep the strand straight during casting and hardening of the concrete. (Fig. A.4).

Before casting, the steel pipes were thoroughly greased with cup grease. The concrete was mixed in a pan-mixer. All specimens of one test series were cast from one batch. The concrete was vibrated with an interior vibrator at four spots in a constant pattern. The vibration was done by the same person throughout the whole test program. For each batch, three 6 by 12-in. cylinders and three 6 by 6-in. cylinders were cast to determine the compressive and splitting strength of the concrete.

The specimens and the cylinders were left in their forms for two days and kept moist by covering them with wet burlap. After two days the forms were struck and the pipes, which were intended to prevent bond between the concrete and the steel outside the bonded length, were pulled out. This could be done with ease.

The specimens and the cylinders were stored in the moist room at a relative humidity of 100 percent for four more days. Afterwards they were brought to a room with a constant relative humidity of 50 percent and a temperature of 73^{o}F. They were kept there until the time of testing. Most pull-out tests were carried out at an age of eight or nine days. Some test series, particularly the tests to be conducted under lateral pressure, were carried out at

a higher age (two to three weeks) because both the preparation and the testing required more time than for standard pull-out tests.

The specimens to be tested under lateral pressure needed a special treatment. After being cured for six days, the surface was carefully smoothed with sand paper. All pores were filled with gypsum plaster (Hydrocal). The surface was painted with a liquid solution of neoprene, which hardened to a rubbery coat of approximately 0.004-in. thickness. The four long faces of the specimen were wrapped into a shim steel with a thickness of 0.004 in. On one side the shim steel was overlapped and sealed with epoxy glue.

A.5 Test Setup

A Tinius Olsen Uceltronic testing machine was used for all tests (Fig. A.5). Its maximum loading capacity was 12,000 lb. Eight different load ranges were available, the lowest one having a range of 120 lb. The machine made it possible to control the pull-out speed exactly since its loading system was completely mechanical. The concrete specimens were placed into a steel cage, which was fixed to the upper head of the testing machine through a hinge (Fig. A.6). The longer end of the steel, sticking through a hole at the bottom plate of the cage, was gripped by a strand grip or the jaws of the testing machine which in turn were fastened to the lower head of the testing machine by another hinge. The two hinges had two degrees of freedom, but they were restrained from rotating around the vertical axis.

Two different principal test setups were used: (a) The steel cage was supported by a thrust bearing at the top, thus permitting the cage, and along with it the concrete prism, to rotate ostensibly freely around the vertical axis. The actual rotational restraint of the thrust bearing, caused by rolling friction, was measured and found to be linearly proportional to the thrust within the range of the applied pull-out forces. The magnitude found was approximately 4 lb in. per 1000 lb of thrust. (b) The steel cage was supported without thrust bearing. In this case the steel cage was completely restrained from rotating around its vertical axis.

Between the concrete prism and the bottom plate of the cage a thin foam rubber plate was placed to compensate for stress concentration due to an uneven concrete surface.

A completely different test setup was necessary for the sustained-load tests. Specimens of standard dimensions were loaded using a cantilever system (Fig. A.7). The applied load, which could be varied by either changing the weight or the lever arm, could be determined with an accuracy of $\pm$ 20 lb.

A.6 Measurements

The basic measurements in all pull-out tests were limited to load and slip readings. The slip was measured by a dial indicator with a reading sensitivity of 0.0001 in. The dial indicator was held by a heavy metal ring which rested on the top surface of the concrete prism (Fig. A.8). The pointer of the dial was kept in contact with the free end of the steel. Thus, the dial recorded the slip of the steel at the end of the bonded length versus the top surface of the concrete prism.

A special system to hold the dial indicator was designed for the sustained-load tests. Shrinkage of the upper half of the concrete prism would affect the readings if the slip would be measured with the system described above over a long period of time (Fig. A.8). In order to eliminate the shrinkage deformations from the dial readings, a frame holding the dial indicator was clamped at midheight to the vertical sides of the concrete prism (Fig. A.7). Thus, the dial readings indicated directly the slip of the steel, which was bonded over a length of only one in. in the center of the specimen, versus the concrete at the same level.

In many pull-out tests containing strand or twisted square bars, the untwisting of the steel versus the rigidly held concrete prism was measured. In other tests the rotation of the unrestrained concrete prism versus the steel was investigated. For this purpose, a five-in. long pointer was glued onto the top of the free end of the steel, and the amount of rotation was read off a scale at the end of the pointer (Fig. A.6).

In tests with bonded lengths larger than two in., the slip was measured on both ends of the bonded length. In addition to the 0.0001-in. dial used to measure the slip at the unloaded end of the strand, two dials with a reading sensitivity of 0.001 in. were clamped to the loaded end of the strand to record the attack-end slip. The pointers of the dials were in contact with the steel plate supporting the concrete specimen.

According to the test setup shown in Fig. A.8, the measured slip at the loaded end of the strand, indicated by the average of the

two dial readings, included the following extraneous deformations in addition to the actual slip between strand and concrete: (a) the deformation of the concrete console around the bonded length; (b) the elastic deformation of the strand between the bonded length and the attachment of the dial indicators to the strand; (c) the deformation of the concrete specimen between the bonded length and the supporting steel plate; and (d) the elastic deformation of the supporting steel plate.

The deformation of the concrete console around the bonded length was primarily a shear deformation. A special test series, BB09-1, was conducted to determine the magnitude of the shear deformation. The test results are discussed in section B.3. The relationship found between the deformation of the concrete console and the unit bond force indicated that the deformation was on the order 0.00015 in. per 1000 lb of unit bond force.

The elastic elongation of the unbonded length of strand could be determined without difficulty. The modulus of elasticity was measured to be 28×10^6 psi, the free length of strand was 9.5 in. For a pull-out force of 1000 lb, the elastic deformation of a 7/16-in. strand (coil II) was determined to be 0.0029 in.

The elastic deformation of the concrete specimen below the bonded length was determined on the basis of a simplified assumption. The bond force was assumed to act at midheight of that part of the bonded length which has slipped more than 0.0001 in. From that point, a distribution of the stresses in the concrete under an angle of 45°

was assumed. A more precise determination of the concrete deformation on the basis of elasticity solutions would have been of little advantage in view of the uncertain assumptions about the concrete properties and the questionable validity of a purely elastic solution. For a bonded length of 3 in. and a force of 2000 lb, the deformation of the concrete was calculated to be 0.0004 in. At 11,000 lb and a bonded length of 20 in., the calculated deformation was approximately 0.004 in.

The elastic deformation of the supporting steel plate was negligible.

A.7 Application of Lateral Pressure

The specimens of seven test series were tested under externally applied lateral pressure. A cross section of the pressure apparatus, is shown in Fig. A.9. The apparatus consisted of a cylindrical steel chamber with end plates. The end plates had a square opening of such dimensions that the concrete prisms wrapped in a 0.004-in. thick shim steel could barely be slipped in. The end of the chamber opening was wider leaving a square ring space between the concrete prisms and the chamber of 1/2 in. Into this space a lead ring, poured in advance, was inserted and pounded in with such effort that the lead was forced not only to fill the space completely but even to withstand pressures up to 4000 psi without significant leaking. The lead was held in place and even compressed further by two end steel plates which were tightened against the steel chamber with six 1/2-in. bolts.

The pressure chamber was connected with an electric hydraulic pump (Fig. A.10). Oil was used as pressure fluid. The pressure was measured with a 10,000-psi Bourdon gage. A close-up of the pressure apparatus with the test specimen in place is shown in Fig. A.11

A.8 Test Procedure

All specimens were loaded with the same speed. The speed of the moving head of the testing machine was held constant at 0.05 in. per minute. At the beginning of the test, the slip dial was set to zero. The first load reading was taken when the dial had moved to 0.0001 in. From then on the load was read at certain slip intervals. The tests were discontinued after the slip had reached a magnitude of 0.15 in.

The test procedure for the specimens being subjected to lateral pressure was basically the same. The desired lateral pressure was applied before the pull-out test was started. It was kept constant during the whole test.

In some tests the attack-end slip was measured in addition to the trail-end slip (Fig. A.8). The two dials at the attack end were recorded by an automatic camera, which was released simultaneously with the readings taken at the trail-end dial.

The test procedure for the sustained-load tests was as follows: Three short-time pull-out tests were conducted on ostensibly identical specimens. The average initial bond force (bond force at a slip of 0.0001 in.) was determined. The sustained-load test specimens were then loaded to different percentages of that initial short-time load.

TABLE A.1

PROPERTIES OF CONCRETE MIXES

Mark	Ratio by weight Cement:Sand:Gravel	Water/Cement Ratio	Average Slump (in.)	Average 8(or 9)-day Compressive Strength (psi)	Average 8(or 9)-day Splitting Strength (psi)
A	1:2.8:3.1	0.65	1.5	5380	400
B	1:1.0:1.6	0.40	1.5	7570	460
C	1:4.7:4.7	1.05	1.5	2370	230
D	1:3.3:3.5	0.65	0.3	5750	410
E	1:2.6:2.8	0.65	7.1	4970	400
F	1:3.9:3.9	0.90	0.5	3400	300

TABLE A.2

STRAND PROPERTIES

Nominal Strand Diameter (in.)	Diameter of Center Wire (in.)	Cross Sectional Area* ($in.^2$)	Pitch (in.)	Angle of Twist** (^{o})	Modulus of Elasticity (ksi)
1/4	0.084	0.0368	3.88	11.5	---
3/8	0.130	0.086	5.06	13.1	---
7/16 (Coil I)	0.147	0.110	5.83	13.3	28.2×10^3
7/16 (Coil II)	0.150	0.118	5.81	13.3	27.9×10^3
1/2	0.171	0.153	6.74	13.1	---

* based on average weight per foot

** $\tan\alpha = \dfrac{\pi \times \text{nominal strand diameter}}{\text{pitch}}$

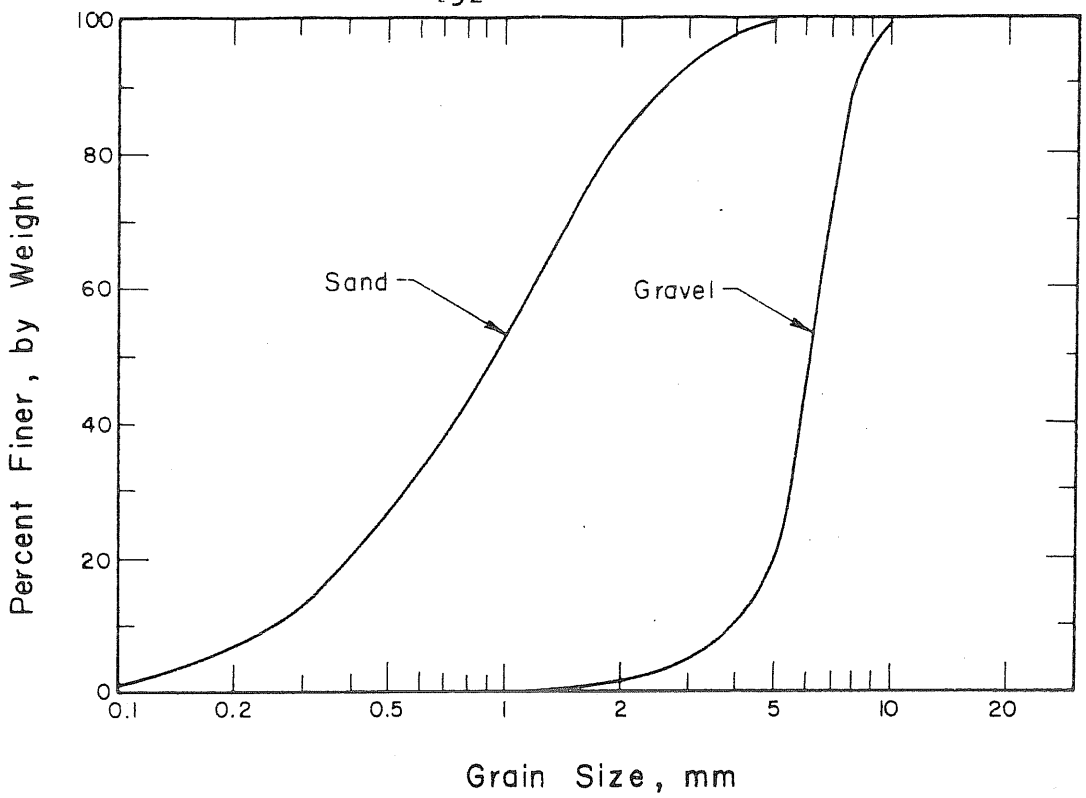

FIG. A.1 SIEVE ANALYSIS FOR FINE AND COARSE AGGREGATES

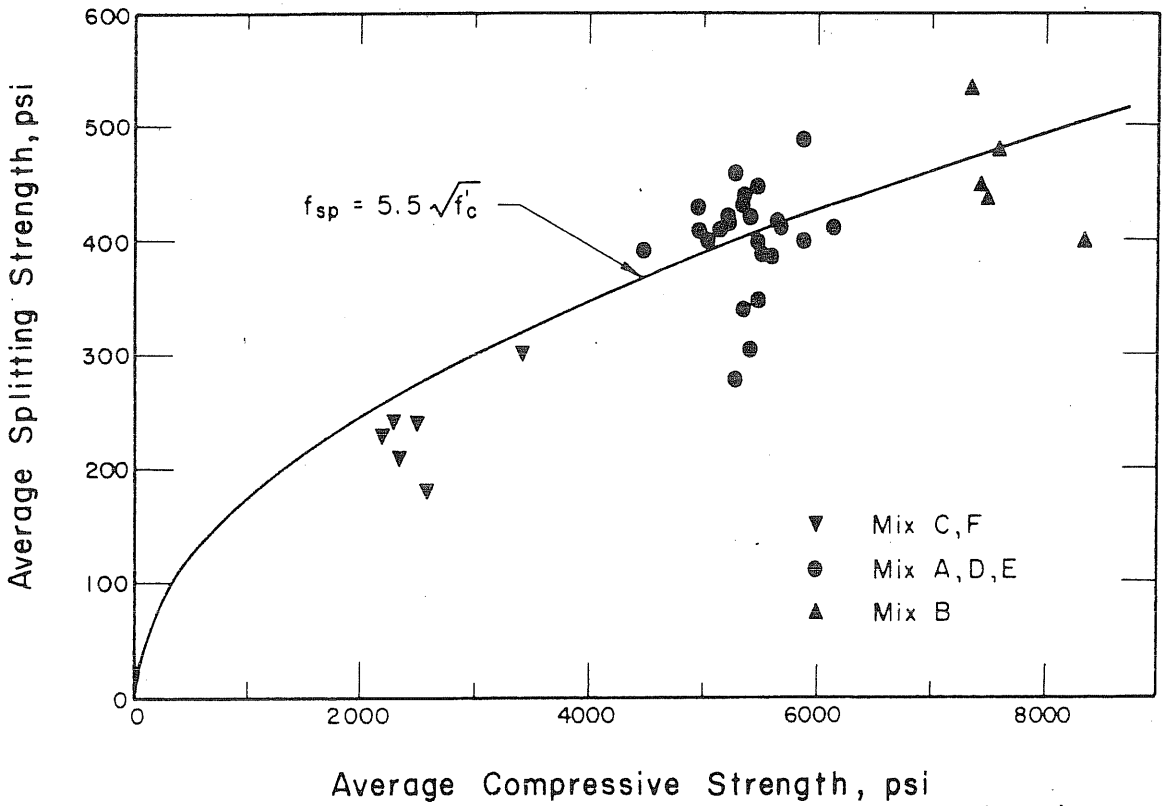

FIG. A.2 SPLITTING STRENGTH vs. COMPRESSIVE STRENGTH FOR 8(or 9)-DAY OLD CONCRETE

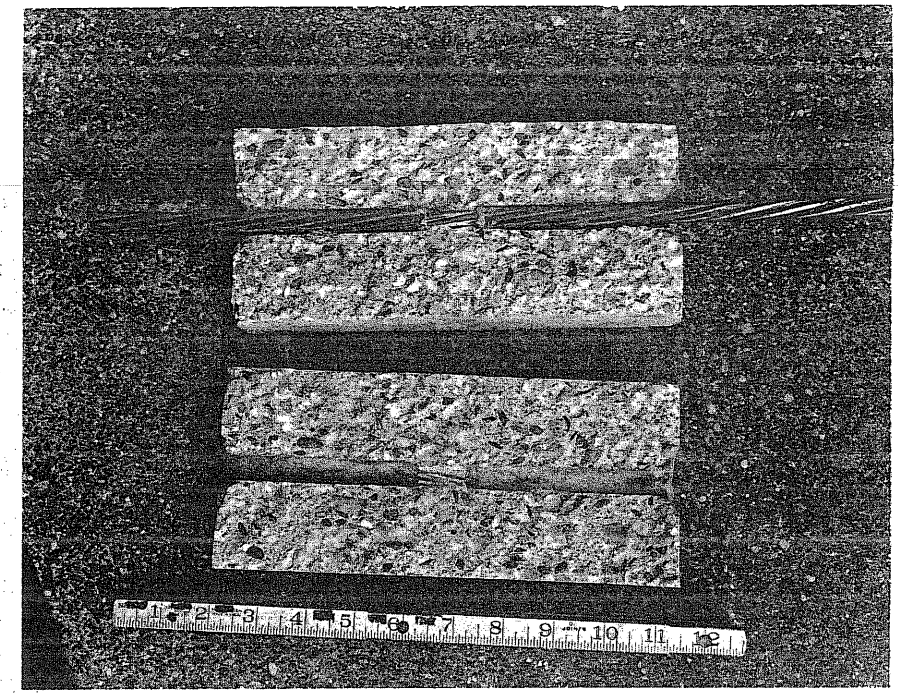

FIG. A.3 TEST SPECIMEN SPLIT IN TWO HALVES

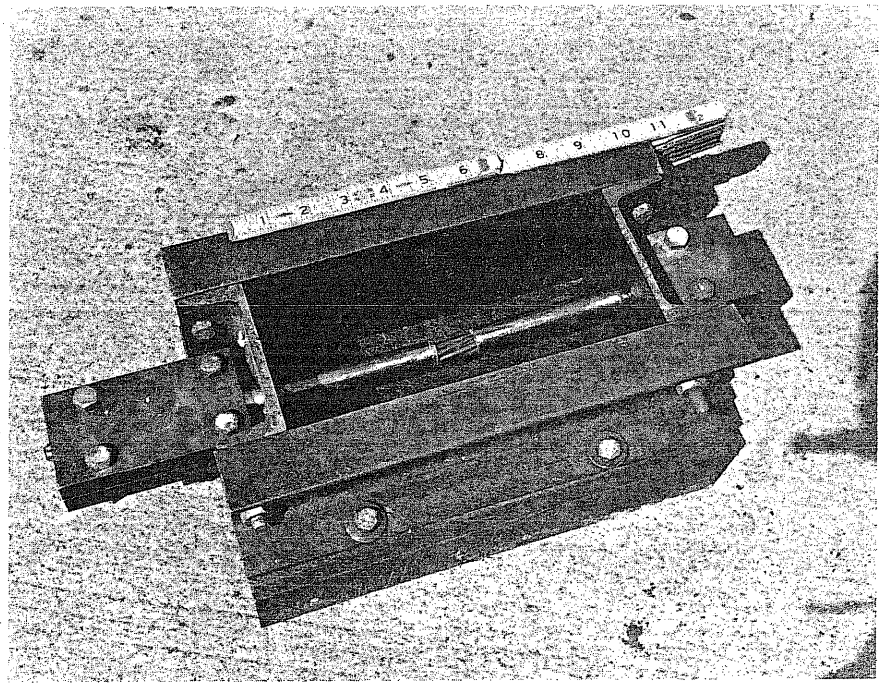

FIG. A.4 SPECIMEN BEFORE CASTING

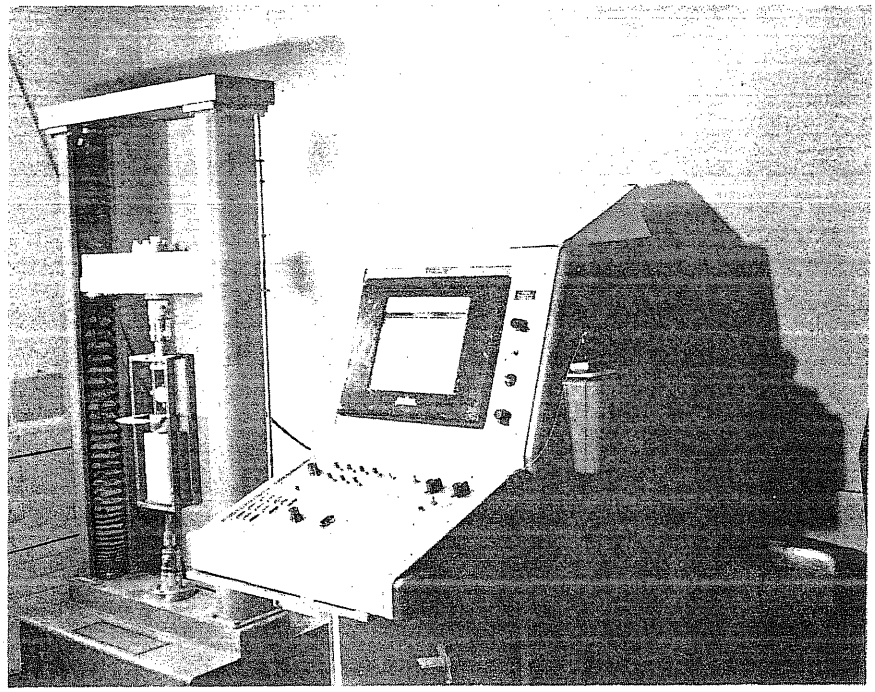

FIG. A.5 TEST SETUP FOR PULL-OUT TESTS

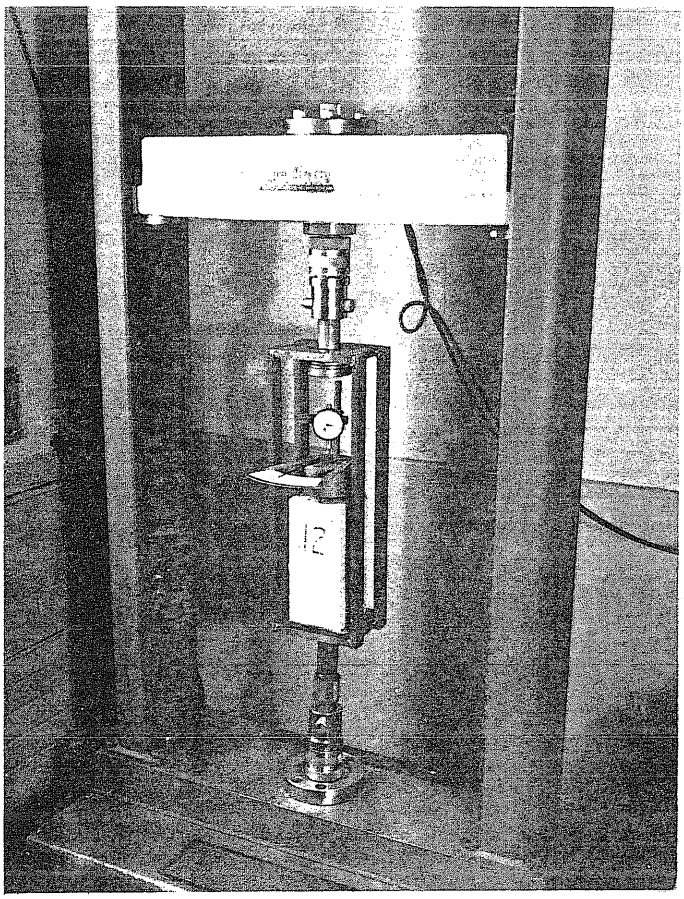

FIG. A.6 TEST SPECIMEN IN PLACE

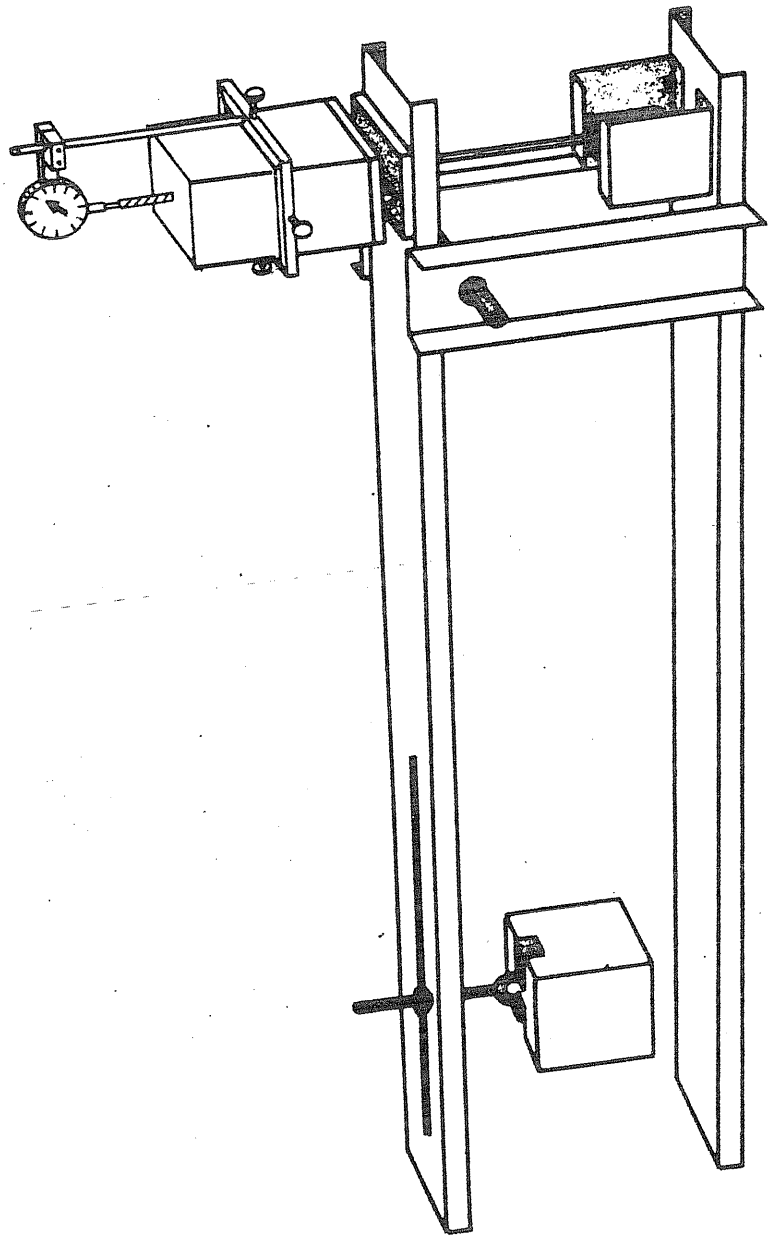

FIG. A.7 TEST SETUP FOR SUSTAINED-LOAD TESTS

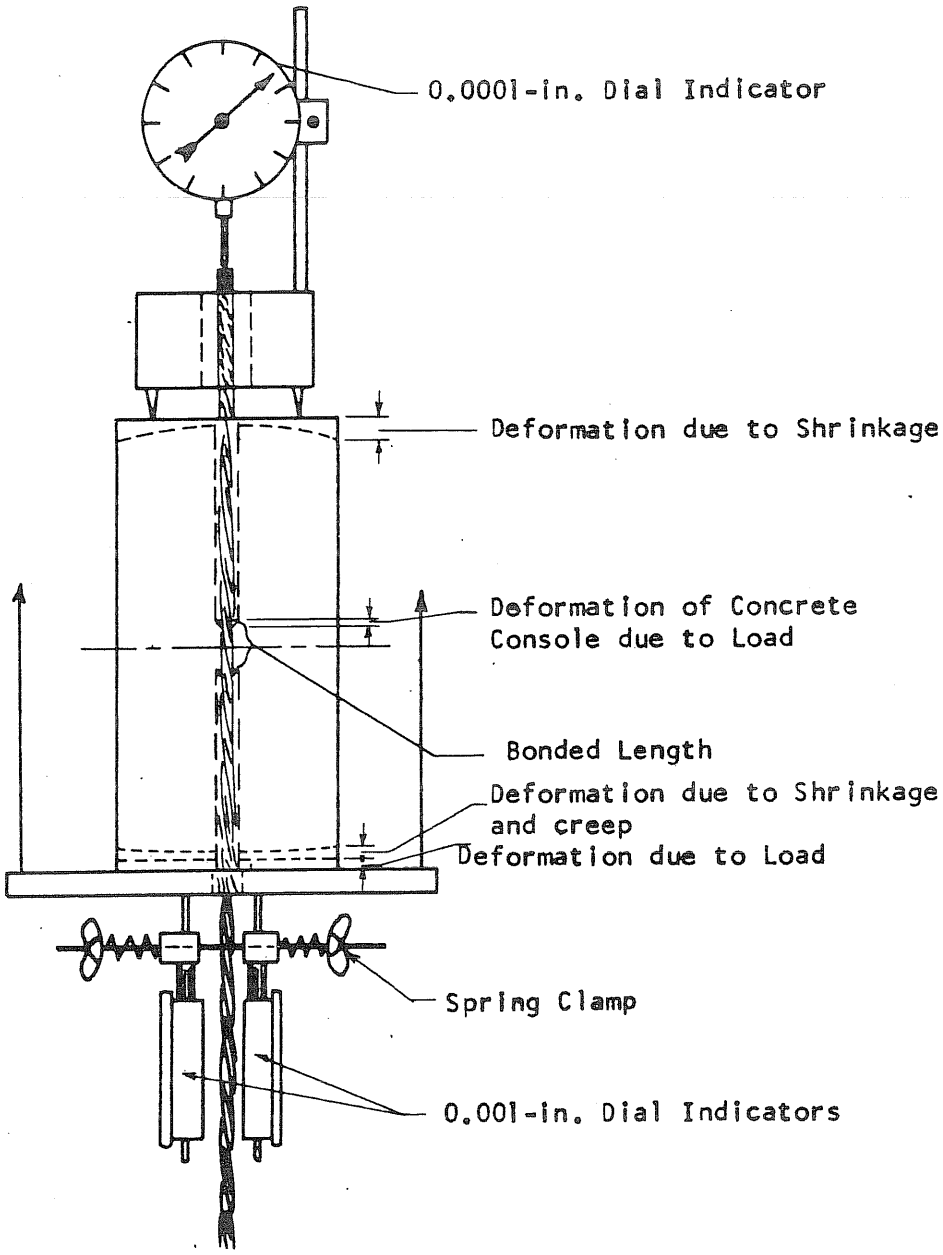

FIG. A.8 TEST SETUP FOR SPECIMENS WITH BONDED LENGTHS EXCEEDING TWO in.

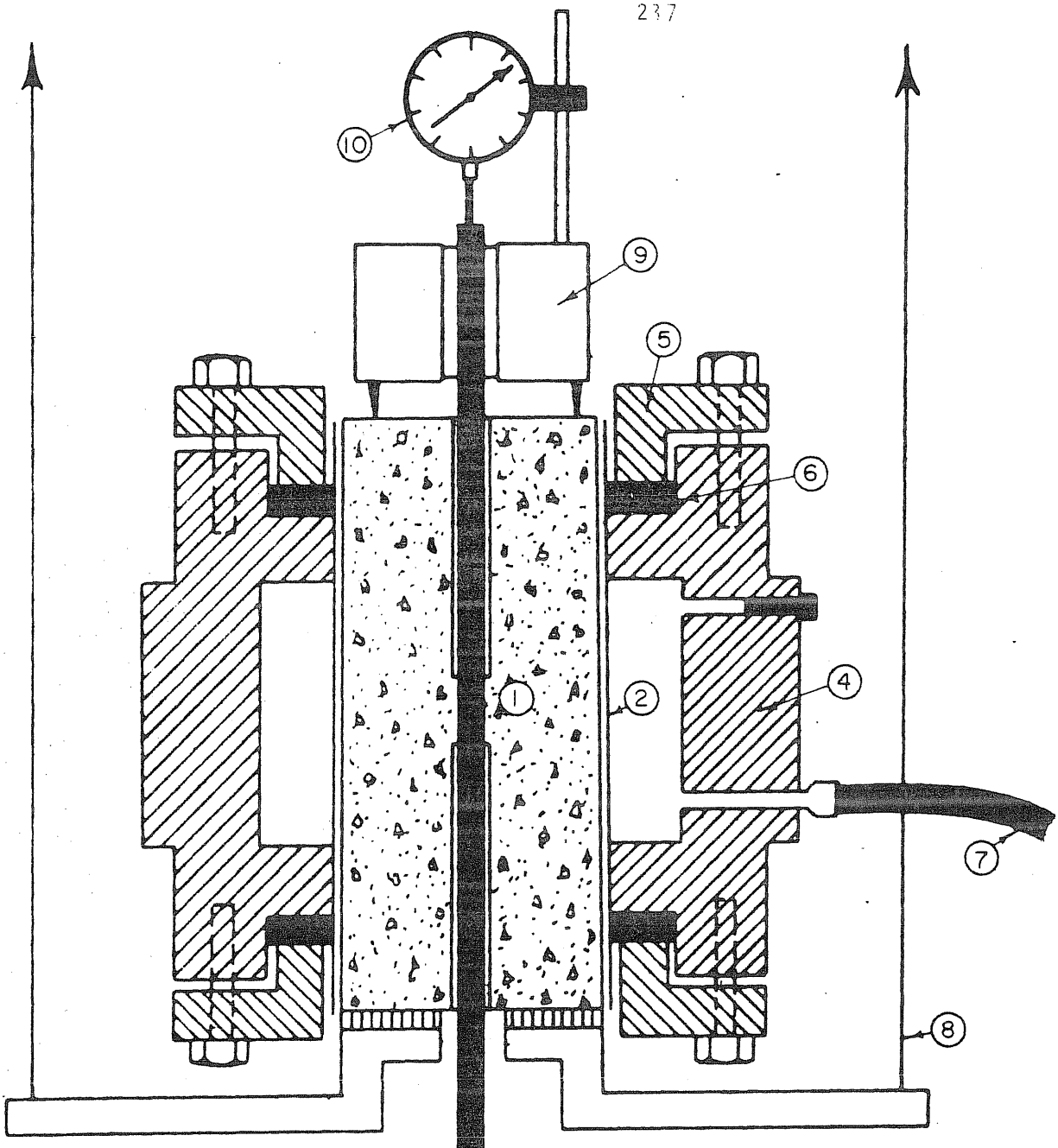

1. Concrete Specimen
2. Shim Steel, 0.004 in.
3. Strand or Wire
4. Pressure Vessel
5. End Plate
6. Lead Packing
7. Pump Line
8. Steel Cage
9. Base for Dial Indicator
10. Dial Indicator

FIG. A.9 TEST SETUP FOR LATERAL-PRESSURE TESTS

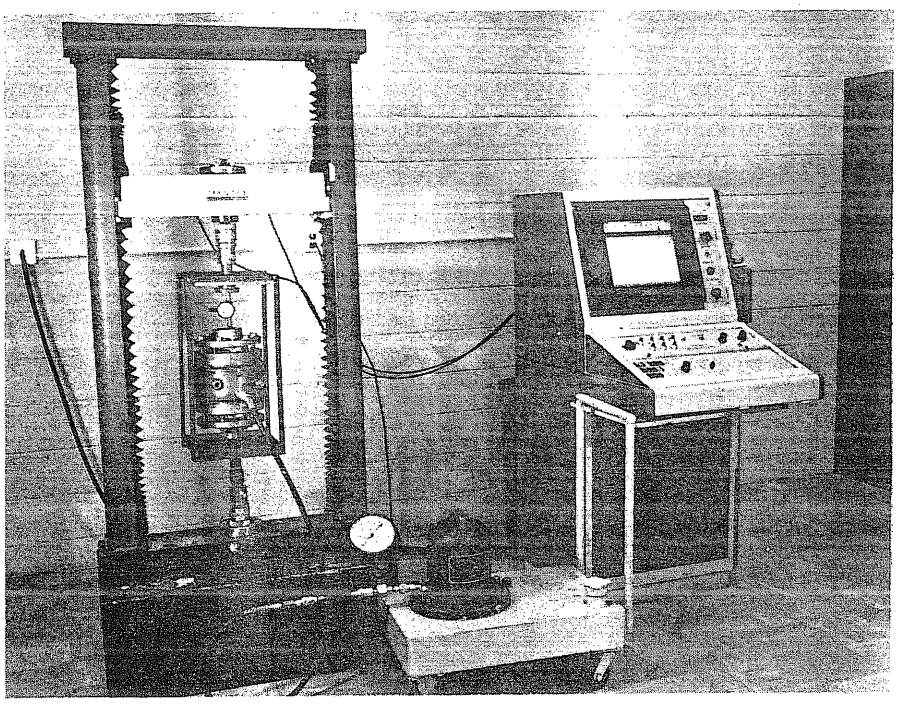

FIG. A.10 TEST SETUP FOR LATERAL-PRESSURE TESTS

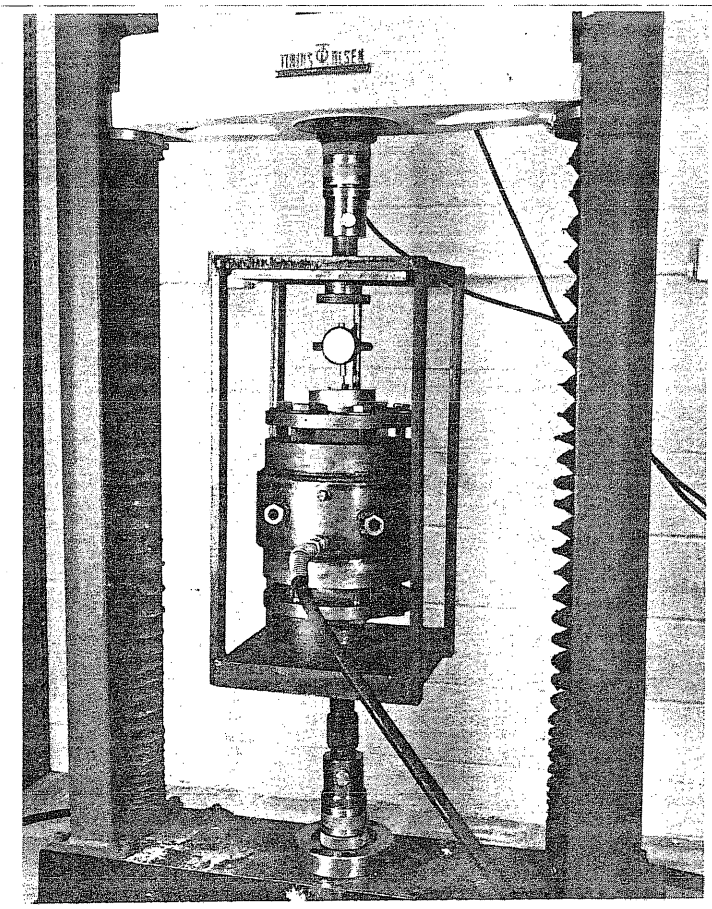

FIG. A.11 TEST SPECIMEN IN PLACE

APPENDIX B: PRESENTATION OF PULL-OUT TEST DATA

B.1 Identification of Test Series

Each test series is identified by a sequence of letters and numerals. The first letter characterizes the type of reinforcement in the pull-out specimen (S = strand, W = wire, Q = square bar, U = straight, nontwisted strand, B = bolt). The second letter represents the type of concrete mix. The proportions of the six different concrete mixes, marked A through F, are given in Table A.1. The third letter, if used, refers to a particular test setup: P stands for the lateral pressure the specimens were subjected to, and L stands for long-time or sustained-load test. The two-digit number following the letters identifies the age of the concrete at which the specimens were tested. The number after the dash represents the numerical sequence of the test series. They were numbered consecutively as long as the specimens shared the same type of steel and concrete mix, and, in addition, were tested in the same test setup.

B.2 Unit Bond Force-Slip Curves

A sequence of simultaneous force and slip measurements provided the basic information about the bond properties of strand. Thus, a measured force-slip relationship is reported for every test. It would have been desirable to express the quality of bond in terms of bond stress, i.e. bond force per unit area, however this was not possible since bond of strand is not only a function of its surface area but also of its geometry. As an alternative, the magnitude of bond was plotted in terms of bond force per unit length, and was called

unit bond force. Although a function of the strand size, this term provides a simple measure of bond. It should be characteristic for every strand. The term of unit bond force will be used for strand and twisted square bars throughout the whole investigation. For plain wires, the magnitude of bond was expressed in terms of bond stress.

The slip was plotted to a logarithmic scale in most graphs. The reason was the large range of slip measurements extending from 0.0001 in. to 0.15 in. The maximum end slip of 7/16-in. strand, prestressed to 160,000 psi, was in the order of 0.07 in. as beam tests indicated. The main interest was therefore concentrated in the slip range below this value. The logarithmic scale offered, for this purpose, a very efficient way of plotting although it had the disadvantage of not lending itself to direct interpretation. In order to provide a perspective of the logarithmic plot, a typical bond-slip relationship for strand and plain wire was plotted in Fig. B.1, using both the linear and the logarithmic scales.

The left axis of the logarithmic plot does not indicate zero slip. It represents the smallest slip value that could be measured reliably. It was observed in all tests that the pointer of the dial indicator started to move at a smaller load than the initial force plotted in the logarithmic graphs.

In some test series, including mainly tests with plain wire and strand tests under externally applied lateral pressure, no bond force-slip data were obtained within the initial slip range from

0.0001 in. to 0.01 in., in extreme cases even to 0.04 in. The hand of the dial indicator turned around for one or several complete revolutions at such a speed that it was impossible to record any readings. In those cases, the initial bond force at a slip of 0.0001 in. was connected graphically with the first bond force data available at larger slip values by a straight line in the semi-logarithmic plot. The straight line seemed to be the most likely and most consistent approach to the actual bond force-slip relation.

Three identical specimens were usually tested to investigate the influence of one variable on bond. Groups of three ostensibly identical bond-slip relationships were plotted in separate graphs. Three or four of those graphs, representing all the individual tests of one series, were combined in one figure.

In Fig. B.2 through B.53, every test series carried out during this investigation is presented in the manner described above. These figures contain the bond-slip relationship of each individual test.

B.3 Correction of Initial Slip Measurements

Measurement of the attack-end slip usually requires a correction for the elongation of the reinforcement. Measurement of the trail-end slip needs no correction for the deformation of the reinforcement. However, it is necessary to make corrections for the deformation of the concrete unless the slip dial is supported immediately adjacent to the bonded length in both the longitudinal and transverse planes.

The test setup used in this investigation, Fig. A.8, required a correction of the slip measurement. The slip was measured only at the trail end in all tests with bonded lengths equal to or shorter than two in. The apparent slip was measured with respect to the edges of the upper surface of the concrete prism upon which the base of the dial indicator rested. The possibility of using a probe to measure the deformation of the concrete immediately adjacent to the trail end of the bonded length was rejected because it was desired to keep the clearance between the concrete and the strand outside the bonded length as small as possible.

The bonded part of the strand transferred the pull-out force over a one-in. high annular console of concrete into the main concrete prism. The high local stresses in the concrete console during the pull-out test led to local deformations which were measured as slip. The overall deflection of the top surface with respect to the trail end of the bonded length was small enough to be negligible.

In order to find out how much concrete deformation was included in the measured slip, tests had to be conducted in such a way that it was possible to measure the concrete deformation separately. Calculation of this deformation involved too many questionable assumptions about the response of the concrete to be of practical value. A series of tests was designed such that virtually no slip would be developed during the test. High strength bolts with a diameter of 3/8 in. and a head filed down to a diameter of 9/16 in. were cast into concrete prisms identical to those used for standard pull-out

tests (Fig. B.54). The underside of the bolt head bore directly on the concrete console. While the edges of the bolt head were not in bond with the surrounding concrete, the shank of the bolt, adjacent to the head, was bonded over a length of one in. The bond condition on the shank was varied. In five specimens the shank was threaded. In four specimens the shank was plain, and in one specimen it was plain and heavily greased. A steel rod, welded to the bolt head, served as an anvil for the dial indicator. Since the bolt head rested on an annular area of 0.14 sq. in., negligible slip should occur between the bolt head and the concrete. Consequently, the dial readings would indicate deformations of the concrete console.

The measured relations between the pull-out force and the movement of the bolt head are shown in Fig. B.54. Bond along the shank affected the results significantly. A clearer perspective of the influence of bond along the shank may be obtained by comparing the average relationships of the three types of tests (Fig. B.55). The curve for the bolts with the threaded shanks may be divided into two regimes: (a) an initial nearly linear portion with a steep slope, and (b) a subsequent nearly linear portion with a relatively flat slope. It should be noted that the curve for the bolt with the greased shank does not exhibit regime (a), and the curve for the bolts with plain shanks represents a compromise between the two extremes.

The movement of the bolt head in the test without bond along the shank must have been related to deformations of the concrete. The concentrated bearing stresses, transmitted from the bolt to the concrete,

cause the concrete immediately under the bolt head to deform under stresses well in the inelastic range. The highly concentrated stress transfer results in a soft force-deformation relationship. The comparatively fast rate of the initial deformation was probably caused by a lack of fit between the concrete console and the bolt head.

The movement of the bolt head in tests with bond along the shank is caused by a concrete deformation, too. However, the initial deformation must represent a shear deformation of the whole concrete console. The pull-out force is transferred to the concrete initially by bond. Since the force transmitted by bond is distributed over a large area compared with the bearing area of the bolt head, the force-deformation relationship is much stiffer than that caused by bearing stresses under the bolt head.

As long as the force in tests with bonded shanks is transferred to the concrete exclusively by bond, the measured deformation represents a shear deformation of the concrete console. After the bond stresses have progressed along the shank so far that steel stresses are induced at the end of the shank, the bolt head starts bearing against the surface of the concrete console. The part of the force that is carried by bond does not undergo any further significant increase since the end of the shank adjacent to the bolt head cannot slip with respect to the surrounding concrete. Thus, the bond strength of the shank cannot be utilized completely. A further increase of the pull-out force causes the load carried by bond to increase only slightly owing to the differential slip of the shank between the attack end and the bolt head.

The rest of the pull-out force is transmitted directly by bearing of the bolt head. Consequently, the force-deformation relation of tests with bonded shanks becomes similar to that of tests without bond along the shank. This is indicated by the approximately parallel slope of the force-deformation curves in Fig. B.55 at slips larger than 0.0003 in.

The bond conditions along the shank determine the load at which bearing of the bolt head becomes effective. The better the bond along the shank is, the more load can be transferred by bond, and consequently the later the bolt head starts bearing.

If the force-deformation relationship for bearing alone is subtracted from the combined relationships caused by bond plus bearing, a relationship should be obtained that indicates the deformation of the concrete console caused only by bond forces. Actually, a somewhat smaller force than that indicated by the force-deformation relation for pure bearing should be subtracted since initially the concrete console deforms due to bond even though the bolt head has not started bearing. The error attributable to this inaccuracy is so small, however, that it may be neglected in this application.

The relationships developed in the manner described above are plotted in Fig. B.56. The initial slope of the two curves represents the relationship between the deformation and the force transferred by bond. The deviation from the initial slope indicates that the bolt head starts bearing against the console. The relatively small further increase of force represents the additional bond forces that were activated by the differential slip.

In pull-out tests with strand, the force is transmitted to the concrete exclusively by bond. Therefore, the force-deformation relationships of these tests should follow the initial slope of the curves plotted in Fig. B.56., and retain this slope even at higher forces since slip is not prevented towards the end of the bonded length by a bolt head. Consequently, a maximum bond stress distribution can develop on the whole length.

In Fig. B.57, the initial portions of the measured force-"slip" relationships were plotted for all strands tested under lateral pressure. At the beginning of the test, the measured "slip" increased approximately linearly with the applied pull-out force. At loads close to the maximum bond force, the measured "slip" started to increase at a faster rate. The maximum bond force, finally, was marked by a rapid increase of the slip and a sudden drop of the load (Fig. B.58). The initial slopes of the bond force-"slip" relationships in Fig. B.57 agree very well with the initial slope of the graph in Fig. B.56, which indicates the shear deformation of the concrete console. The agreement of the measured "slip" data and the predicted deformation of the concrete console confirmed the conclusion that the deformations of the concrete console were measured in the pull-out tests as slip.

The increasing rate at which the measured "slip" progressed near the maximum bond force may be explained by a gradual failure of bond between the strand and the concrete. The gradual failure must be regarded as a progressive type of rupture proceeding from the attack end of the bonded length towards the trail end. It must be emphasized

that, although described as gradual, the failure took place within a slip range of approximately 0.0005 in. (Fig. B.57).

The average deformation (Fig. B.57) was approximately 0.00015 in. per 1000 lb of pull-out force. This amount had to be subtracted from the measured "slip" in order to obtain the actual slip between strand and concrete. Instead of using an average correction, however, each individual test was corrected by an amount that was indicated by the slope of the initial part of the individually measured force-"slip" relationship, plotted to a linear scale. A typical example, showing the measured and the corrected bond force-slip relationships of test series SBP 24-1, is presented in Fig. B.58.

A few pull-out tests were conducted with a bonded length larger than one in. According to the above, the shear deformations are proportional to the shear stresses which, in this case, are equal to the bond stresses. For this reason, the measured "slip" in tests with bonded lengths larger than one in. were corrected in proportion to the unit bond force.

TABLE B.1 PROPERTIES OF TEST SPECIMENS CONTAINING STRAND

Test Series	Number of Tests	Concrete Properties: Mix	Compressive Strength (psi)	Splitting Strength (psi)	Slump (in.)	Water/Cement Ratio	Steel: Strand Diameter (in.)	Bonded Length (in.)	Applied Lateral Pressure (psi)	Age at Testing (days)	Remarks
SA09-1	12	A	5590	390	1.5	0.65	1/4	0.5,1,1.5,2	0	9	
SA09-2	12	A	5380	420	2.3	0.65	3/8	0.5,1,1.5,2	0	9	
SA08-3	12	A	5560	390	1.5	0.65	7/16	0.5,1,1.5,2	0	8	
SA09-4	12	A	5350	440	1.5	0.65	1/2	0.5,1,1.5,2	0	9	
SA08-5	9	A	4900	410	1.5	0.65	7/16	1	0	8	
SA09-6	5	A	4950	430	1.5	0.65	7/16	1	0	9	
SA09-7	4	A	5640	410	1.5	0.65	7/16	1	0	9	
SA23-8	12	A	5930	480	2.5	0.65	1/4,3/8,7/16,1/2	1	0	23	
SA08-9	12	A	5210	420	2.2	0.65	1/4,3/8,7/16,1/2	1	0	8	
SA08-10	12	A	5890	490	1.5	0.65	1/4,3/8,7/16,1/2	1	0	8	
SA08-11	12	A	5430	450	1.7	0.65	1/4,3/8,7/16,1/2	1	0	8	
SA08-12	6	A	5480	350	1.5	0.65	7/16	1	0	8	
SA08-13	3	A	5640	420	1.5	0.65	7/16	1	0	8	dry cured
	3		5240	460			7/16	1	0	8	moist cured
SA08-14	4	A	5850	400	2.2	0.65	7/16	1	0	8	
SA09-15	15	A	5370	305	1.5	0.65	7/16*	1	0	9	
SA09-16	15	A	5150	410	1.5	0.65	7/16*	1	0	9	
SA08-17	9	A	5350	340	1.5	0.65	7/16*	1	0	8	
SA09-18	14	A	5280	280	1.5	0.65	7/16*	1,3,8,15,20	0	9	
SA10-19	8	A	5230	415	1.5	0.65	7/16*	1,3,8	0	10	

* 7/16-in. Strand (Coil II)

TABLE B.2 PROPERTIES OF TEST SPECIMENS CONTAINING STRAND

Test Series	Number of Tests	Mix	Concrete Properties: Compressive Strength (psi)	Splitting Strength (psi)	Slump (in.)	Water/Cement Ratio	Steel: Nominal Strand Diameters (in.)	Bonded Length (in.)	Applied Lateral Pressure (psi)	Age at Testing (days)	Remarks
SB09-1	12	B	7450	440	1.5	0.40	1/4,3/8,7/16,1/2	1	0	9	
SB09-2	12	B	7390	450	1.5	0.40	1/4,3/8,7/16,1/2	1	0	9	
SB08-3	12	B	7560	480	1.7	0.40	1/4,3/8,7/16,1/2	1	0	8	
SB18-4	3	B	8600	490	1.7	0.40	7/16	1	0	18	dry cured
	3		8600	---			7/16	1	0	18	moist cured
SC09-1	12	C	2580	180	1.5	1.05	1/4,3/8,7/16,1/2	1	0	9	
SC09-2	12	C	2340	210	1.5	1.05	1/4,3/8,7/16,1/2	1	0	9	
SC08-3	12	C	2270	260	1.5	1.05	1/4,3/8,7/16,1/2	1	0	8	
SC08-4	12	C	2470	260	1.0	1.05	1/4,3/8,7/16,1/2	1	0	8	
SD09-1	4	D	5320	410	0.2	0.65	7/16	1	0	9	
SD09-2	4	D	6180	410	0.5	0.65	7/16	1	0	9	
SE09-1	4	E	4460	390	7.7	0.65	7/16	1	0	9	
SE09-2	4	E	5470	400	6.5	0.65	7/16	1	0	9	
SF09-1	12	F	3400	300	0.5	0.90	1/4,3/8,7/16,1/2	1	0	9	
SAL12-1	16	A	6000 7140	400 440	1.8	0.65	7/16	1 1	0 0	12 129	Sustained-Load tests
SAL11-2	10	A	6500 7000	430 460	1.0	0.65	7/16*	1	0	11 451	
SBL12-1	11	B	8700 8800	450 460	3.0	0.40	7/16*	1	0	12 446	

* 7/16-in. Strand (Coil II)

TABLE B.3 PROPERTIES OF TEST SPECIMENS SUBJECTED TO LATERAL PRESSURE

Test Series	Number of Tests	Concrete Properties: Mix	Compressive Strength (psi)	Splitting Strength (psi)	Slump (in.)	Water/Cement Ratio	Steel: Strand or Wire	Bonded Length (in.)	Applied Lateral Pressure (psi)	Age at Testing (days)
SAP15-1	4	A	6600	500	1.5	0.65	7/16-in. Strand	1	0	15
	1							1	1150	
SAP22-2	2	A	6450	460	2.0	0.65	7/16-in. Strand	1	0	22
	2							1	2150	
SAP23-3	3	A	5340	470	1.5	0.65	7/16-in. Strand	1	0	23
	3							1	1000	
	3							1	2000	
	1							1	2400	
	1							1	2500	
SBP24-1	3	B	8670	430	1.2	0.40	7/16-in. Strand	1	0	24
	3							1	1000	
	1							1	1500	
	3							1	2000	
	1							1	2500	
WAP15-1	6	A	6300	460	3.0	0.65	Wire d = 0.147 in.	1	0	15
	1							1	1000	
	1							1	1150	
	1							1	2150	
WAP17-2	3	A	5900	470	1.5	0.65	Wire d = 0.147 in.	1	0	17
	3							1	1000	
	3							1	2000	
WBP66-1	3	B	8220	530	2.5	0.40	Wire d = 0.147 in.	1	0	66
	2							1	1000	
	3							1	2000	

TABLE B.4 PROPERTIES OF TEST SPECIMENS CONTAINING STEEL OTHER THAN STRAND

Test Series	Number of Tests	Concrete Properties: Mix	Compressive Strength (psi)	Splitting Strength (psi)	Slump (in.)	Water/Cement Ratio	Steel	Bonded Length (in.)	Applied Lateral Pressure (psi)	Age at Testing (days)	Remarks
WA08-1	12	A	5040	400	1.7	0.65	Center Wire of	1	0	8	
WB08-1	12	B	8310	400	1.5	0.40	1/4,3/8,7/16,1/2-in.	1	0	8	
WC08-1	12	C	2180	230	1.5	0.65	Strand	1	0	8	
WB18-2	3	B	8600	490	1.7	0.40	Center Wire of 7/16-in. Strand	1	0	18	dry cured
	3		8600	480				1	0	18	moist cured
QB09-1	17	B	7320	535	3.0	0.40	Square Bars, a = 5/16 in.	1	0	9	
UA09-1	5	A	5520	370	1.7	0.65	Nontwisted 3-Wire and 7-Wire Strand	1	0	9	
BB09-1	10	B	7400	---	1.5	0.40	Bolts, d = 3/8 in.	1	0	9	

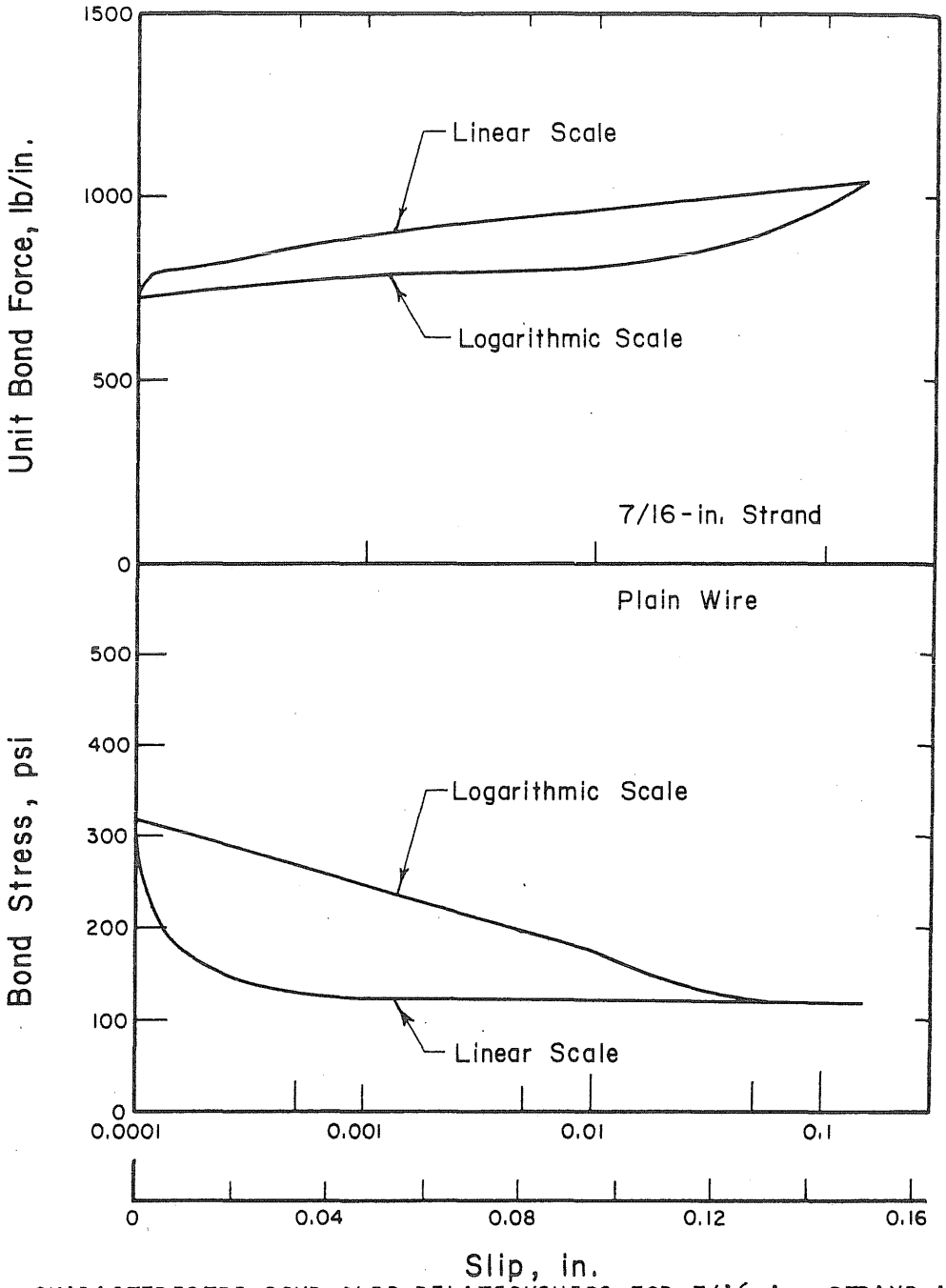

FIG. B.1 CHARACTERISTIC BOND-SLIP RELATIONSHIPS FOR 7/16-in. STRAND AND PLAIN WIRE WITH SLIP VALUES PLOTTED TO LINEAR AND LOGARITHMIC SCALES

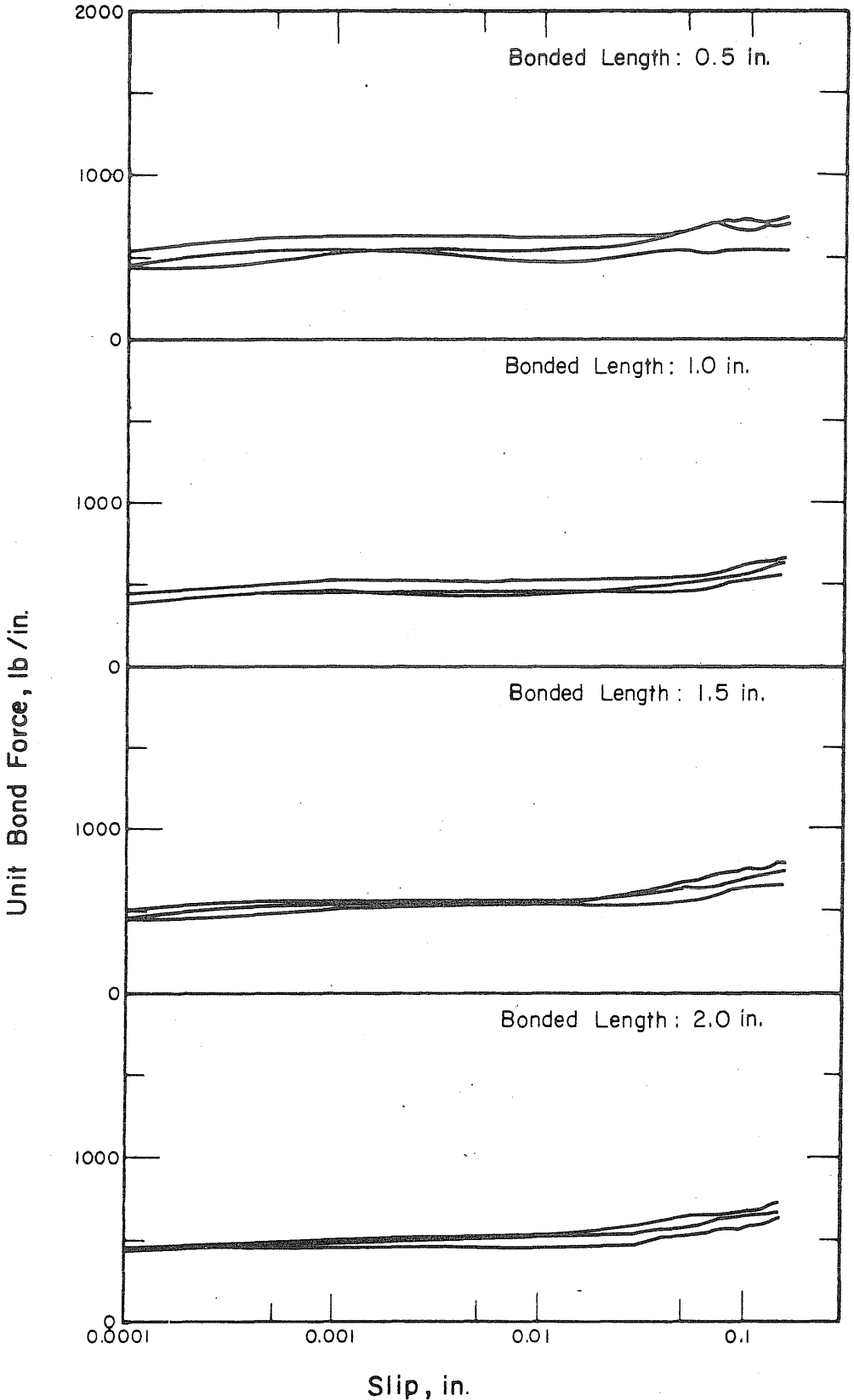

FIG. B.2 UNIT BOND FORCE-SLIP RELATIONSHIPS OF 1/4-in. STRAND FOR VARIOUS BONDED LENGTHS, SERIES: SA09-1

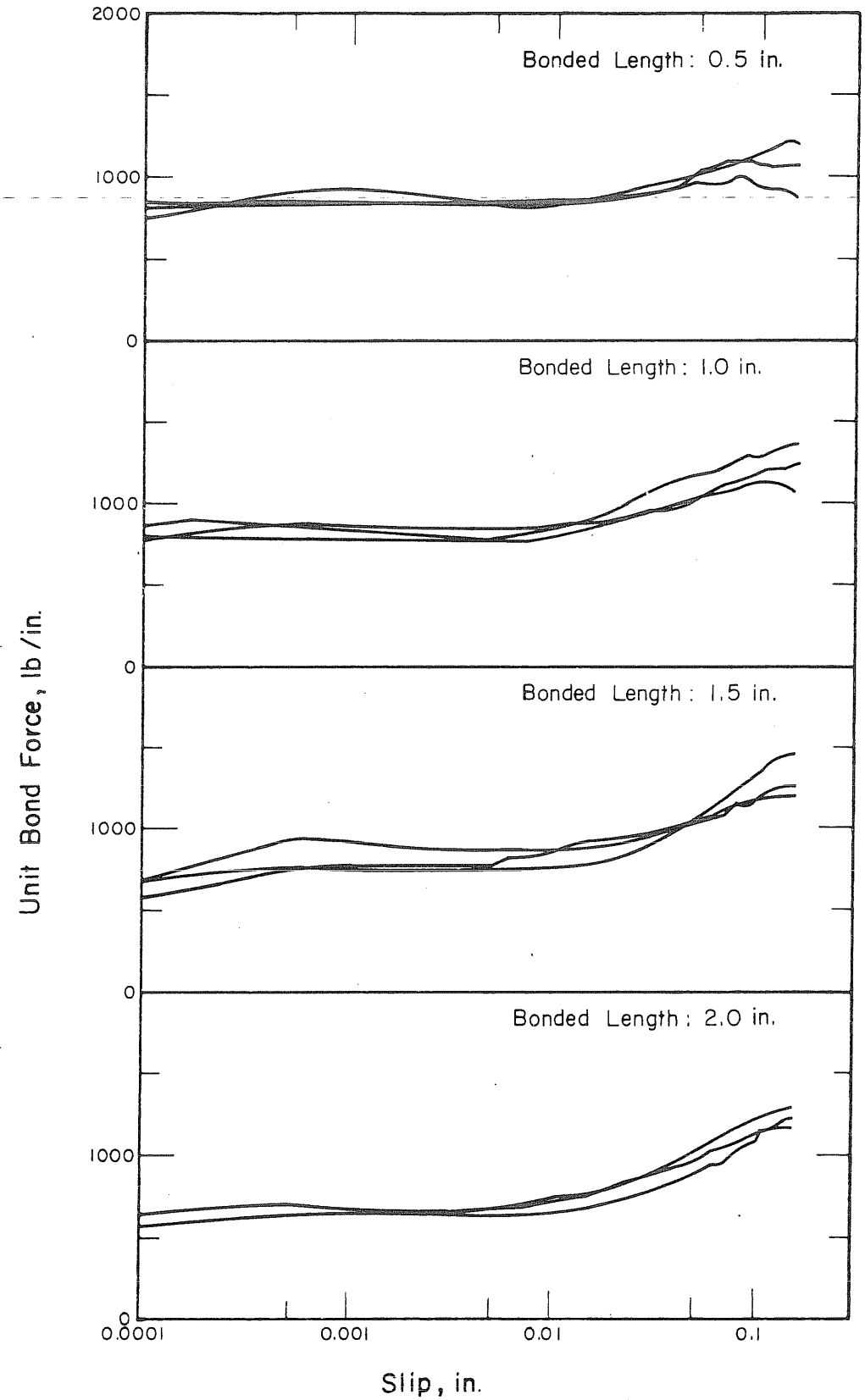

FIG. B.3 UNIT BOND FORCE-SLIP RELATIONSHIPS OF 3/8-in. STRAND FOR VARIOUS BONDED LENGTHS, SERIES: SA09-2

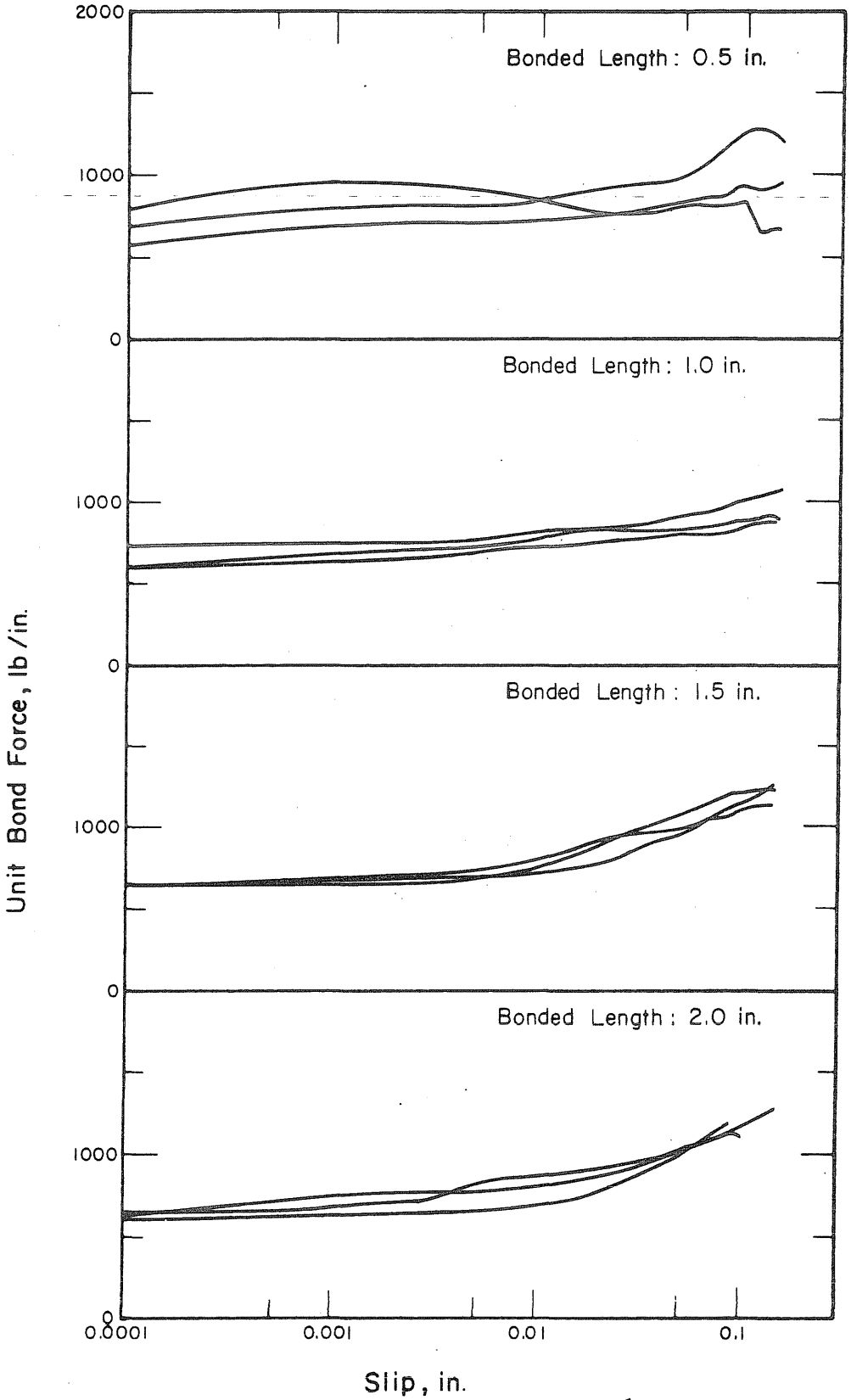

FIG. B.4 UNIT BOND FORCE-SLIP RELATIONSHIPS OF 7/16-in. STRAND FOR VARIOUS BONDED LENGTHS, SERIES: SA08-3

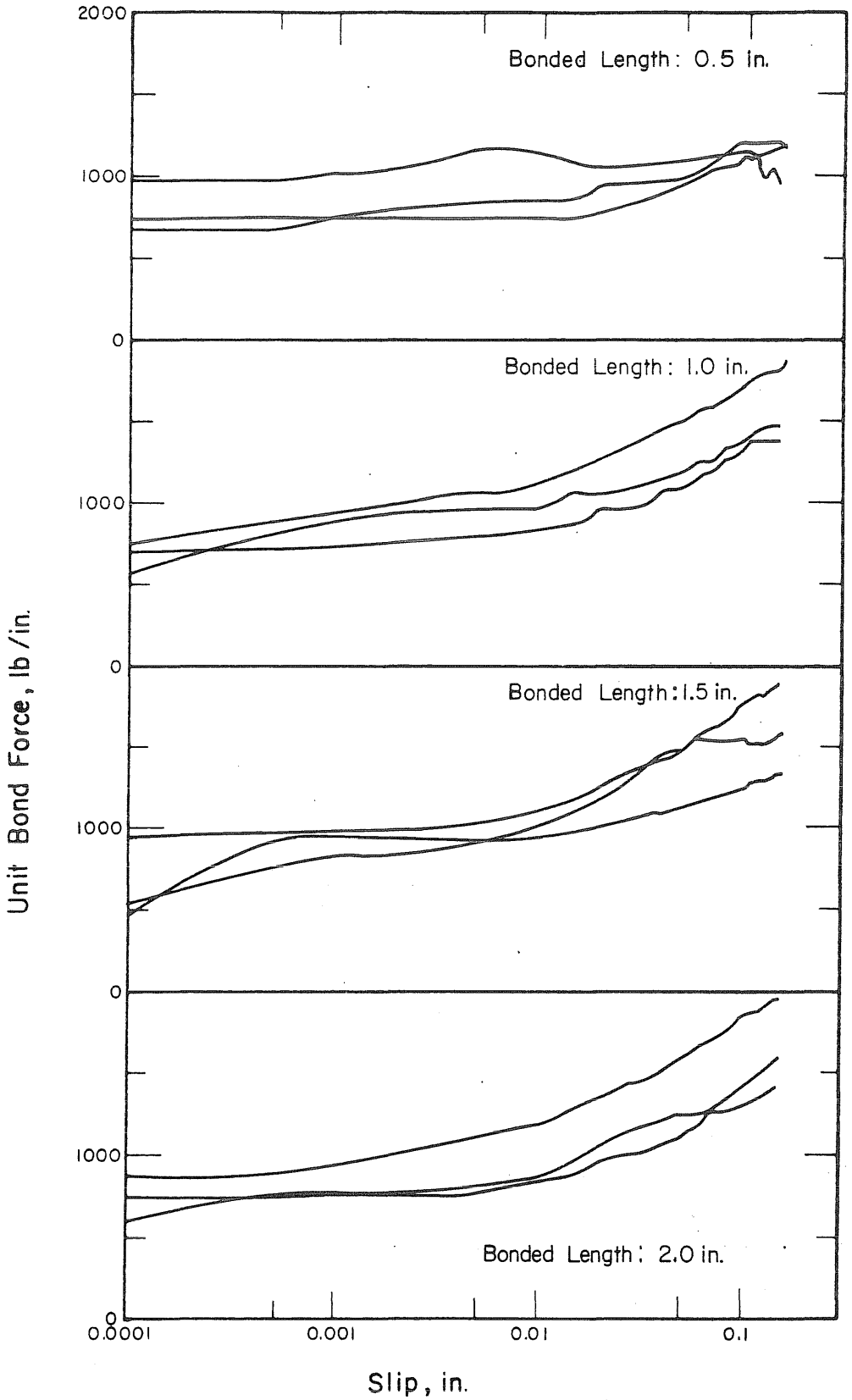

FIG. 3.5 UNIT BOND FORCE-SLIP RELATIONSHIPS OF 1/2-in. STRAND FOR VARIOUS BONDED LENGTHS, SERIES: SA09-4

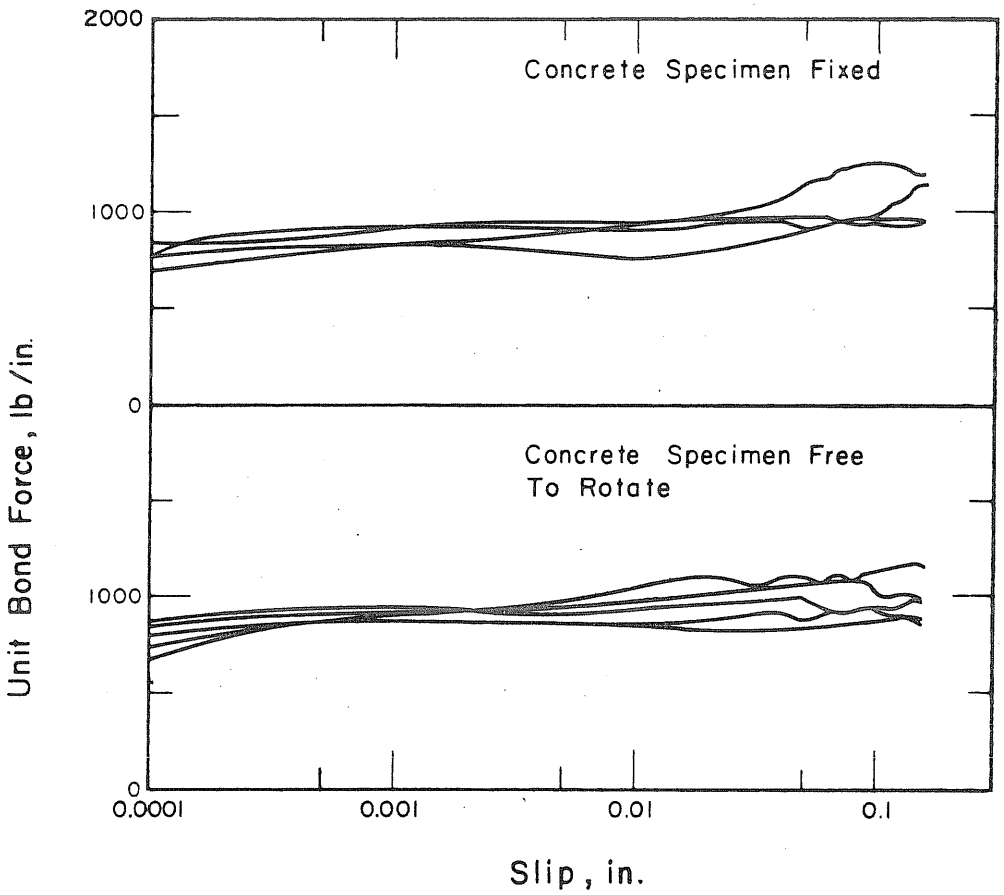

FIG. B.6 UNIT BOND FORCE-SLIP RELATIONSHIPS OF 7/16-in. STRAND FOR DIFFERENT TEST SETUPS, SERIES: SA08-5

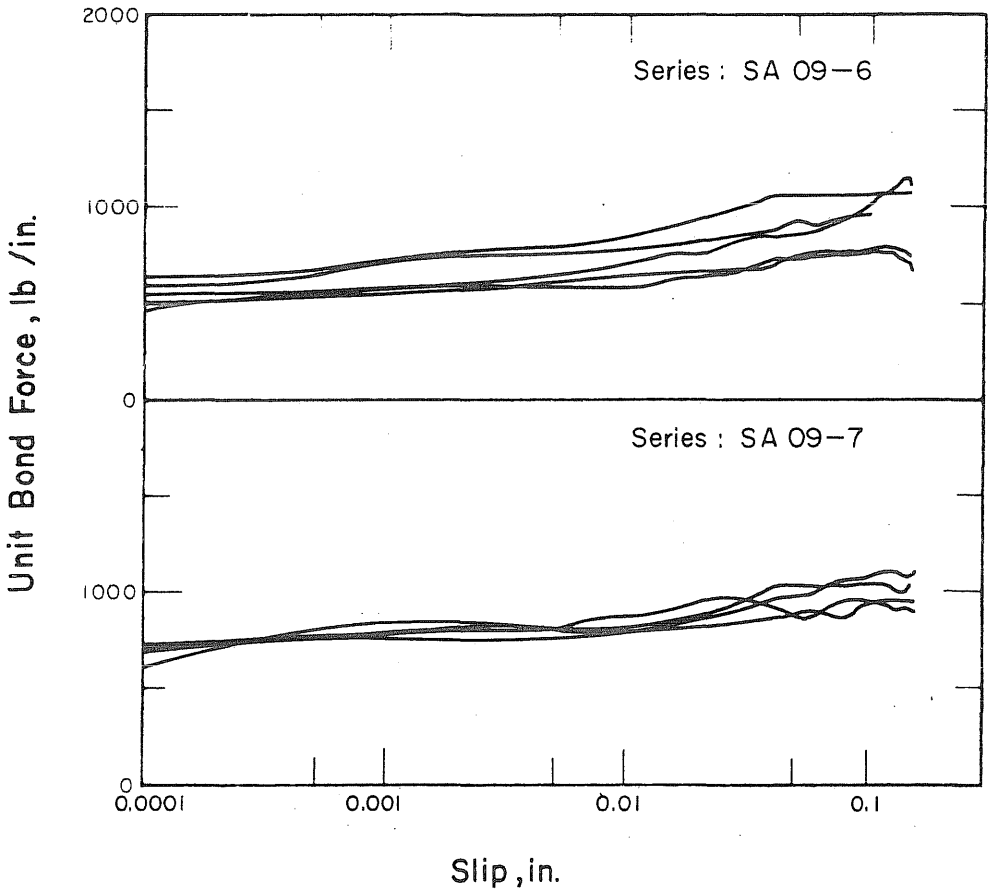

FIG. B.7 UNIT BOND FORCE-SLIP RELATIONSHIPS OF 7/16-in. STRAND, SERIES: SA09-6, SA09-7

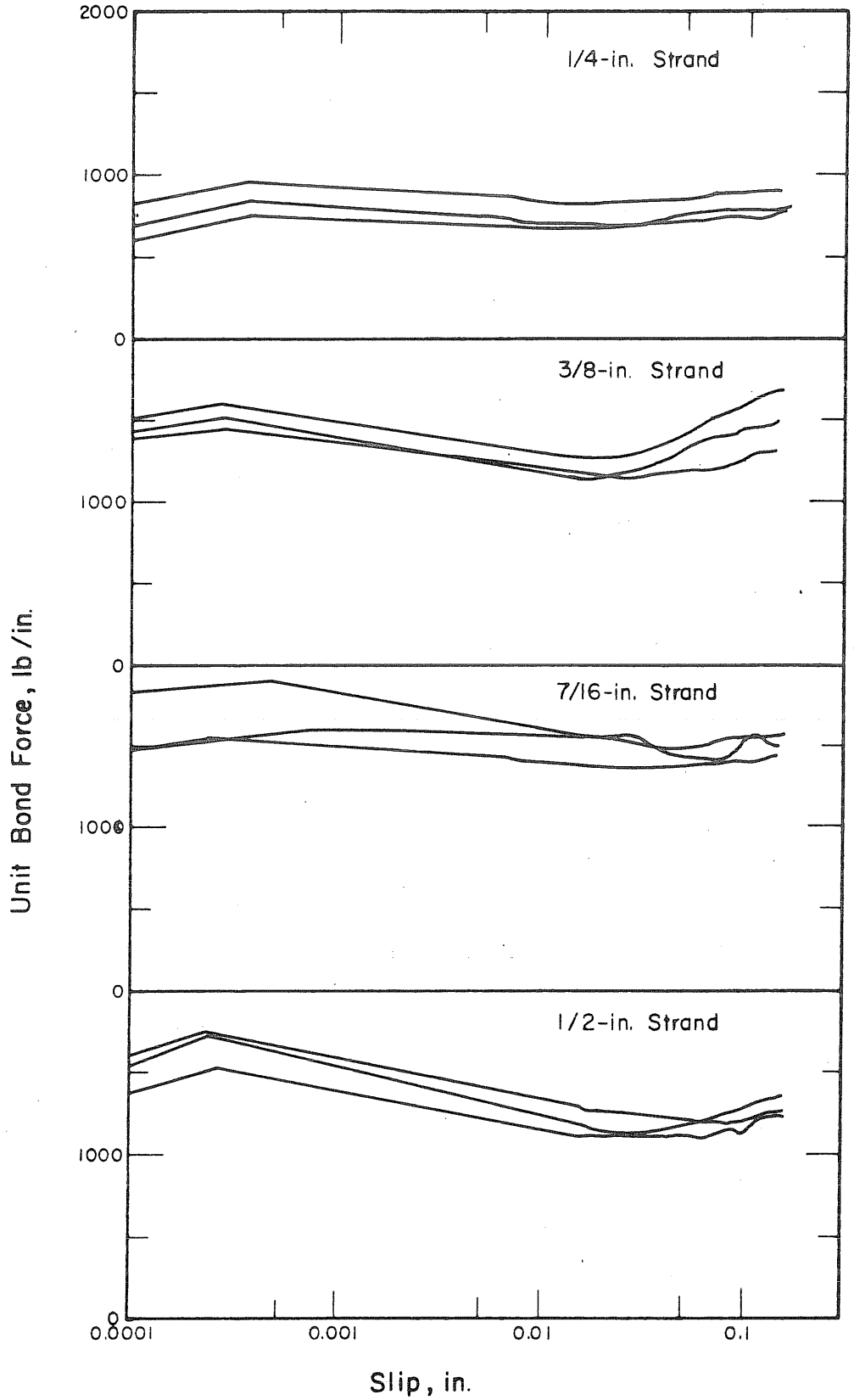

FIG. B.8 UNIT BOND FORCE-SLIP RELATIONSHIPS FOR VARIOUS STRAND SIZES, SERIES: SA23-8

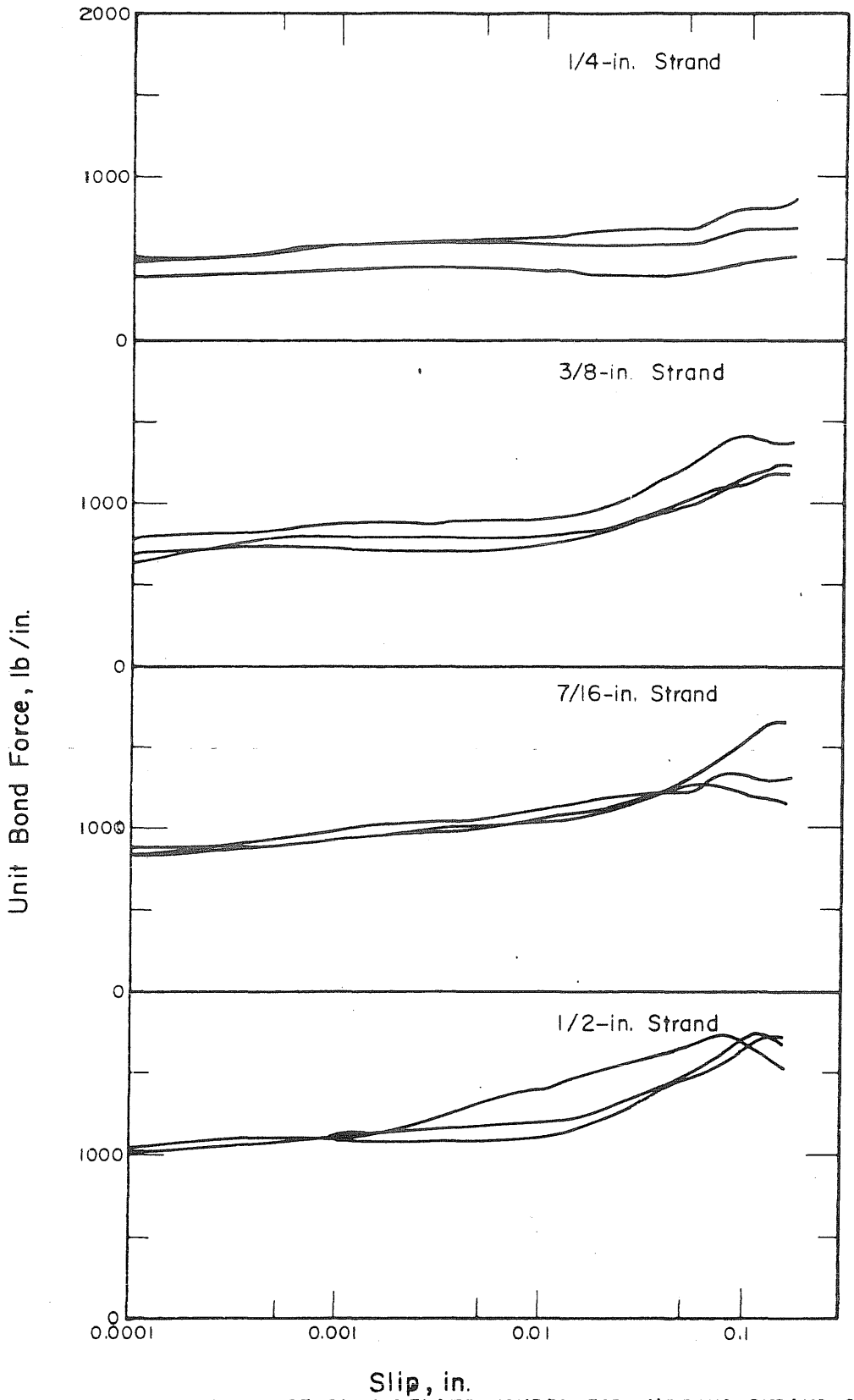

FIG. B.9 UNIT BOND FORCE-SLIP RELATIONSHIPS FOR VARIOUS STRAND SIZES, SERIES: SA08-9

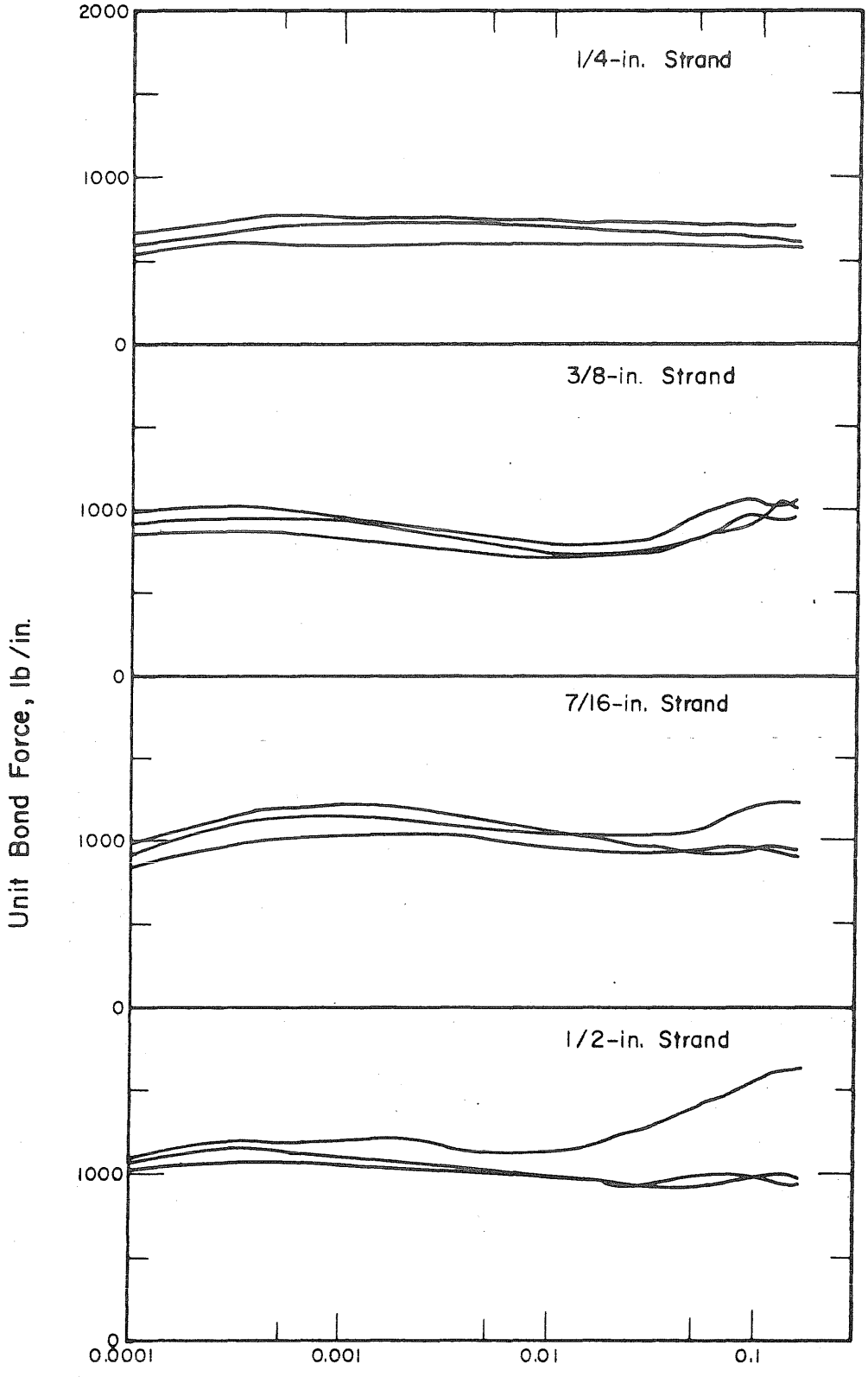

FIG. B.10 UNIT BOND FORCE-SLIP RELATIONSHIPS FOR VARIOUS STRAND SIZES, SERIES: SA08-10

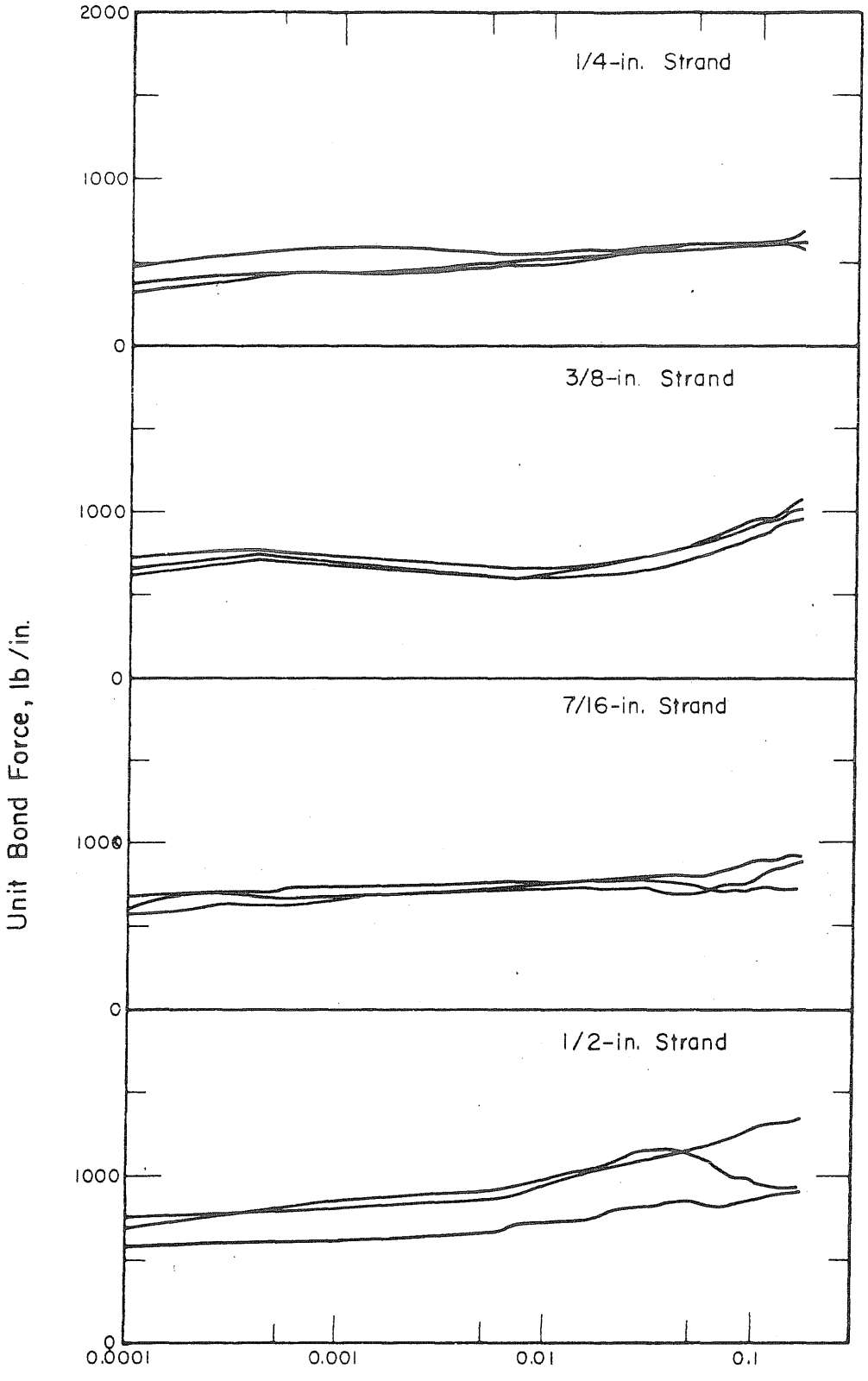

FIG. B.11 UNIT BOND FORCE-SLIP RELATIONSHIPS FOR VARIOUS STRAND SIZES, SERIES: SA08-11

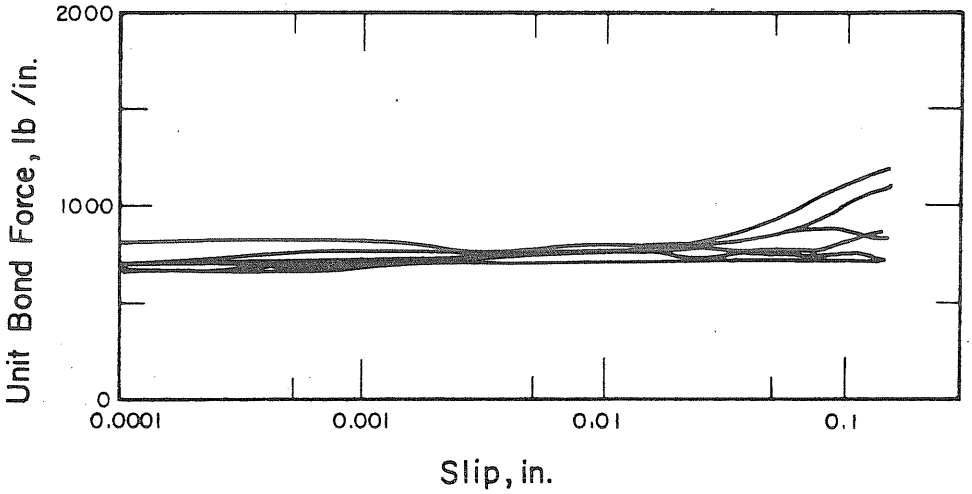

FIG. B.12 UNIT BOND FORCE-SLIP RELATIONSHIPS OF 7/16-in. STRAND, SERIES: SA08-12

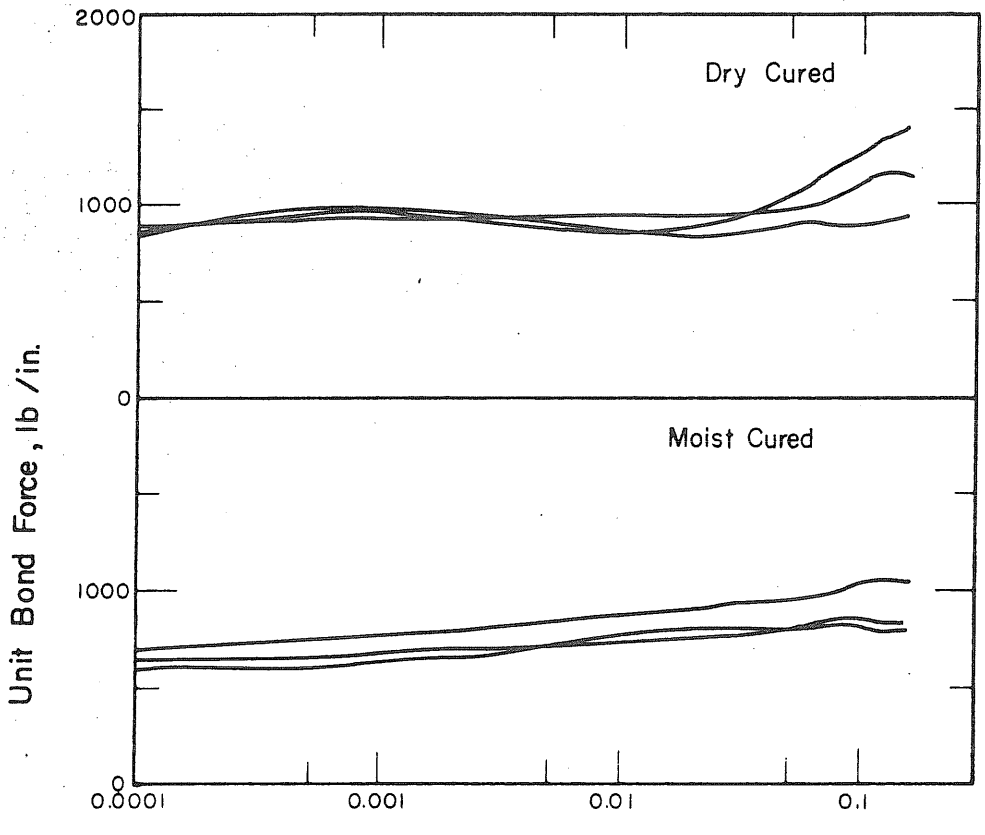

FIG. B.13 UNIT BOND FORCE-SLIP RELATIONSHIPS OF 7/16-in. STRAND FOR DIFFERENT CURING CONDITIONS, SERIES: SA08-13

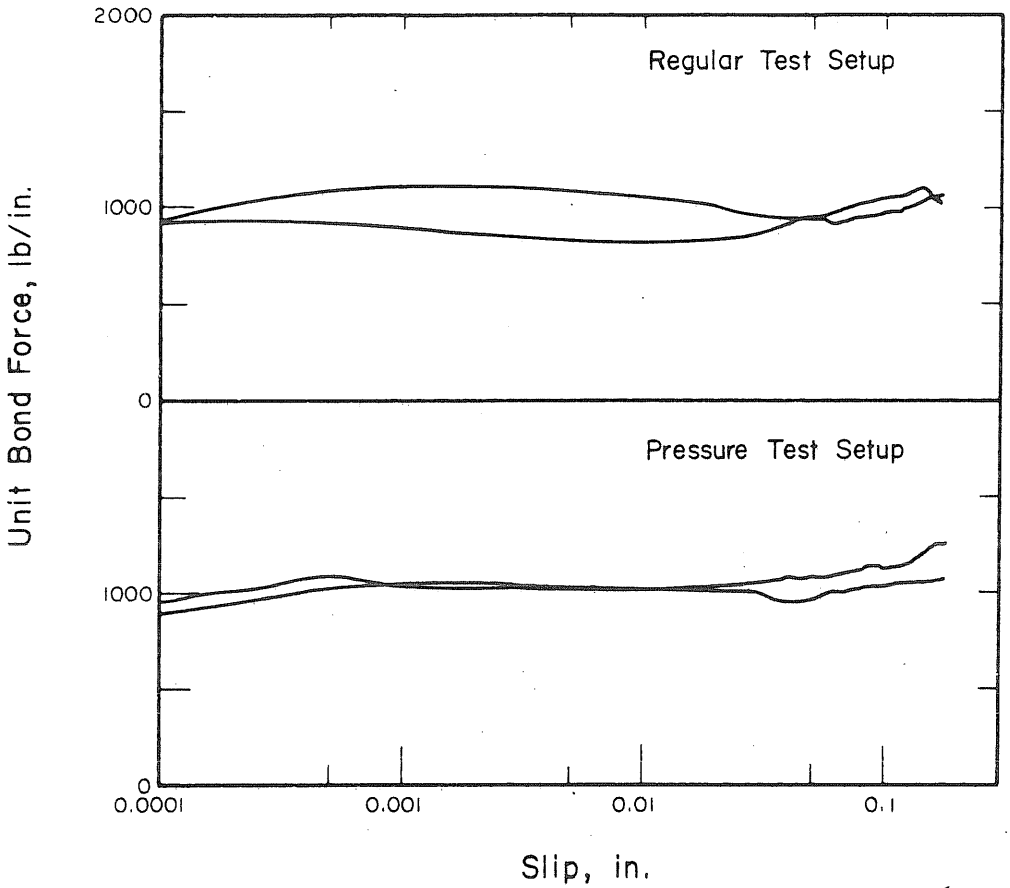

FIG. B.14 UNIT BOND FORCE-SLIP RELATIONSHIPS OF 7/16-in. STRAND FOR DIFFERENT TEST SETUPS, SERIES: SA08-14

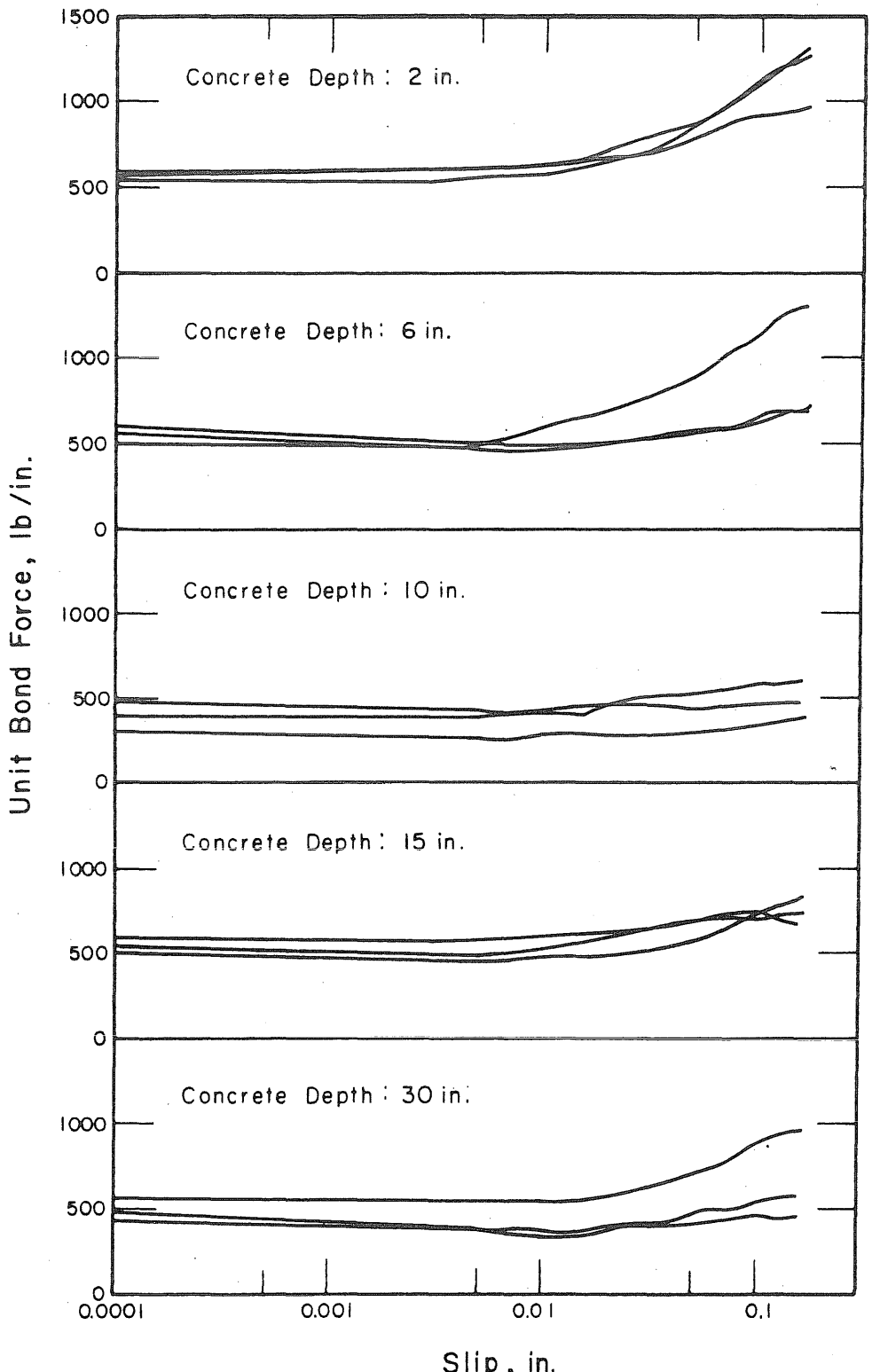

FIG. B.15 UNIT BOND FORCE-SLIP RELATIONSHIPS OF 7/16-in. STRAND FOR DIFFERENT CONCRETE DEPTHS UNDER THE STRAND, SERIES: SA09-15

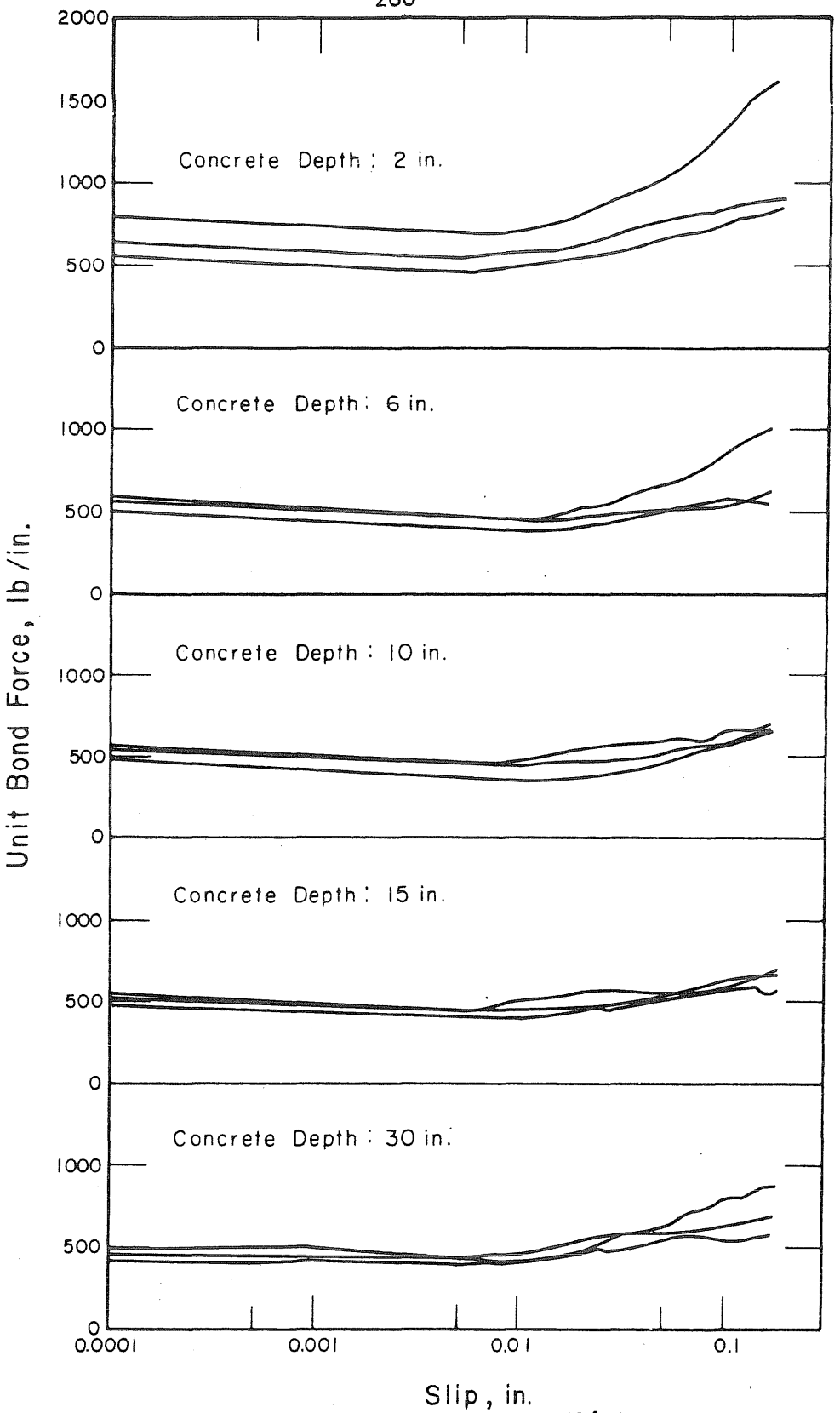

FIG. B.16 UNIT BOND FORCE-SLIP RELATIONSHIPS OF 7/16-in. STRAND FOR DIFFERENT CONCRETE DEPTHS UNDER THE STRAND, SERIES: SA09-16

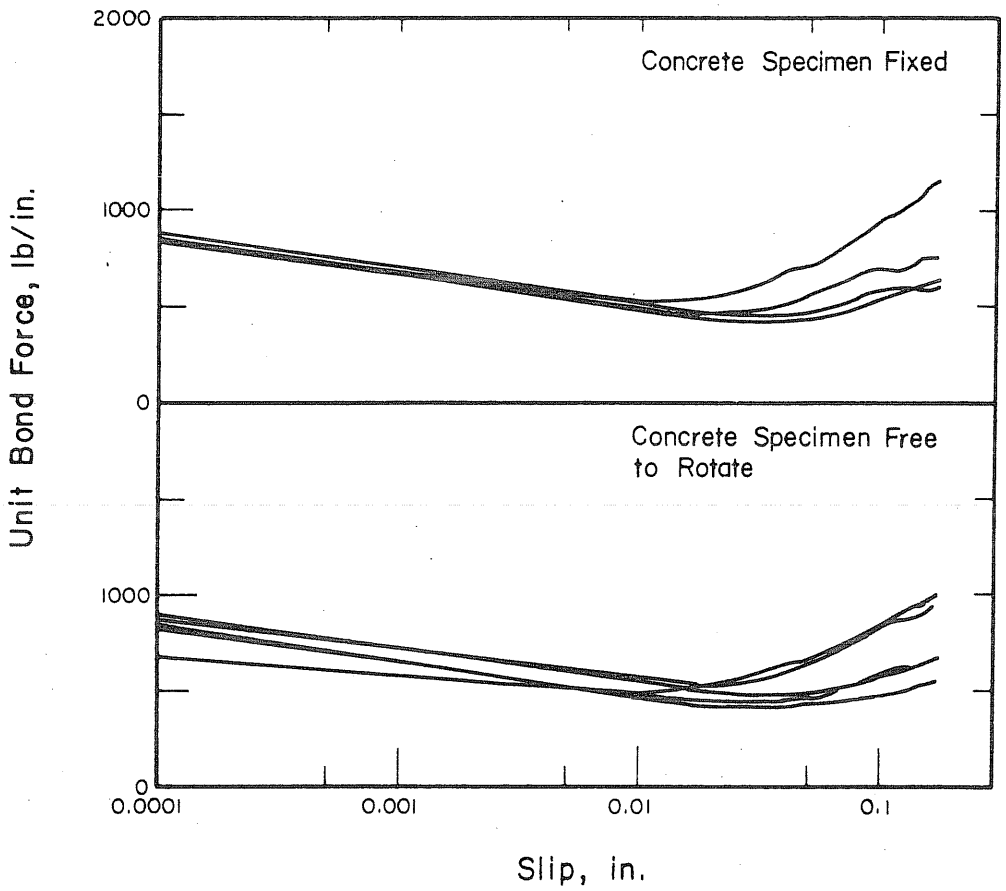

FIG. B.17 UNIT BOND FORCE-SLIP RELATIONSHIPS OF 7/16-in. STRAND FOR DIFFERENT TEST SETUPS, SERIES: SA08-17

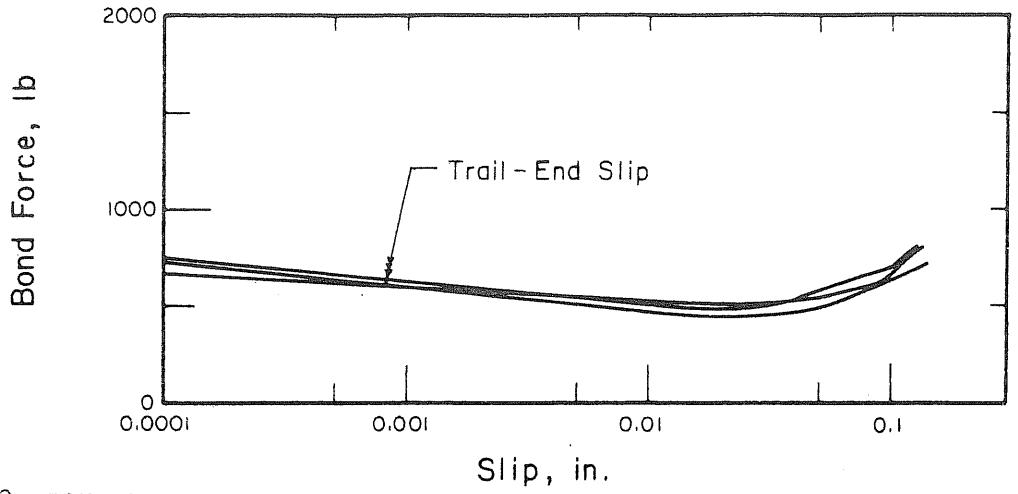

FIG. B.18 BOND FORCE-SLIP RELATIONSHIPS OF 7/16-in. STRAND FOR A BONDED LENGTH OF ONE in., SERIES: SA09-18

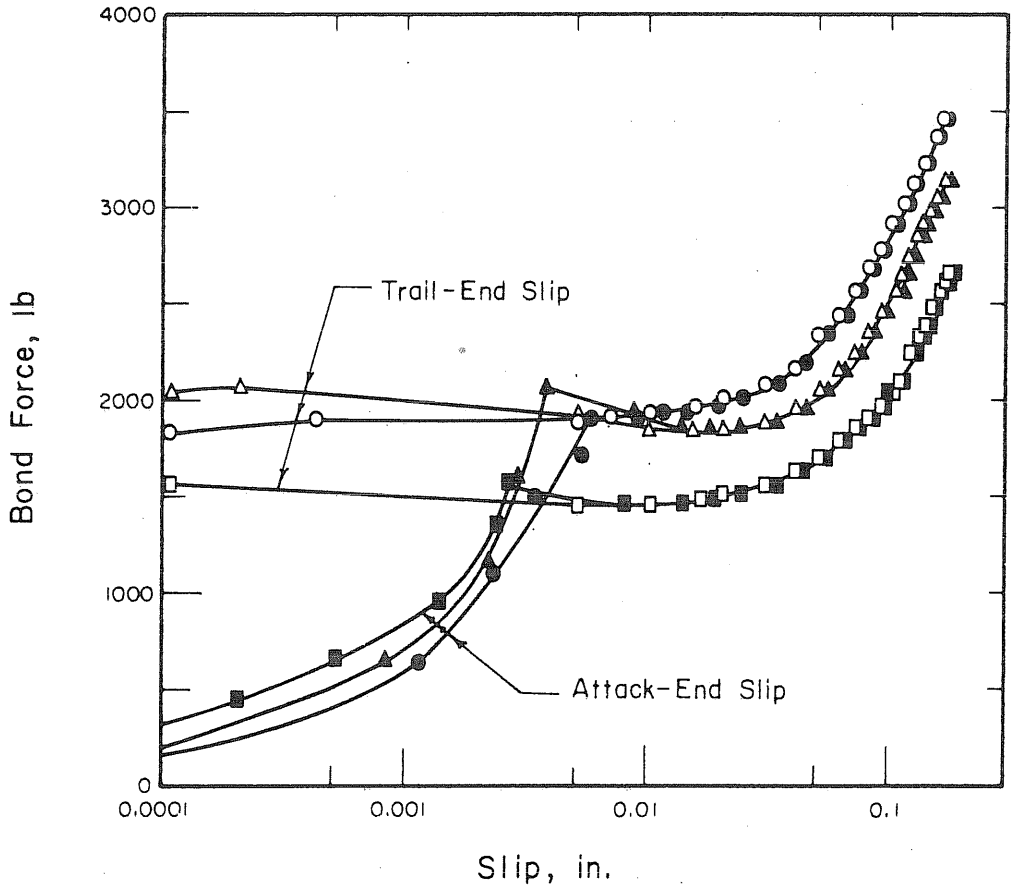

FIG. B.19 BOND FORCE-SLIP RELATIONSHIPS OF 7/16-in. STRAND FOR A BONDED LENGTH OF 3 in., SERIES: SA09-18

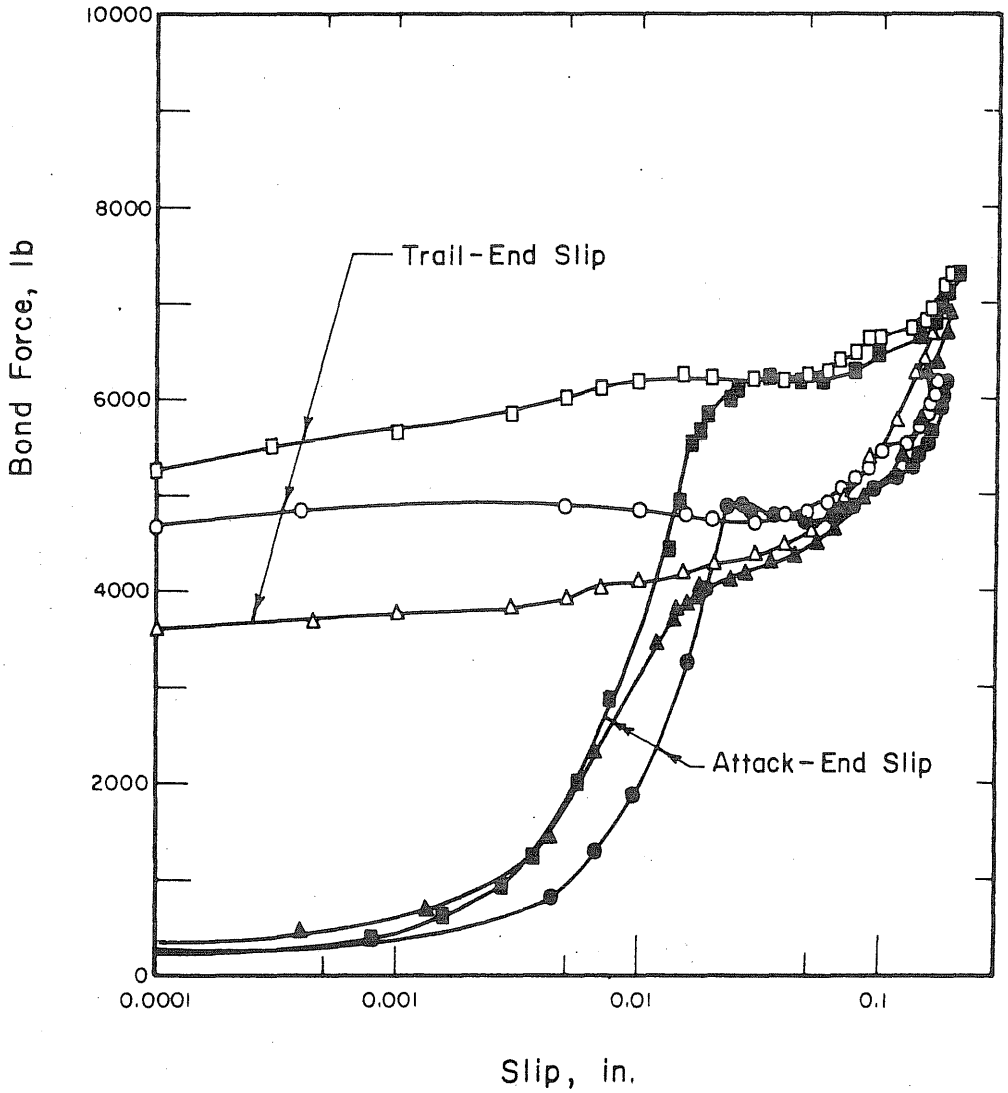

FIG. B.20 BOND FORCE-SLIP RELATIONSHIPS OF 7/16-in. STRAND FOR A BONDED LENGTH OF 8 in., SERIES: SA09-18

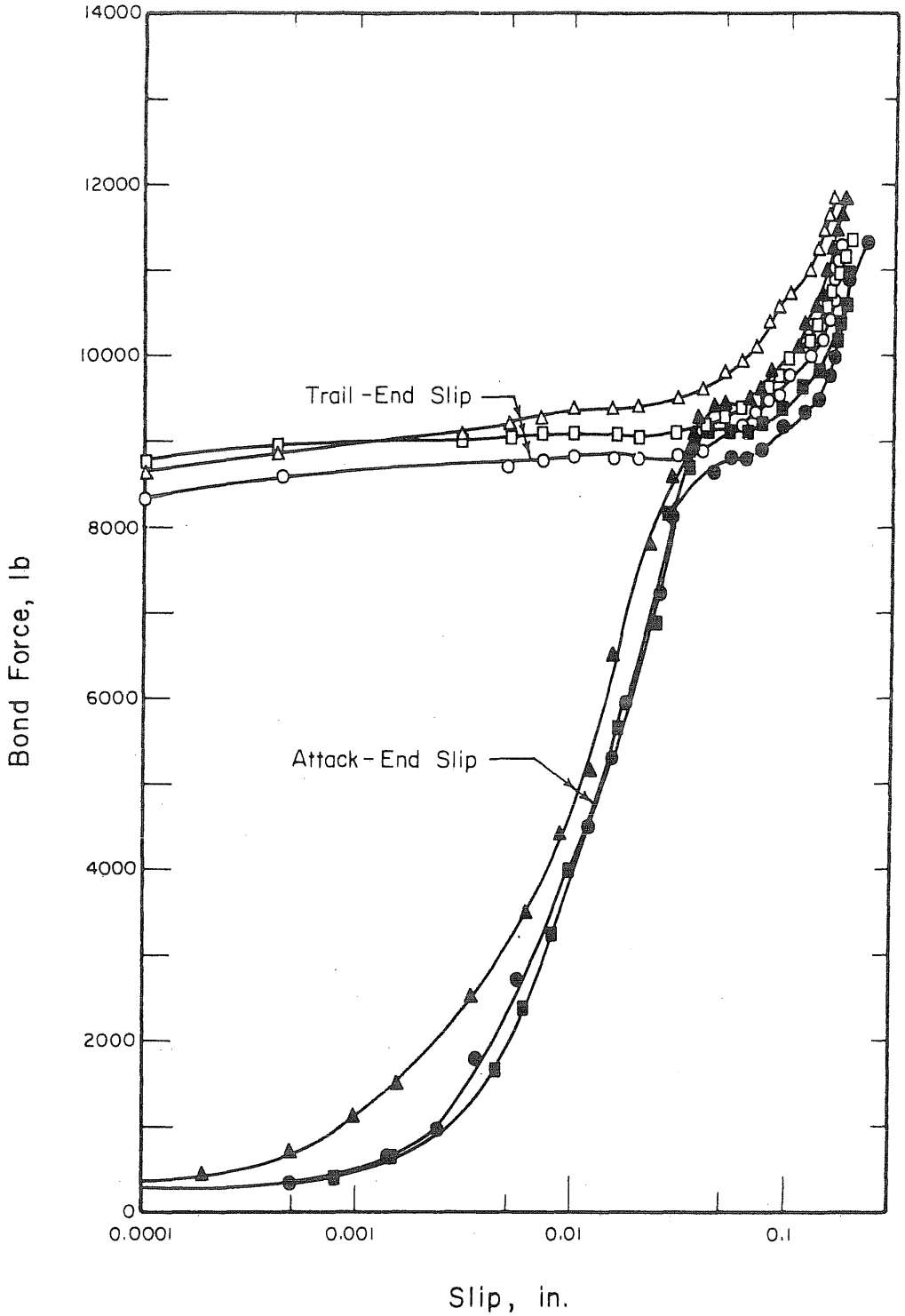

FIG. B.21 BOND FORCE-SLIP RELATIONSHIPS OF 7/16-in. STRAND FOR A BONDED LENGTH OF 15 in., SERIES: SA09-18

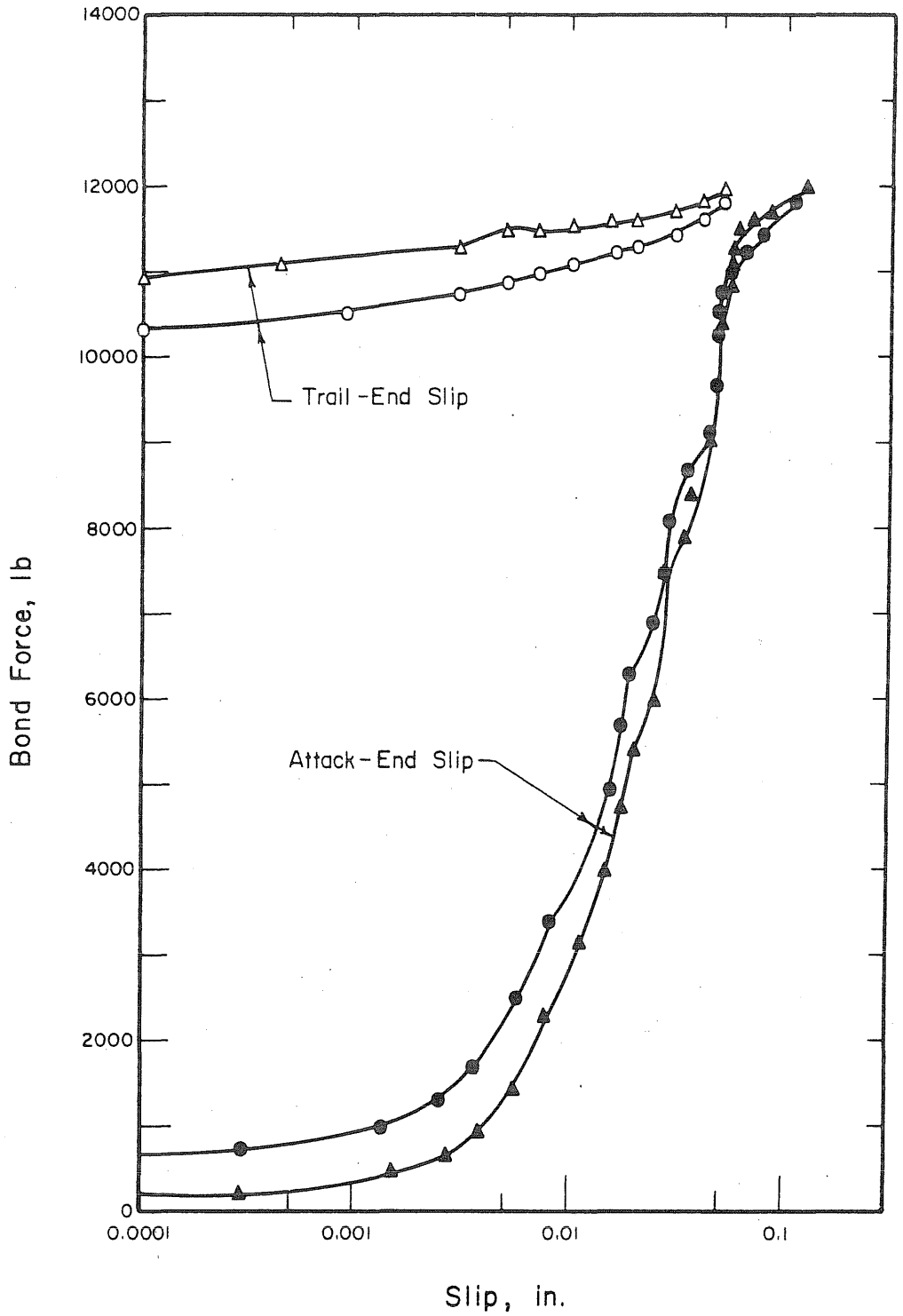

FIG. B.22 BOND FORCE-SLIP RELATIONSHIPS OF 7/16-in. STRAND FOR A BONDED LENGTH OF 20 in., SERIES: SA09-18

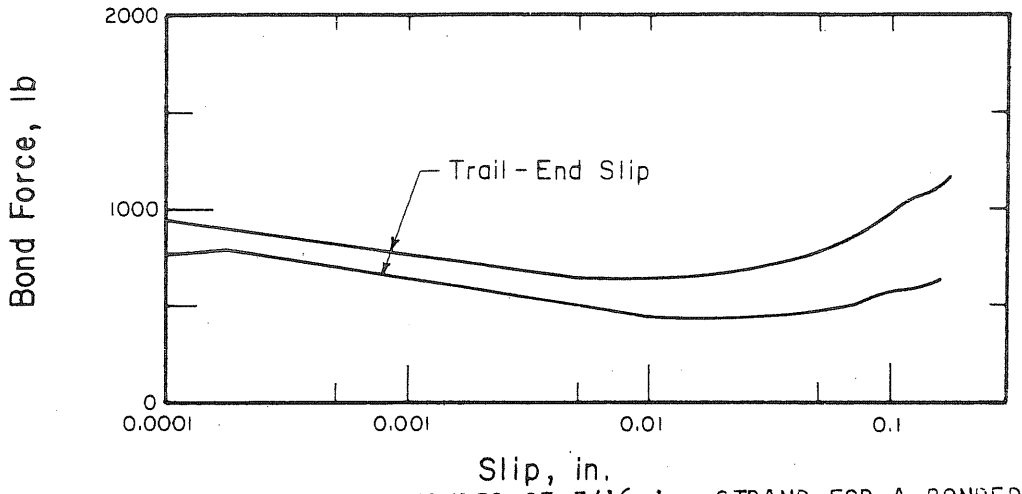

FIG. B.23 BOND FORCE-SLIP RELATIONSHIPS OF 7/16-in. STRAND FOR A BONDED LENGTH OF ONE in., SERIES: SA10-19

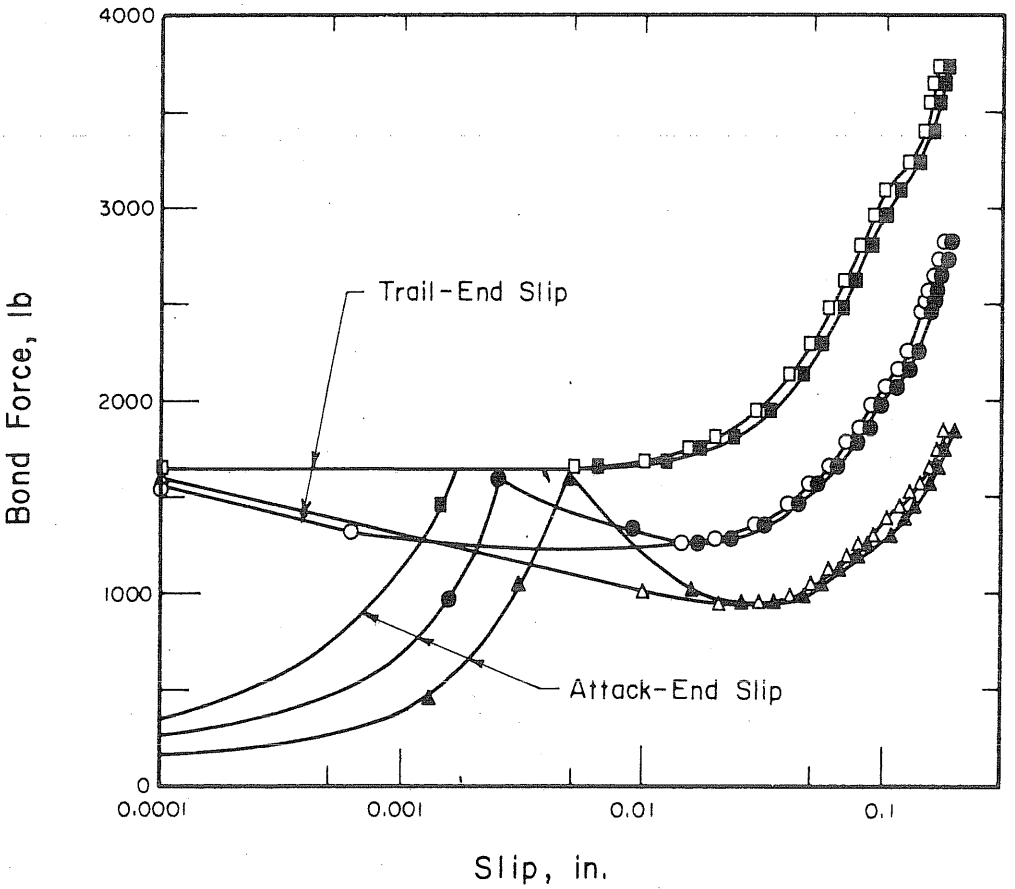

FIG. 24 BOND FORCE-SLIP RELATIONSHIPS OF 7/16-in. STRAND FOR A BONDED LENGTH OF 3 in., SERIES: SA10-19

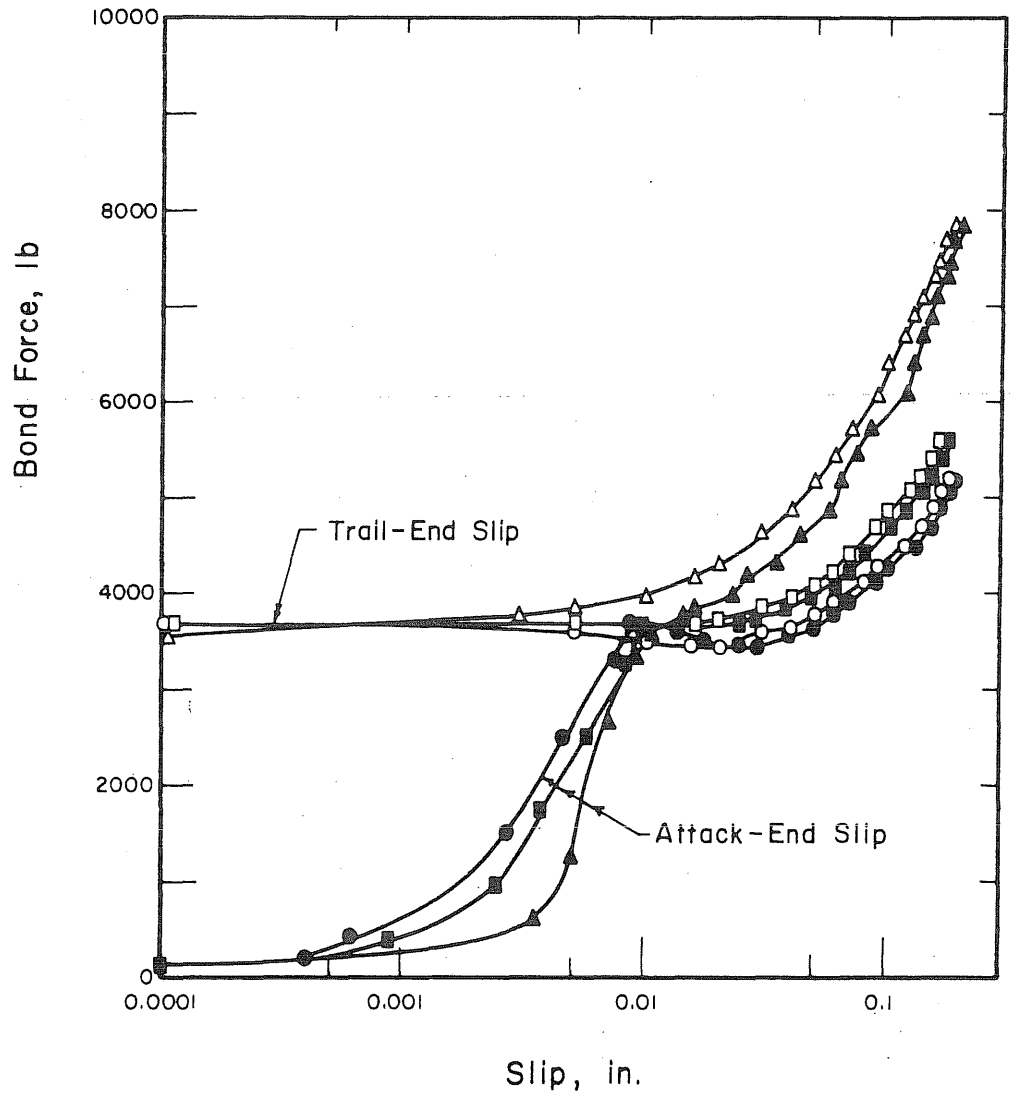

FIG. B.25 BOND FORCE-SLIP RELATIONSHIPS OF 7/16-in. STRAND FOR A BONDED LENGTH OF 8 in., SERIES: SA10-19

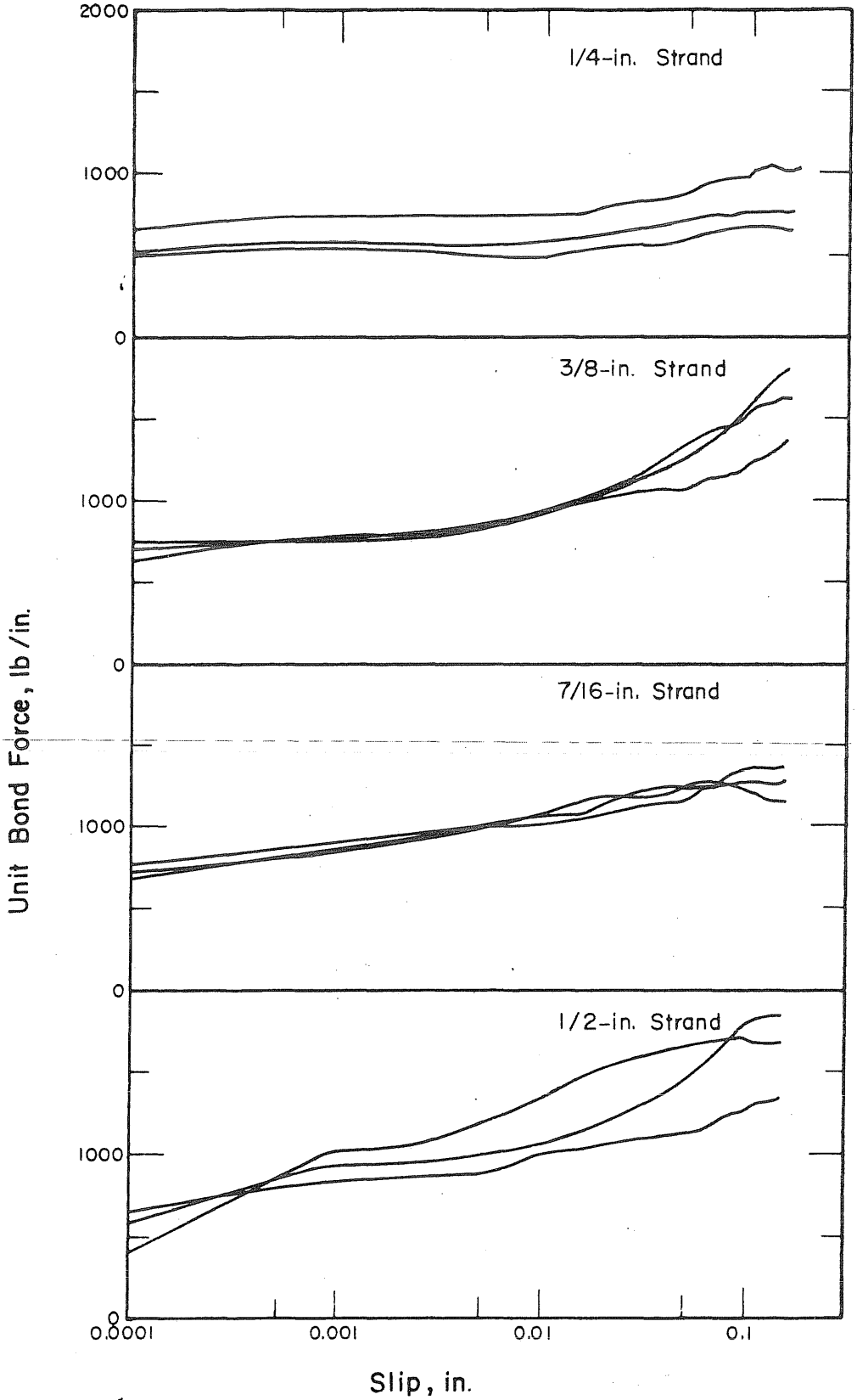

FIG. B.26 UNIT BOND FORCE-SLIP RELATIONSHIPS FOR VARIOUS STRAND SIZES, SERIES: SB09-1

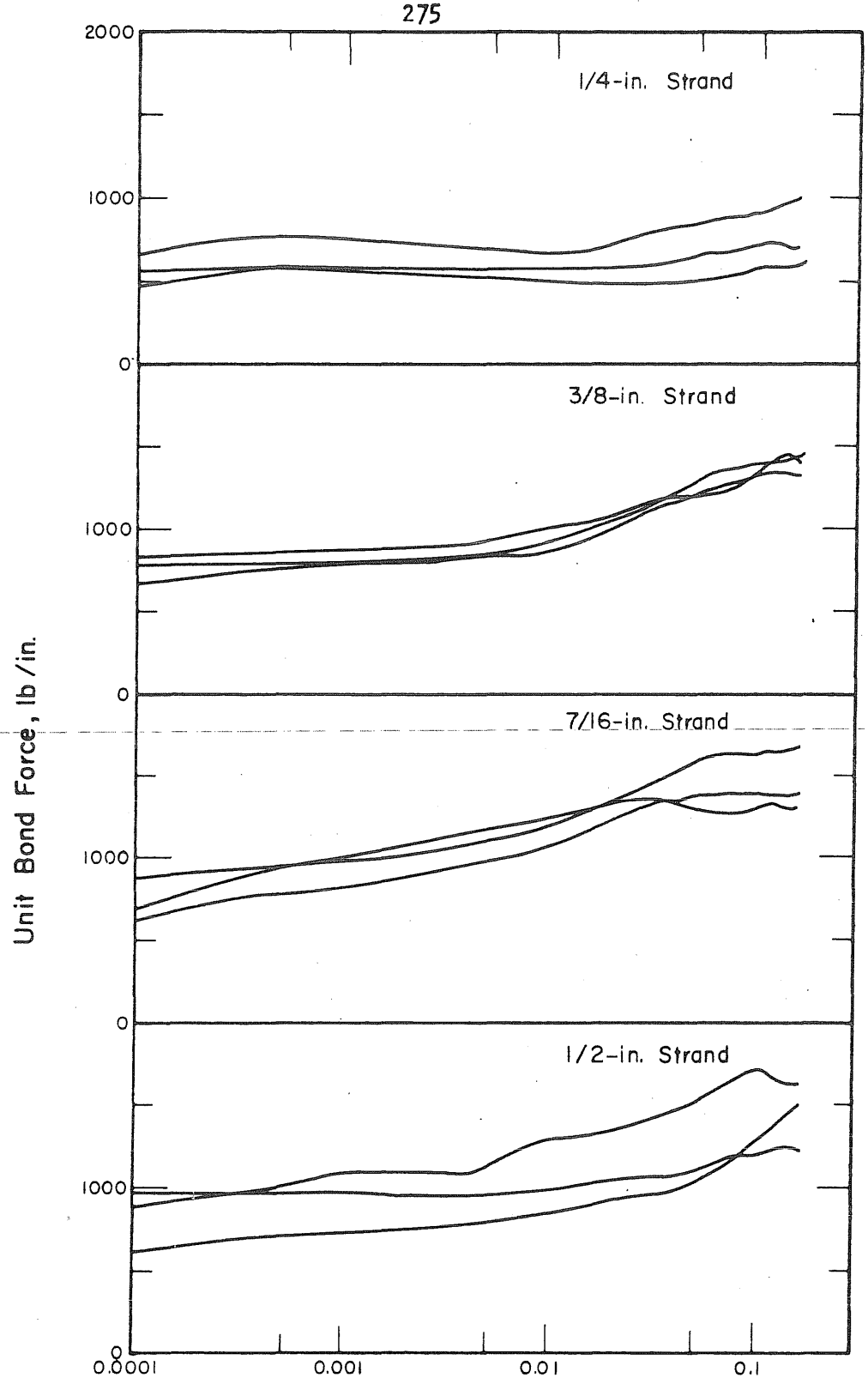

FIG. B.27 UNIT BOND FORCE-SLIP RELATIONSHIPS FOR VARIOUS STRAND SIZES, SERIES: SB09-2

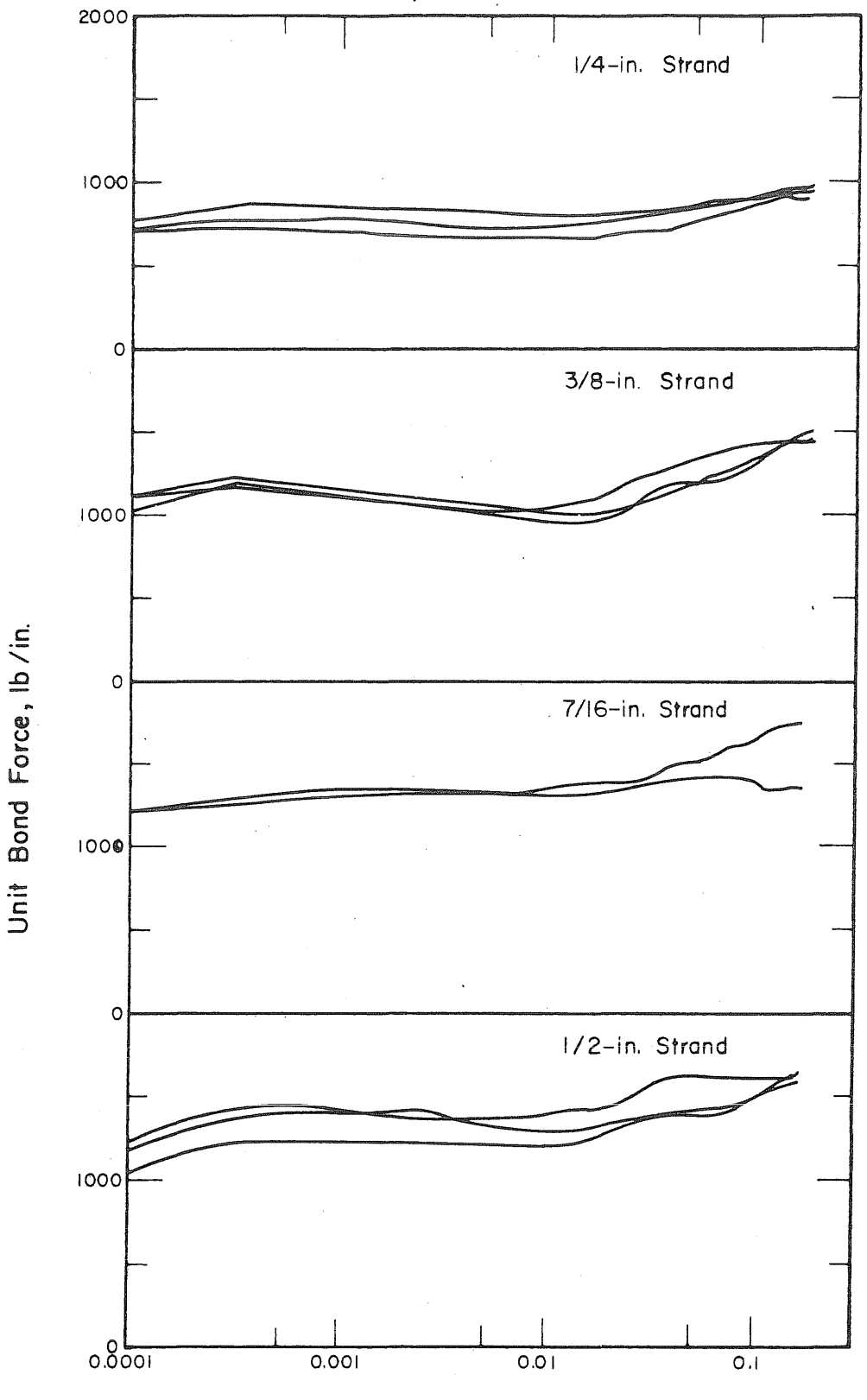

FIG. B.28 UNIT BOND FORCE-SLIP RELATIONSHIPS FOR VARIOUS STRAND SIZES, SERIES: SB08-3

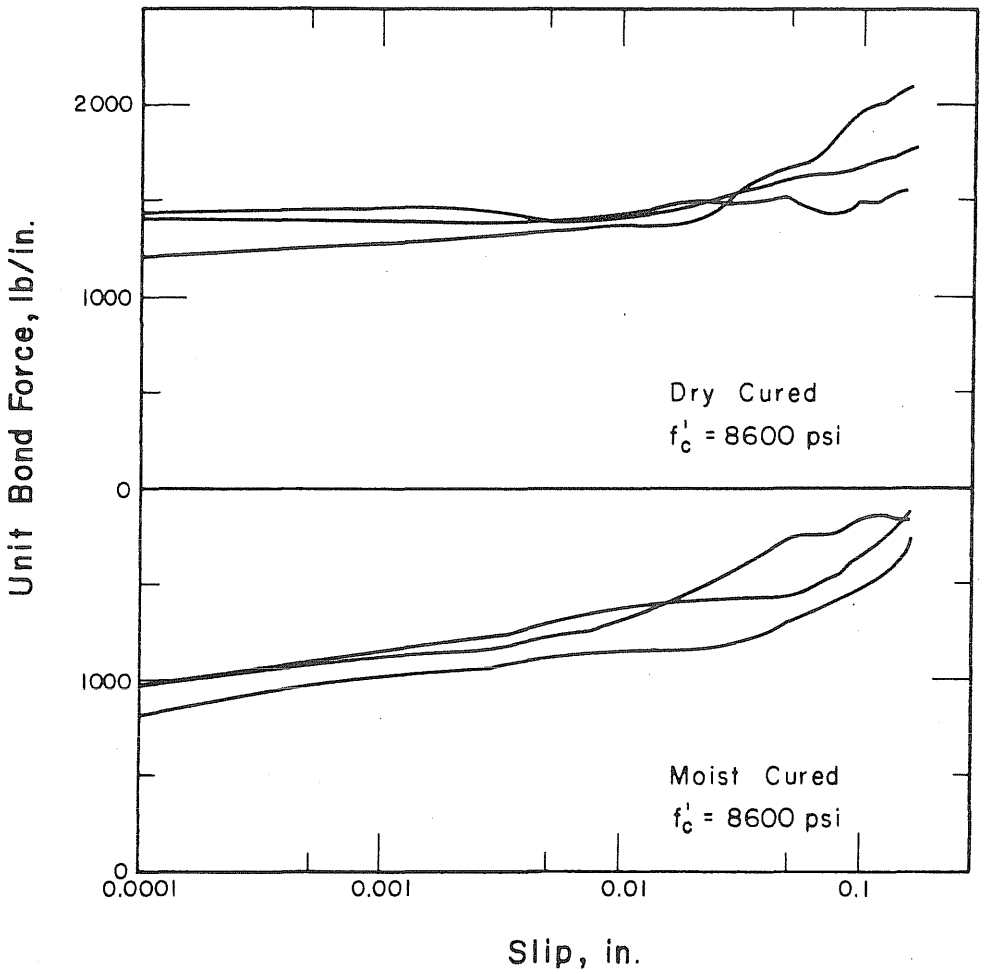

FIG. B.29 UNIT BOND FORCE-SLIP RELATIONSHIPS OF 7/16-in. STRAND FOR DIFFERENT CURING CONDITIONS, SERIES: SB18-4

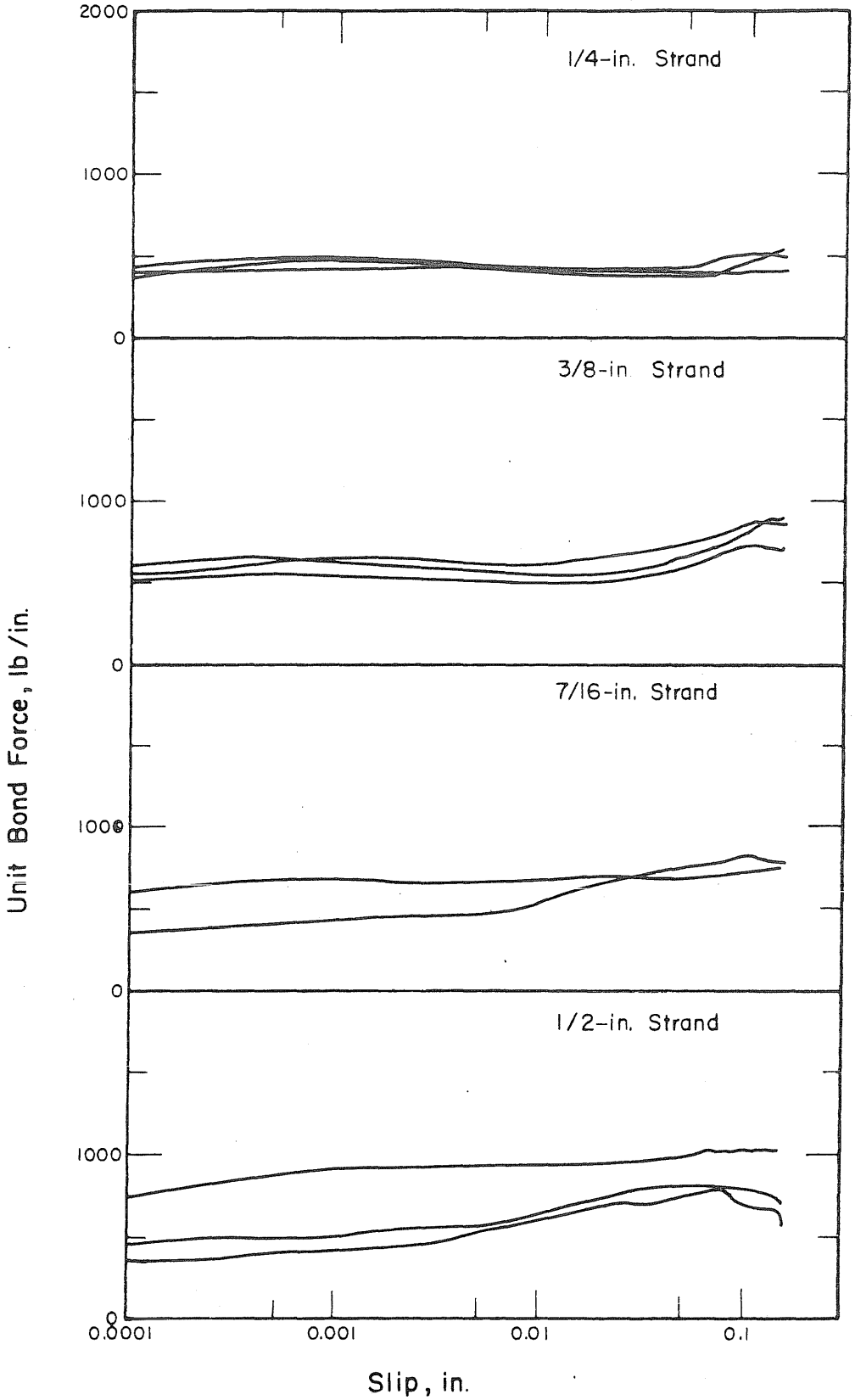

FIG. B.30 UNIT BOND FORCE-SLIP RELATIONSHIPS FOR VARIOUS STRAND SIZES, SERIES: SC09-1

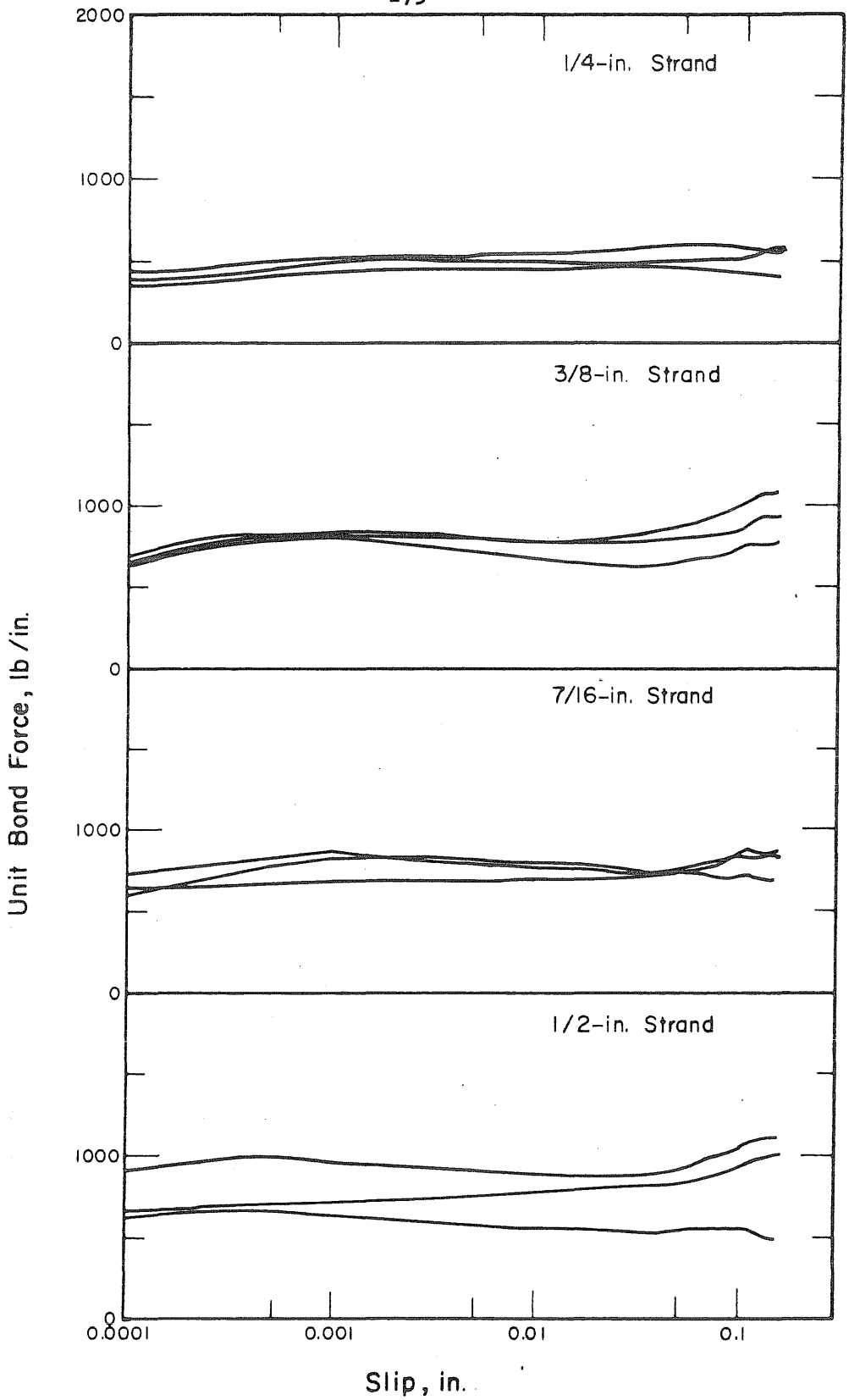

FIG. B.31 UNIT BOND FORCE-SLIP RELATIONSHIPS FOR VARIOUS STRAND SIZES, SERIES: SC09-2

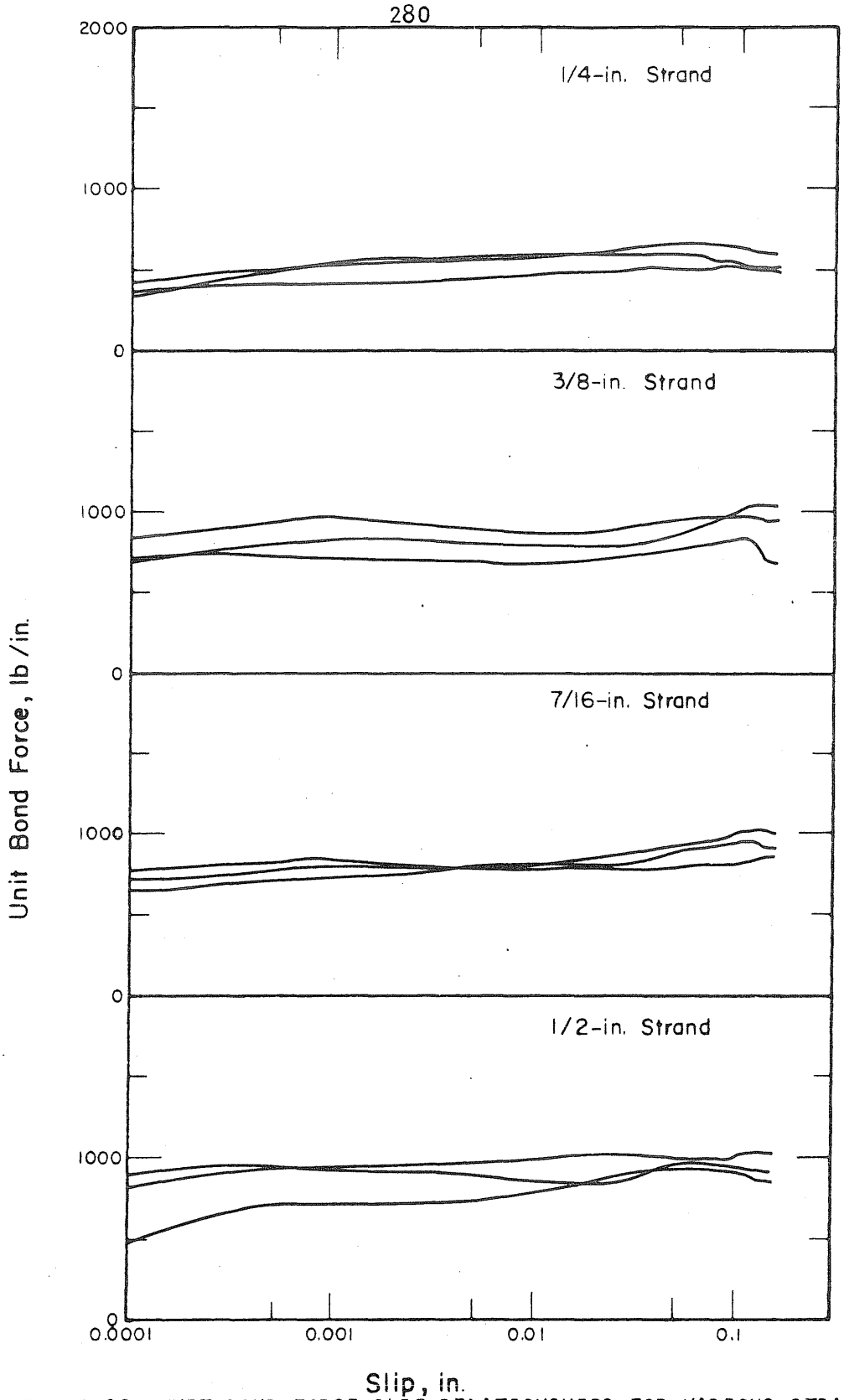

FIG. B.32 UNIT BOND FORCE-SLIP RELATIONSHIPS FOR VARIOUS STRAND SIZES, SERIES: SC08-3

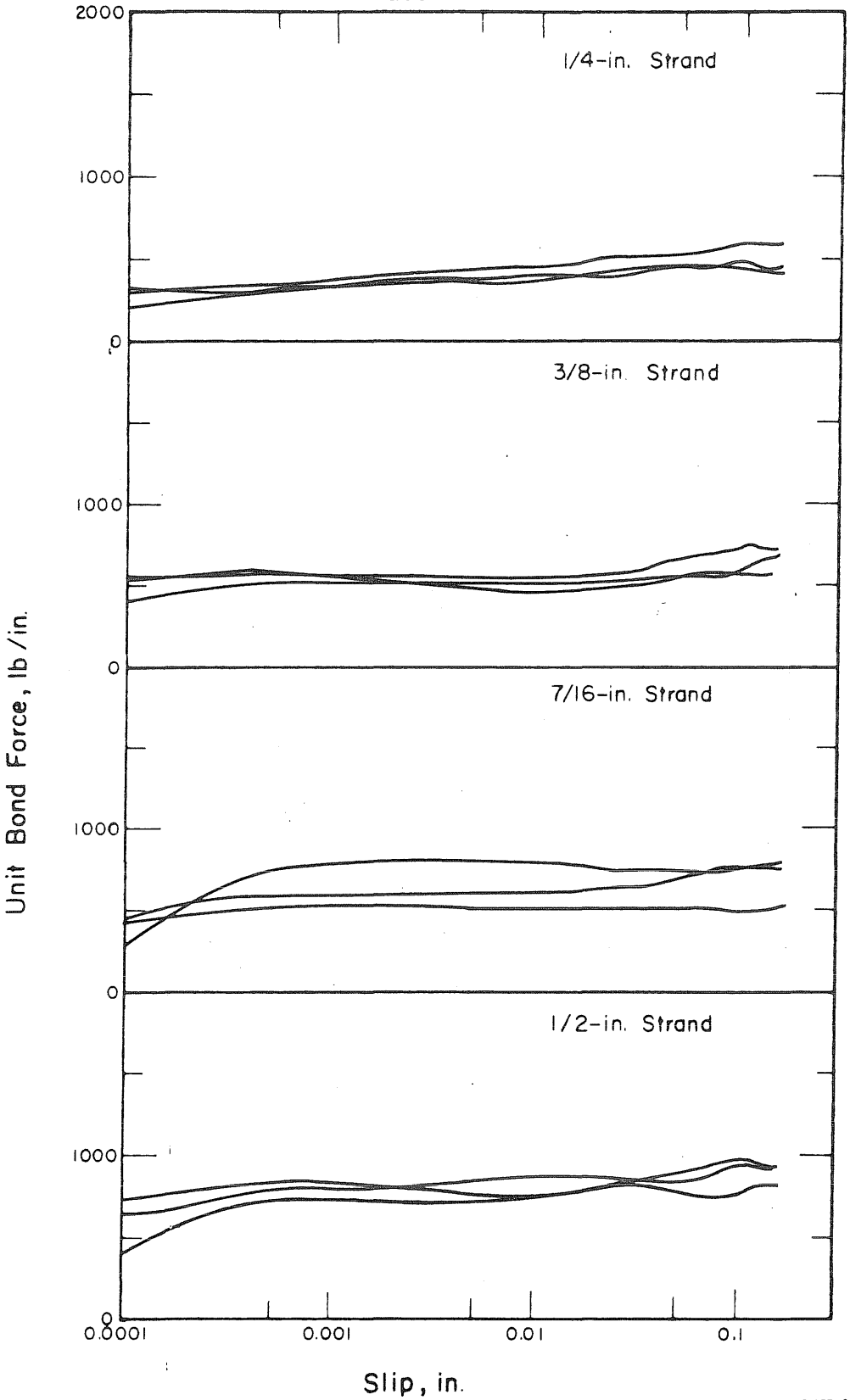

FIG. B.33 UNIT BOND FORCE-SLIP RELATIONSHIPS FOR VARIOUS STRAND SIZES, SERIES: SC08-4

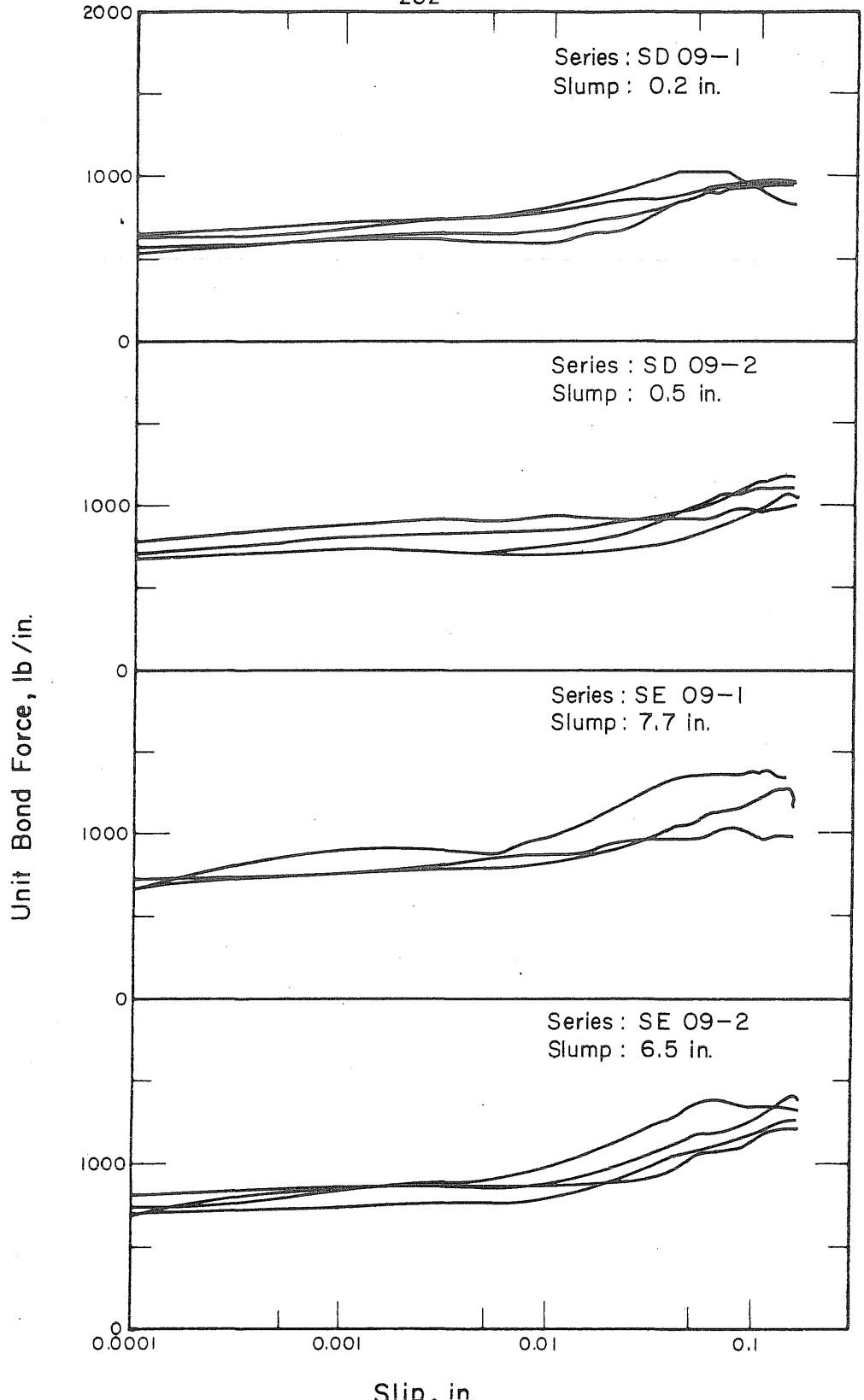

FIG. B.34 UNIT BOND FORCE-SLIP RELATIONSHIPS OF 7/16-in. STRAND FOR VARIOUS CONCRETE CONSISTENCIES, SERIES: SD09-1, SD09-2, SE09-1, SE09-2

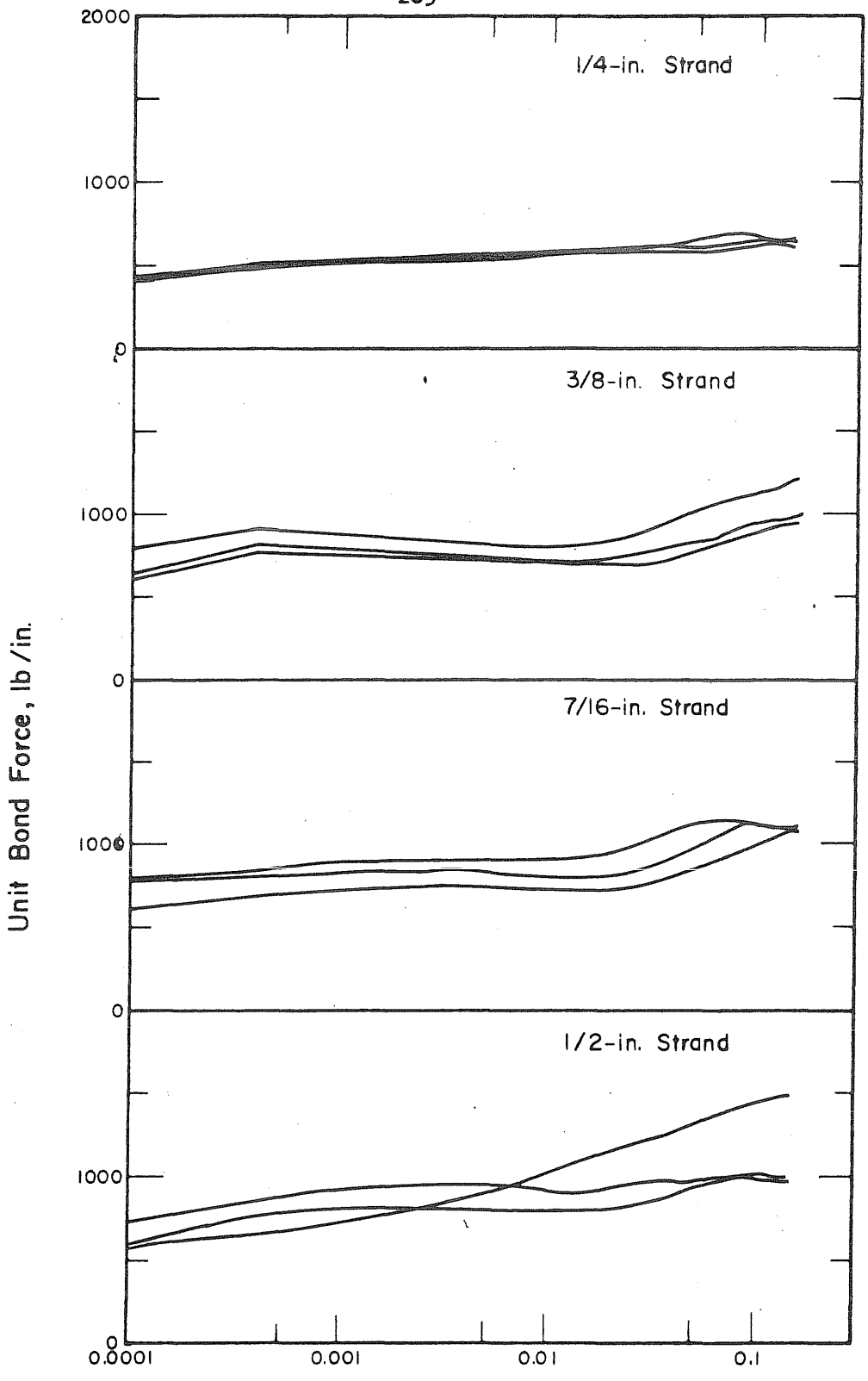

FIG. B.35 UNIT BOND FORCE-SLIP RELATIONSHIPS FOR VARIOUS STRAND SIZES, SERIES: SF09-1

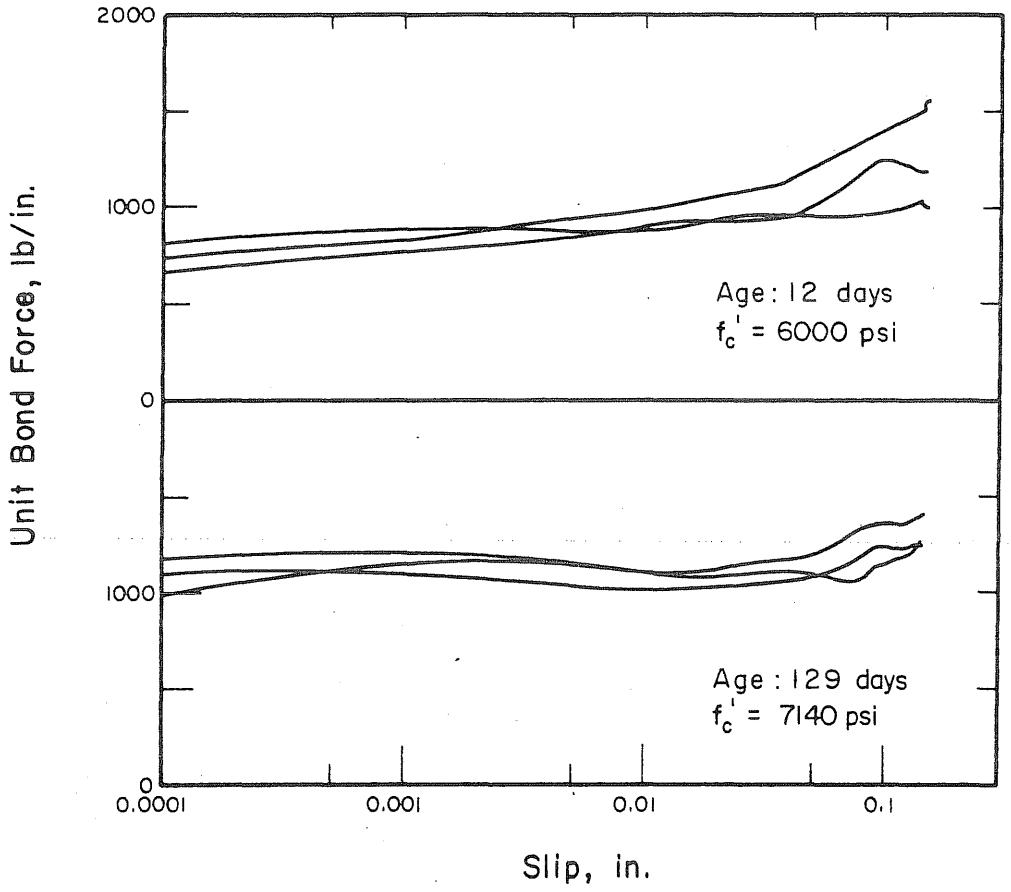

FIG. B.36 UNIT BOND FORCE-SLIP RELATIONSHIPS OF 7/16-in. STRAND AT DIFFERENT AGES, SERIES: SAL12-1

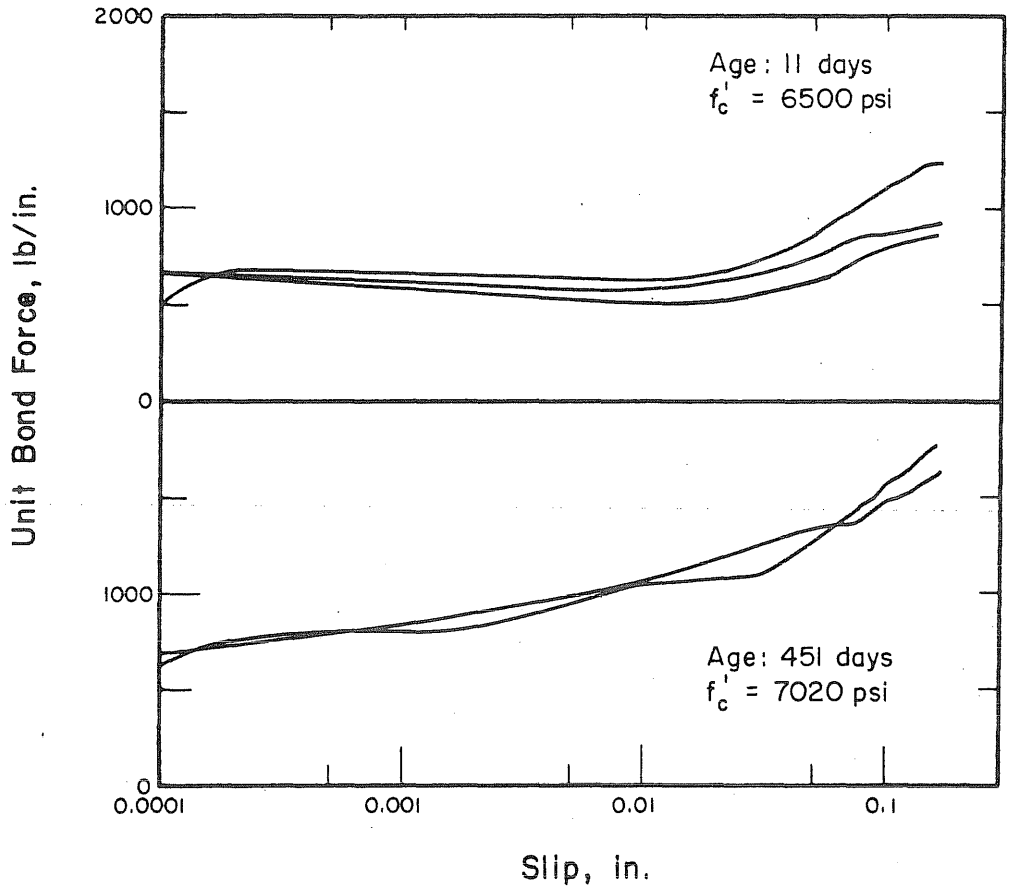

FIG. B.37 UNIT BOND FORCE-SLIP RELATIONSHIPS OF 7/16-in. STRAND AT DIFFERENT AGES, SERIES: SAL11-2

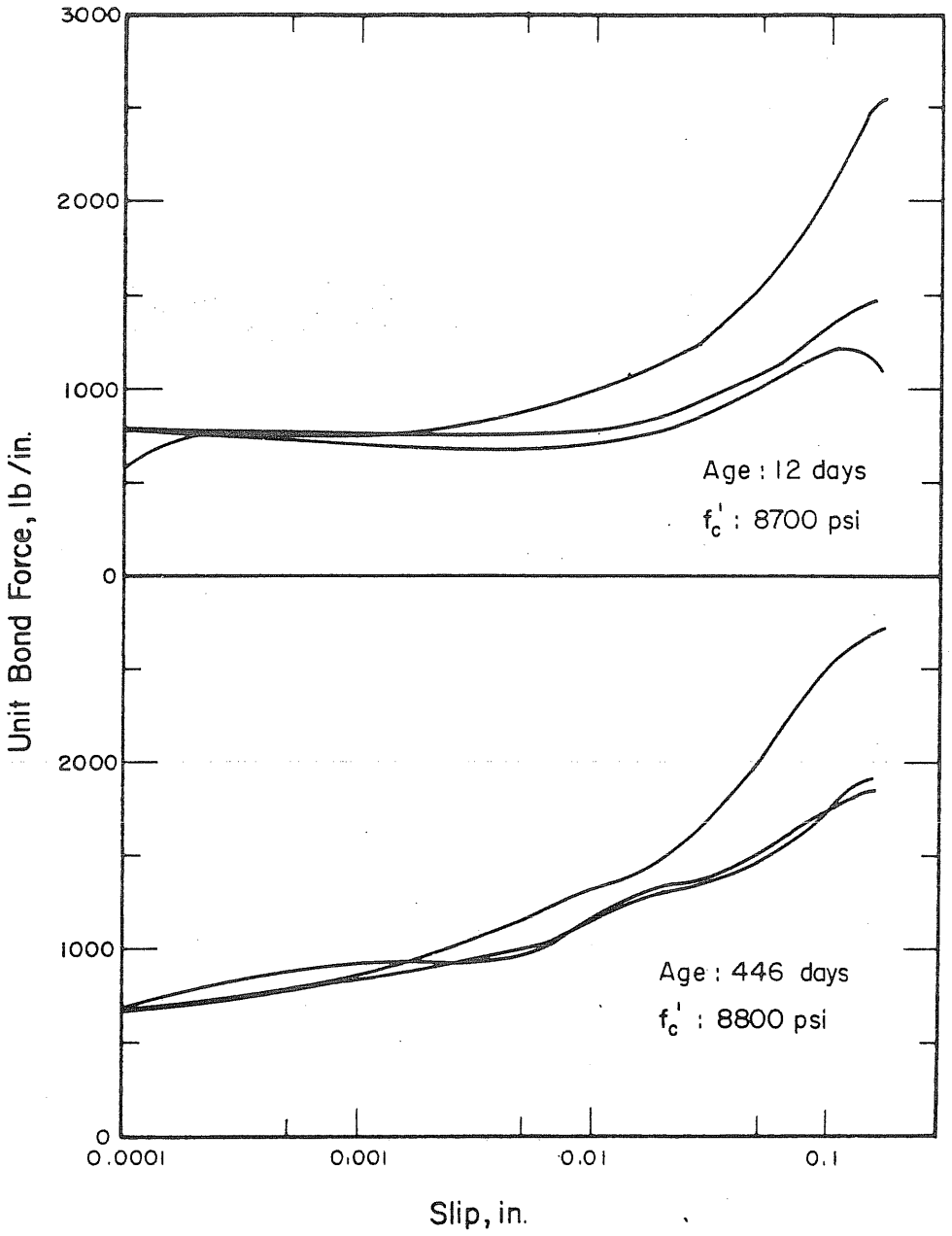

FIG. B.38 UNIT BOND FORCE-SLIP RELATIONSHIPS OF 7/16-in. STRAND AT DIFFERENT AGES, SERIES: SBL12-1

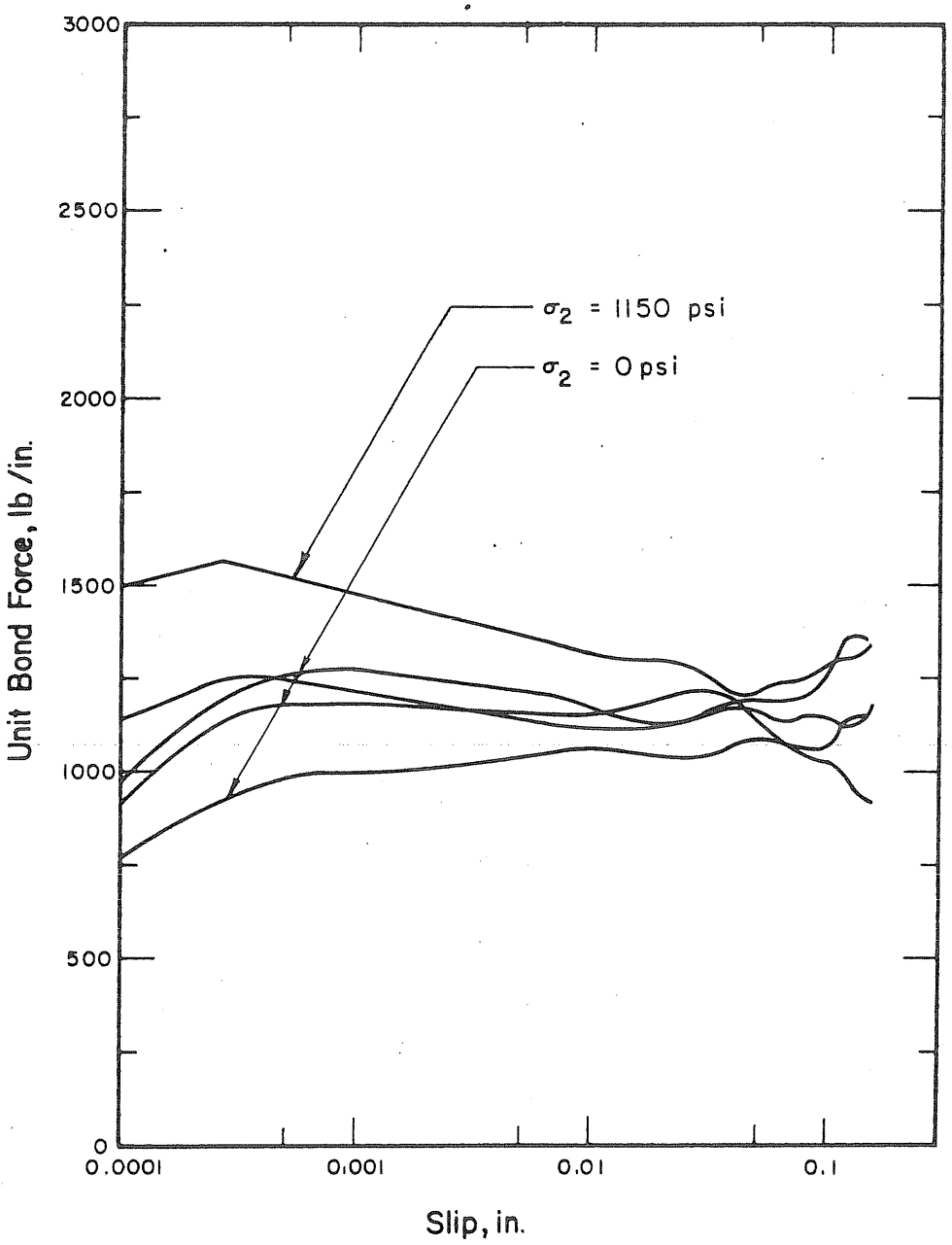

FIG. B.39 UNIT BOND FORCE-SLIP RELATIONSHIPS OF 7/16-in. STRAND FOR DIFFERENT LATERAL PRESSURES, SERIES:SAP15-1

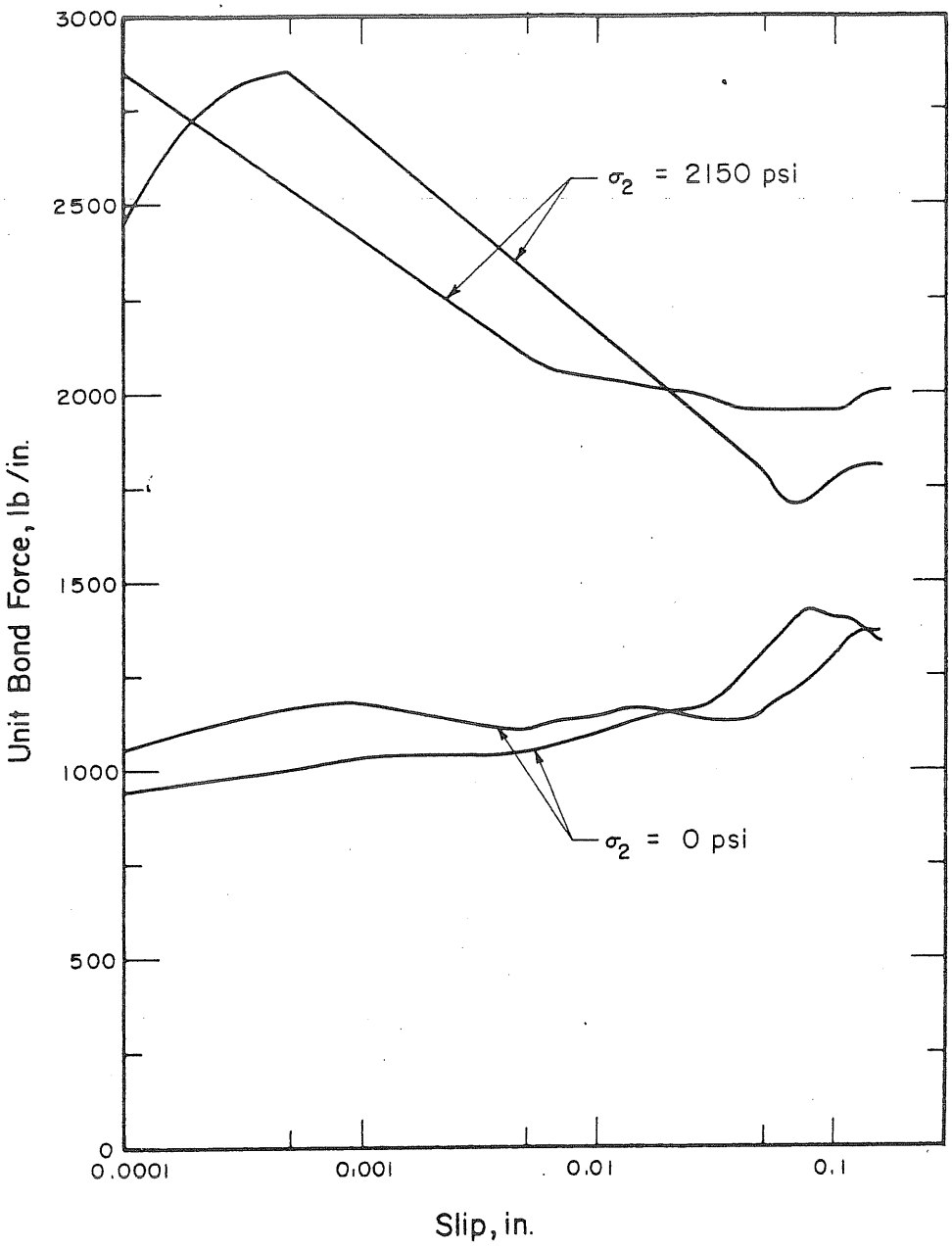

FIG. B.40 UNIT BOND FORCE-SLIP RELATIONSHIPS OF 7/16-in. STRAND FOR DIFFERENT LATERAL PRESSURES, SERIES: SAP22-2

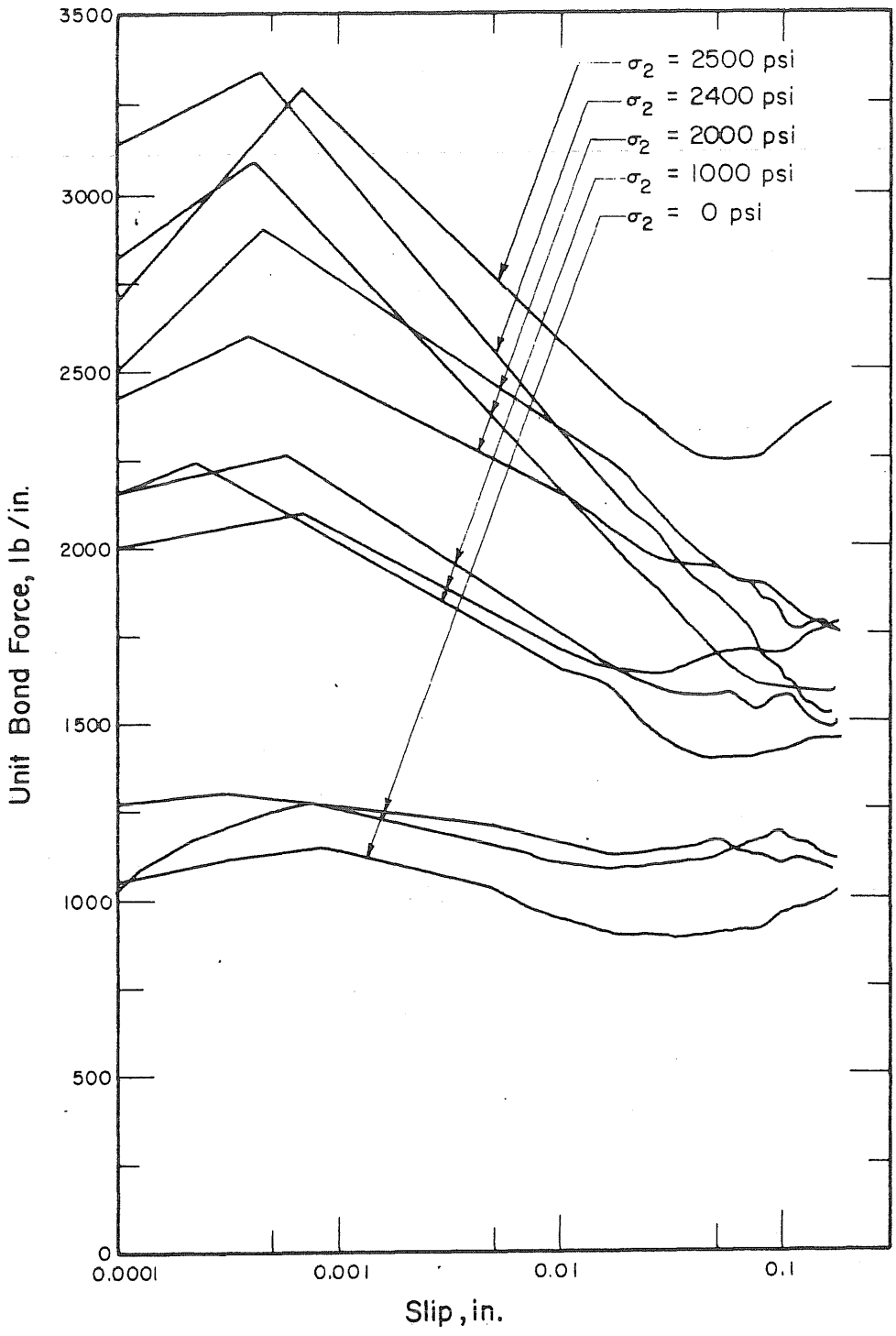

FIG. B.41 UNIT BOND FORCE - SLIP RELATIONSHIPS OF 7/16-in. STRAND FOR DIFFERENT LATERAL PRESSURES, SERIES: SAP23-3

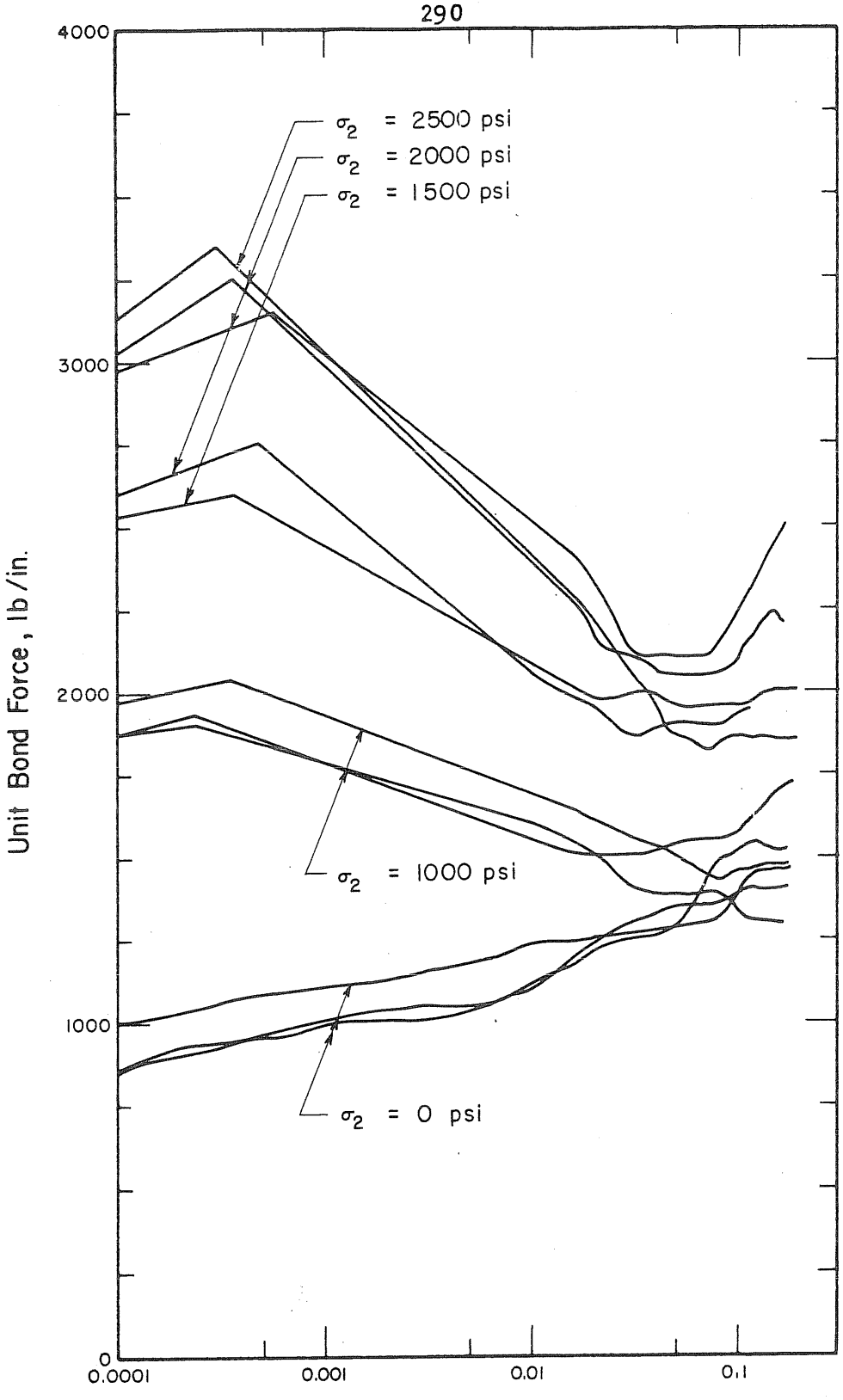

FIG. B.42 UNIT BOND FORCE-SLIP RELATIONSHIPS OF 7/16-in. STRAND FOR DIFFERENT LATERAL PRESSURES, SERIES: SBP24-1

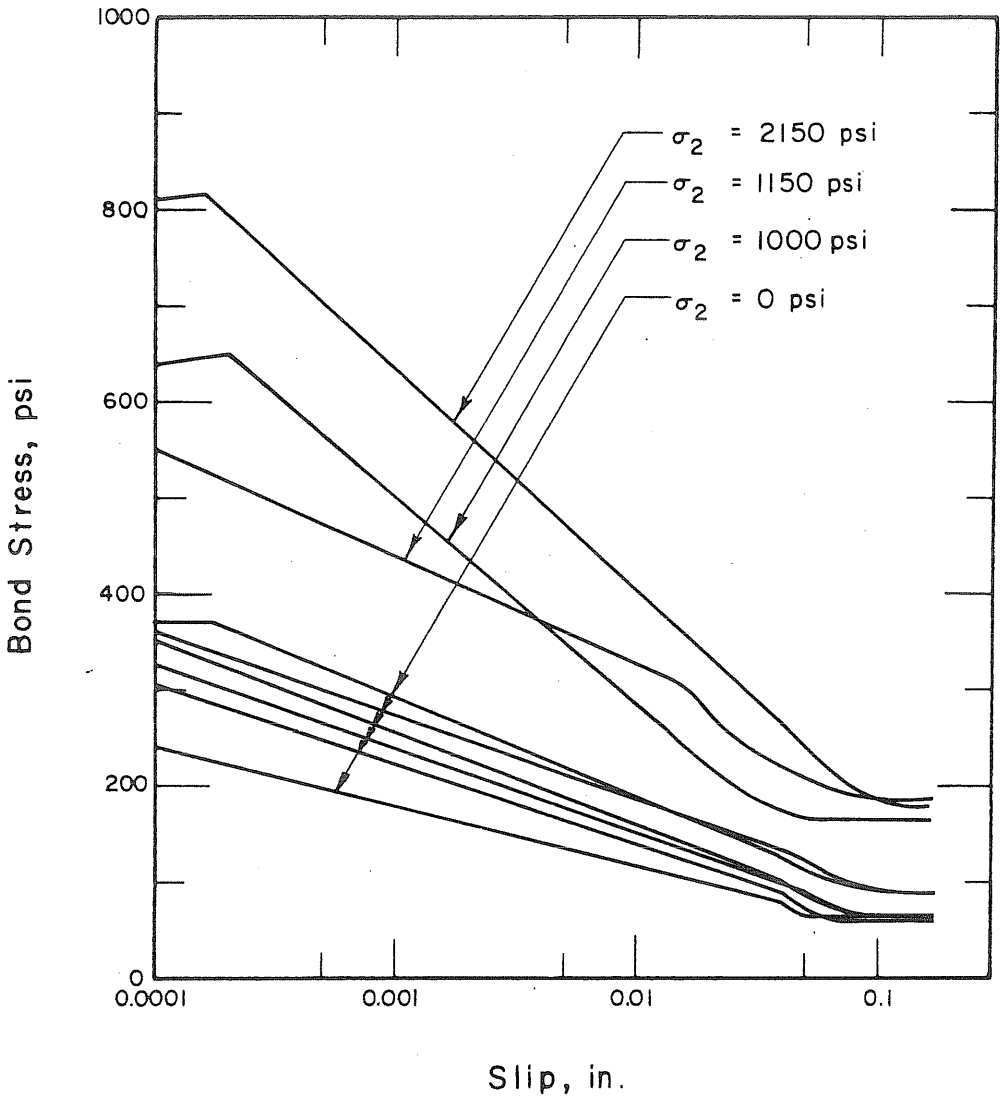

FIG. B.43 BOND STRESS - SLIP RELATIONSHIPS OF CENTER WIRE FROM 7/16-in. STRAND FOR VARIOUS LATERAL PRESSURES, SERIES: WAP15-1

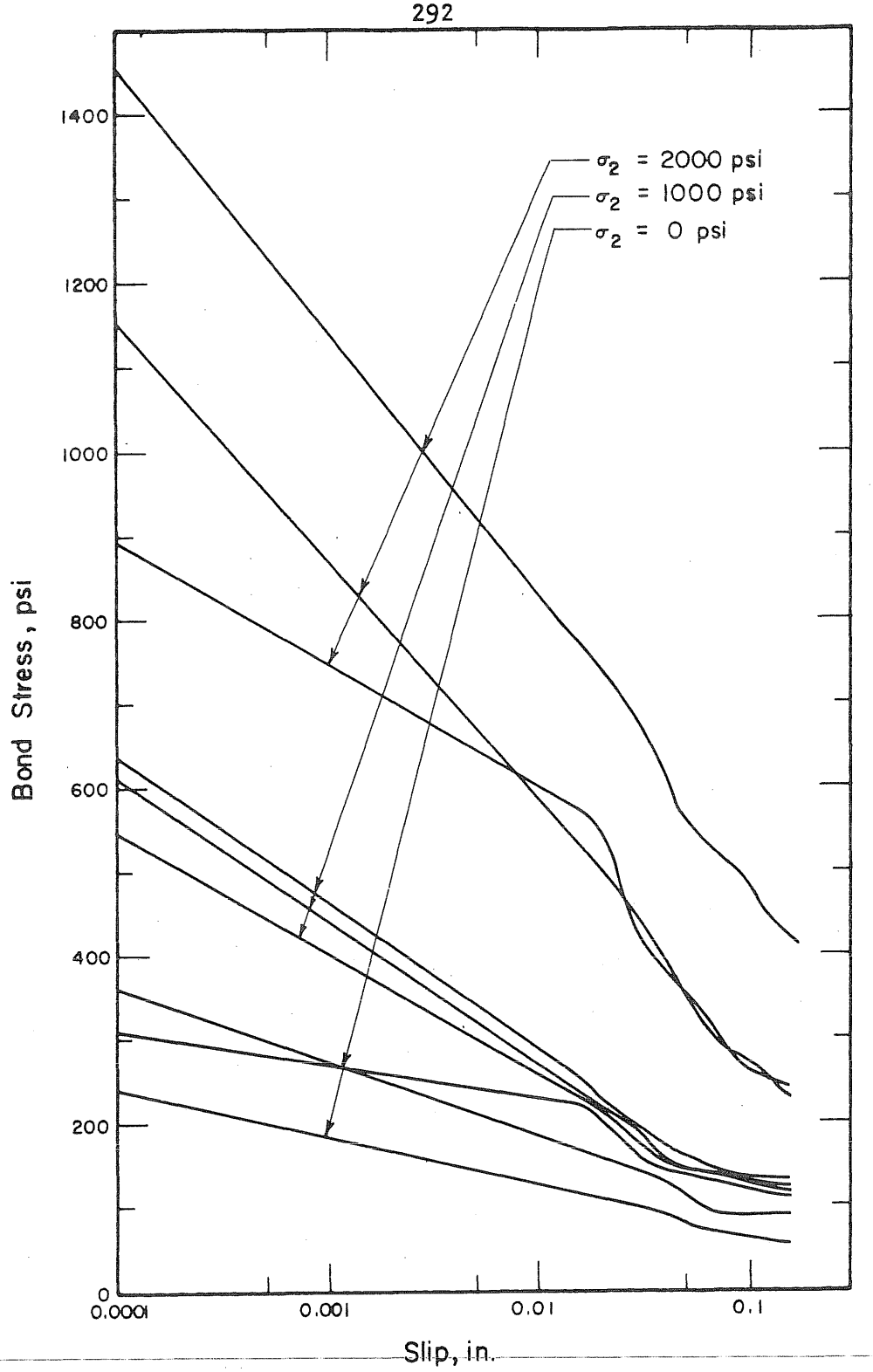

FIG. B.44 BOND STRESS - SLIP RELATIONSHIPS OF CENTER WIRE FROM 7/16-in. STRAND FOR VARIOUS LATERAL PRESSURES, SERIES:WAP17-2

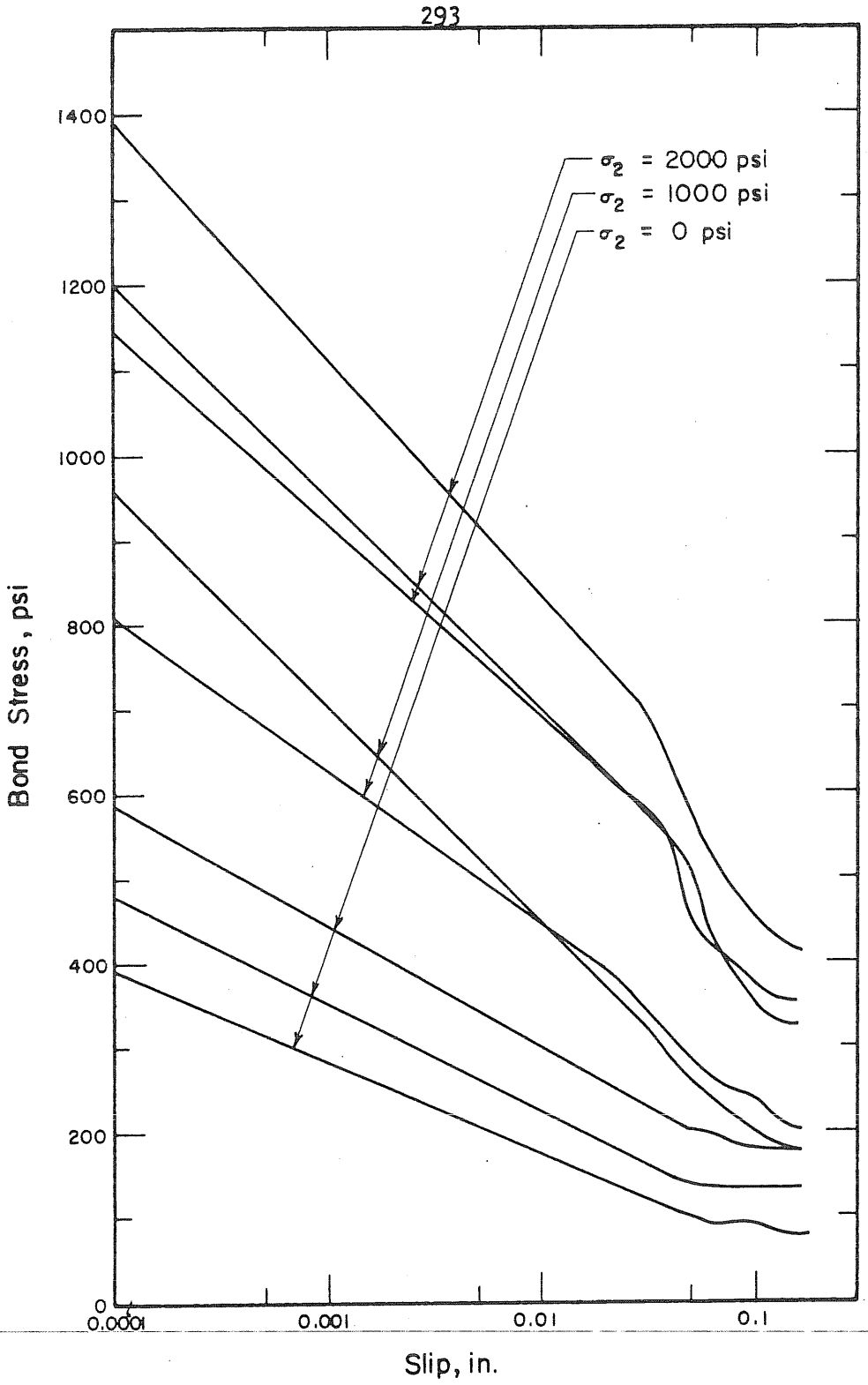

FIG. B.45 BOND STRESS - SLIP RELATIONSHIPS OF CENTER WIRE FROM 7/16-in. STRAND FOR VARIOUS LATERAL PRESSURES, SERIES: WBP66-1

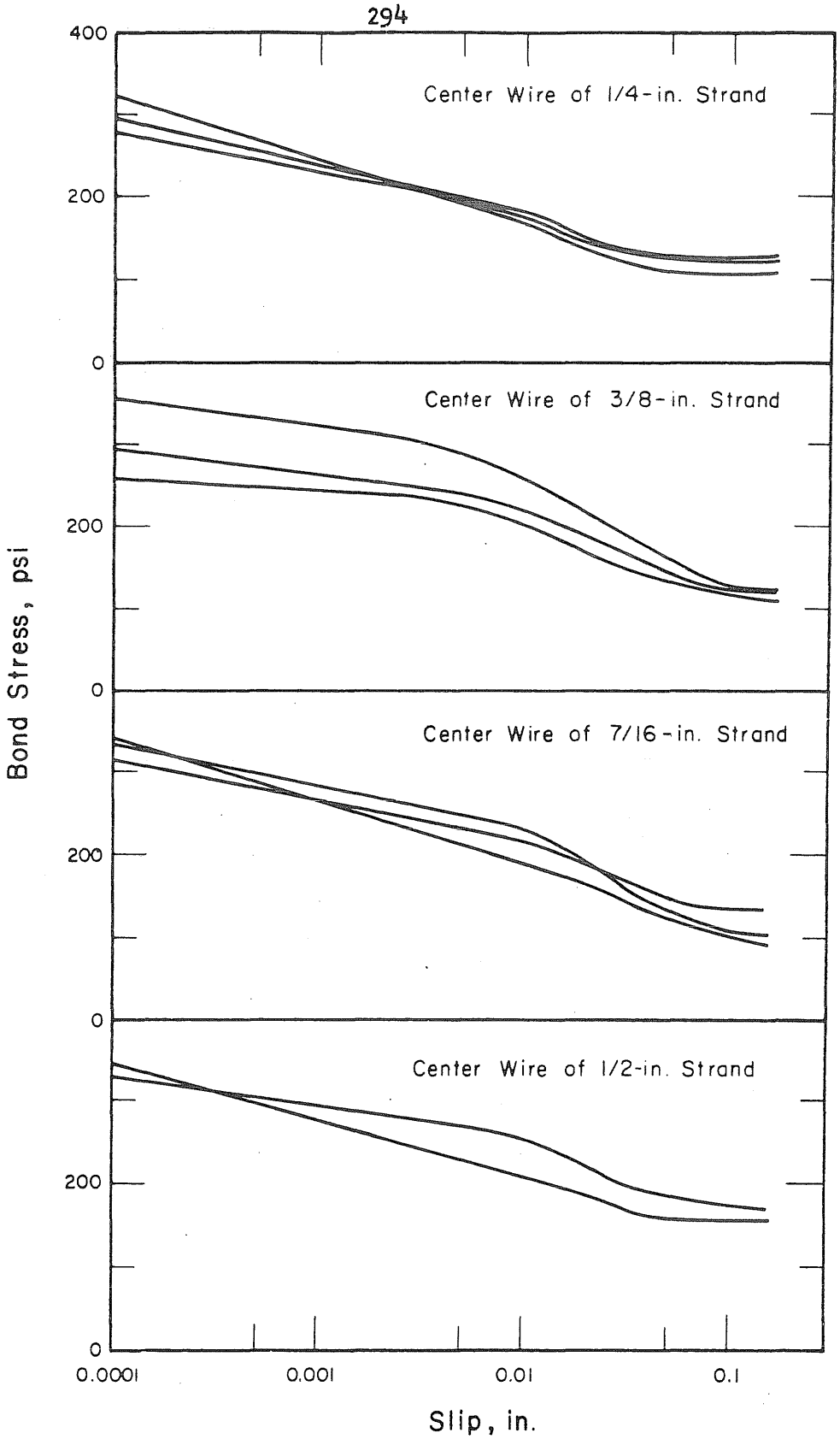

FIG. B.46 BOND STRESS - SLIP RELATIONSHIPS OF CENTER WIRE FROM DIFFERENT STRAND SIZES, SERIES: WA08-1

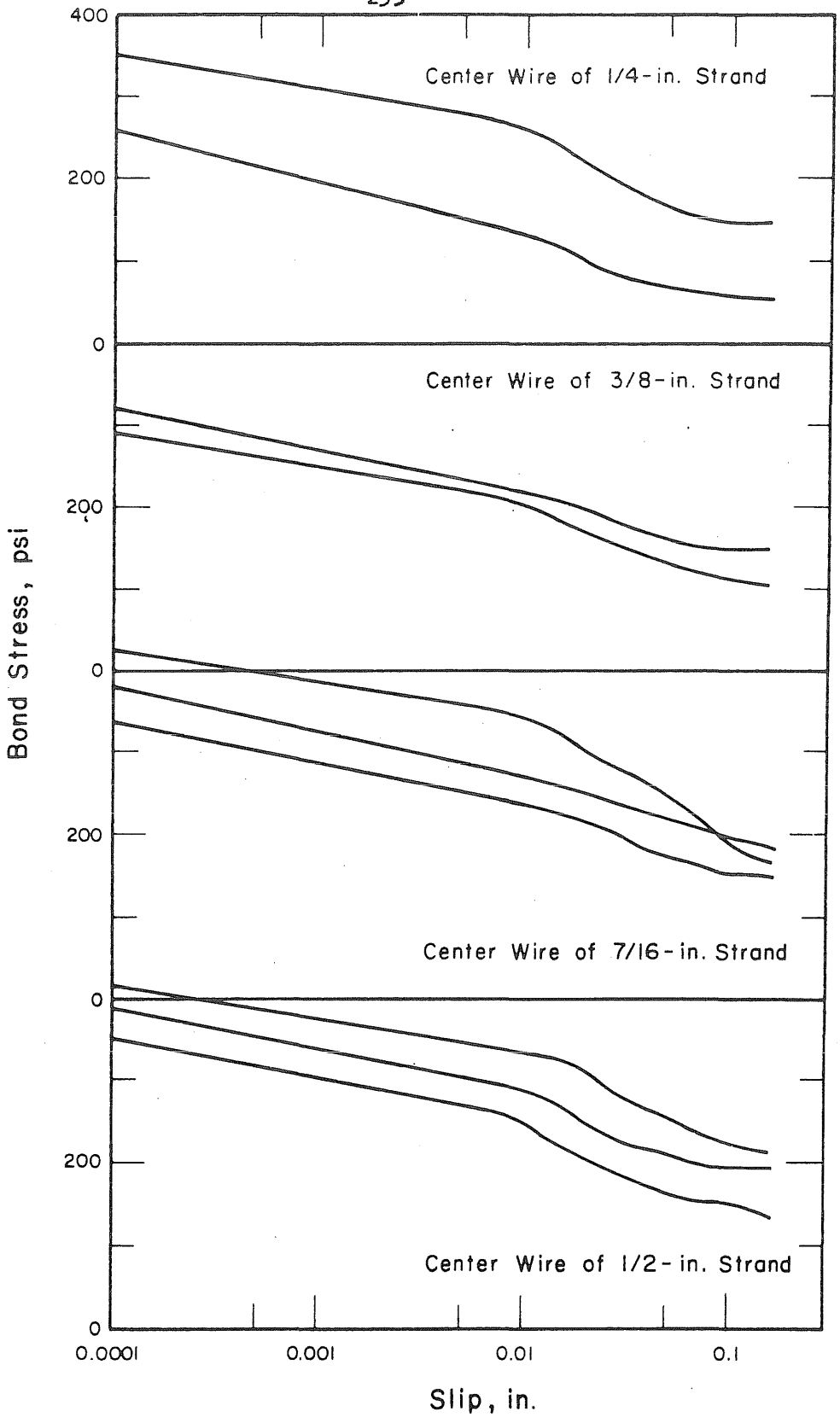

FIG. B.47 BOND STRESS - SLIP RELATIONSHIPS OF CENTER WIRE FROM DIFFERENT STRAND SIZES, SERIES: WB08-1

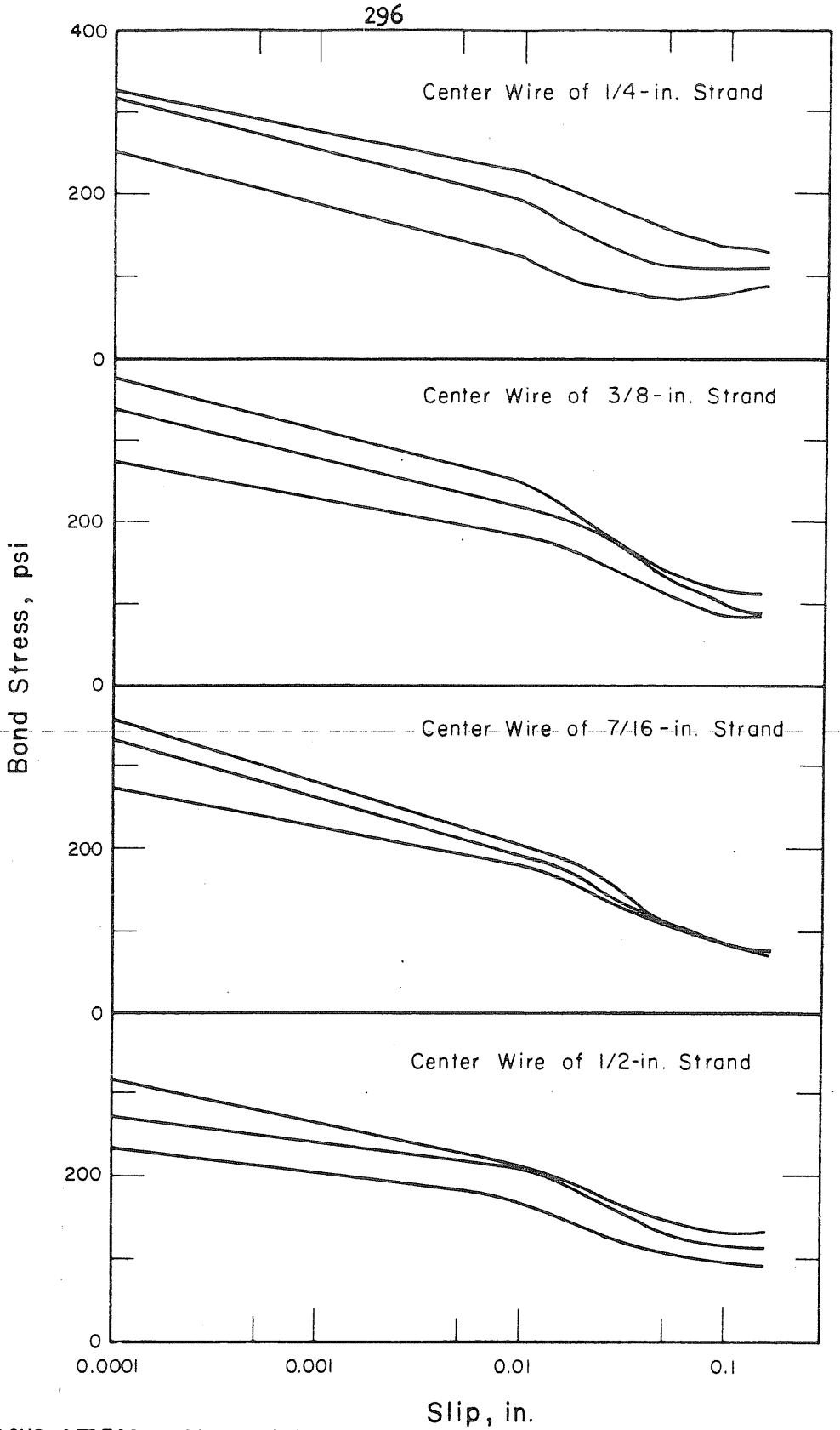

FIG. B.48 BOND STRESS - SLIP RELATIONSHIPS OF CENTER WIRE FROM DIFFERENT STRAND SIZES, SERIES: WC08-1

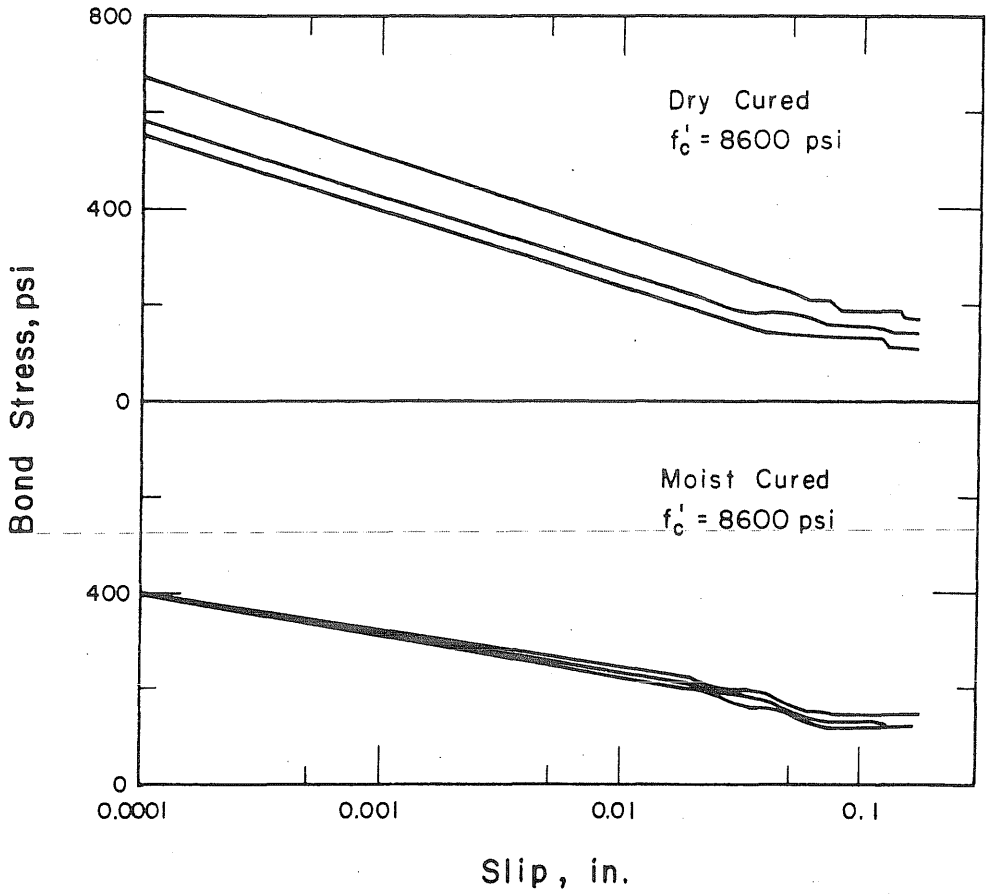

FIG. B.49 BOND STRESS-SLIP RELATIONSHIPS OF PLAIN CENTER WIRE FROM 7/16-in. STRAND FOR DIFFERENT CURING CONDITIONS, SERIES: WB18-2

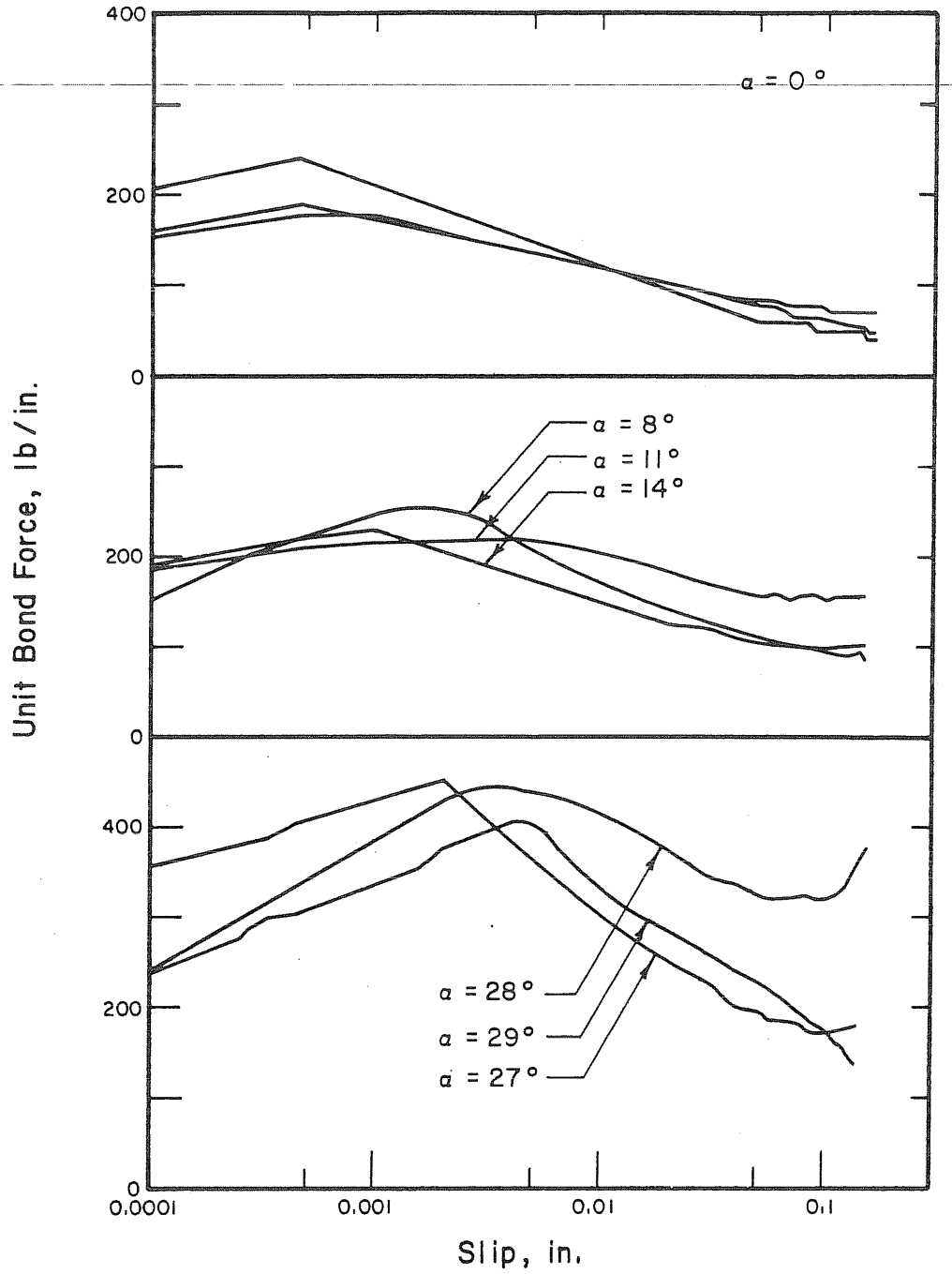

FIG. B.50 UNIT BOND FORCE-SLIP RELATIONSHIPS OF 5/16-in. SQUARE BARS, CONCRETE SPECIMENS FREE TO ROTATE, SERIES: QB09-1

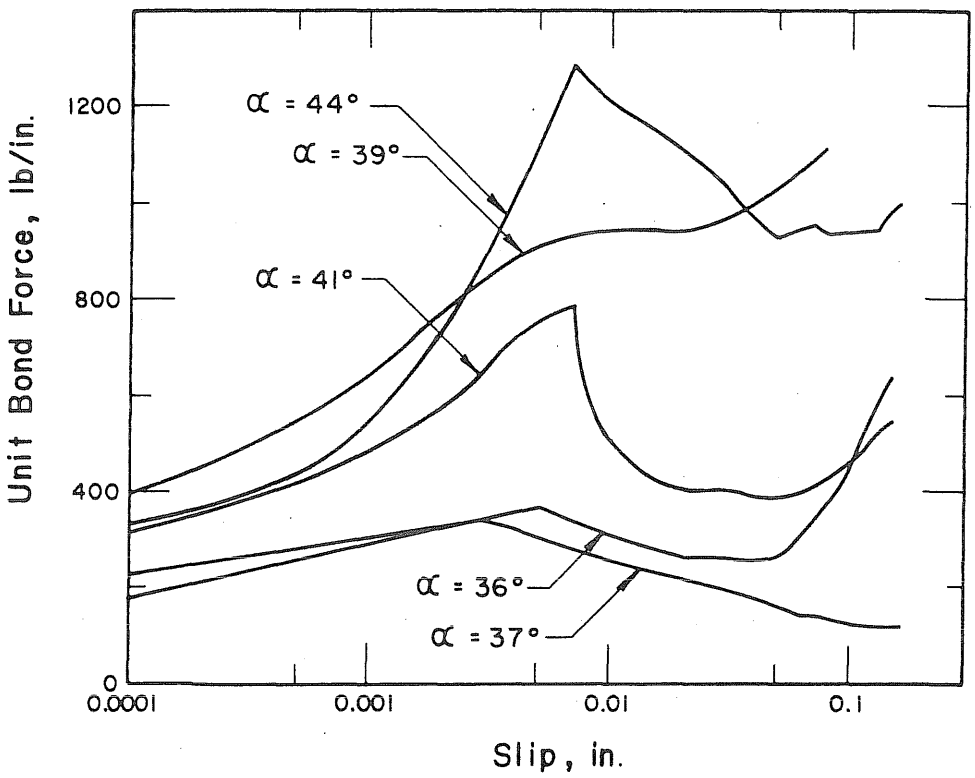

FIG. B.51 UNIT BOND FORCE-SLIP RELATIONSHIPS OF 5/16-in. SQUARE BARS, CONCRETE SPECIMENS FREE TO ROTATE, SERIES: QB09-1

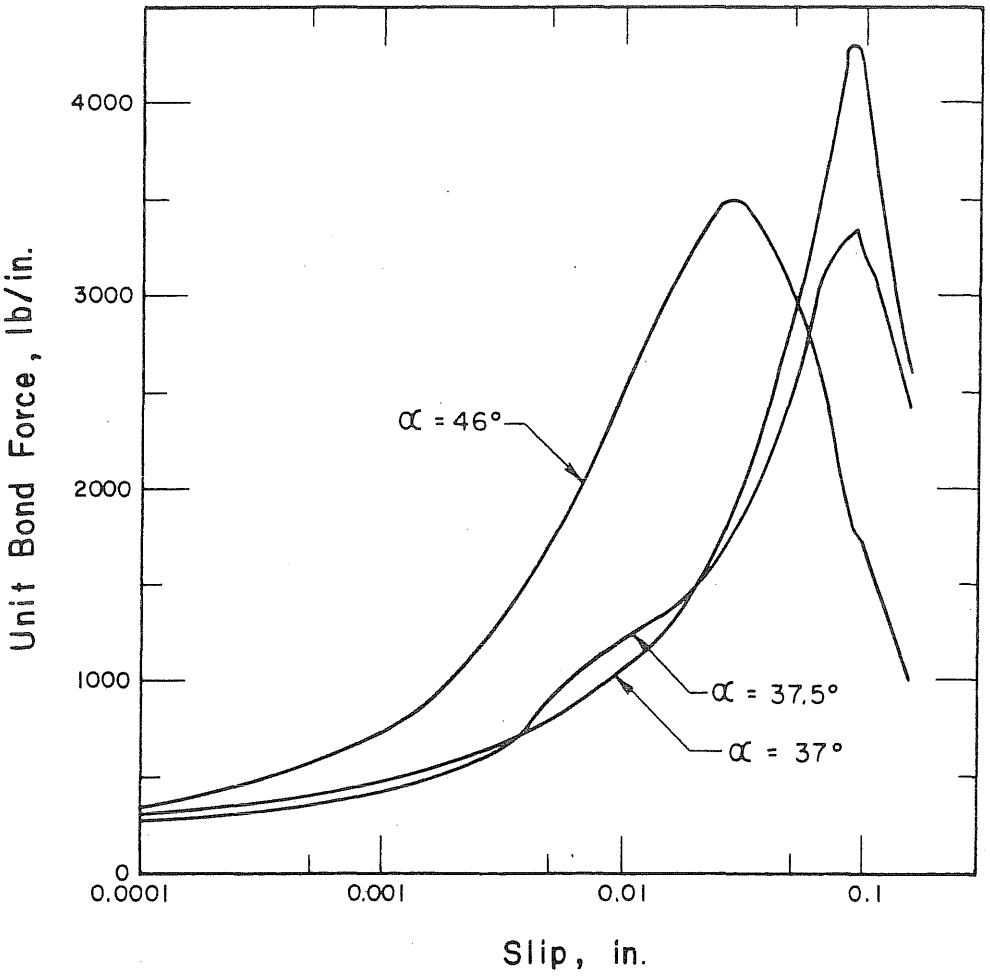

FIG. B.52 UNIT BOND FORCE-SLIP RELATIONSHIPS OF 5/16-in. SQUARE BARS, CONCRETE SPECIMEN AND STRAND FIXED AGAINST ROTATION, SERIES: QB09-1

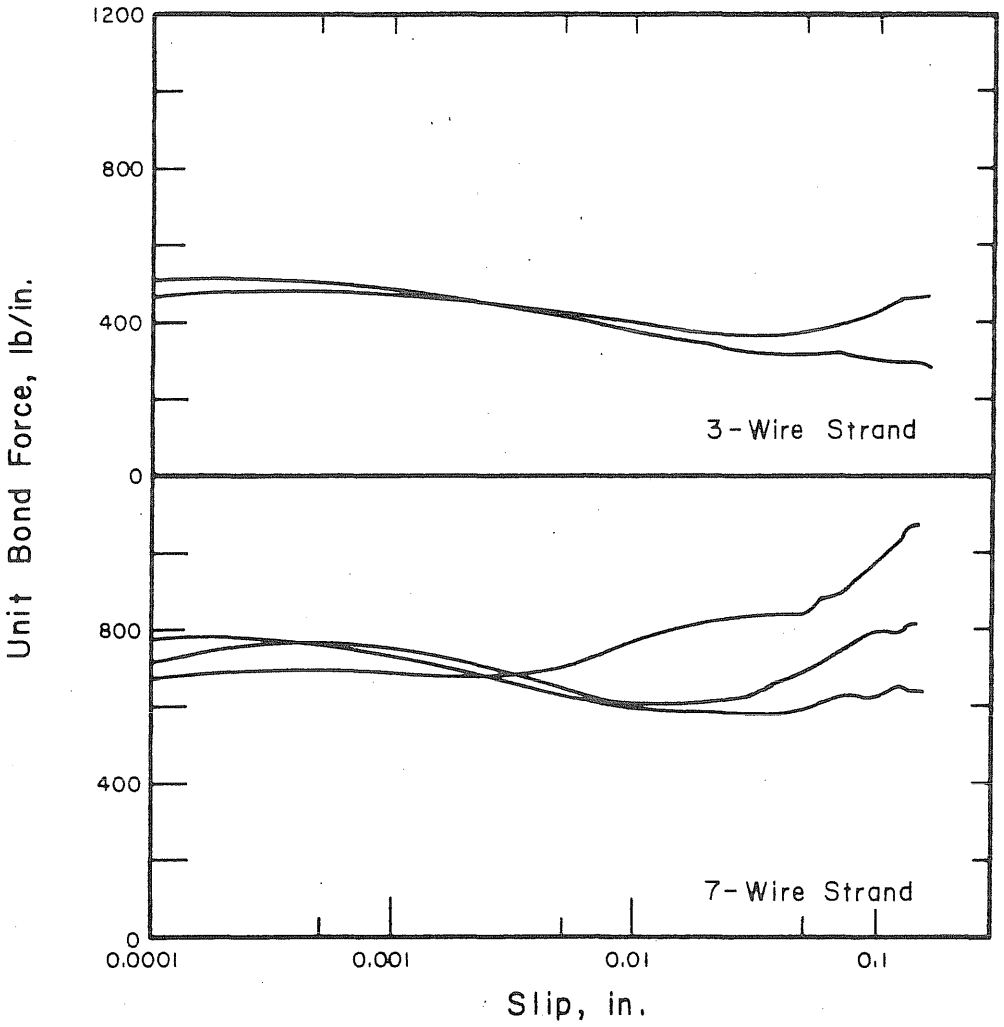

FIG. B.53 UNIT BOND FORCE-SLIP RELATIONSHIPS OF "STRAIGHT" (NONTWISTED) 3-WIRE AND 7-WIRE STRAND FABRICATED WITH CENTER WIRE FROM 7/16-in. STRAND, SERIES: UA09-1

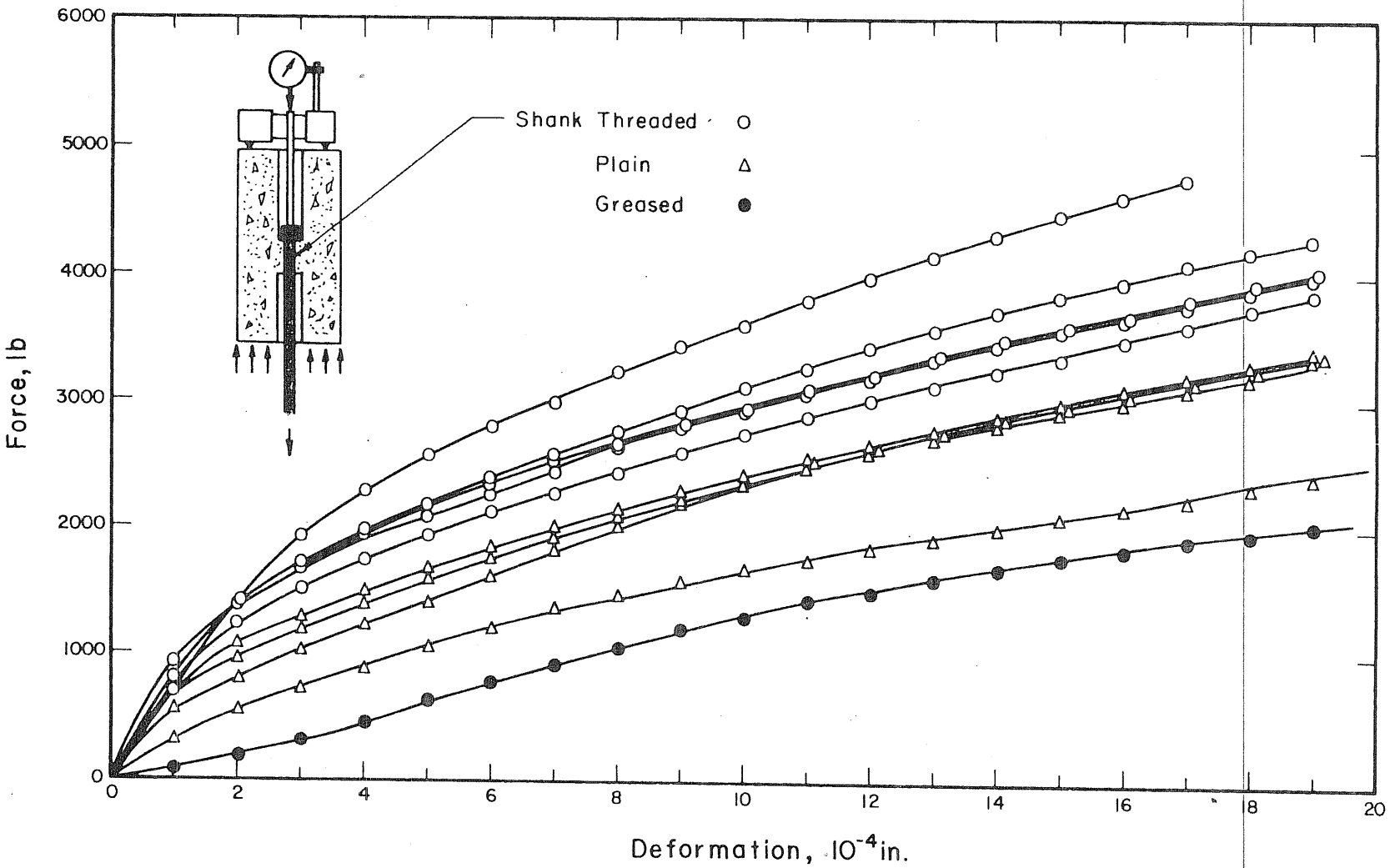

FIG. B.54 DEFORMATION OF THE CONCRETE UNDER THE HEAD OF THE BOLT WITH RESPECT TO THE TOP SURFACE OF THE SPECIMEN, SERIES: BB09-1

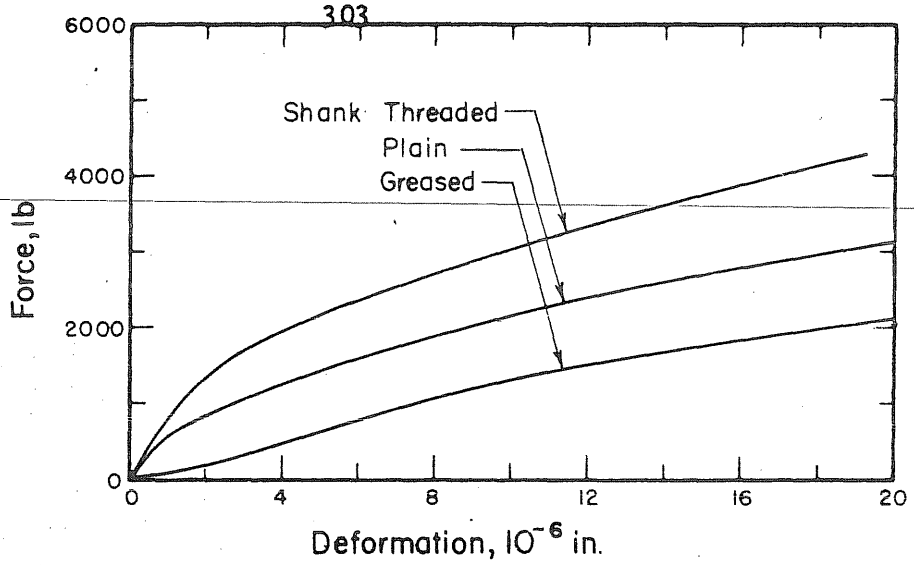

FIG. B.55 AVERAGE DEFORMATIONS OF CONCRETE CONSOLE, SERIES: BB09-1

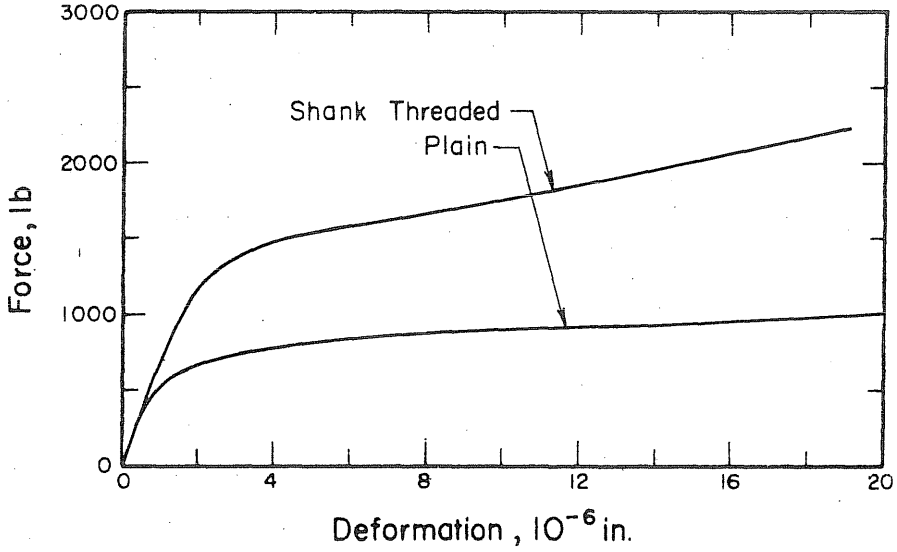

FIG. B.56 AVERAGE DEFORMATIONS OF CONCRETE CONSOLE CAUSED BY BOND STRESSES ALONG THE SHANK OF THE BOLT, SERIES: BB09-1

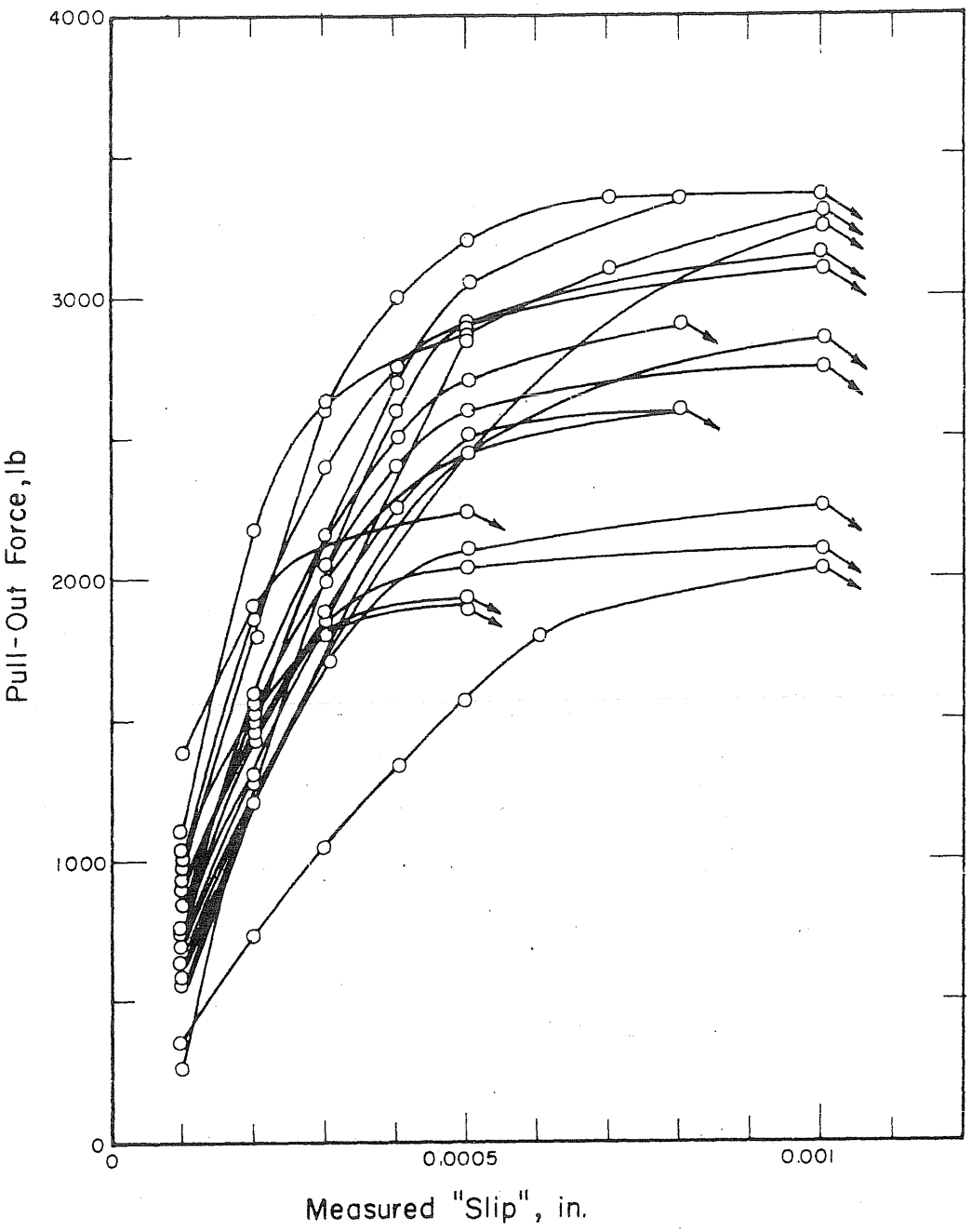

FIG. B.57 PULL-OUT FORCE vs. APPARENT SLIP RELATIONSHIPS FOR TESTS WITH STRAND SUBJECTED TO LATERAL PRESSURE

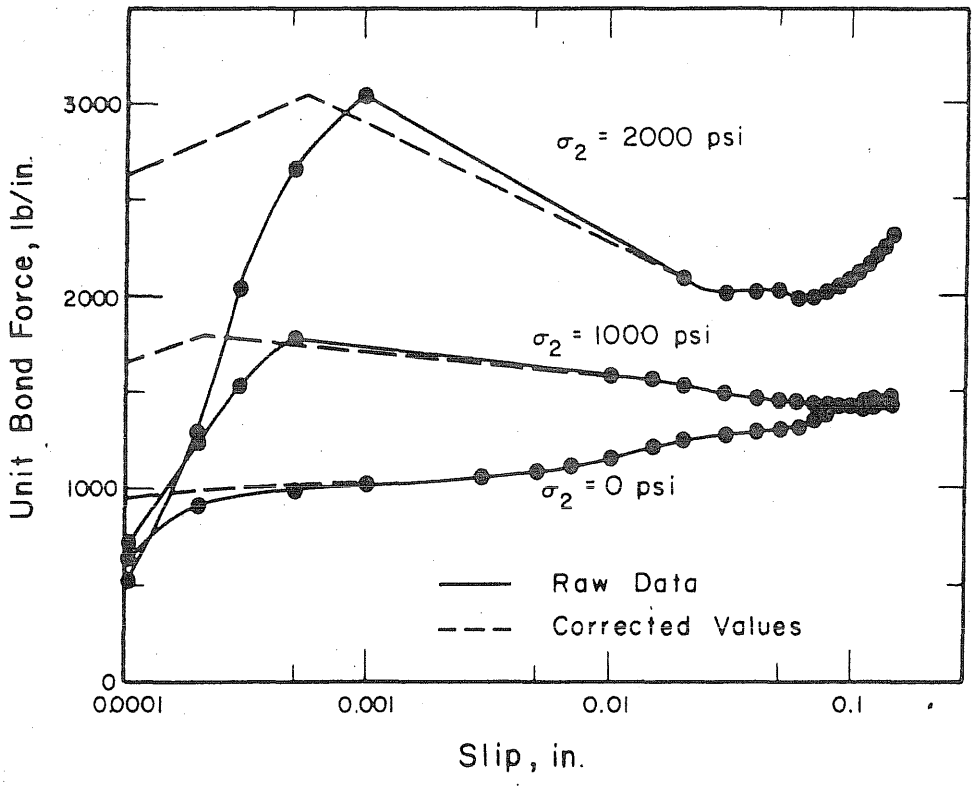

FIG. B.58 COMPARISON OF CORRECTED VALUES WITH RAW DATA, SERIES: SBP24-1

APPENDIX C: CONTACT STRESS BETWEEN STEEL AND CONCRETE

C.1 Introductory Remarks

The following two sections contain a discussion of the contact stresses acting normal to the surface of a reinforcing bar embedded in concrete. The stresses considered are caused (a) by lateral pressure applied externally to the concrete specimen, and (b) by shrinkage of the concrete. The calculations are based on the assumption that concrete is a homogeneous linearly elastic material.

C.2 Contact Stress Caused by Externally Applied Pressure

If a cylinder of homogeneous elastic material is subjected to a uniform lateral pressure, the radial and tangential stresses on every element within the cylinder are of the same magnitude as the externally applied pressure. If the cylinder contains a core with a material of different stiffness characteristics, the radial and tangential stresses vary across the cross section. Therefore, the normal stresses acting on a steel bar embedded in a concrete cylinder that is subjected to an external lateral pressure differ in magnitude from the stresses acting on the surface of the concrete cylinder.

The cross section of the pull-out specimens subjected to lateral pressure was square (4 by 4 in.) with the strand or plain wire embedded in the center of the cross section. The calculation of the contact pressure between the steel and the concrete is based on the assumption that both concrete and steel are homogeneous linearly elastic materials. By considering the cross section of the concrete prism to be a circular area with a diameter of four in. instead of a square area, the problem

may be reduced to that of a thick-walled hollow cylinder submitted to uniform pressure on the inner and outer surface. The pressure on the outer surface is equal to the externally applied pressure. The pressure on the inner face is generated when the deformation of the concrete cylinder directed inward is restrained by the steel which forms the core of the cylinder.

The general solution for the stresses in a thick-walled cylinder is given by Timoshenko (1951)

$$\sigma_r = \frac{A}{r^2} + 2C \tag{C.1}$$

$$\sigma_t = -\frac{A}{r^2} + 2C \tag{C.2}$$

with

$$A = \frac{a^2 b^2 (p_o - p_i)}{b^2 - a^2} \tag{C.3}$$

$$2C = \frac{p_i a^2 - p_o b^2}{b^2 - a^2} \tag{C.4}$$

where σ_r = normal stress in the radial direction, σ_t = normal stress in the circumferential direction, r = radial coordinate, a = radius of steel core or inner radius of concrete cylinder, b = outer radius of concrete cylinder, p_o = external pressure, and p_i = contact pressure between steel and concrete.

Under the influence of the inner pressure p_i, the radius of the steel core, a, shortens by

$$e_1 = \frac{-ap_i}{E_s}(1 - \nu_s) \qquad (C.5)$$

where E_s = modulus of elasticity, and ν_s = Poisson's ratio for steel.

Any radius of the concrete cylinder, which is subjected to an externally applied uniform pressure p_o and an internal pressure p_i, deforms by

$$e = \frac{1}{E_c}\left[-\frac{(1+\nu_c)A}{r} + 2C(1-\nu_c)r\right] \qquad (C.6)$$

where E_c = modulus of elasticity and ν_c = Poisson's ratio for concrete. By substituting the constants A and C, the inner radius, a, of the concrete cylinder can be shown to shorten by

$$e_2 = \frac{a}{E_c(b^2 - a^2)}\left\{p_i\left[b^2(1+\nu_c) + a^2(1-\nu_c)\right] - 2b^2p_o\right\} \qquad (C.7)$$

The displacements of the steel, e_1, and the displacements of the concrete, e_2, should match at their common boundary. Thus, the unknown contact pressure, p_i, is

$$p_i = \frac{2nb^2p_o}{(b^2-a^2)(1-\nu_s) + n[b^2(1+\nu_c) + a^2(1-\nu_c)]} \qquad (C.8)$$

or

$$p_i = kp_o \qquad (C.9)$$

where n = modular ratio of steel and concrete, and k is a constant for given geometric dimensions and elastic material properties according to Eq. (C.8). The factor k depends on the modular ratio n. The influence of n, however, is very small considering the possible range of the modular ratio for steel and concrete (Fig. C.1).

Using Poisson's ratio of 0.3 for steel and a modular ratio of n = 8, the factor k for 7/16-in. strand varied from 1.67 to 1.54, when Poisson's ratio of concrete was varied from 0.10 to 0.20. For the center wire from 7/16-in. strand, k varied from 1.68 to 1.55.

The theoretical distribution of the radial and circumferential stress along the diameter of a test specimen with center wire from 7/16-in. strand is shown in Fig. C.2. A similar distribution is obtained for specimens with strand.

The elastic solution derived above was based on the assumption that every cross section of the specimen through the bonded length was in a state of plane stress. The fact that the stress distribution along the bonded length was nonuniform because the bonded length was only one in. while the external stress was applied to the concrete over a length of five in. was not taken into account. The stiffness of the concrete specimen was large enough to make this effect negligibly small. The small error in the analysis of substituting a cylindrical concrete specimen for a prism was neglected in view of the uncertainties in the parameters involved.

The result from the elastic solution indicates that the contact pressure between steel and concrete was 60 percent higher than the stress applied externally to the concrete prism. It must be noted,

however, that the applicability of an elastic solution to this case demands some stringent conditions. The materials in contact must be homogeneous and linearly elastic. The moduli of elasticity and Poisson's ratios must be known. Furthermore, a perfect contact between the steel and the concrete is required. It is evident that none of these conditions is fulfilled exactly. Therefore, some consideration must be given to the effect of the contact conditions on the actual magnitude of the contact pressure.

(1) The magnitude of the contact stress due to an externally applied pressure is very sensitive to any relative displacement between the steel and the concrete. According to Eq. C.7, a reduction in the radius of the steel (center wire) by as little as 3.7×10^{-5} in. would cause the contact pressure between steel and concrete to disappear despite an externally applied stress of 1000 psi. Only 1.5×10^{-5} in. would be required to change the value of k (Eq. C.9) from 1.6 to 1.0.

A relative displacement between steel and concrete of the above order of magnitude is possible for several reasons. During the pull-out tests, the steel contracts elastically by an amount depending on the axial stress in the steel and Poisson's ratio. This effect may easily be taken into account by replacing Eq. C.5 with

$$e_1 = \frac{-a(1-\nu_s)p_i}{E_s} - \frac{a\nu_s P}{2E_s A_s} \qquad (C.10)$$

where P = total pull-out force, and A_s = cross sectional area of the steel. The last term in the above expression was divided by two because it was assumed that the steel stress decreases approximately linearly from the attack end of the bonded length to the trail end.

The new expression for k taking into account the elastic contraction of the steel due to the axial tensile force was found to be

$$k = \frac{2nb^2 p_o - (b^2 - a^2)\nu_s \frac{P}{2A_s}}{(b^2 - a^2)(1-\nu_s) + n\,[b^2\,(1 + \nu_c) + a^2(1-\nu_c)]} \qquad (C.11)$$

The variation of k with the pull-out force is shown in Fig. C.3 both for 7/16-in. strand and plain wire. According to those relations which were based on average values of n = 8 and ν_c = 0.15, the value of k varied in the tests, depending on the pull-out forces and applied lateral stresses, from approximately 1.3 to 1.5.

A further reduction of k may be expected by the inelastic deformation of the concrete immediately surrounding the steel. Especially at higher external lateral pressures (3000 to 4000 psi), the stress-strain relationship for the concrete near the steel is likely to be far in the inelastic range. Any reduction in the stiffness of the concrete, even if it is limited to a thin layer around the steel, leads to a decrease in contact pressure. Consider, for instance, a test specimen which contains a layer of concrete with reduced modulus of elasticity around the steel with a thickness of roughly 0.1 in. (Fig. C.4). Using the assumed moduli of elasticity and the theoretical expression for k given in Fig. C.4, k was found to be 1.03 in comparison to k = 1.60 for a concrete of uniform stiffness ($E = 4 \times 10^6$ psi). The distribution of the radial stress is indicated in the figure.

The concrete around the strand may become inelastic even at smaller external stresses than mentioned above because the contact stresses may be increased through shrinkage by several hundred psi.

(2) The magnitude of the contact stress is very sensitive to the quality of the material-to-material contact between steel and concrete. Caused by bleeding and settlement of the fresh concrete, it is possible, or even likely, that air pores get trapped between the two materials. This reduces the area of true contact, increases locally the stress in the concrete, and causes therefore the concrete to become inelastic at relatively low external pressures. In a case of extremely bad contact, it is conceivable, although unlikely, that the value of k may drop below 1.0.

(3) In discussing the magnitude of k, the question, of course, arises of measuring the contact pressure. Within current limits of instrumentations the experimental determination of k does not seem to yield any advantages, even if very small pressure gages would be available. Any measuring device would lead to such disturbances locally that the accuracy of the measurement would be questionable.

Summarizing the above discussion, it must be concluded that the contact stress is extremely sensitive to the smallest change in the conditions of contact. All evidence points to the fact that the factor of k = 1.6 calculated for the perfect elastic case is too high. The trend of all the factors influencing the contact between steel and concrete seems to indicate that the actual value for k is much closer to 1.0 than to 1.6. It was therefore decided to use k = 1.0

in the analysis of the test data. It should be kept in mind that, under certain circumstances, k may be as high as 1.1 or 1.2. Because of the uncertainties involved, however, it would be unreasonable to differentiate for different cases.

C.3 Contact Stress Caused by Shrinkage of Concrete

Since a satisfactory method of measuring the contact stresses due to shrinkage between concrete and a reinforcing bar is not available, these stresses have to be estimated by a theoretical approach.

The calculation is based on the same assumptions as in the previous section. The concrete specimen is considered as a thick-walled cylinder submitted to uniform pressure on the inner surface. The inner pressure is generated when the concrete tends to shrink but is restrained by the steel forming the core of the cylinder.

Longitudinal shrinkage of the concrete specimen produces stresses parallel to the steel bar because of the restraint that bond poses to free shrinkage in that direction. If these longitudinal stresses are neglected, any element of the cross section may be considered as being in a state of plane stress. The stresses in the concrete cylinder which are set up when the concrete surrounding the steel tends to shrink are determined by Eq. C.1 through C.4. The external pressure, p_o, in that case is equal to zero.

According to Eq. C.6 the radial displacement, d_1, of the inner radius of the concrete cylinder due to the restraining pressure p_i,

which the steel bar exerts on the concrete, is

$$d_1 = \frac{a\, p_i}{E_c(b^2 - a^2)}\left[(1 + \nu_c)b^2 + (1 - \nu_c)a^2\right] \qquad (C.12)$$

where the terms on the right side of the equation have the same meaning as those of Eq. C.7.

Subjected to the shrinkage pressure p_i, the radius of the steel bar decreases by

$$d_2 = \frac{-p_i\, a}{E_s}(1 - \nu_s) \qquad (C.13)$$

If the steel had been replaced by concrete, the radius of the circular area taken by the steel would shrink by the amount

$$d_3 = - aS \qquad (C.14)$$

where S is the linear shrinkage strain of the concrete.

In order to satisfy compatiblity, the total deformation of the concrete at radius a must equal the deformation of the steel, or

$$d_3 + d_1 = d_2 \qquad (C.15)$$

Substituting into this expression Eq. C.12 through C.14, the shrinkage pressure p_i may be determined by

$$p_i = \frac{S(b^2 - a^2)}{\frac{1}{E_c}\left[b^2\,(1+\nu_c) + a^2\,(1-\nu_c)\right] + \frac{1}{E_s}(b^2 - a^2)(1-\nu_s)} \qquad (C.16)$$

If dimensions of the test specimens with plain center wire and realistic material properties (a = 0.073 in., b = 2.0 in., $E_c = 4 \times 10^6$ psi, $\nu_c = 0.15$, $E_s = 29 \times 10^6$ psi, $\nu_s = 0.3$) are inserted into Eq. C.16, a contact stress between the concrete and the wire of approximately 300 psi is obtained for a shrinkage strain of 10×10^{-5}.

Shrinkage strains of dry cured concrete measured over a period ranging from the second to the eighth day after casting were found to be in the order of 15×10^{-5} (Fig. 6.9). It may be assumed, however, that a large amount of shrinkage has taken place during the first two days when no measurements were taken. Therefore, it is not absurd to assume contact stresses between concrete and reinforcing steel due to shrinkage to be in the order of several hundred psi.

The method of calculating the shrinkage stresses may not be very accurate for several reasons. In the calculation, it was assumed that shrinkage was distributed uniformly over the entire cross section. This assumption is not realistic because of the nonuniform process of drying of the concrete. Furthermore, even if the shrinkage strains, needed to calculate the shrinkage stresses, can be determined accurately in the early stages of hardening of the concrete, it appears to be difficult to relate realistic stiffness properties of the concrete to the early shrinkage deformations.

Another very important consideration should be mentioned here. Although the shrinkage stresses are relatively small compared with the compressive strength of the concrete, they cause the concrete to creep. Consequently, the shrinkage stresses are gradually reduced with time, a phenomenon which poses another uncertainty in the theoretical determination of the shrinkage stresses.

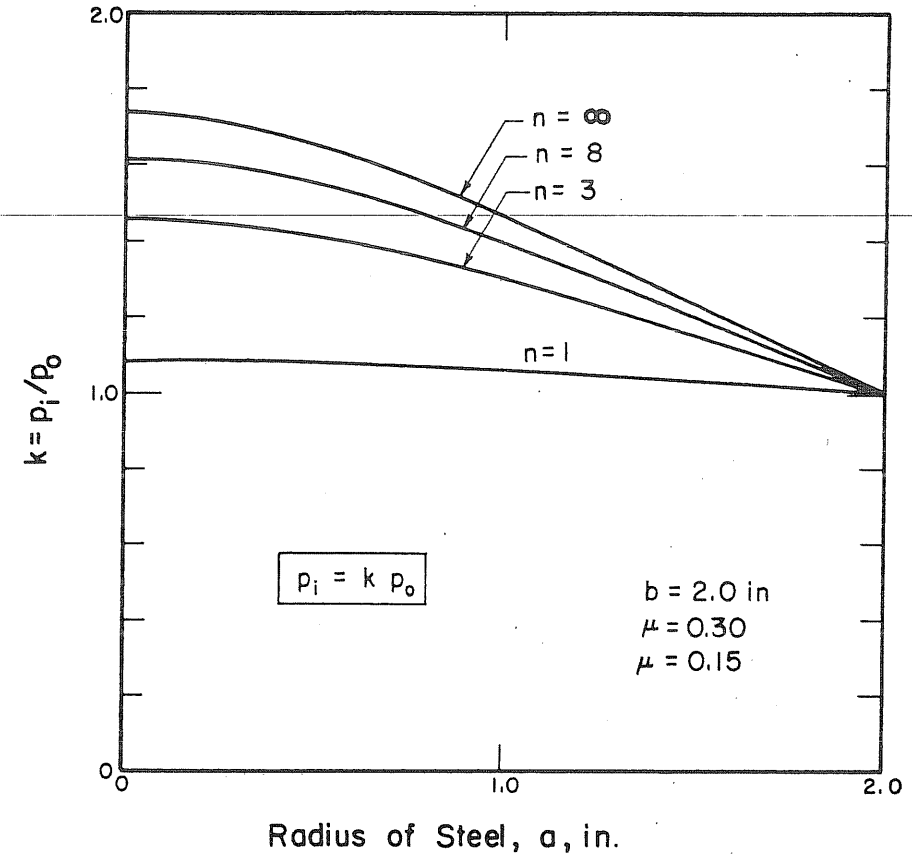

FIG. C.1 VARIATION OF CONTACT PRESSURE WITH RADIUS OF STEEL FOR VARIOUS MODULAR RATIOS $n = E_{steel}/E_{concrete}$

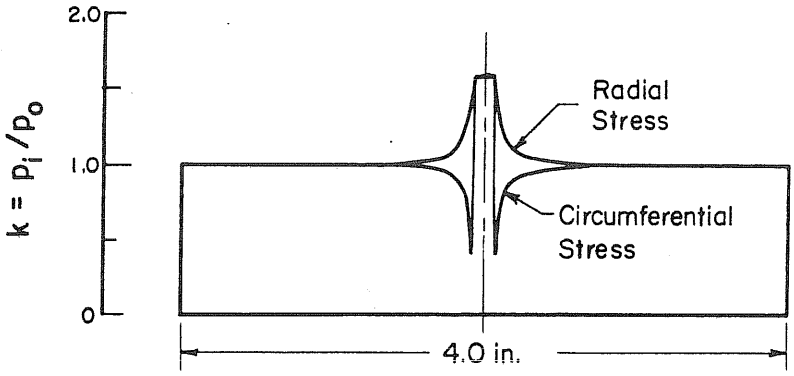

FIG. C.2 DISTRIBUTION OF RADIAL AND CIRCUMFERENTIAL STRESSES ALONG DIAMETER OF CONCRETE SPECIMEN WITH CENTER WIRE FROM 7/16-in. STRAND

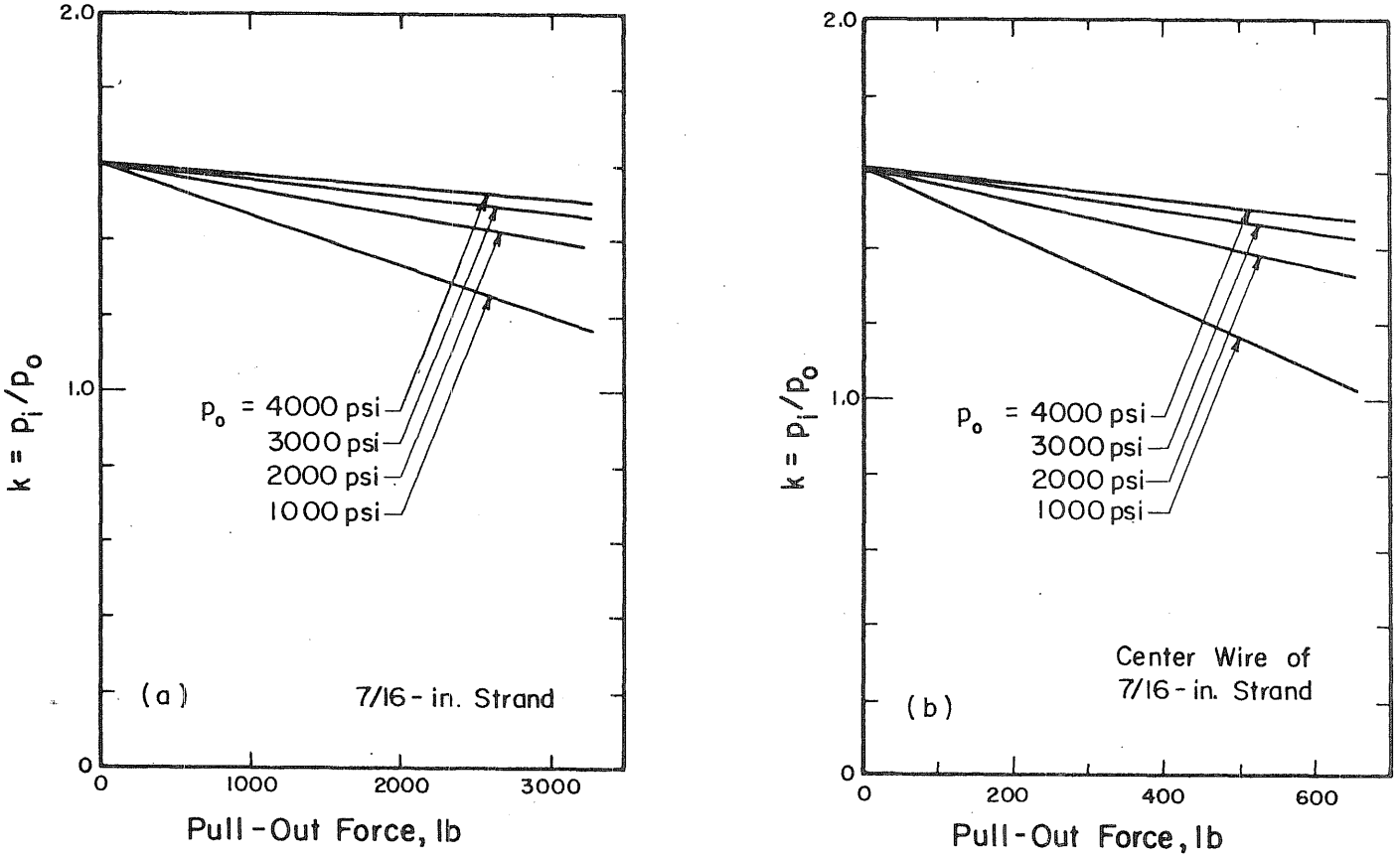

FIG. C.3 VARIATION OF RATIO $k = p_i/p_o$ WITH PULL-OUT FORCE FOR SPECIMENS WITH (a) 7/16-in. STRAND AND (b) CENTER WIRE FROM 7/16-in. STRAND

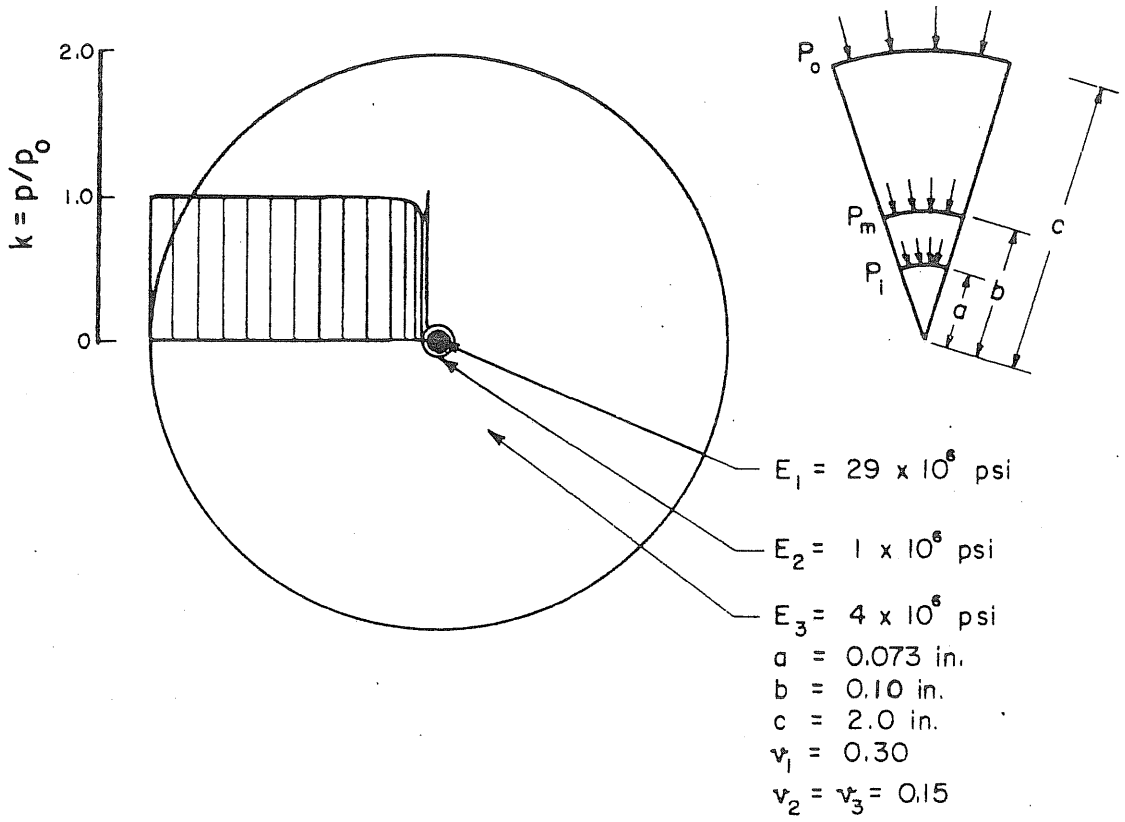

$$p_i = \frac{4\, n_1\, n_2\, b^2\, c^2\, (b^2-a^2)\, P_o}{\left\{(b^2-a^2)(1-\nu_1) + n_1\left[b^2(1+\nu_2) + a^2(1-\nu_2)\right]\right\}\left\{\left\langle n_2(b^2-d^2)\left[c^2(1+\nu_3) + b^2(1-\nu_3)\right]\right\rangle\right.}$$

$$\left. + (c^2-b^2)\left[a^2(1+\nu_2) + b^2(1-\nu_2)\right]\right\} - 4\, n_1\, a^2\, b^2\, (c^2-b^2)$$

FIG. C.4 DISTRIBUTION OF RADIAL STRESSES ALONG RADIUS OF CYLINDER SUBJECTED TO EXTERNAL PRESSURE AND CONTAINING CORES OF DIFFERENT MATERIALS

APPENDIX D: COMPUTATION OF THE STRESS DISTRIBUTION IN A SHEAR KEY

In Chapter II, it was assumed that the initial bond strength is determined by a shear failure of concrete keys which are interlocked with a microscopically rough steel surface. In the following section, a method of calculating the stress distributions in one of those concrete keys subjected to bond forces is discussed for various assumptions about the local transfer of stress from the steel to the concrete.

A profile of the surface of a cold drawn wire as measured by Rehm (1961) with a profile meter is shown in Fig. D.1a. Numerous measurements made by Rehm indicated that the depth-to-width ratio remained approximately constant for all indentations at approximately 1:10 to 1:15.

For the purpose of the calculations, it was assumed that the steel surface was marred by a large number of rectangular indentations as shown in Fig. D.1c. Furthermore, it was assumed that the deformable concrete key was attached to a rigid mass of concrete.

When force is to be transmitted from the steel to the concrete, an individual concrete key may be subjected to forces as indicated in Fig. D.2a. The bond forces are assumed to be transferred from the steel to the concrete only through the top surface of the shear key. The shear forces along the vertical face of the concrete key are neglected.

The horizontal forces, P_2, represent lateral contact pressures caused either by shrinkage or externally applied forces.

The uppermost part of the shear key has the tendency to deflect in the negative y-direction under the loading shown. Since the steel prevents any deflection in this direction, the upper part of the concrete key was fixed with respect to movement in the y-direction over a distance where negative deflections would take place. The resulting deflection of the shear key due to the loading shown in Fig. D.2a is shown in Fig. D.2b.

Three loading cases were investigated (Fig. D.3): case I, with a vertical force on the top surface of the shear key, and case II and III which involved combinations of vertical and horizontal forces.

For the calculation of the stresses and deflections of the shear key, use was made of an existing computer program (Pecknold, 1969). The solution was based on finite element methods. Triangular, two-dimensional elements were used as indicated in Fig. D.4. The concrete was assumed to be elastic and in a state of plane stress.

The calculation provided the normal and shear stresses for each of the elements shown in Fig. D.4. Deflections in the x- and y-directions were obtained at each node.

Solutions were obtained for the following conditions:

(a) depth-to-width ratio of the shear key = 1/10

(b) modulus of elasticity of concrete = 4×10^6 psi

(c) Poisson's ratio for concrete = 0. (Calculations using Poisson's ratio of 0.2 indicated that the effect of different ratios on the stresses was very small).

The loads acting on the shear key as indicated in Fig. D.3 were determined such that their relative values, P_1 and P_2, reflected a regular pull-out test on plain wire without applied lateral pressure (case I), a pull-out test with a lateral pressure of 1000 psi (case II), and a pull-out test with a lateral pressure of 2000 psi (case III). The test results were taken from Fig. 8.3.

By assuming that the loads P_1 and P_2 are transferred only through the shear key and that the bonded area is pitted by a given number of square indentations of the same size, it was possible to assign relative values for P_1 and P_2 to an individual shear key for each loading case.

Because of the many simplifying assumptions made, it was not attempted to find actual forces and stresses but to determine relative values. For this reason, the normal stresses and shear stresses plotted for the fixed edge of a shear key for each loading case are given without dimensions (Fig. D.5 through D.7).

The stress distributions indicate that high tensile stresses in the y-direction exist near the top of the shear key in all three loading cases. This is the location where the "shear failure" will start. Having failed at the top, the failure will progress along the presumably fixed edge of the shear key.

In Fig. D.8, the directions of the principal stresses in the upper half of the shear key are shown for load case I. Figure D.9 presents lines of equal principal tension in the upper part of the shear key for all three load cases. Again it is shown that very

high tensile stresses are concentrated in the upper fixed corner of the shear key. It should be noted, however, that a sharp corner as assumed in Fig. D.1c does not exist (compare with Fig. D.1b). Consequently, the stress concentrations will be less pronounced in the actual case.

The relative magnitudes of the principal tension corresponding to failure loads in actual pull-out tests indicate that the shear key of load case I is subjected to smaller stresses than the load cases II and III. Therefore, a comparatively higher failure load should be expected in pull-out tests of case I. Because of the disturbance of stresses inflicted by the sharp corner of the assumed shear key and the purely elastic solution of the problem, no quantitative conclusion can be drawn from that result.

The calculation demonstrated that the initial failure conditions in bond tests with or without lateral pressure are alike and can be explained by a material failure of the interlocking structure between steel and concrete.

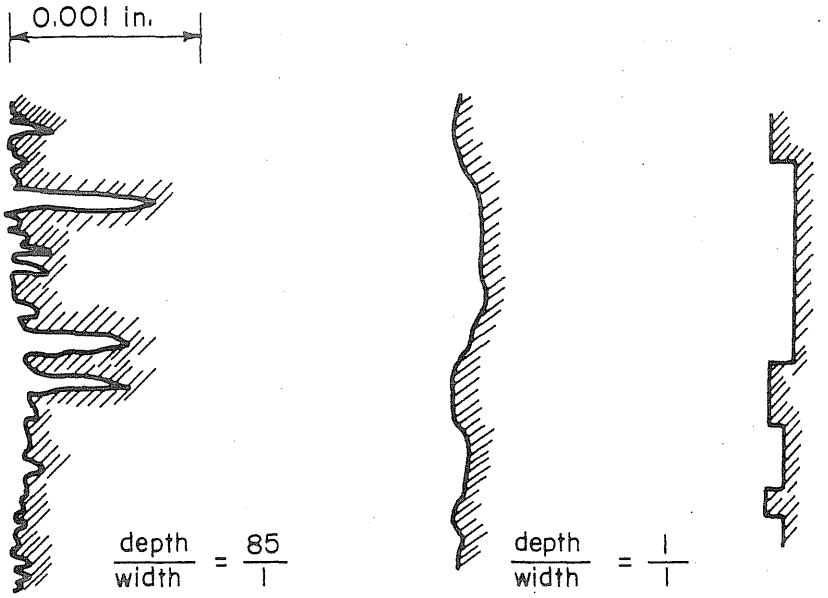

(a) Measured by Rehm (b) In Detail (c) Simplified

FIG. D.1 SURFACE PROFILE OF COLD DRAWN WIRE

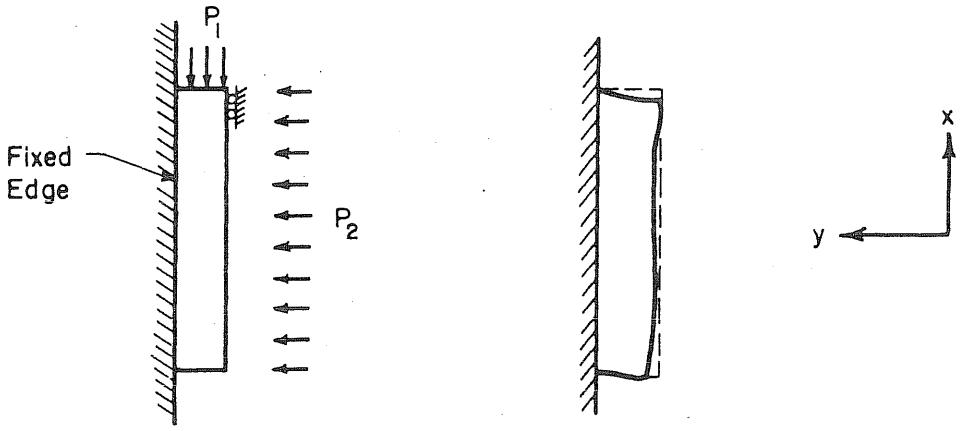

(a) Assumed Load Distribution (b) Deflection of Shear Key

FIG. D.2 ASSUMED DISTRIBUTION OF LOAD AND DEFLECTION FOR AN INDIVIDUAL SHEAR KEY

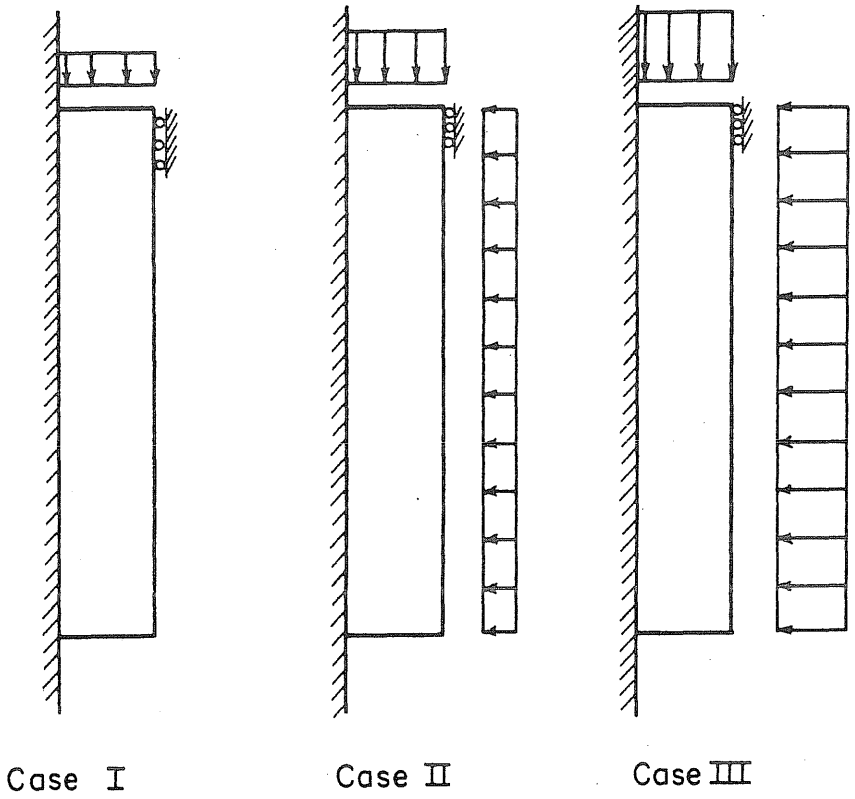

FIG. D.3 LOAD CASES INVESTIGATED

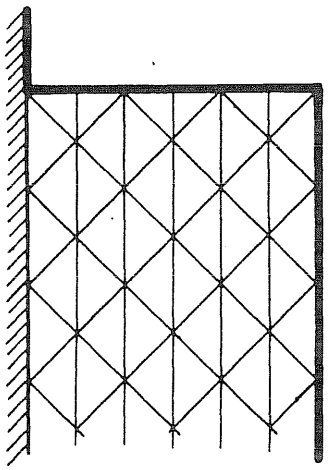

FIG. D.4 FINITE ELEMENT GRID USED

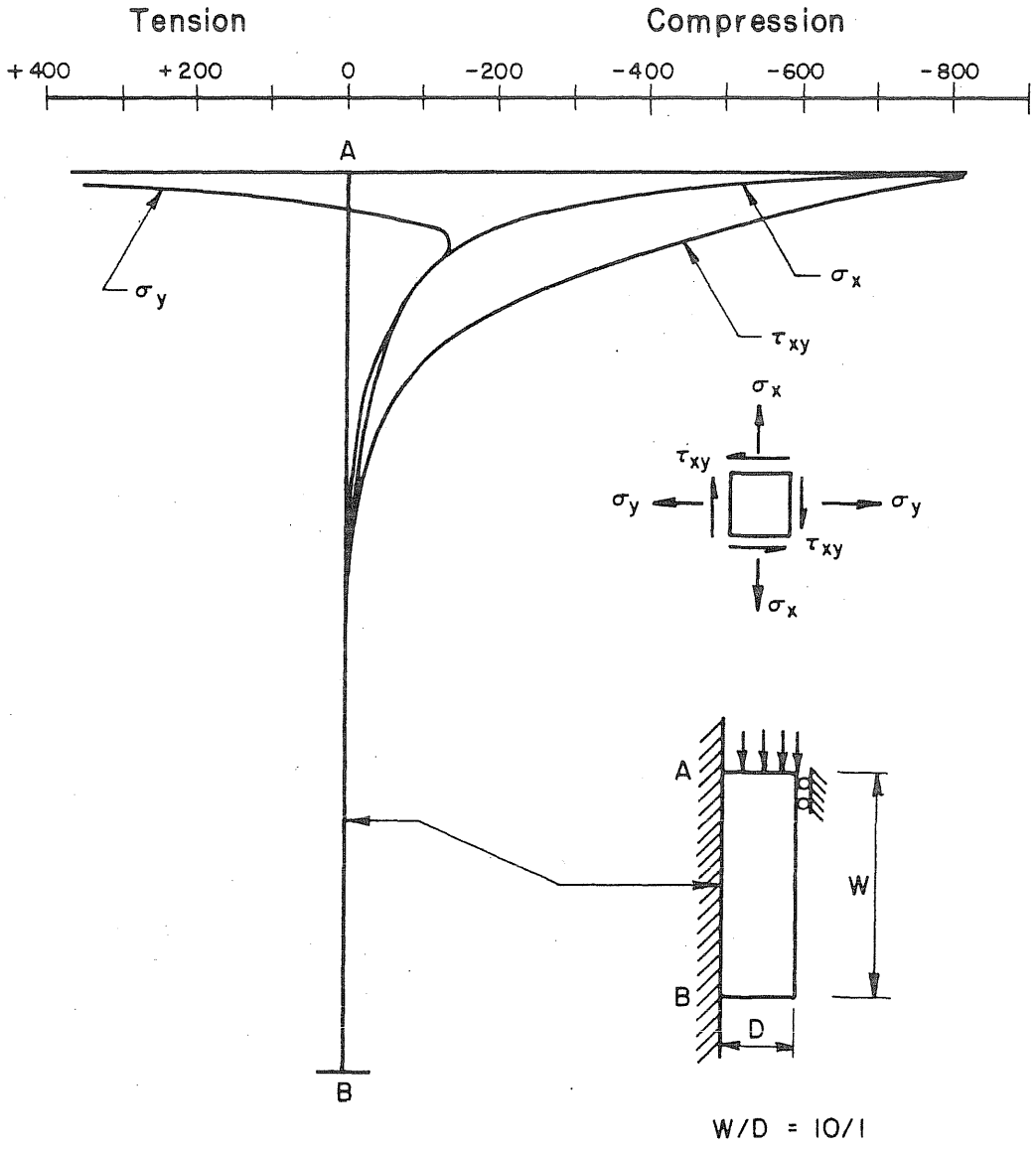

FIG. D.5 STRESS DISTRIBUTION ALONG FIXED EDGE OF SHEAR KEY, LOAD CASE I

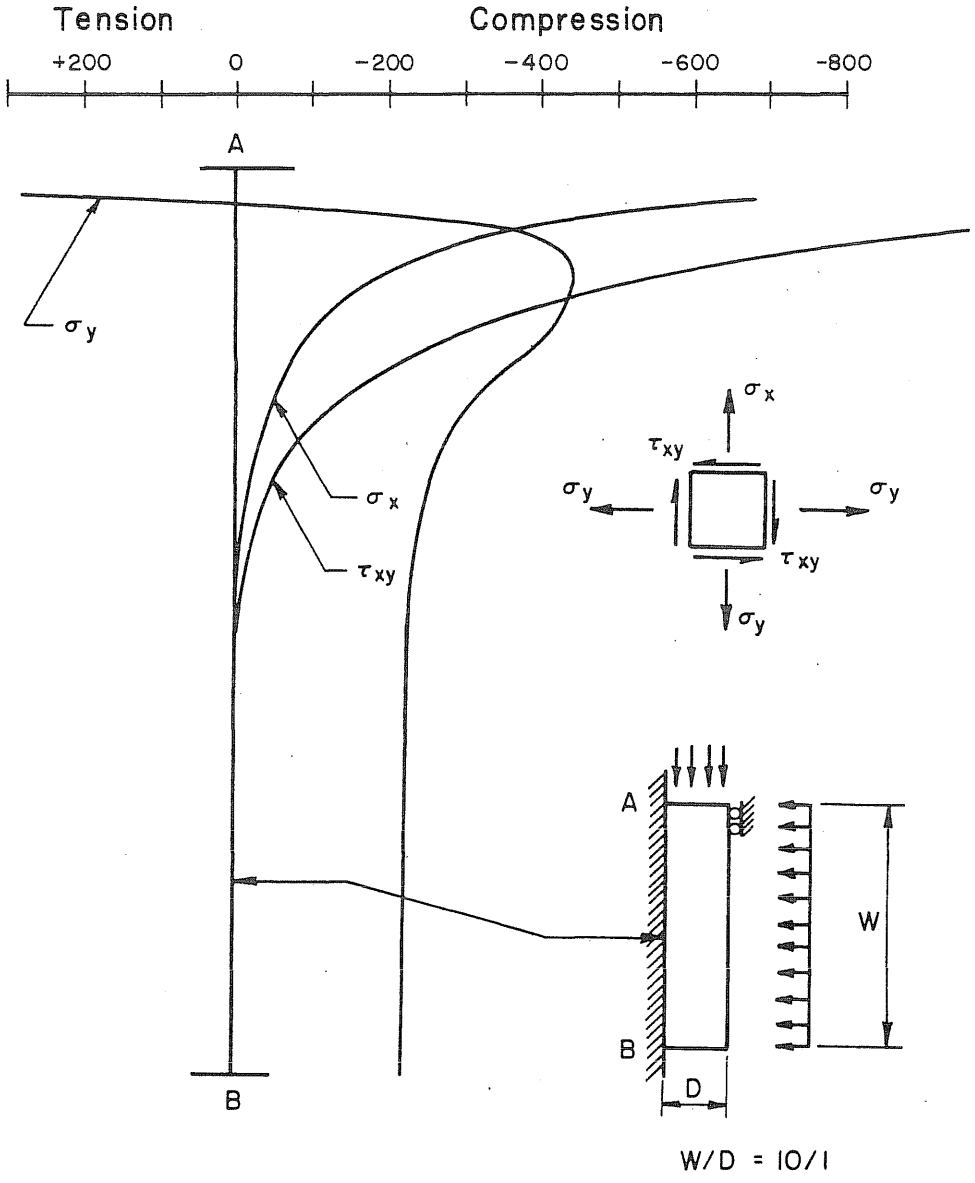

FIG. D.6 STRESS DISTRIBUTION ALONG FIXED EDGE OF SHEAR KEY, LOAD CASE II

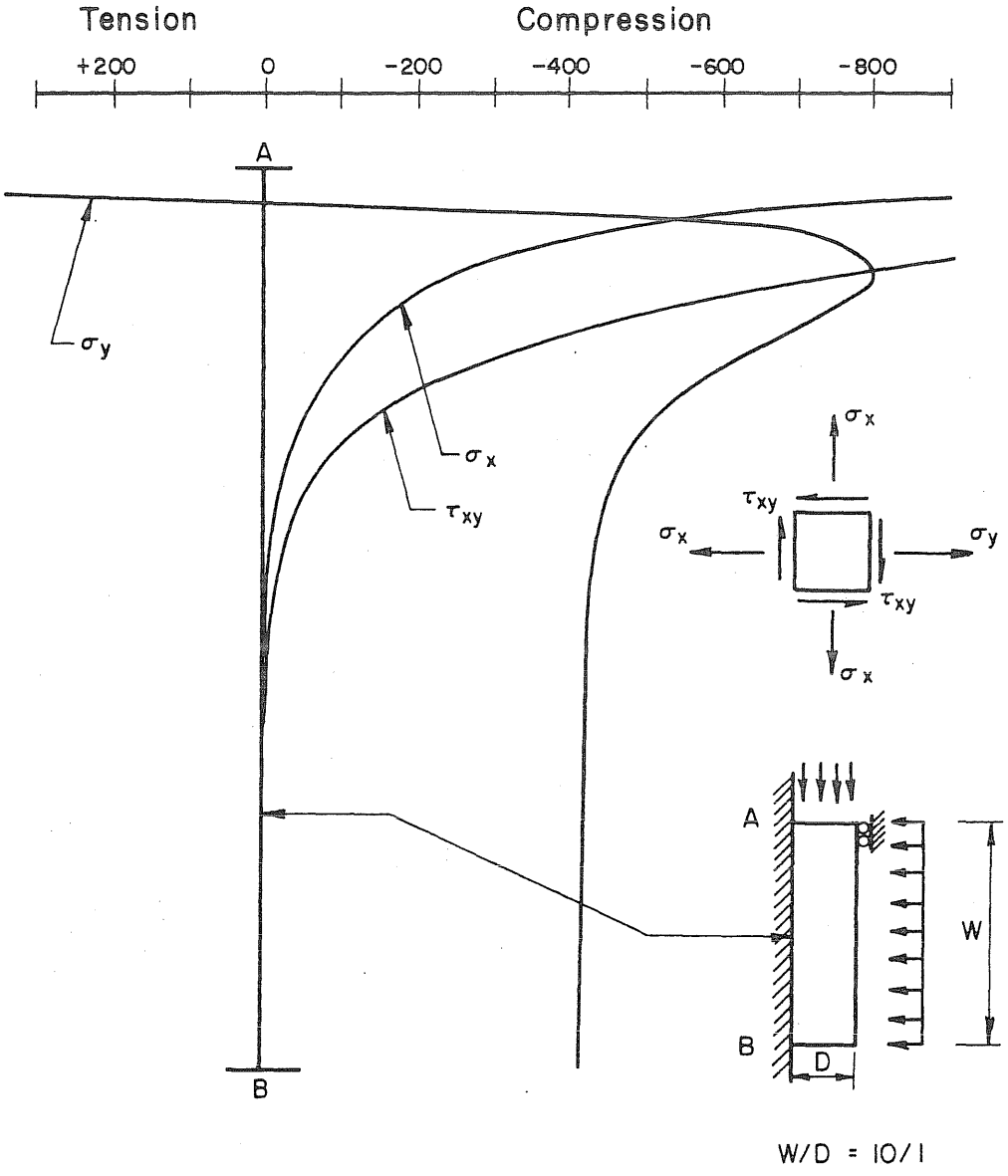

FIG. D.7 STRESS DISTRIBUTION ALONG FIXED EDGE OF SHEAR KEY, LOAD CASE III

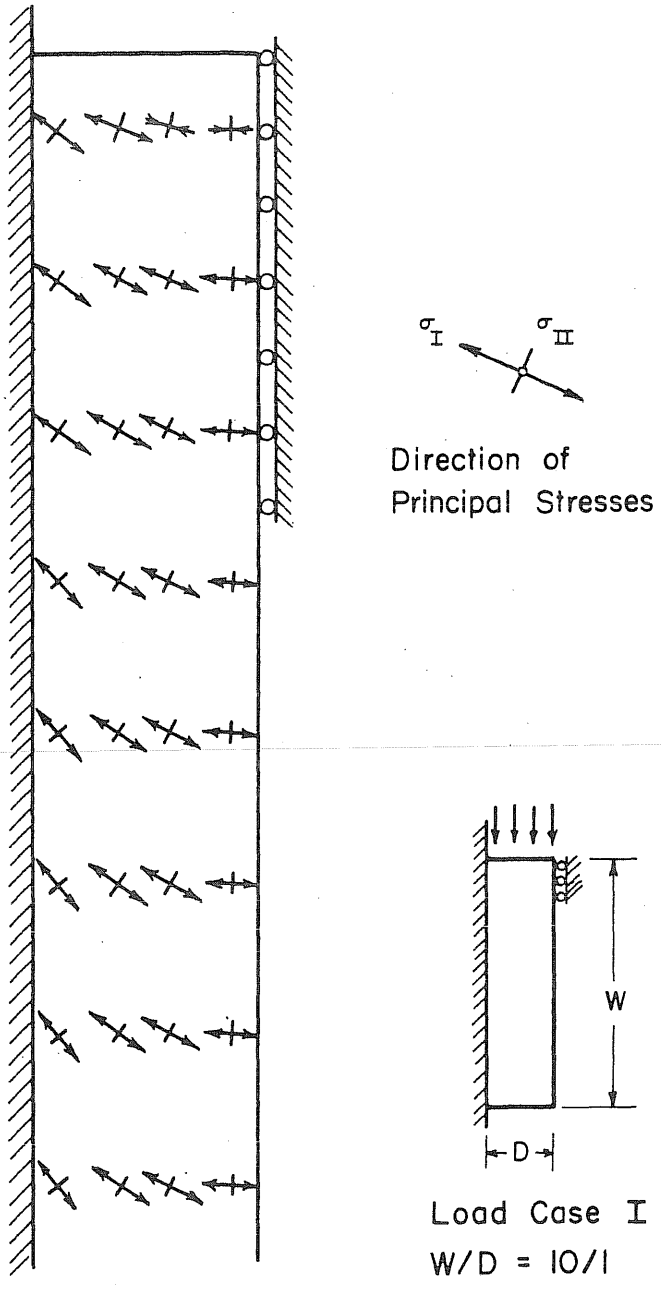

FIG. D.8 DIRECTION OF PRINCIPAL STRESSES IN UPPER HALF OF SHEAR KEY, LOAD CASE I (μ_c = 0, W/D = 10/1)

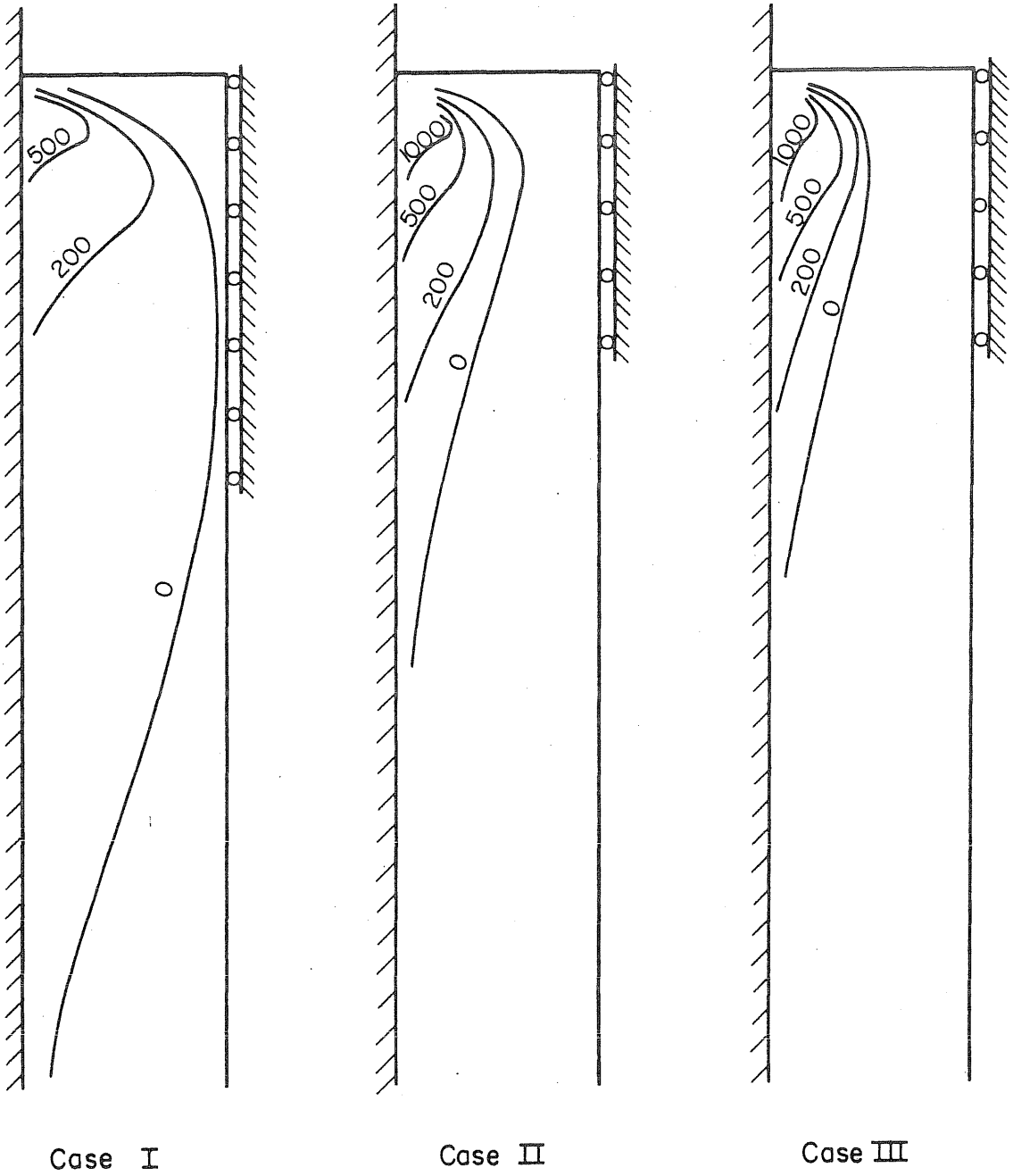

FIG. D.9 LINES OF EQUAL PRINCIPAL TENSILE STRESSES

APPENDIX E: THEORETICAL DETERMINATION OF BOND-SLIP RELATIONSHIPS FOR LONG EMBEDMENT LENGTHS

E.1 Determination of Bond-Slip Relationship for a Given Bonded Length on the Basis of Results from One-in. Pull-Out Tests

The objective of the calculation described in the following section is the prediction, on the basis of results from one-in. pull-out tests, of the bond-slip relationship of strand for any given bonded length. Given are the unit bond force-slip relationship of strand which is assumed to be characteristic for bond between strand and concrete, the stress-strain curve of the strand, and the trail-end slip for which the bond-slip relationship is to be calculated.

The calculation which is to be carried out with the aid of a digital computer is a simple iteration procedure. It is based on the relationship that the change of the slip is equal to the absolute sum of the changes in deformation of the strand and the concrete, or

$$\frac{ds}{dx} = \frac{de_s}{dx} + \frac{de_c}{dx} \qquad (E.1)$$

where s = slip, e_s = deformation of strand, e_c = deformation of concrete, and dx = differential length regarded.

Since the deformation of the concrete is small compared with the deformation of the steel, the last term of Eq. E.1 was neglected. Thus, the basic assumption of the calculation was reduced to the simple relation that the change in slip is equal to the change in deformation of the strand.

The iteration is started at the trail end of the bonded length where the slip and the steel stress (= zero) are known. The bonded length is divided into a number of iteration intervals.

With the given unit bond force-slip relationship, the bond force developed at the end of the first iteration interval can be determined by assuming that the unit bond force corresponding to the given trail-end slip remains constant along the iteration interval considered. Using the known stress-strain relationship of strand, the deformation of the strand at the end of the first iteration length can be calculated. Since it was assumed above that the change in deformation of the steel is equal to the change in slip, the slip at the end of the first iteration interval is determined by the sum of the trail-end slip and the calculated deformation of the strand. Now a new unit bond force corresponding to the calculated slip can be picked from the given unit bond force-slip relation for the second iteration interval. This procedure is continued until the sum of the iteration intervals equals the bonded length for which the bond-slip relationship is to be calculated.

The length of the iteration intervals may be chosen to suit any "accuracy" of the solution desired. For the relatively slowly changing unit bond-slip relationship of strand, an iteration length of 0.5 in. was found to be sufficient.

The degree of agreement of the theoretical solution with the actual test results depends merely on the accuracy with which the unit bond force-slip relationship of the one-in. pull-out tests represents the actual bond-slip relation between strand and concrete.

E.2 Calculation of the Anchorage Length of Strand in a Pretensioned Prestressed Member

The objective of the calculation method described in the following is to determine the anchorage length of strand in a pretensioned prestressed member for any given prestress on the basis of results from one-in. pull-out tests. Given are the unit bond force-slip relationship of strand which is assumed to be typical for bond between strand and concrete, the stress-strain curve of the strand, and the prestress for which the anchorage length is to be calculated.

The calculation consists of a simple iteration procedure based on the same assumptions as discussed in Section E.1. The iteration is started at the end of the anchorage length (in the interior of the beam) where the conditions both for the steel stress and the slip are known. At this point, the steel stress is equal to the effective prestress while the relative slip between the strand and the concrete is equal to zero.

Since the smallest slip measurable in the pull-out tests was 0.0001 in., the shape of the bond-slip relation for slips smaller than this value is not known exactly. Consequently, it was assumed that one in. from the end of the anchorage length towards the end of the prestressed member (equal to the bonded length of the pull-out test) a slip of 0.0001 in. is developed after the release of the prestressing force. The strand force at that point is equal to the effective prestressing force minus the initial bond force as indicated by the unit bond force-slip relationship at a slip of 0.0001 in.

The rest of the anchorage length is divided in equal intervals the length of which depends on the accuracy of the solution desired. Assuming that the bond stress corresponding to a slip of 0.0001 in. of the measured unit bond force-slip relationship remains constant over the first iteration interval, the strand force transferred to the concrete by bond on this length can be determined. This force must be subtracted from the prestressing force existing at the beginning of the interval in order to obtain the prestressing force at the end of the first interval. According to the assumptions made in Section E.1, the slip at the end of the first interval is equal to the deformation of the strand corresponding to the differential prestressing force. Using this slip value, a new unit bond force may be picked from the unit bond force-slip relationship to calculate the prestressing force at the end of the second interval. The iterations are continued until the prestressing force in the strand becomes zero. The anchorage length is determined by the sum of the iteration intervals required plus the initial length of one in.

The degree of agreement of the calculation with actual test results depends on the accuracy with which the unit bond force-slip relationships of pull-out tests represent the typical bond-slip relation between strand and concrete.

APPENDIX F: DESCRIPTION AND DISCUSSION OF PRESTRESSED-BEAM TESTS

F.1 Introduction

The objective of the prestressed-beam tests described in this section was to check experimentally the theoretical projection of results from one-in. pull-out tests to practical problems involving bond between prestressing strand and concrete. In particular, the end slip and the anchorage length of 7/16-in. strand for two different depths of concrete under the strand were to be investigated.

Five pretensioned prestressed concrete beams reinforced with two 7/16-in. strands were cast. The beams were 9 ft long and had a cross section of 6 by 12 in. In three beams, the strand was placed 2 in. from the bottom, in two beams 2 in. from the top. The concrete strength of all beams was roughly 5600 psi.

The anchorage length was determined immediately after the release of the prestressing force by measuring the strain distribution of the concrete at the level of the reinforcement. In two beams, the end slip and the anchorage length were measured, in addition, at various time intervals after release of the prestress: 1, 6, 15, and 35 days.

With each of the three beams with the reinforcement near the bottom, a set of three pull-out specimens was cast and tested after the prestress had been released. The theoretical determination of anchorage length and end slip was based on the results of those tests.

F.2 Materials

F.2.1 Concrete

The same type of cement and aggregates used for the pull-out specimens was used for the beams (see Appendix A).

The mix proportions of the concrete were identical to those of mix A listed in Table A.1.

The slump of the concrete, the age at the time of testing, the apparent modulus of elasticity (determined from tests on three 6 by 12-in. cylinders), and the strength characteristics are listed in Table F.1 for each individual beam.

The compressive strength of the concrete was determined from tests on three 6 by 12-in. cylinders. The splitting strength was found from three 6 by 6-in. cylinders.

F.2.2 Steel

The reinforcing strand used in the beams consisted of seven-wire (round wire) strand with a nominal diameter of 7/16 in. The properties of the strand such as cross sectional area, pitch, angle of twist, and the apparent modulus of elasticity are listed in Table A.2. The strand used in the beams was cut from coil II.

The surface of the strand was clean and free of corrosion.

F.3 Description of Specimens

The exterior dimensions of all five beams tested were identical. The length was 9.0 ft, the cross section was 6 by 12 in. (Fig. F.1). The beams were reinforced with two 7/16-in. strands which were placed 2 in. from the bottom in three beams, and 10 in. from the bottom in two beams. No stirrups were used. The average prestress in the strand before release was 175 ksi.

The beams were identified by a series of letters and numerals: The first two letters, PB, stand for prestressed beam, the third letter

(B or T) identifies the level of the reinforcement referring either to the bottom or the top level. The numeral after the dash represents the numerical sequence of the beams.

F.4 Prestressing

The strands were prestressed between two concrete blocks anchored to the test floor of the laboratory using a hydraulic jack (Fig. F.2). The two strands of each beam were stressed simultaneously. The tension was controlled by dynamometers placed under the strand grips at both ends of the prestressing bed.

The strands were stressed until the average load indicated by the four dynamometers was 20.5 kips per strand which corresponded to a stress of 174 ksi. After tightening the nuts on the tie rods against the bearing plate on which the hydraulic jack rested, the hydraulic pressure was released. The load of each strand was adjusted by turning the nuts such that the two dynamometers of each strand indicated an average prestress of 174 ksi.

Prestressing of the strands took place at least 36 hours before casting in order to allow for initial losses of prestress due to relaxation of the steel and slip of the wedges in the strand grips.

F.5 Casting and Curing of Specimens

The forms were made of steel channels. A plastic sheet was placed on the bottom of the forms and slightly oiled in order to reduce friction between the beam and the form after the prestressing force was released.

The strands were cleaned with acetone immediately before casting.

Each beam was cast from one batch of concrete. A set of three or six 6 by 12-in. cylinders and three 6 by 6-in. cylinders was cast with each beam. In addition, three one-in. pull-out specimens, prepared in the same manner as described in Section A.4, were cast with those beams in which the strand was placed two-in. above the bottom.

The concrete was placed into the forms in one layer and vibrated with an interior vibrator.

The beams, the cylinders, and the pull-out specimens were cured in the same manner. For the first two days, the specimens were left in their forms and kept moist by covering them with wet burlap. After two days, the forms, except the bottom form supporting the beams, were struck. After keeping the specimens moist for another four days, the specimens were uncovered and left exposed to the laboratory environment until the time of testing (three days).

F.6 Transfer of Prestress

In all cases, the prestressing force was transferred to the beam on the ninth day.

The release of prestress was accomplished by loosening the nuts on the tie rods thus transferring the prestressing force to the extended hydraulic jack. Then, the valves of the hydraulic system were opened. Using this procedure, it was possible to release the prestressing force of both strands simultaneously into the beam within a few seconds. However, the release was gentle enough to allow reliable slip measurements between strand and concrete at the end of the beam.

F.7 Instrumentation and Measurements

Four aluminum center-hole dynamometers were used to determine the prestressing force applied.

In order to measure the concrete deformation, two lines of small steel discs with conical holes in the center were glued to the surface of the beam at the level of the reinforcement. The relative displacement of those reference points was measured with a 10-in. Whittemore mechanical strain gage. The spacing of the reference points is indicated in Fig. F.3.

In addition, special brackets with reference points were attached to the end of the beams in order to measure the average strains at sections closer than 10 in. to the end of the beam (Fig. F.3). Since the bracket was unstrained, the strain gage readings indicated only the deformation of the concrete within the gage interval. The sensitivity with which the strains could be measured was $\pm$ 0.01 percent.

A pair of 0.001-in. dial indicators was clamped to each strand at the ends of the beam in order to measure the end slip between the strand and the concrete. The slip of the strand was measured with respect to the end face of the concrete beam.

Slip- and strain measurements were taken immediately before the release of the prestress (zero reading) and immediately afterwards. These measurements corresponded to the instantaneous deformations of the concrete. For the beams PBB-3 and PBT-2, additional measurements were taken at the following ages after transfer: 1, 6, 15 and 35 days.

For each beam, three 6 by 12-in. cylinders were tested after the prestress had been transferred in order to determine the compressive strength and the modulus of elasticity of the concrete. At the same time, a set of three 6 by 6-in. cylinders was tested to obtain the splitting strength. As modulus of elasticity of the concrete, the secant modulus determined at 50 percent of the compressive strength was chosen.

In connection with those beams that were cast with the reinforcement located two in. above the bottom, three pull-out specimens were tested in the same manner as described in Appendix A.

F.8 Discussion of Test Results

F.8.1 Evaluation of Test Data

The anchorage length in a pretensioned prestressed member is defined as the length of strand necessary to transfer the entire effective prestressing force of the pretensioned reinforcement to the concrete by bond. The effective prestressing force immediately after release is equal to the pretensioning force minus the force lost by the instantaneous deformation of the strand and the concrete.

The anchorage length can be determined approximately by measuring the strain distribution of the concrete at the level of the reinforcement. According to the definition of the anchorage length, a constant strain distribution must be obtained theoretically in the center part of the beam between the two anchorage zones. The strain in the anchorage zone decreases from the constant strain at the end of the anchorage length to zero at the end of the beam. The anchorage length is therefore determined by the distance between the end of the beam and the cross section that develops the maximum concrete strain.

Because of a certain shear lag between the location of the actual stress transfer at the surface of the strand and the exterior surface of the concrete, the anchorage length determined by the concrete strain distribution may be slightly larger than the actual anchorage length. However for small concrete covers, this error is negligibly small.

In practice, it is difficult to determine exactly the cross section at which the full concrete strain is developed because of the unavoidable scatter of the strain measurements and the slightly asymptotical approach of the strain distribution to the constant strain plateau.

In order to obtain comparable results from various tests, the length of strand required to develop 90 percent of the full concrete strain (which corresponds to 90 percent of the full prestressing force) was determined and called L(90). This value could be measured with greater reliability. According to calculations discussed in Section 13.3, the full anchorage length is obtained approximately by multiplying L(90) by 1.12.

F.8.2 Effective Prestress

The prestress of the strand immediately before release of the prestressing force into the concrete was, on the average, 167 ksi (Table F.2). The difference in the individual prestress of the two reinforcing strands was less than three percent in each beam.

The effective prestress between the two anchorage zones of the beam immediately after release of the initial prestress was found

to be, on the average, 159 ksi. The average effective prestress of each beam, listed in Table F.2, was determined by subtracting from the prestress measured before release the steel stress corresponding to the average concrete strain measured in the center part of the beam.

The effective prestress decreases with time due to creep and shrinkage of the concrete.

F.8.3 Concrete Strains

The measured strain distributions on both sides of each beam are shown in Fig. F.4 through F.8. It was noted that in beams with the reinforcement near the bottom, the strains measured on both sides of the beam differed significantly. They varied by as much as 25 percent. The prestressing forces of the two reinforcing strands, however, immediately before release of the prestress varied by less than 3 percent. An eccentricity of 0.1 in. of the resultant force would cause the stresses on the two faces of the beam to differ by approximately 20 percent of the smaller stress. Therefore, the variation in the measured strains does not appear unreasonable.

F.8.4 Anchorage Length

The lengths L(90) measured for both anchorage zones of each strand are listed for every beam in Fig. F.4 through F.8 and in Table F.2. The values varied from 18 to 28 in. for the beams with the strand located 2 in. above the bottom. The average was 22 in. According to the calculation described in Section 13.3, the full anchorage length (112 percent of L(90)) may be expected to be on the average 25 in. This value corresponds to a length of approximately 57 times the nominal strand diameter.

For the two beams with the strand located near the top surface, the measured values for L(90) varied from 26 to 30.5 in. The average was roughly 28.5 in. This corresponds to a full anchorage length of approximately 32 in. or a length of 73 times the strand diameter.

On the average, the anchorage length in beams with the reinforcement placed 10 in. above the bottom was 28 percent larger than that developed in beams with the strand placed 2 in. above the bottom. This difference is consistent with data from pull-out tests which were performed to study the influence of the settlement of concrete under the strand (Chapter 7). The results of those pull-out tests indicated that, on the average, the settlement of a 10-in. thick layer of concrete under the strand reduces the bond strength, compared to that developed by specimens with a 2-in. thick layer, by approximately 25 percent for an average slip of 0.05 in. (Fig. 7.2). The end slip developed in the beams was roughly 0.10 in.

It should be noted that the average anchorage length of all beams measured at the release end was practically identical to that measured at the fixed end. The same result was true for the average values of the end slip.

F.8.5 End Slip

The end slip of each strand measured immediately after release of the prestressing force is listed in Table F.2. For beams with the strand placed near the bottom, the end slip ranged from 0.051 to 0.076 in., with an average value of 0.068 in. For beams with the strand near the

top surface, the end slip ranged from 0.088 to 0.109 in. with an average value of 0.096 in. The larger slip of the strand placed near the top of the beam is related to the reduced bond strength because of the effect of settlement.

F.8.6 Effect of Time on Anchorage Length and End Slip

In two beams (PBB-3 and PBT-2), the end slip and the strain distribution were measured at various time intervals after the release of the prestress: immediately, and at 1, 6, 15 and 35 days. The strain distributions are plotted separately for each side of the two beams in Fig. F.9 and F.10.

The measured lengths L(90) indicated by arrows in Fig. F.9 and F.10, are listed in Table F.3. It was observed that L(90) did not change over the time of observation. The small variations shown in Table F.3 are due to the scatter of the test results. The end slip, measured to an accuracy of 0.001 in., did not change either with time for both beams (Table F.3).

It should be noted that the prestressing force did not stay constant with time because of creep and shrinkage deformations of the concrete. Figure F.11 presents the variation of the average concrete strain with time in the center part of the two beams. Using these strains, the average loss of prestress in the strand can be calculated. The effective prestress of the two beams is plotted as a function of time in Fig. F.12. The graphs indicate that the prestressing force decreased by approximately eight percent over a period of 35 days.

F.8.7 Comparison of Test Data with Results from Other Investigations

Comparing test results related to bond which were obtained in different laboratories is difficult because bond is sensitive to various parameters that defy simple definition, such as,

(1) surface roughness of the steel (see Section 12.4)

(2) irregularities in the shape of strand (see Section 12.4)

(3) curing conditions of the concrete (see Section 6.4)

(4) shrinkage conditions of the concrete (see Section 6.3, 6.5)

The reference given in parentheses refers to the sections in which the effect of the particular variable on bond is discussed.

The difference in the magnitude of the anchorage length observed in literature may be a result of variations of test conditions of the type mentioned above.

Table F.4 lists the average anchorage length for 7/16-in. strand measured by other investigators or extrapolated from results of tests with other strand sizes. The major conditions under which the tests were performed are given, if reported, in the table.

The required interpolations or extrapolations were made with the following assumptions:

(1) the length required to transfer a given percentage of the prestressing force to the concrete is linearly proportional to the amount of prestressing force transferred.

(2) The anchorage length increases in linear proportion to the effective prestress.

(3) The anchorage length increases in linear proportion to the strand diameter.

The first assumption is based on the results of the theoretical (Fig. 13.5) and experimental (Fig. F.4 through F.8) determination of the steel stress distribution within the anchorage zone or the recognition of the fact that the bond-slip response for strand is virtually flat.

The second assumption is confirmed fairly well for strand by theoretical considerations based on results from pull-out tests (Fig. 13.7) as well as by test results (Kaar, 1963).

The third assumption is justified by results of pull-out tests (Fig. 5.7) and beam tests (Kaar, 1963). Although the results indicate that, for a given prestress, the anchorage length of small strand sizes may be slightly shorter in proportion to the nominal diameter than that for large strand sizes, the error is small.

The anchorage lengths measured and extrapolated for 7/16-in. strand and an effective prestress of 175 ksi differ significantly. The difference may be caused by the effect of various experimental parameters as mentioned above. Concluding from the scatter in the test results of three ostensibly identical beams (Table F.2) and data from many pull-out tests, a fair amount of scatter between the anchorage lengths measured in different laboratories must be expected. It was not possible to assign statistical weights to the various values because of lack of information on experimental details.

With a few exceptions, the anchorage length of 7/16-in. strand manufactured in the U. S. is around 27 in. or 62 times the

nominal strand diameter. This length would be required to develop the effective prestress of 175 ksi immediately after transfer. According to the Building Code Requirements for Reinforced Concrete (ACI 318-63), (1963), this would be the maximum allowable prestress for strand with a strength of 250 ksi. The Code requires that the effective prestress immediately after transfer be less than 0.7 times the strength of the strand or 175 ksi.

On the basis of data obtained in the course of this investigation and tests made elsewhere, the influences of the major variables appear to be as follows.

(1) Concrete Strength: Conclusions about the effect of concrete strength are not consistent throughout the available body of experimental data.

The pull-out tests on strand with diameters ranging from 1/4 in. to 1/2 in. reported here indicated that the bond strength of strand increases at a rate of approximately ten percent per 1000 psi of concrete strength.

Rüsch and Rehm (1963) who conducted an extensive investigation to study the anchorage length of 16 different, mostly deformed, prestressing steels found that, in general, the anchorage length decreased with increasing concrete strength. Their results for strand, however, obtained from only three beam tests, each with a different concrete strength, were not conclusive.

Ratz et al (1958) report a significant influence of the concrete strength on the anchorage length of 0.19-in. strand (see Table F.4).

It must be mentioned, however, that in most of the tests only the end slip of the strand was measured while the anchorage length was determined analytically.

Janney (1954) found that concrete strength has a relatively small effect on the transfer length of plain wire.

The most comprehensive study on the effect of concrete strength on the transfer length of strand was carried out by Kaar et al (1963). It was found that the concrete strength had practically no influence on the anchorage length of strands with diameters up to 1/2 in.

In view of the practical range of variation for concrete strength in prestressed concrete members, it appears that the effect of concrete strength may be ignored in practical considerations with the caution that a large accidental reduction in concrete strength may increase the anchorage length by approximately ten percent per 1000 psi of concrete compressive strength.

(2) Manner of Release: The anchorage length of strand up to 1/2-in. diameter may be as much as 20 percent larger at the end where the prestress is released suddenly than at the end where it is transferred slowly (Kaar, 1963; Rüsch, 1963). The difference may be even larger for 0.6-in. strand (Kaar, 1963).

(3) Surface Characteristics: Rusted strand and deformed strand developed shorter anchorage lengths than clean strand (Preston, 1963; Hanson, 1969).

(4) Time-Dependent Effects: The anchorage length of strand did not increase with time up to one year (Kaar, 1963; Rüsch, 1963;

Section F.8.6). However, it must be noted that the prestressing force of the strand decreased considerably in all investigations because of creep and shrinkage of the concrete and relaxation of the steel.

F.9 Results from Pull-Out Tests

The bond-slip relationships of three sets of pull-out tests cast in connection with those beams in which the strand was placed two in. from the bottom are presented in Fig. F.13. Since the concrete strength and the curing conditions were practically identical for all three sets of test specimens, an average unit bond-slip relationship (Fig. F.14) was used as a basis for the analytical method, described in Section 13.3, to determine the anchorage length and the end slip of strand in the beams PBB-1 through PBB-3.

F.10 Conclusions

The following may be concluded from the results of five prestressed-beam tests described in this section:

(1) The anchorage length of clean seven-wire (round wire) 7/16-in. strand, prestressed to approximately 165 ksi and placed no more than 2 in. above the bottom of the beams with respect to the direction of casting, was found to be, on the average, 25 in. or equal to 57 nominal strand diameters. This value was obtained by releasing the prestress at a relatively slow rate. The concrete strength was roughly 5600 psi. The age of the concrete at the time of transfer was nine days.

(2) The anchorage length of the same strand and measured under identical conditions was found to be, on the average, 32 in. or equal to 73 strand diameters when placed 10 in. above the bottom of the beam with respect to the direction of casting.

(3) The anchorage length and the end slip of the strand did not increase with time during a period of 35 days. During the observation period the effective prestress decreased by approximately 8 percent.

TABLE F.1

CONCRETE PROPERTIES OF PRESTRESSED BEAMS

Beam	Slump (in.)	Age at Release of Prestress (days)	Modulus of Elasticity (10^6 psi)	Compressive Strength (psi)	Splitting Strength (psi)
PBB-1	1.5	9	3.8	5290	450
PBB-2	1.5	9	3.7	5510	360
PBB-3	1.0	9	3.8	5490	380
PBT-1	1.25	9	3.9	5970	390
PBT-2	1.5	9	3.7	5690	400

TABLE F.2

TEST DATA FOR PRETENSIONED PRESTRESSED BEAMS

		Beam				
		PBB-1	PBB-2	PBB-3	PBT-1	PBT-2
Prestress before Release (ksi)		169.7	168.7	165.7	160.1	169.7
Effective Prestress after Release (ksi)		161.4	160.8	157.5	154.1	163.1
L(90) measured at Release End (in.)	South	22	20	23.5	30	27
	North	21	20.5	20.5	30	27
L(90) measured at Fixed End (in.)	South	24	19	24	30.5	26
	North	22	18	28	27.5	29
Average L(90) (in.)		22.5	19.4	24.0	29.5	27.2
Approximate Anchorage Length (in.)		25.0	21.5	27.0	33.0	30.5
End Slip measured at Release End (in.)	South	0.068	0.051	0.076	0.094	0.100
	North	0.064	0.067	0.064	0.090	0.109
End Slip measured at Fixed End (in.)	South	0.071	0.075	0.071	0.097	0.088
	North	0.073	0.062	0.070	0.097	0.093
Average End Slip (in.)		0.069	0.064	0.070	0.095	0.097

TABLE F.3

TEST DATA FOR THE BEAMS PBB-3 and PBT-2

Beam	Time After Release	Effective Prestress (ksi)	L(90) at Release End (in.)	L(90) at Fixed End (in)	L (90) Average (in.)	End Slip at Release End (in.)	End Slip at Fixed End (in.)	End Average (in.)
			23.5	24.0		0.076	0.071	
	1 hr.	157.5	20.5	28.0	24.0	0.064	0.071	0.070
			24.0	23.5		0.076	0.071	
	1 day	155.3	20.5	29.0	24.3	0.064	0.070	0.070
			23.5	23.5		0.076	0.071	
PBB-3	6 days	152.7	21.5	27.0	23.9	0.064	0.069	0.070
			23.5	23.5		0.076	0.071	
	15 days	149.2	21.5	27.0	23.9	0.064	0.069	0.070
			24.0	23.0		0.076	0.070	
	35 days	145.2	21.0	26.5	23.6	0.063	0.072	0.070
			27.0	26.0		0.100	0.088	
	1 hr.	163.1	27.0	29.0	27.2	0.109	0.093	0.097
			28.0	27.5		0.100	0.088	
	1 day	160.6	28.5	29.0	28.3	0.109	0.093	0.097
			27.0	25.0		0.099	0.088	
PBT-2	6 days	157.5	29.0	28.5	27.4	0.109	0.092	0.097
			26.0	26.0		0.099	0.088	
	15 days	154.0	28.0	28.0	27.0	0.109	0.092	0.097
			24.5	27.0		0.099	0.092	
	35 days	150.7	28.0	27.5	26.8	0.109	0.090	0.097

TABLE F.4

COMPARISON OF TEST RESULTS FROM OTHER INVESTIGATIONS FOR 7/16-in. STRAND

Investigator	Cross Section b x d (in.)	Depth of Concrete Below Center Line of Strand (in.)	Concrete Compressive Strength at Transfer (psi)	Age at Transfer (days)	Effective Prestress at Transfer (ksi)	Measured Transfer Length L(% of Stress Transferred) Release Slow (in.)	Measured Transfer Length L(% of Stress Transferred) Release Sudden (in.)	Anchorage Length L(100) Extrapolated to f_{se} = 175 ksi Release Slow (in.)	Anchorage Length L(100) Extrapolated to f_{se} = 175 ksi Release Sudden (in.)	Remarks
Debly (1956)	6 x 12	2.5	4300	9	148	L(100) 24		28.5		
		1.75,3.25	4670	14	167	32		33.5		
Ratz, Holmjanski and Kolner (1958)			2400		170	L(100) 43		44		extrapolated from 7x1.6 mm-strand
			3600		170	27		27.5		
			4800		170	18		18.5		
			6000		170	11.5		12		
Dinsmore, Deutsch, and Montemayor (1958)	4 x 10	2	6000	8,12	160	L(100) 19		21		beam tests by Montemayor
Rüsch and Rehm (1963)			1950	8	127	L(100) 34	L(100) 39	47	54	extrapolated from
	5.5 x 5.5	1,4.5	2900	4	127	41.5	41.5	57	57	7x3 mm-strand
			3900	3	128	31.5	31.5	43	43	
Kaar, LaFraugh and Mass (1963)		2.6	1660	1	172	L(100) 25.5	L(100) 32	26	32.5	interpolated between 3/8-in. and 1/2-in. strand
	7.3 x 5.3	1.75,3.50	3330	3	162	28	33.5	30.5	36	
		1.75,3.50	5000	22	153	24	29	27.5	33	
Preston (1963)	4.5 x 3.5	1.75	4120	2	176	L(100) 27		27		extrapolated from 1/2-in. strand
			4200		153	23.5		27		
Hanson and Hulsbos (1965)	I-Beams 9 x 18	1.5,3.25	5720	7	155	L(85) 14		18.5		
Over and Au (1965)	3 x 3	1.5	4840		150	L(100) 32.5		38		interpolated between 3/8-in. and 1/2-in. strand
Hanson (1969)	10.5 x 7	3,4.5	6480	7	172	L(95) 27	L(95) 28.5	29	30.5	
This Investigation	6 x 12	2	5600	7	160	L(90) 24.5		27		
		10	5600	7	159	32		35		

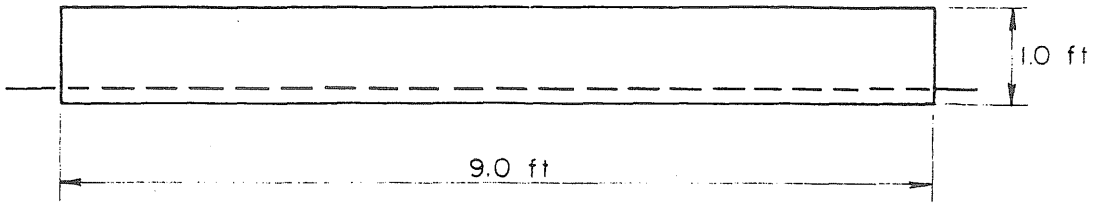

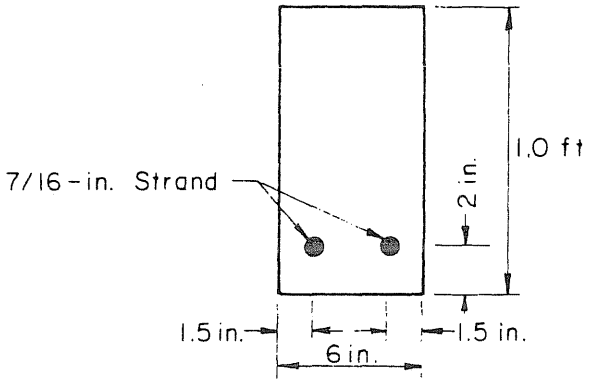

Beams :

PBB — 1
PBB — 2
PBB — 3

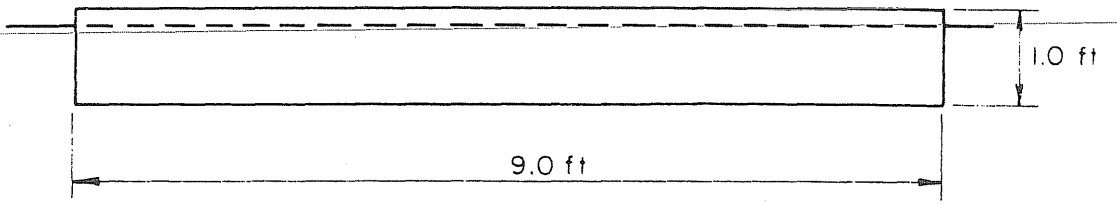

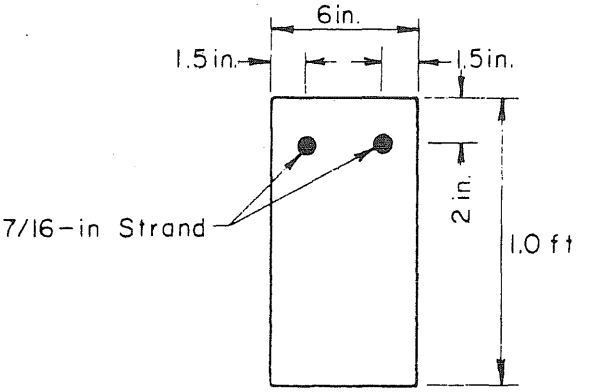

Beams :

PBT — 1
PBT — 2

FIG. F.1 BEAM DIMENSIONS

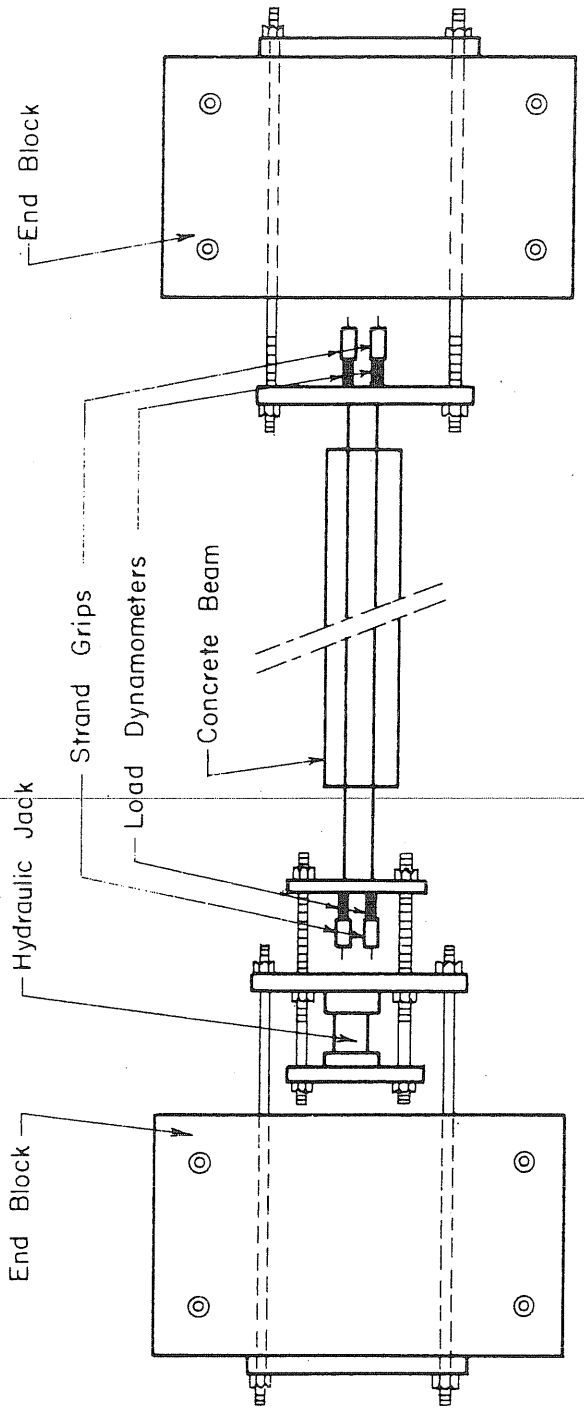

FIG. F.2 TEST SETUP

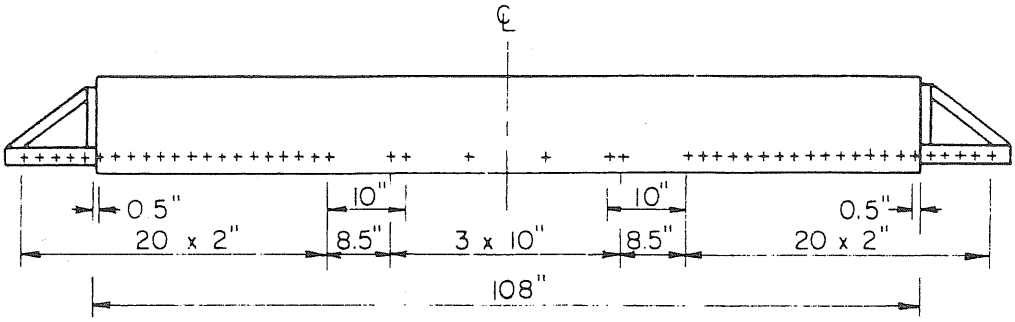

FIG. F.3 ARRANGEMENT OF STRAIN GAGE POINTS

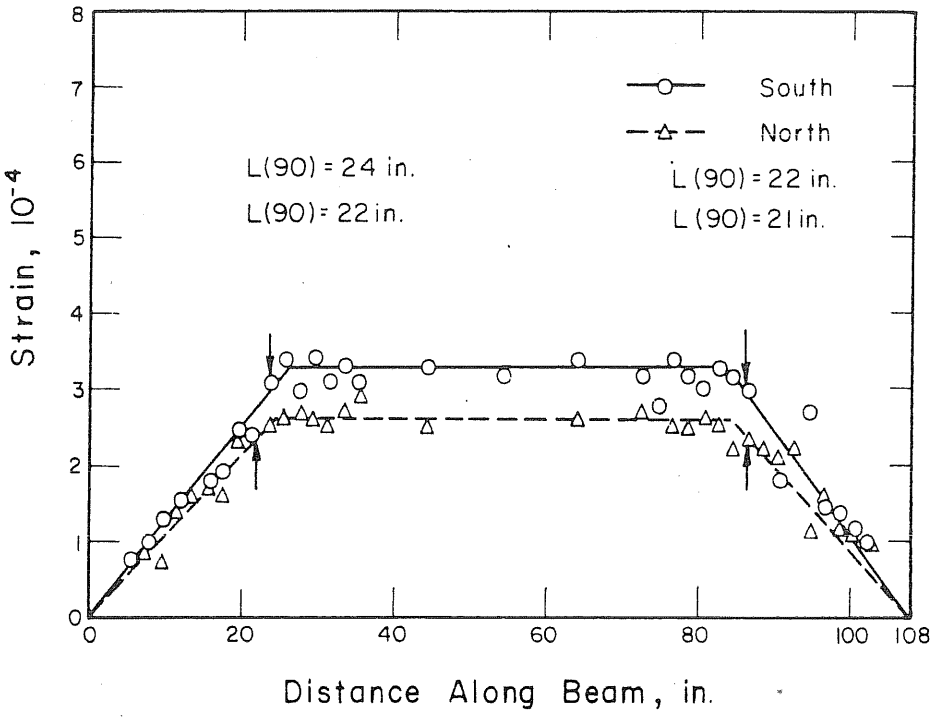

FIG. F.4 STRAIN DISTRIBUTION AFTER RELEASE OF PRESTRESS, BEAM: PBB-1

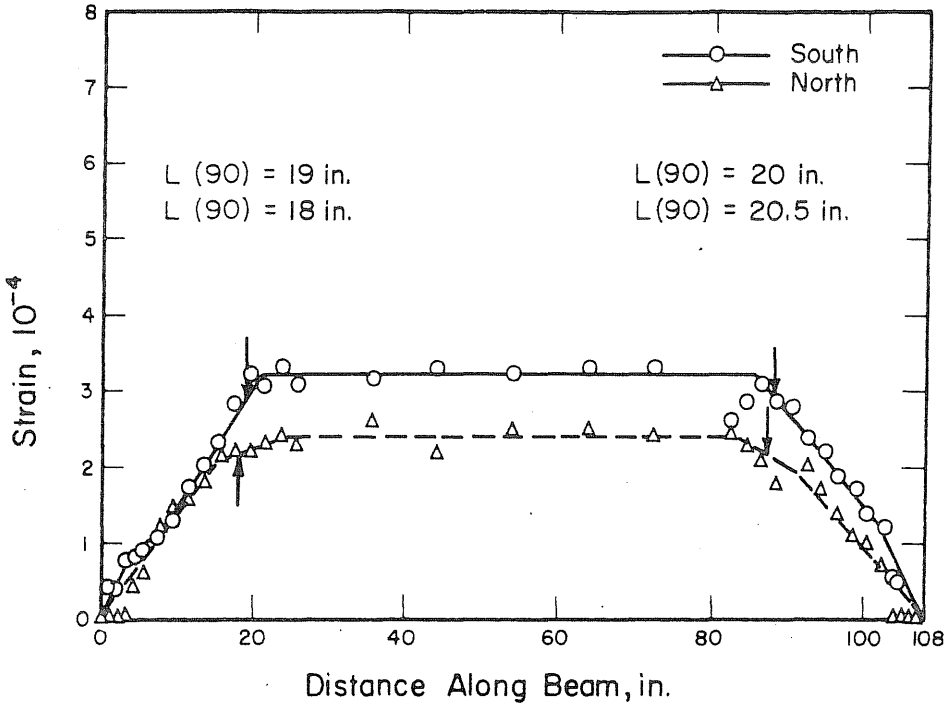

FIG. F.5 STRAIN DISTRIBUTION AFTER RELEASE OF PRESTRESS, BEAM: PBB-2

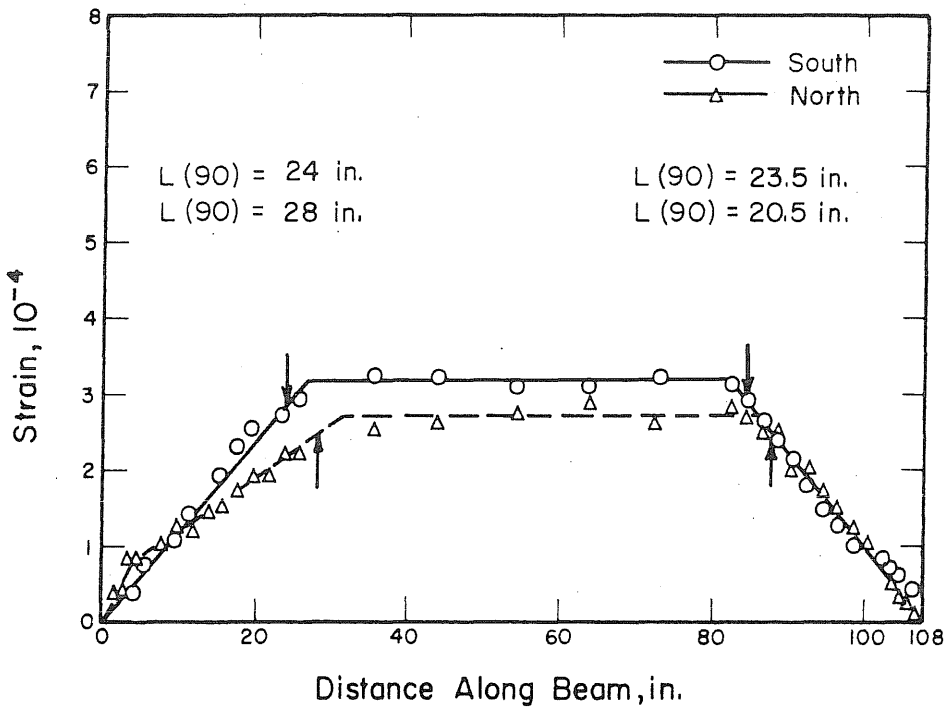

FIG. F.6 STRAIN DISTRIBUTION AFTER RELEASE OF PRESTRESS, BEAM: PBB-3

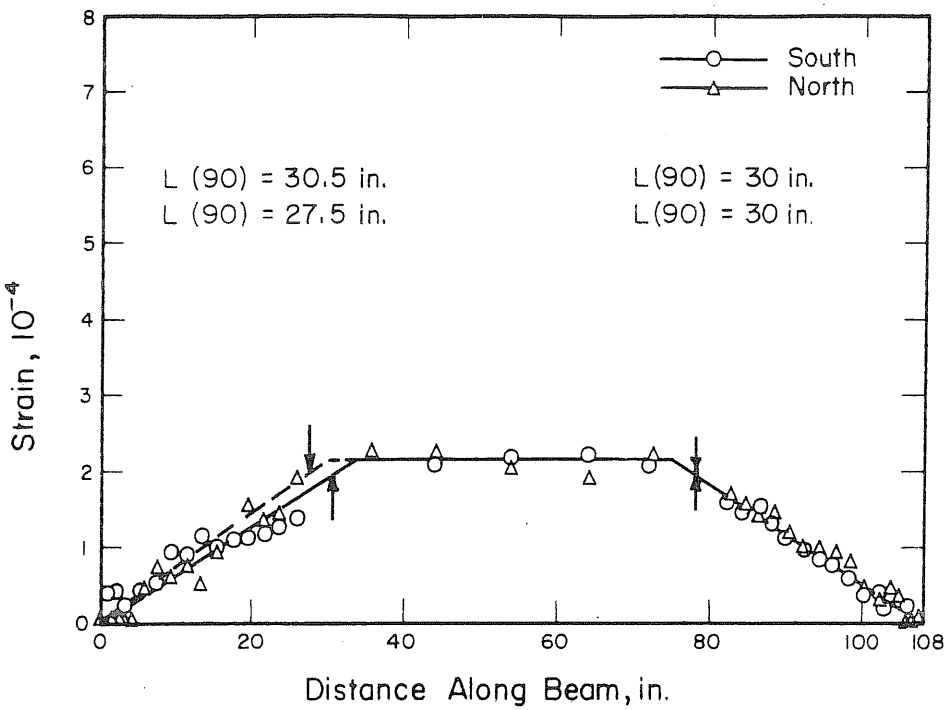

FIG. F.7 STRAIN DISTRIBUTION AFTER RELEASE OF PRESTRESS, BEAM: PBT-1

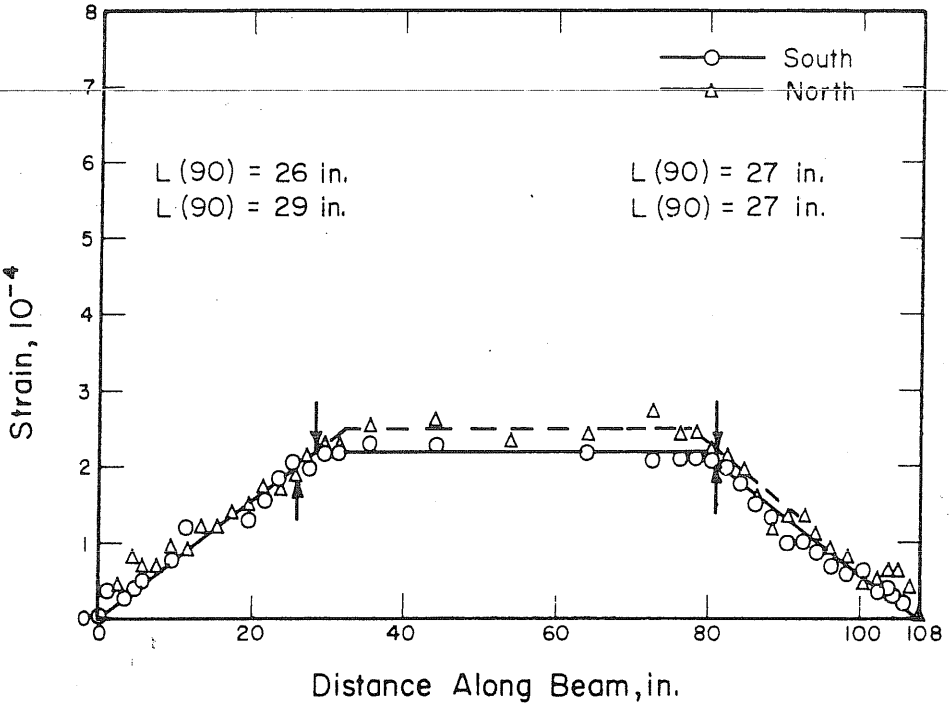

FIG. F.8 STRAIN DISTRIBUTION AFTER RELEASE OF PRESTRESS, BEAM: PBT-2

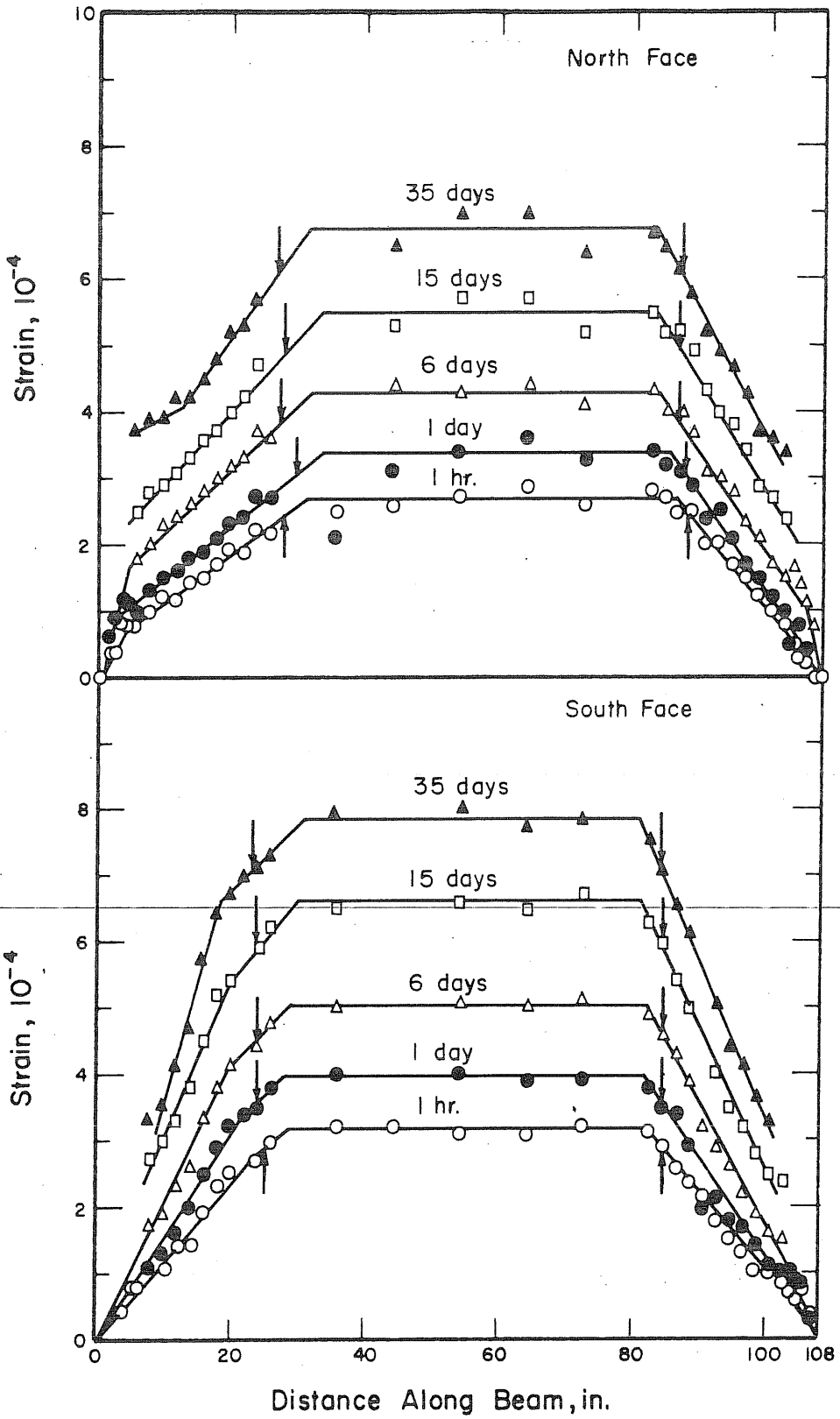

FIG. F.9 VARIATION OF CONCRETE STRAIN WITH TIME, BEAM: PBB-3

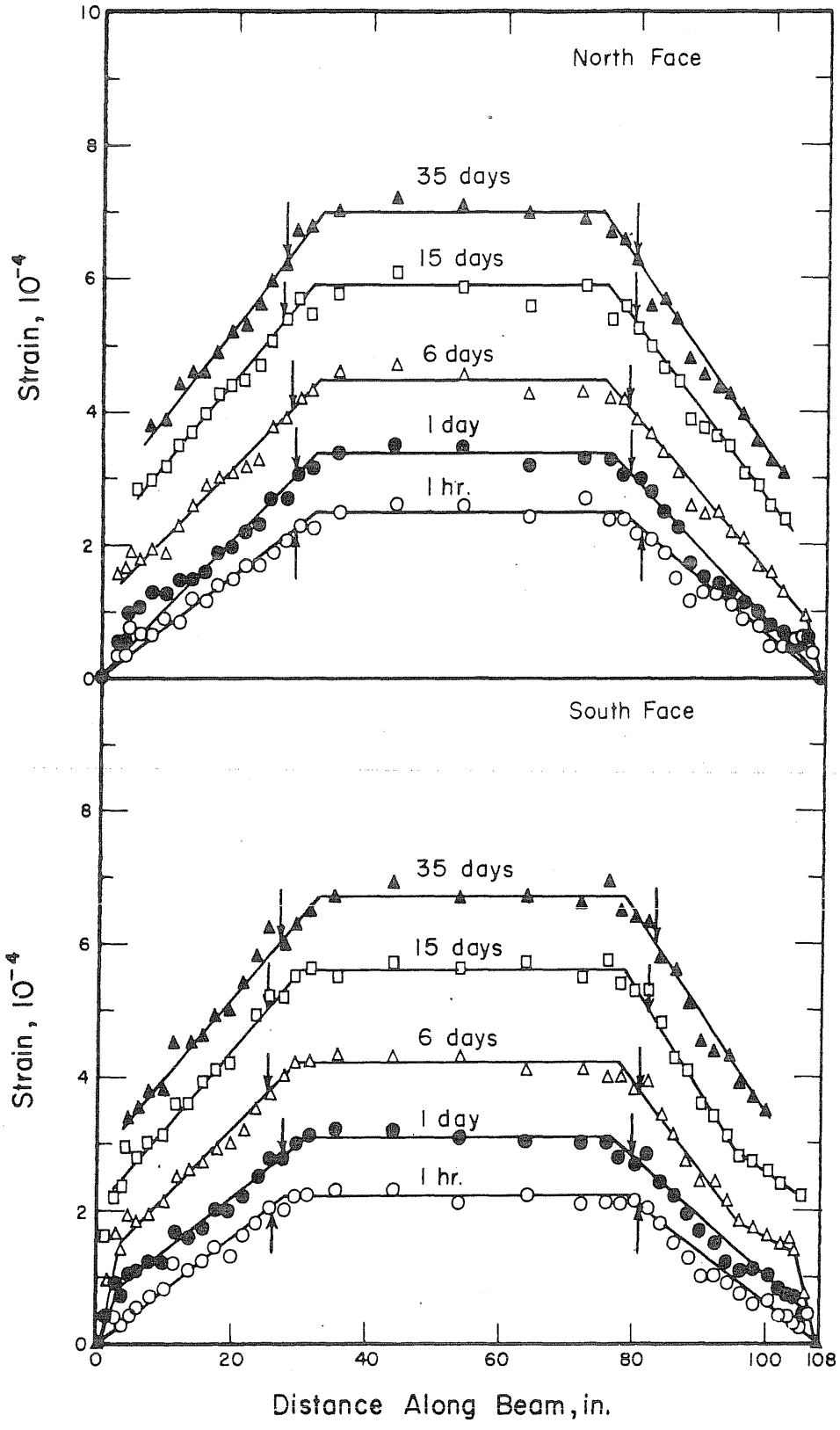

FIG. F.10 VARIATION OF CONCRETE STRAIN WITH TIME, BEAM: PBT-2

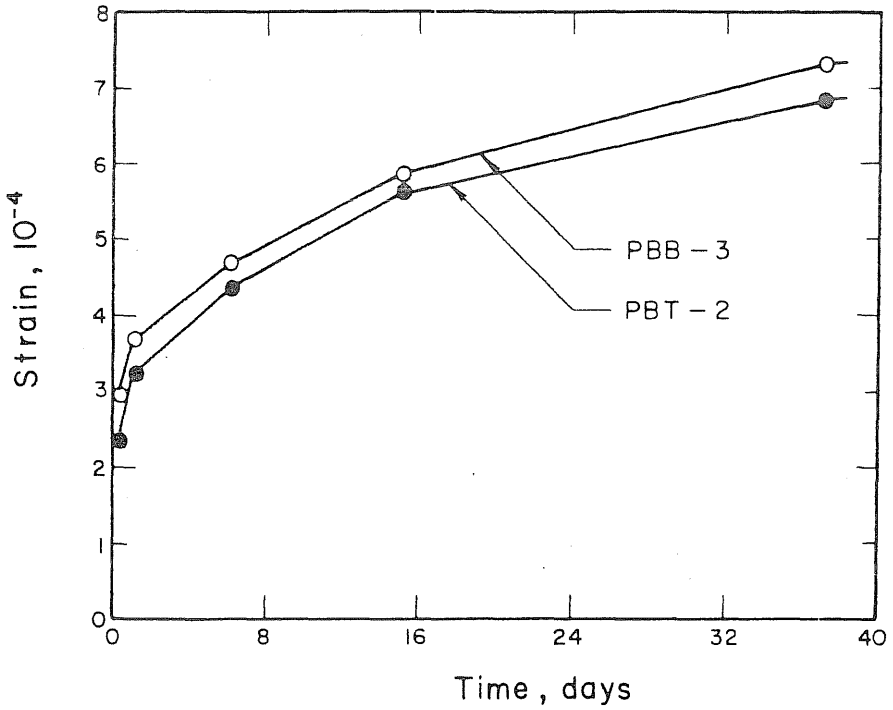

FIG. F.11 VARIATION OF CONCRETE STRAIN WITH TIME, BEAMS: PBB-3 and PBT-2

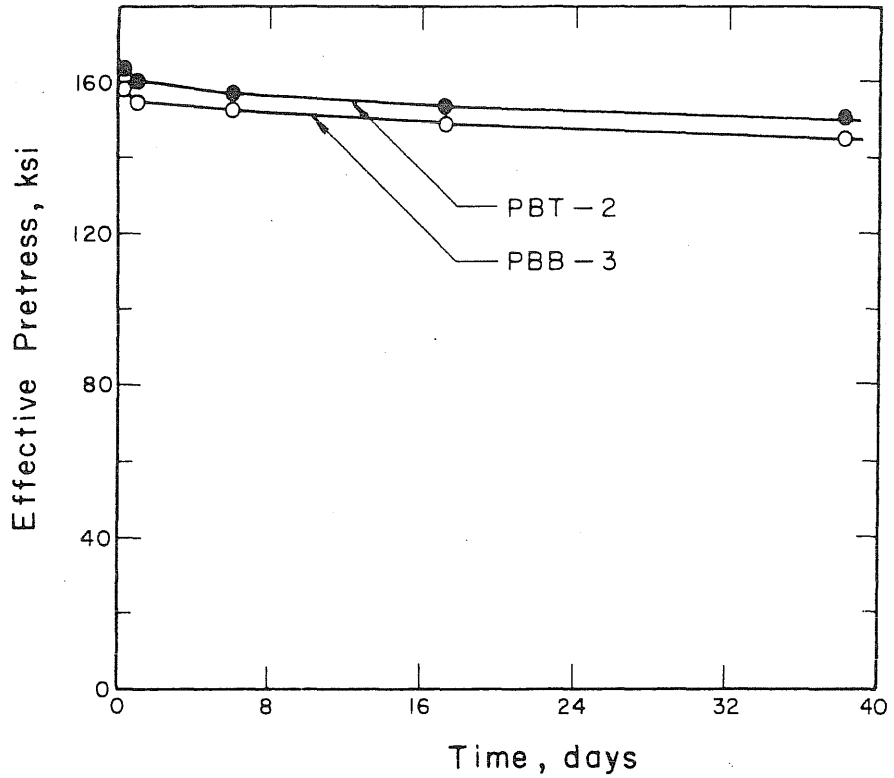

FIG. F.12 LOSS OF PRESTRESS WITH TIME, BEAMS: PBB-3 and PBT-2

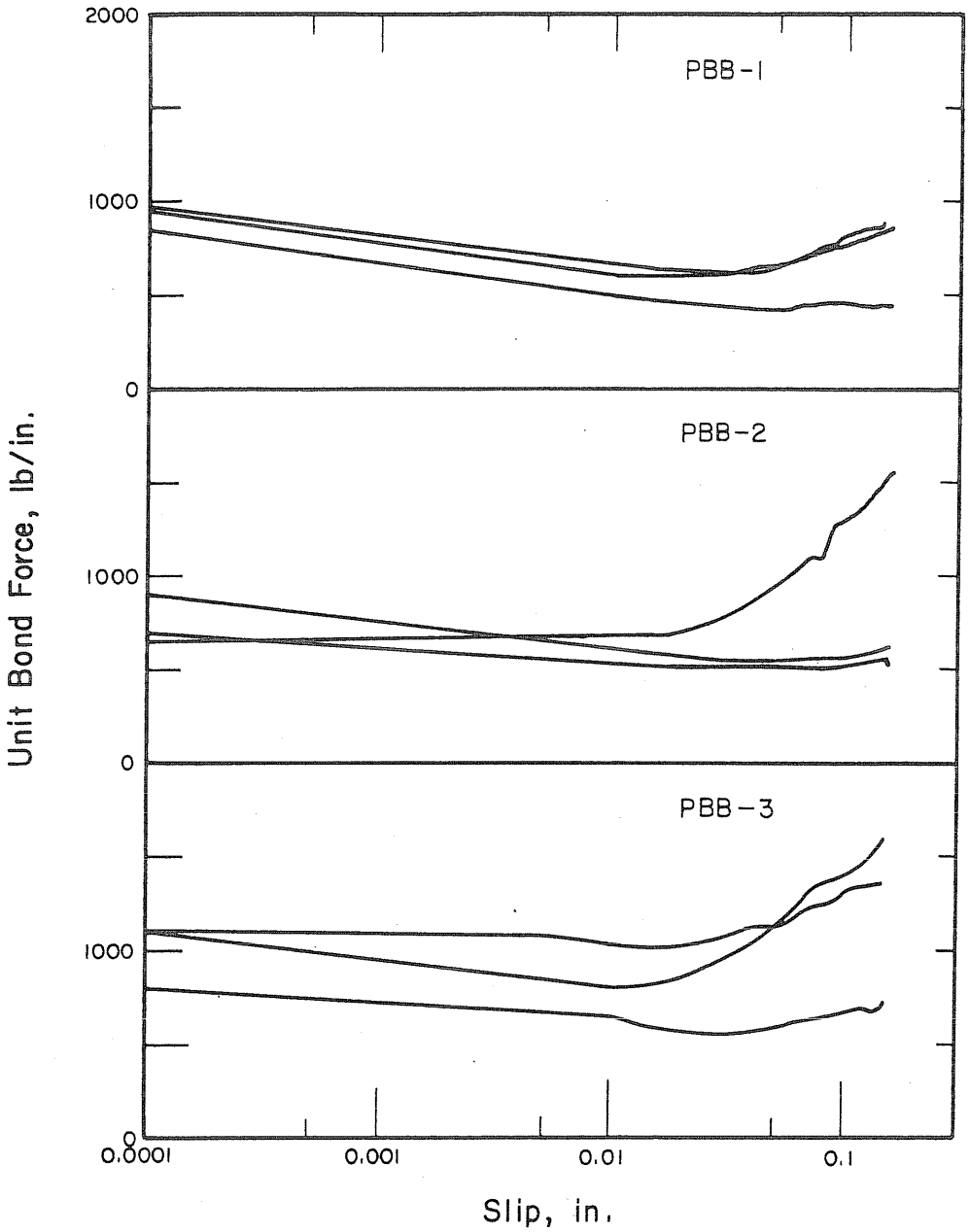

FIG. F.13 UNIT BOND FORCE-SLIP RELATIONSHIPS OF 7/16-in. STRAND FROM PULL-OUT SPECIMENS TESTED TOGETHER WITH THE PRESTRESSED BEAMS: PBB-1, PBB-2, PBB-3

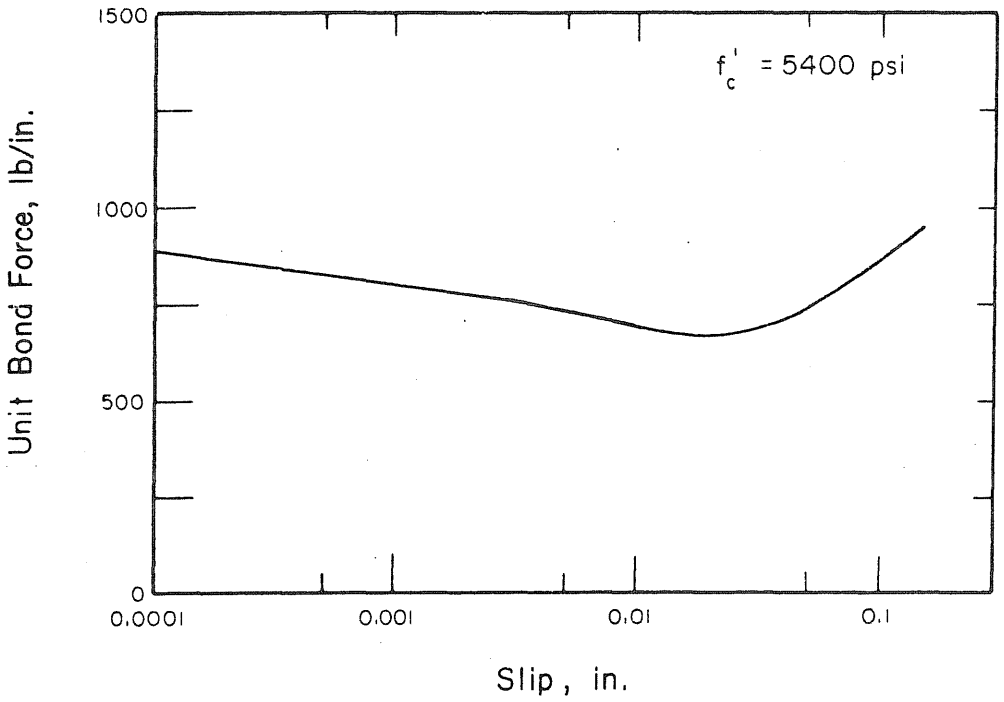

FIG. F.14 AVERAGE UNIT BOND FORCE-SLIP RELATIONSHIP OF 7/16-in. STRAND FROM PULL-OUT SPECIMENS TESTED TOGETHER WITH THE PRESTRESSED BEAMS: PBB-1, PBB-2, PBB-3